An investigation into the role of pericytes in regulation of vascular morphology and function using murine models of inflammation

A thesis submitted for the degree of

Doctor of Philosophy
University of London

By

DI (FH) Michaela Finsterbusch

Centre for Microvascular Research
William Harvey Research Institute
Barts & The London School of Medicine and Dentistry
Queen Mary University of London
Charterhouse Square
London EC1M 6BQ
United Kingdom

ACKNOWLEDGEMENTS

I want to thank all those who supported me throughout my PhD project, both in a professional and also personal manner, and without whom the progress of this work would not have been achieved.

I would like to express my gratitude to my supervisor Prof. Sussan Nourshargh for giving me the possibility to work in her team, providing me this interesting theme and for her time and supervision. I acknowledge Prof. Nourshargh and all the members of the Microvascular Research group for their constructive scientific support and advice. I wish to thank especially Doris for her warm welcome and for introducing me to the field of pericytes, and Mathieu for all his time and help. Many thanks also go to Abby and Beeny for their patience with me asking millions of times for tail vein injections, and Tomeu who always had helping hands for me. A big thank you goes to Natalie, the good soul in the lab, for her help and support. I would like to express my gratitude to my colleague and friend Krishma, who went through this journey with me including all the ups and downs and always had an open ear and heart for me. My gratitude goes also to the students Shimona, Clare, Giulia, Andrew, Emma, Chris and Suborno not at least for the barrel of fun at lunchtimes and legendary Friday nights but also for creating such a good atmosphere to work in, their encouragements and support in all kinds of ways, and their friendship that developed throughout my time at the WHRI.

A big “thank you” goes to Thomas, who always supported me in various forms, gave me motivation and the strength to believe in my abilities, and to my family for their love and faith they have had in me not just during these three years.

I wish to thank also Prof. Rod Flower, Prof. Chris Thiemermann and Dr. Martin Carrier for acting as my examiners in several progress assessments.

Furthermore, I would like to thank the British Heart Foundation for funding my studentship.

ABSTRACT

Leukocyte recruitment to sites of inflammation is a crucial event in host defense against pathogens and tissue injury. Although there is at present much interest in deciphering the mechanisms of leukocyte transendothelial cell migration, little attention has been paid to the subsequent steps, *i.e.* leukocyte migration through the pericyte layer and the venular basement membrane. In this context, results from this group previously demonstrated that neutrophils preferentially transmigrate through gaps between adjacent pericytes, regions associated with sites of low matrix protein expression within the vascular basement membrane. The aim of this thesis was to extend these findings by investigating the impact of inflammatory mediators on pericyte morphology and vascular basement membrane deposition using both *in vitro* and *in vivo* models.

Flow cytometry analysis of pericyte-like C3H/10T1/2 cells and primary lung pericytes revealed the expression of key pro-inflammatory molecules on their surface (including cytokine receptors and adhesion molecules) and the regulation of these molecules upon cytokine stimulation. Using the murine cremaster muscle model it was further demonstrated that key neutrophil chemoattractants (*i.e.* LTB_4, KC, C5a and fMLP) induced neutrophil transmigration that was associated with a change in pericyte morphology (as quantified through enlargement of gaps between adjacent pericytes). These changes in pericyte gap size were neutrophil-dependent and mediated by endogenously generated TNF as demonstrated in neutrophil-depleted mice and $TNFR^{-/-}$ mice, respectively. In addition, TNF appeared to mediate post-inflammatory BM deposition in response to LTB_4 and was required for chemoattractant-induced vascular permeability.

Hence, the results of the present work have demonstrated the ability of pericytes to respond to both cytokines and chemoattractants, suggesting an active role for pericytes in the regulation of inflammatory responses. In addition, findings provide the first evidence for chemoattractant-induced changes in vascular morphology and barrier functions of venular walls *in vivo* via the release of endogenous TNF as a secondary mediator, effects that may contribute to the pro-inflammatory properties of these stimuli.

TABLE OF CONTENTS

LIST OF FIGURES

LIST OF TABLES

ABBREVIATIONS

7-AAD	7-Aminoactinomycin D
ActD	Actinomycin D
Ang1/2	Angiopoietin 1/2
Ang II	Angiotensin II
ANOVA	Analysis of variance
αSMA	alpha smooth muscle actin
ATTC	American type culture collection
BBB	Blood-brain barrier
BM	Basement membrane
bp	Base pair
BSA	Bovine serum albumin
CAM	Cell adhesion molecule
Cat	Catalase
CCL2	Chemokine: C-C motif ligand 2
CD	Cluster of differentiation
CNS	Central nervous system
DAMP	Damage-associated molecular pattern
DC	Dentritic cell
DMEM	Dulbecco's modified eagle's medium
DMSO	Dimethyl sulfoxide
DNA	Deoxyribonucleic acid
dNTP	Deoxynucleotide triphosphate
EAP	Endothelial adhesive platform
EC	Endothelial cell
EGF	Endothelial growth factor
EGFP	Enhanced green fluorescent protein
EDTA	Ethylene diamine tetraacetic acid
ELISA	Enzyme-linked immunosorbent assay
ESAM	Endothelial cell-selective adhesion molecule
ESL-1	E-selectin ligand-1
FBS	Fetal bovine serum
FGF	Fibroblast growth factor
FISH	Fluorescence in situ hybridisation
fMLP	Formyl-Methionyl-Leucyl-Phenylalanine
FPR2	N-formyl peptide receptor 2

GAG	Glycoaminoglycan
GFP	Green fluorescent protein
GM-CSF	Granulocyte-macrophage colony-stimulating factor
GPCR	G-protein-coupled receptor
GS	Goat serum
GTP	Guanosine triphosphate
h	Hours
HBP	Heparin-binding protein
HBSS	Hank's balanced salt solution
ICAM-1	Intracellular adhesion molecule-1
i.d.	Intradermal
IFN-γ	Interferon gamma
Ig	Immunoglobulin
IL	Interleukin
IL-1β	Interleukin-1 beta
IL-1R	Interleukin-1 receptor
i.m.	Intramuscular
i.p.	Intraperitoneal
I/R	Ischemia reperfusion injury
i.s.	Intrascrotal
i.v.	Intravenous
IVM	Intravital microscopy
JAM	Junctional adhesion molecule
KC	Keratinocyte-derived chemokine
kg	Kilogram
KO	Knockout
LER	Low expression region
LFA-1	Lymphocyte function-associated antigen-1
LPS	Lipopolysaccharide
LSM	Laser scanning microscope
LTB_4	Leukotriene B_4
Lys	Lysozyme
M	Mol
mAb	Monoclonal antibody
MeOH	Methanol
MFI	Mean fluorescence intensity
µg	Microgram

mg	Milligram
µl	Microliter
ml	Millilitre
µm	Micrometre
mM	Millimolar
mm	Millimetre
MAC-1	Macrophage antigen-1
MAPK	Mitogen-activated protein kinase
MCP-1	Macrophage chemotactic protein-1
MHC	Major histocompatibility complex
MIF	Macrophage inhibitory factor
Min	Minutes
MIP-2	Macrophage inflammatory protein-2
mm	Millimetre
MMP	Matrix metalloproteinase
MPO	Myeloperoxidase
mRNA	Messenger ribonucleic acid
MRP14	Myeloid-related protein-14
ND	Not detected
NE	Neutrophil elastase
ng	Nanogram
NG-2	Neuron-glia antigen 2
NLRP3	Nod-like receptor family pyrin-containing domain 3
PAF	Platelet-activating factor
PAMP	Pathogen-associated molecular pattern
PBS	Phosphate buffered saline
PCR	Polymerase chain reaction
PDGF-B	Platelet-derived growth factor B
PDGFR-β	Platelet-derived growth factor receptor beta
PE	Phycoerythrin
PECAM-1	Platelet endothelial cell adhesion molecule-1
PFA	Paraformaldehyde
PI3Kγ	Phosphoinositol 3-kinase gamma
PSGL-1	P-selectin glycoprotein ligand-1
PRR	Pattern recognition receptors
PVC	Perivascular cell
qPCR	quantitative polymerase chain reaction

RA	Rheumatoid arthritis
RFI	Relative fluorescence intensity
RGD	Arginine-glycine-aspartic acid
ROCK	Rho kinase
ROM	Reactive oxygen metabolites
ROS	Reactive oxygen species
s	Second
S1P	Sphingosine-1-phosphate
SD	Standard deviation
SDF-1α	Stromal-derived factor 1 alpha
SDS	Sodium dodecyl sulphate
SEM	Standard error of the mean
SM22α	Smooth muscle protein-22 alpha
SOD	Superoxide dismutase
SYK	Spleen tyrosine kinase
TAE	Tris-Acetate-eDTA
TEM	Transendothelial migration
TGF-β	Transforming growth factor beta
TLR	Toll-like receptor
TNF-α	Tumour necrosis factor alpha
TNFR	Tumour necrosis factor receptor
U	Unit
UV	Ultraviolet
V	Volt
VCAM-1	Vascular cell adhesion molecule-1
VEGF	Vascular endothelial growth factor
VLA-4	Very late antigen-4
vSMC	Vascular smooth muscle cell
v/v	Volume/volume
VVO	Vesiculo-vacuolar organelle
WT	Wild type
w/v	Weight/volume

PUBLICATIONS ARISING FROM THIS WORK

Finsterbusch M, Voisin MB & Nourshargh S (2013). **Chemoattractant-induced TNF plays a pivotal role in vascular morphology and permeability.** Manuscript in preparation for Blood

LIST OF PRESENTATIONS

Finsterbusch M, Voisin MB & Nourshargh S (2012). **A role for TNFα as a secondary mediator of LTB_4-induced inflammatory responses.** William Harvey Day (London, 16th October 2012). *Poster presentation.*

Finsterbusch M, Voisin MB & Nourshargh S (2012). **A role for TNFα as a secondary mediator of LTB_4-induced inflammatory responses.** William Harvey Research Institute Annual Review (London, 11th July 2012). *Poster presentation. First prize winner for outstanding poster presentation.*

Finsterbusch M, Voisin MB & Nourshargh S (2012). **LTB_4 induces changes in vascular morphology.** International Vascular Biology Meeting (Wiesbaden, Germany, 2nd – 5th June 2012). *Poster presentation.*

Finsterbusch M, Voisin MB & Nourshargh S (2011). **LTB_4 induces changes in vascular morphology.** London Vascular Biology Forum (London, 7th December 2011). *Poster presentation. First prize winner for outstanding poster presentation.*

Finsterbusch M, Voisin MB & Nourshargh S (2011). **LTB_4 induces changes in vascular morphology.** William Harvey Day (London, 19th October 2011). *Poster presentation.*

Finsterbusch M, Voisin MB & Nourshargh S (2011). **LTB_4 induces changes in vascular morphology.** 24th UK Adhesion Meeting (Birmingham, 22nd September 2011). *Poster presentation.*

Finsterbusch M, Voisin MB & Nourshargh S (2011). **LTB_4 induces changes in vascular morphology.** 23rd UK Adhesion Meeting (London, 23rd June 2011). *Poster presentation.*

STATEMENT OF ORIGINALITY

The approach and experiments presented here are novel. The author has personally undertaken all the work described here, unless stated otherwise.

CHAPTER 1: GENERAL INTRODUCTION

1.1 General vascular biology

The cardiovascular system is an organ system that provides distribution of blood throughout the body. This process of circulation serves to transport oxygen, proteins, nutrients, blood cells, hormones, enzymes and other molecules to and from tissues. Thereby, it plays a role in maintaining homeostasis, tissue regeneration and reorganisation, regulation of body temperature and pH and immune response. The cardiovascular system is formed by the heart, blood, and blood vessels. Higher developed organisms such as vertebrates exhibit a closed cardiovascular system with blood flowing within a closed network of blood vessels. Blood vessel walls are composed of three layers – tunica interna, tunica media and tunica externa – composed of a variety of cell types such as endothelial cells (ECs), perivascular cells (including both pericytes and vascular smooth muscle cells (vSMCs)) and fibroblasts (Figure 1). Depending on the composition of vessel walls, different types of blood vessels (arteries, veins and capillaries) exhibit distinct properties to allow varying levels of blood flow, pressure and vascular permeability for active and passive transport of molecules and cells.

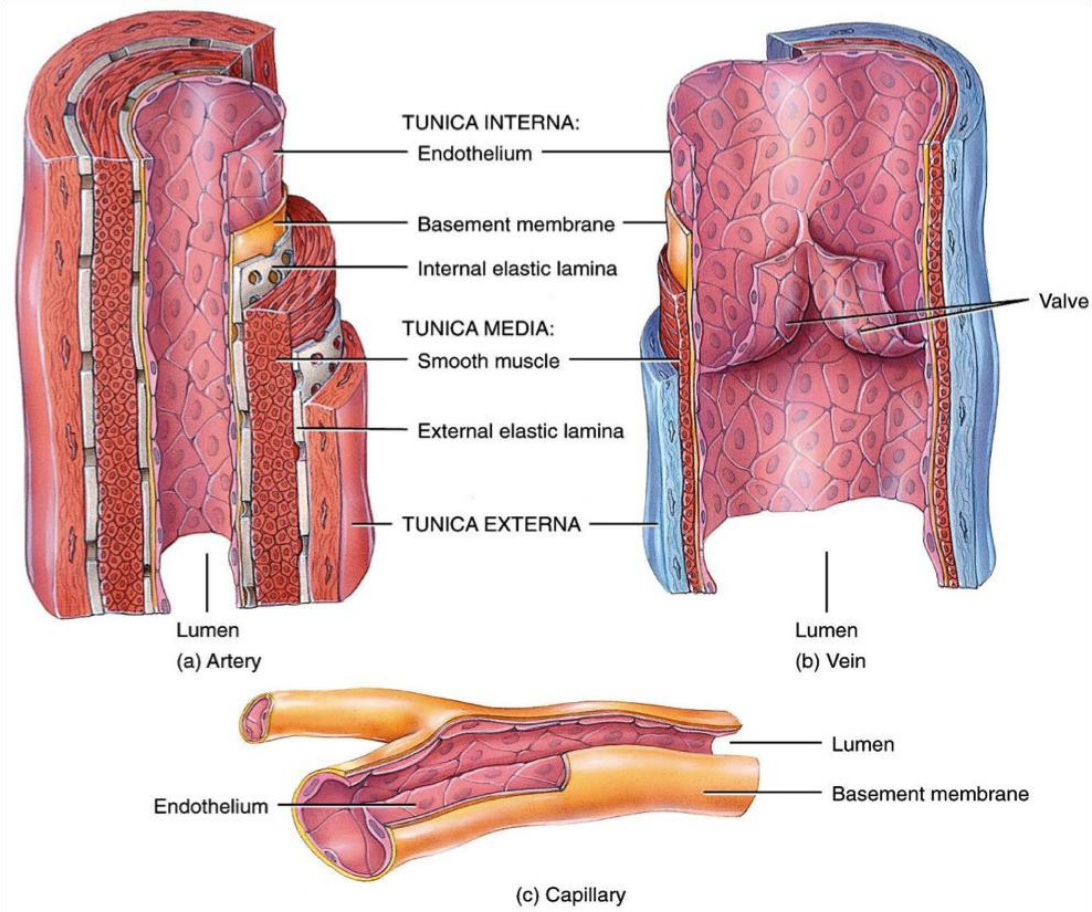

Figure 1.1: Components of blood vessel walls. Blood vessel walls consist of three structural layers: the tunica intima, tunica media and tunica externa. The tunica intima forms the inner lining of blood vessels and includes the endothelium surrounded by connective tissue basement membrane and elastic lamina. The tunica media (middle layer) is primarily muscular tissue with high variations among different vessel types and a role in regulating vessel diameter and blood flow. The outermost layer of vessel walls is the tunica externa (also called tunica adventia) which consists of elastic and collagenous fibres and plays a role in anchoring the vessel to surrounding tissue. Modifications of the composition of vessel walls among different vessel types (such as arteries, veins and capillaries) account for their specific function to accommodate varying levels of blood flow and pressure. Arteries **(a)** comprise a high amount of smooth muscle cells, which makes the walls thicker than those of veins **(b)** and enables high blood pressure and flow in arteries. In contrast, capillaries **(c)** have extremely thin walls, with only the tunica interna and sporadic perivascular cells. The thin wall of capillaries permits molecule exchange between blood and tissue. (Figure from Tortora and Derrickson, 2009, Principles of Anatomy & Physiology, 12th edition).

1.2 Pericytes at a glance

1.2.1 Location, characteristics and identification of pericytes

Pericytes are located around the endothelium of all vessel types and are generally described as mural cells which are embedded within vascular basement membrane (BM)(Shimada et al., 1992; Wang et al., 2006) (Figure 1.2).

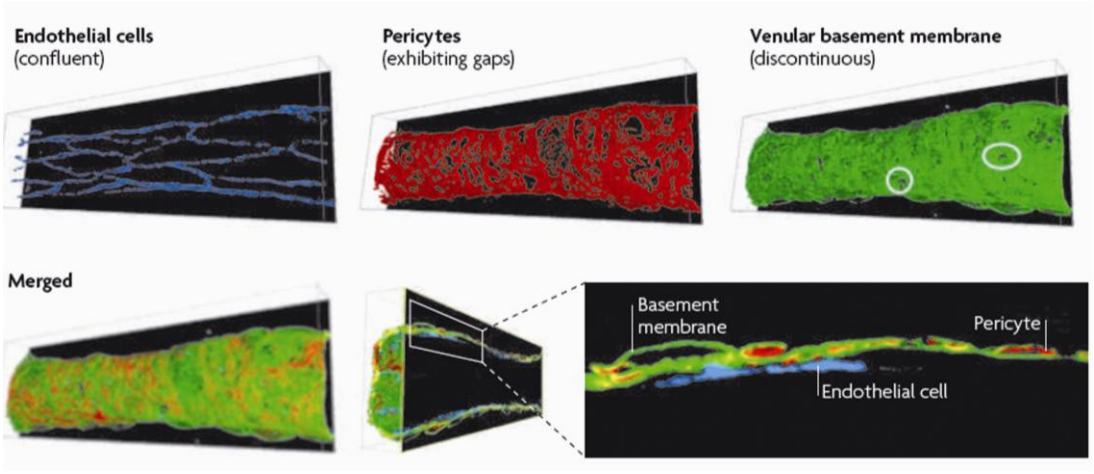

Figure 1.2: Location of pericytes within vascular walls. Confocal images of postcapillary venules of immunofluorescently labelled cremaster muscle are shown. Vessel walls are composed of endothelial cells (ECs) (shown in blue, labelled for platelet endothelial cell adhesion molecule, PECAM-1), pericytes (shown in red, labelled for α-smooth muscle actin, αSMA) and BM proteins (shown in green, labelled for laminin). The endothelium provides the first barrier to components of the blood and shows a confluent cell layer surrounding the lumen. In contrast, pericytes and BM exhibit a discontinuous network with pericytes exhibiting gaps between adjacent cells and BM exhibiting low expression regions (LERs). Pericytes are embedded in the vascular BM, which is thought to be generated by both pericytes and ECs. (Figure from (Nourshargh et al., 2010).

Pericytes are also known as adventitial cells, perivascular cells, mural cells, Rouget cells, periendothelial cells and pericapillary cells and were first described in 1871 and 1873 by the scientists Eberth and Rouget as cells closely associated with underlying endothelium of small blood vessels. More than 50 years later, in 1923, the term “pericyte” was introduced by Zimmermann due to their close proximity to ECs. Pericytes are long cells (~50-70 µm length), possess a large kidney-shaped nucleus and processes along the abluminal surface of EC tubes. However, pericytes are multipotent cells and morphological differences exist depending on

vessel type (Figure 1.3), vascular bed, developmental stage, species and pathological conditions (Diaz-Flores et al., 1991; Morikawa et al., 2002b). Similar to pericytes, also vSMC and other cells such as astrocytes, epithelial cells, fibroblasts and macrophages occupy the periendothelial compartments. This makes the correct identification of pericytes difficult. Being derived from the same mesenchymal stem cell lineage (Armulik et al., 2005), pericytes and vSMC are especially hard to be distinguished from each other. vSMC are located at arteries and arterioles with intermediate cells – resembling both pericytes and vSMCs – around capillaries (Diaz-Flores et al., 1991; Hirschi and D'Amore, 1996; Shimada et al., 1992). On the other side of the capillary bed, pericytes are thought to be located at post-capillary venules and collecting venules. Whereas pericytes form a loose network with gaps between adjacent cells, classical vSMCs are tightly wrapped around arterioles, arteries and veins. However, both, pericytes and vSMCs are closely related and thus, clear differentiation between these cell types is not always possible.

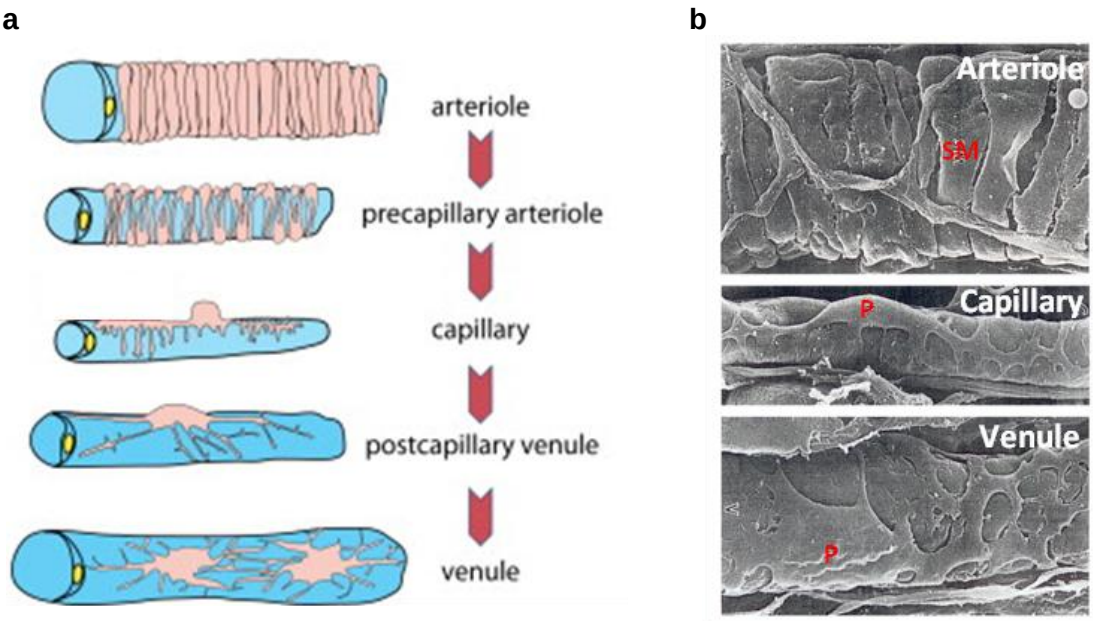

Figure 1.3: Morphology of perivascular cells on different vessel types. Schematic diagram **(a)** and electron microscopic images **(b)** of perivascular cells illustrating morphological differences between vSMCs and pericytes depending on the vessel type. vSMCs on arterioles (SM in "b") exhibit a spindle-shaped morphology with few cytoplasmic processes and are tightly wrapped around the entire abluminal side of the endothelium. Capillary pericytes (P in "b") in contrast cover only a small proportion of the endothelium. They show a rounded cell body with few major processes running parallel to the vessel. These primary processes give rise to multiple secondary processes that are perpendicularly orientated. Pericytes investing venules exhibit a stellate shape with many branching processes covering a great part of the underlying endothelium. (**(a)** figure modified from *(Armulik et al., 2011)*; **(b)** modified from *(Shimada et al., 1992)*).

The lack of an absolute marker for pericytes significantly hampered the study of these mural cells. Although several markers for pericytes have been described, including neuron-glia antigen 2 (NG-2), alpha smooth muscle actin (αSMA), platelet-derived growth factor receptor beta (PDGFR-β) and desmin, none of them is completely specific for pericytes or recognises all pericytes. Differences in their expression are seen in different species, vascular beds, developmental stage and vessel types (Chan-Ling et al., 2004; Hughes and Chan-Ling, 2004; Murfee et al., 2005; Nehls and Drenckhahn, 1991). Furthermore, pericytes have been shown to be able to differentiate into vSMCs and vice versa (Nehls and Drenckhahn, 1993) and also into other cell types such fibroblasts (Sundberg et al., 1996), chondroblasts (Farrington-Rock et al., 2004), osteoblasts (Brighton et al., 1992; Diaz-Flores et al., 1992; Canfield et al., 1996; Doherty et al., 1998) and adipocytes (Farrington-Rock et al., 2004; Schor et al., 1995), which makes the study of pericytes especially *in vitro*

even harder. Thus, today a series of criteria (location, morphology and gene/protein expression) are used to define pericytes and the interpretation of data needs to be handled with care (Armulik et al., 2011).

1.2.2 Physiological functions of pericytes

Role of pericytes in vessel development (vasculogenesis and angiogenesis)

The close association of pericytes with ECs provides mechanical support and stability for the vessel wall, and mediates EC functions (Lindahl et al., 1997). Pericyte-EC crosstalk occurs through soluble factors as well as direct contact between these two cell types via membrane invaginations extending from the pericyte into EC vaginations ("peg and socket" connections) (Diaz-Flores et al., 1991) (Figure 1.4). These membrane invaginations might contain tight junction- and gap junction-like structures as suggested by a study using human brain sections and electron microscopy (Cuevas et al., 1984), or with freeze fracture replicas of human brain ECs and pericytes *in vitro (*Larson et al., 1987*)*. In addition, electron microscopic studies have described adhesion plaques between ECs and pericytes (Courtoy and Boyles, 1983). These connection points provide mechanical linkage via endothelial fibronectin-rich cytoplasmic fibrils that are attached to the plasma membrane of pericytes and opposing ECs. However, the functional evidence for these pericyte-EC interactions *in vivo* is less known.

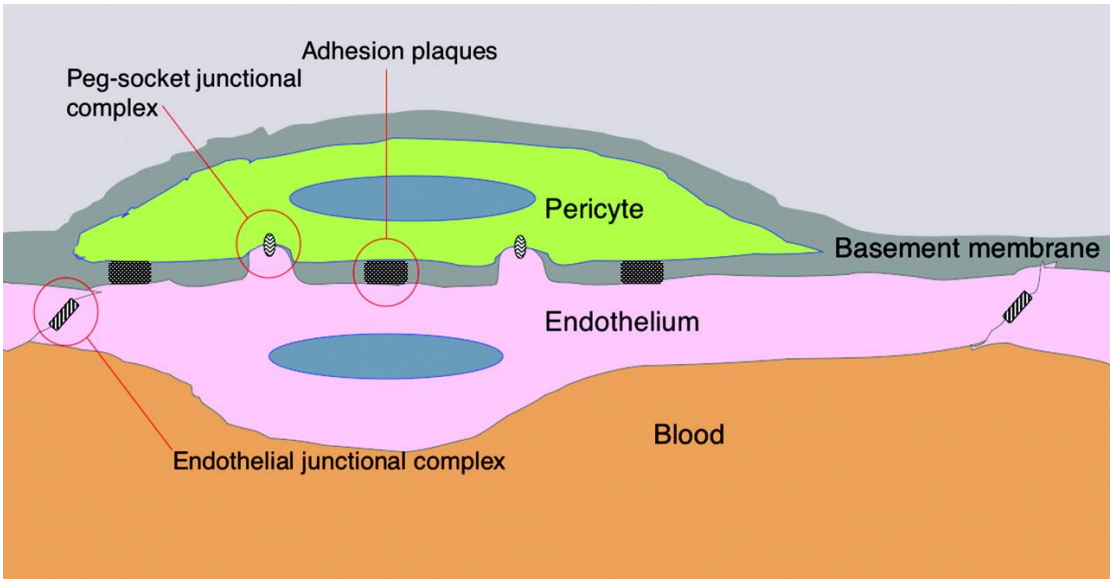

Figure 1.4: Pericyte-EC interactions. Connection points between EC and pericytes include "peg and socket" contacts, representing specific pericyte protrusions into EC invaginations, and adhesive plaques, which often coincide with gaps in the BM. (Figure from *(Armulik et al., 2005)*).

Recent development of genetic mouse models has helped to gain a better understanding into signaling through soluble factors between pericytes and ECs. A principal function of pericytes appears to be during vessel maturation and remodelling by regulating endothelial metabolism, growth and motility through paracrine and juxtacrine signaling. Several mediators have been identified which are involved in pericyte recruitment to the endothelium and vessel stabilization during developmental vasculogenesis or angiogenesis: transforming growth factor (TGF)-β, angiopoietins (Ang) 1 and 2, platelet-derived growth factor (PDGF)-B, stromal-derived factor (SDF)-1α, sphingosine-1-phosphate (S1P) and vascular endothelial growth factor (VEGF) (Armulik et al., 2005). The interplay between these signaling factors is highly complex and most factors involved are pleiotropic with different effects on pericytes and/or ECs. TGF-β initiates the differentiation of precursor cells (undifferentiated mesenchymal cells) into pericytes or vSMCs *in vitro* (Darland and D'Amore, 2001). On the other hand, after recruitment TGF-β suppresses EC proliferation, a process that is dependent on direct contact of the ECs with pericytes (Orlidge and D'Amore, 1986; Orlidge and D'Amore, 1987). Genetic depletion of genes involved in the TGF-β signaling pathways (e.g. *tgfb1*, *alk1*, *alk5* and *tgfbr2*) leads to embryonic lethality with severe vascular defects, similar effects that were also described for knockouts of PDGF-B pathway genes or

ang1 or tie2 null mice (Armulik et al., 2011). Mice deficient for *pdgfb*, *pdgfrb, ang1* or *tie2* genes die prenatally due to mural cell deficiency and consequently vascular dysfunction (Leveen et al., 1994; Soriano, 1994; Patan, 1998; Suri et al., 1996), indicating an important role for pericytes in vascular development and stabilisation. Besides promoting EC differentiation and quiescence, pericyte-EC interactions during pericyte recruitment to newly formed vascular tubes is associated with BM matrix deposition and assembly (Stratman et al., 2009). Both, ECs and pericytes generate components of the vascular BM (Mandarino et al., 1993; Cohen et al., 1980; Hallmann et al., 2005; Stratman et al., 2009) in which they are embedded and which further contributes to the mechanical stability of the vessel.

Pericyte contractility: Role in regulation of blood flow?

Pericytes were first described as contractile cells more than 100 years ago by Rouget in 1873 and Zimmermann in 1923. These mural cells envelope the underlying endothelium with their processes and express contractile microfilaments (e.g. actin and myosin) and intermediate filaments (e.g. desmin and vimentin) (Herman and D'Amore, 1985; Fujimoto and Singer, 1987; Nakano et al., 2000), suggesting a potential role for pericytes in regulation of vascular tone and blood flow. Furthermore, primary bovine retinal pericytes and pericytes of rat brain sections possess receptors for vasoactive factors such as endothelin-1, angiotensin II, prostacyclin, catecholamines and vasopressin (Takahashi et al., 1989; Ferrari-Dileo et al., 1996; van Zwieten et al., 1988). *In vitro* studies using primary rat pericytes demonstrated cell contraction or shape change in response to angiotensin II (Ang II), bradykinin, serotonin, lipopolysaccharide (LPS) and reactive oxygen metabolites (ROMs) (Khoury and Langleben, 1998; Speyer et al., 2000; Murphy and Wagner, 1994; Kerkar et al., 2001). Contractility changes of pericytes were further seen *ex vivo* in brain slices or whole retinas, resulting in pericyte-mediated constriction of capillaries (Peppiatt et al., 2006). An indication for the role of pericyte contraction in regulating capillary blood flow is given by a recent study using brain slices and isolated retinas, and *in vivo* imaging (Yemisci et al., 2009). In this study, oxidative-nitrative stress induced pericyte contraction in a model of ischemia reperfusion injury (I/R), causing capillary constriction and erythrocyte flow obstruction. However, direct evidence of pericyte contraction or indeed regulation of vascular tone and blood flow *in vivo* is limited. A study by Fernandez-Klett et al., recently showed impaired erythrocyte flow caused by pericyte-dependent capillary

constriction *in vivo* using real-time imaging of pericytes in the cerebral cortex of mice (Fernandez-Klett et al., 2010). In contrast to arterioles, however, there was no evidence for capillary-mediated functional hyperemia in this model. In summary, the mechanisms and impact of pericyte contraction are poorly understood at present and this issue was addressed as part of the present project.

Pericytes and the blood-brain barrier (BBB)

The degree of pericyte coverage lies between 10-70% of the vessel area and depends on the organ and vessel-type. Their density and coverage seem to be positively correlated with the endothelial barrier properties in distinct organs. In fact, the highest ratio of pericytes to ECs is found in the central nervous system (CNS) and retina (1:1, 1:3, respectively) as compared to a reported 1:100 in striated muscles (Shepro and Morel, 1993; Dalkara et al., 2011). This is likely due to pericytes having a role in supporting the blood-brain and the blood-retinal barrier where higher levels of barrier function are necessary. Indeed, recent studies have demonstrated a crucial role of pericytes in the maturation and maintenance of the BBB both *in vitro* and *in vivo* (Armulik et al., 2010; Daneman et al., 2010; Dohgu et al., 2005; Nakagawa et al., 2007; Bell et al., 2010). In this context, pericytes negatively regulate both paracellular and transcellular permeability via the establishment and tightening of BBB-specific intercellular junctions as shown in *in vitro* models of the BBB (Dohgu et al., 2005; Nakagawa et al., 2007; Al et al., 2011) and by inhibiting EC transcytosis *in vivo* by a yet unknown mechanism (Armulik et al., 2010; Daneman et al., 2010).

Further functions of pericytes

Pericytes are considered to possess multipotent stem and/or progenitor cell properties similar to mesenchymal stem cells, adipocyte progenitors, muscle stem cells and even neural stem cells. In fact, pericytes isolated from multiple tissues (e.g. skeletal muscle, pancreas, retina and adipose tissue) exhibit multilineage progenitor properties and are able to differentiate into osteocytes, adipocytes, macrophages/dentritic cells (DCs), ECs, vSMCs, skeletal muscle, neural cells and chondrocytes (Diaz-Flores et al., 1992; Doherty et al., 1998; Farrington-Rock et al., 2004; Schor et al., 1990; Crisan et al., 2008; Cai et al., 2009; Dore-Duffy et al.,

2006). The capability of pericytes to differentiate into several cell types harbours their potential use in regenerative medicine in the future, however, a closer identification and function of these cells *in vivo* is required.

Recent studies have indicated that pericytes are much more heterogeneous within tissues and across different tissue beds (specialised pericytes e.g. in glomeruli, brain, retina, liver) than previously believed. Besides the specialised pericytes of the CNS regulating BBB functions, hepatic stellate cells (also called Itoh cells) are considered as specialised pericytes in the liver with a role in hepatocyte proliferation and liver regeneration (Sato et al., 2003). In addition, pericytes in the kidney (also known as mesangial cells) are important for blood ultrafiltration by branching or splitting glomerular capillaries and thereby increasing capillary surface area (Betsholtz, 2004).

In conclusion, the heterogeneous morphology and similarity of pericytes to other cell types led to misinterpretation of results in the past and has hampered the study of pericytes in general. Thus, pericyte functions are still poorly understood.

1.2.3 Pericytes and disease

Loss of pericytes or disrupted pericyte functions are associated with several pathologies including diabetic retinopathy, multiple sclerosis, tumour angiogenesis, calcification of vascular tissue, central nervous system dementia and hypertension (Wallow et al., 1993; Verbeek et al., 1999; Yamagishi et al., 1999; Collett and Canfield, 2005; Sima et al., 1985; Morikawa et al., 2002a). These pathologies often go along with changes in pericyte morphology, decreased pericyte/EC interactions and increased vessel permeability. Diabetic retinopathy for example is associated with apoptosis of retinal capillary pericytes, leading to decreased capillary tone, dilatation and in turn the formation of micro-aneurysms (Sima et al., 1985; Barber et al., 2011). By supporting angiogenesis and stabilising the tumour neovasculature, there is currently much interest in the role of pericytes in tumour development. Similar to physiological angiogenesis, PDGFR-B/PDGFR-β signalling appears to recruit pericytes to tumour blood vessels (Abramsson et al., 2002; Furuhashi et al., 2004). However, compared to healthy tissue, pericyte recruitment occurs to a lesser extent and pericyte-EC contact is diminished with pericyte processes extending away from the endothelium into the tumour parenchyma (Morikawa et al., 2002b).

Defective pericyte coverage and impaired EC-pericyte crosstalk may contribute to the leakiness of tumour vessels (Hobbs et al., 1998; Hashizume et al., 2000). In addition to morphological changes, tumour pericytes exhibit variations in marker expression. The exact cause of the abnormal behaviour of pericyte on tumour vessels, however, is still unknown and variations exist in the involvement of certain pathways between different tumor-types (Nisancioglu et al., 2010; Bergers and Song, 2005). Recent studies have further suggested that pericytes may serve as myofibroblast precursors and as such, to have a potential role in fibrogenesis in several organs, as well as in cystic fibrosis (Fabris and Strazzabosco, 2011; Schrimpf and Duffield, 2011; Wei et al., 2011). Specifically, fibrosis develops under conditions of chronic inflammation and is characterised by excessive deposition of extracellular matrix proteins by myofibroblasts, leading to scar formation and finally organ failure. Similar to tumour pericytes, pericytes involved in fibrosis display changes in marker expression and morphology (Armulik et al., 2011). The exact source of myofibroblast progenitors is currently unknown, but might include several other cells beside pericytes, including resident fibroblasts, epithelial cells, bone marrow-derived cells and ECs.

1.3 Pericytes and inflammation

Pericytes are associated with several diseases characterised by inflammatory components (see previous paragraph). Thus, these mural cells are considered to play a role in inflammation. Inflammation is characterised by the recruitment and migration of leukocytes from the vascular lumen through the vessel wall into the surrounding tissue. Being located at the interface between circulating blood and interstitial tissue, pericytes possess a potential strategic position in the vasculature to regulate immunological responses. In the following sections an introduction into the general aspects of inflammation is given in order to give an entry into the possible roles of pericytes in this process.

1.3.1 Inflammation and immunity

Inflammation is part of a multi-cellular response in host defence initiated by invasion of pathogens such as viruses, bacteria, fungi or parasites and/or cell damage. It serves as a protective mechanism to overcome the initial cause of infection or injury

by eliminating these harmful stimuli, and promoting tissue repair (Serhan et al., 2008). Inflammatory responses occur in vascularised tissue and are defined by the activation and transmigration of leukocytes, and plasma protein efflux to sites of infection or injury. The classical signs of inflammation include *dolor* (pain), *calor* (heat), *rubor* (redness), *tumor* (swelling) and *functio laesa* (loss of function) (Majno and Joris, 2004). These symptoms are largely induced by the effects of inflammatory mediators on local blood vessels. Redness and heat develop due to increased blood flow; swelling is caused by increased vascular permeability that allows leakage of plasma fluid (exudates) and pain is caused by the release of chemicals that stimulate local sensory nerve endings. However, if uncontrolled, all these symptoms can also eventually lead to loss of organ/tissue function.

Immunity is also known as host defence, which in higher developed organisms involves both, non-specific (innate immunity) and specific components (adaptive immunity). The non-specific or innate immunity is the first line of the body's defence mechanism, representing the natural resistance defence response and has a vital role in initiating subsequent adaptive immune responses (Abbas A and Lichtman A, 2005). It consists of physical and chemical components (such as ECs and antimicrobial factors presented on their surface), phagocytic leukocytes (such as neutrophils, monocytes and macrophages) and soluble proteins (e.g. components of the complement system, chemokines and cytokines). Resident cells (e.g. tissue macrophages, dentritic cells and mast cells) mediate the earliest steps of inflammation (Figure 1.5). They express surface and intracellular pattern recognition receptors (PRR) such as toll-like receptors (TLRs) (Takeuchi and Akira, 2010) through which they are able to recognise broad structures of potentially harmful material released by invading microorganisms (pathogen-associated molecular patterns; PAMPs) or damaged cells (damage-associated molecular patterns; DAMPs) (Bianchi, 2007). Following activation, resident cells release pro-inflammatory mediators such as cytokines (e.g. tumour necrosis factor α (TNF) and interleukin-1β (IL-1β)), chemokines (e.g. macrophage chemotactic protein-1 (MCP-1/CCL2) and macrophage inflammatory protein-2 (MIP-2/CXCL2) and other chemoattractants (e.g. leukotriene B_4 (LTB_4)) to indicate the site of infection (Bianchi, 2007; McDonald et al., 2010; Sadik et al., 2011). These mediators trigger a cascade of events leading to a transient vasoconstriction of arterioles and consequently increase in blood flow, increased permeability of the microvasculature to protein-rich plasma and transmigration of leukocytes. These events can collectively lead to the triggering of the infection being resolved or confined.

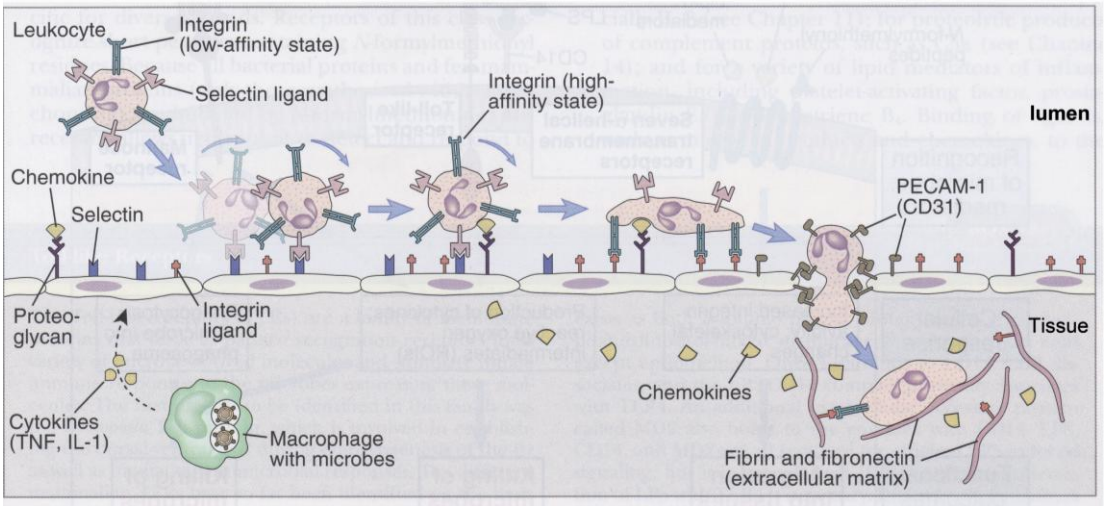

Figure 1.5: Leukocyte Recruitment. During inflammation, tissue macrophages recognise and phagocytose pathogens such as microbes and release pro-inflammatory mediators (e.g. TNF and IL-1β), that act on local ECs as well as circulating leukocytes. Following upregulation of adhesion molecules (e.g. selectins and ligands for integrins) on ECs and generation of chemokines, leukocyte capturing and rolling is initiated. Arrest and firm adhesion of chemokine-activated leukocytes is mediated by integrins, which switch from a low affinity state to a high-affinity state. After adhesion strengthening, leukocytes crawl along the EC layer to preferred sites, where they finally transmigrate through the vessel wall. This process is known as the leukocyte adhesion cascade. (Figure modified from (Abbas A and Lichtman A, 2005)).

Neutrophils are the most abundant type of leukocytes in human blood (40-60%) and are the first cells to be recruited to the tissue. Their main roles are to phagocytose and finally destroy pathogens. During inflammation, neutrophils mobilise from the bone marrow, resulting in neutrophilia and ensuring sufficient supply during tissue inflammation (Phillipson and Kubes, 2011). Like macrophages, neutrophils express surface receptors for common bacterial components and are able to engulf and phagocytose microorganisms and cellular debris (Finlay and Hancock, 2004). When activated, neutrophils themselves release numerous factors such as granular anti-microbial substances and degrading proteases as well as oxygen-derived free radicals that can be cytotoxic for both pathogens and host tissue (Finlay and Hancock, 2004). Thus, excessive and uncontrolled neutrophil activation may lead to injury of host cells and vascular and/or tissue damage.

Furthermore, neutrophils generate and secrete pro-inflammatory cytokines and chemokines that can in turn amplify inflammatory reactions via recruitment and/or activation of other cell types. Neutrophil influx in acute inflammation is commonly

followed by an influx of monocytes that mature into macrophages and help in the clearing the infections via phagocytosis of pathogens (Finlay and Hancock, 2004). In conditions where pathogens are able to resist innate immunity, priming of the adaptive immune response, which initiates the slower but highly specific immune response, is critical (Abbas A and Lichtman A, 2005). In contrast to innate immune cells, cells of the adaptive immunity (B- and T-lymphocytes) target highly specific structures of microbial molecules (antigens) and develop memory to specific pathogens. Following pathogen elimination, in the final resolving phase of inflammation, repair mechanisms are activated promoting tissue healing (e.g. by promoting fibroblast growth and adherence) (Finlay and Hancock, 2004).

Inflammation can be acute - lasting for a short period of time (minutes to days) - or chronic (lasting days to years). Whereas acute inflammatory responses are transient and generally involve neutrophils and plasma exudation, chronic inflammation occurs when the inflammatory insult/trigger is persistent (e.g. during autoimmune diseases) and involves primarily macrophages/monocytes and lymphocytes. Collectively, immunity is a highly regulated and carefully balanced process. Disruption of regulatory mechanisms can lead to chronic inflammation and severe pathological conditions such as rheumatoid arthritis (RA), atherosclerosis and asthma. Therefore, understanding the intricacies of the immune system - especially the mechanisms mediating leukocyte recruitment - is key to the development of novel anti-inflammatory therapies.

1.3.2 The leukocyte adhesion cascade

During inflammation, leukocytes have to breach the vessel wall, which forms a complex physical barrier of cellular (the endothelium and the pericyte sheath) and non-cellular components (vascular BM) between the blood and the extravascular tissue (Nourshargh et al., 2010). Extensive studies and development of advanced microscopy techniques over the last decades have considerably extended our knowledge of the mechanisms of leukocyte transmigration. Transmigration of inflammatory cells largely occurs within postcapillary venules and involves penetration of the endothelium as a first barrier. ECs form a confluent monolayer of cobble-stone shaped cells (10-15 µm wide and 25-40 µm long) lining the vascular lumen. It is now well established that leukocyte transendothelial migration is driven

by specific interactions between adhesion molecules on immune cells and ECs (Ley et al., 2007) (Figure 1.6). The sequence of cellular and molecular responses involved in this process is commonly known as the leukocyte adhesion cascade which involves multifactorial and complex steps: capture of circulating leukocytes, rolling of these cells on the luminal side of the endothelium, followed by slow rolling and arrest, adhesion strengthening, intraluminal crawling and paracellular and transcellular migration through the endothelium.

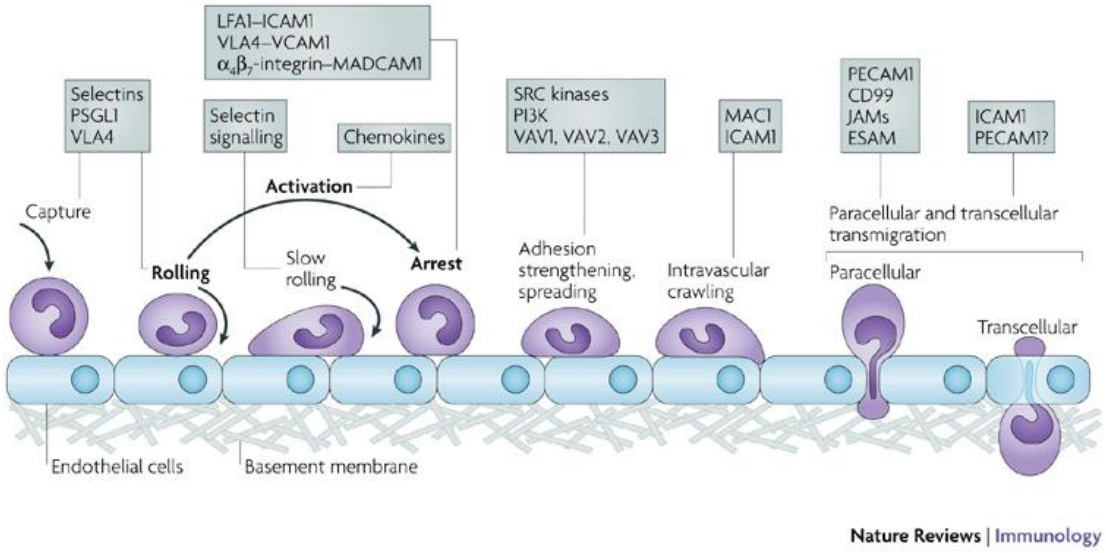

Figure 1.6: The leukocyte adhesion cascade. Initially, the leukocyte adhesion cascade was divided into three steps: rolling (mediated by selectins), activation (mediated by chemokines) and arrest/firm adhesion of leukocytes (mediated by integrins). These original steps are shown in bold. Recent insight into the mechanism of leukocyte transendothelial migration has identified additional steps such as slow rolling, adhesion strengthening, intraluminal crawling and transcellular migration through the endothelium. Selectin signalling initiates the transition from rolling into slow rolling and eventually adhesion and cell spreading. Intravascular crawling of leukocytes to preferred sites of transmigration occurs via adhesion molecules such as macrophage antigen-1 (Mac-1) and intercellular adhesion molecule -1 (ICAM-1). Final transmigration through the endothelium involves molecules such as PECAM-1, junctional adhesion molecules (JAMs), cellular adhesion molecules (CAMs) and CD99. (Figure from *(Ley et al., 2007)*).

Leukocyte capture and rolling

Pro-inflammatory mediators released by resident cells act transiently by binding to specific high-affinity receptors on their target cell such as leukocytes and ECs. Activation of the endothelium results in the upregulation and/or redistribution of adhesion molecules (such as selectins) (Nourshargh et al., 2010). Selectin expression (E-selectin and P-selectin) on ECs initiates leukocyte capture (also called tethering) through binding to leukocytic P-selectin glycoprotein ligand-1 (PSGL-1), E-selectin ligand-1 (ESL-1), CD44 and other glycosylated ligands (Kansas, 1996; Vestweber and Blanks, 1999). To date three selectins have been described in the literature: E-selectin, which is specifically expressed by inflamed ECs, L-selectin, found on most leukocytes and P-selectin which is expressed on ECs and activated platelets (Ley et al., 2007). Selectin ligands are all fucosylated carbohydrate structures containing sulphated-sialyl-Lewis^x and are expressed on leukocytes (McEver, 2002). Leukocyte binding to selectins further mediates secondary leukocyte tethering, allowing cells that do not express ligands for selectins to get recruited to sites of inflammation (Sperandio et al., 2003).

Leukocyte capture is followed by rolling along the endothelial surface which is enabled by a high on- and off-rate of formed selectin bonds to leukocyte receptors, leading leukocytes to detach from the endothelium and subsequently form new adhesive interactions (Alon et al., 1995). These selectin bonds are so-called catch bonds that rely on high shear rates along the vessel wall and become stronger under conditions of pulling forces, such as shear stress (Finger et al., 1996; Lawrence et al., 1997). Formation of long membrane tethers containing PSGL-1 at discrete sticky patches, so-called “slings”, allow leukocytes to roll along the endothelium at conditions of high shear stress (Sundd et al., 2012). These “slings” are formed at the back of rolling neutrophils and swing to the front of the cells as they roll forward to reattach to the underlying endothelium. Rolling of leukocytes along the luminal side of the vessel wall is prerequisite for the subsequent steps of the leukocyte adhesion cascade as blockade of selectins using antibodies completely abolishes leukocyte adhesion and transmigration (Kanwar et al., 1997). Besides mediating direct interaction between leukocytes and ECs, selectins also provide signalling properties. Selectin-mediated binding triggers signalling events in both leukocytes and ECs which further induces integrin activation and subsequent integrin-mediated firm adhesion (Simon et al., 2000). Selectin engagement can induce phosphoinositide 3-kinase-γ (PI3Kγ) (Puri et al., 2005), spleen tyrosine

kinase (SYK) (Zarbock et al., 2007) and p38 mitogen-activated protein kinase (MAPK)-dependent pathways (Simon et al., 2000), but the precise mechanisms remain unclear.

Leukocyte adhesion, arrest and intravascular crawling to sites of transmigration

Leucocyte activation and arrest is primarily triggered by chemokines (e.g. CXCL1 and CXCL2) that are presented on the abluminal surface of ECs by glycoaminoglycans (GAGs) (Rot, 2010). This leads to the formation of a chemotactic gradient which guides neutrophils through the vasculature to sites of injury (Phillipson and Kubes, 2011). Chemokines and chemoattractants act through specific G-protein-coupled receptors (GPCRs) on leukocytes. Following binding to GPCRs, a complex intracellular signalling network triggers rapid integrin activation by increasing integrin avidity, a mechanism that is referred to as inside-out signalling (Ley et al., 2007).

Integrins are heterodimeric proteins consisting of an α- and a β-subunit and are expressed on the cell surface of leukocytes. Under quiescent conditions, integrins exhibit a non-active conformation associated with low affinity (Kinashi, 2005) (Figure 1.7a). Increase in integrin affinity corresponds to changes of the molecule conformation and signal transduction properties. This leads from a low-affinity state to intermediate affinity and finally high-affinity state that increases their affinity to adhesion molecules on ECs through the opening of the ligand-binding pocket, increased ligand-binding energy and decreased ligand dissociation (Kinashi, 2005). Integrin valency on the other hand is associated with lateral clustering of integrin molecules on the cell surface which allows multivalent interactions with the ligand and therefore increases integrin binding avidity (Figure 1.7b). Activation of integrins thus, induces binding of leukocyte integrins (mainly β_1 and β_2 integrins) to EC adhesion molecules (e.g. intercellular adhesion molecule 1 (ICAM-1) and vascular cell adhesion molecule 1 (VCAM-1)) (Campbell et al., 1996; Campbell et al., 1998; Constantin et al., 2000; Kim et al., 2003; Shamri et al., 2005). This process represents the transition from selectin-mediated rolling to integrin-mediated firm arrest. The main integrins involved in adhesion strengthening and consequently leukocyte arrest are lymphocyte function-associated antigen 1 (LFA-1; also known as $\alpha_L\beta_2$ integrin), macrophage antigen-1 (Mac-1; $\alpha_M\beta_2$) with a high affinity to ICAM-1,

and very late antigen 4 (VLA-4; $\alpha_4\beta_1$ integrin) with a high affinity to its ligand VCAM-1.

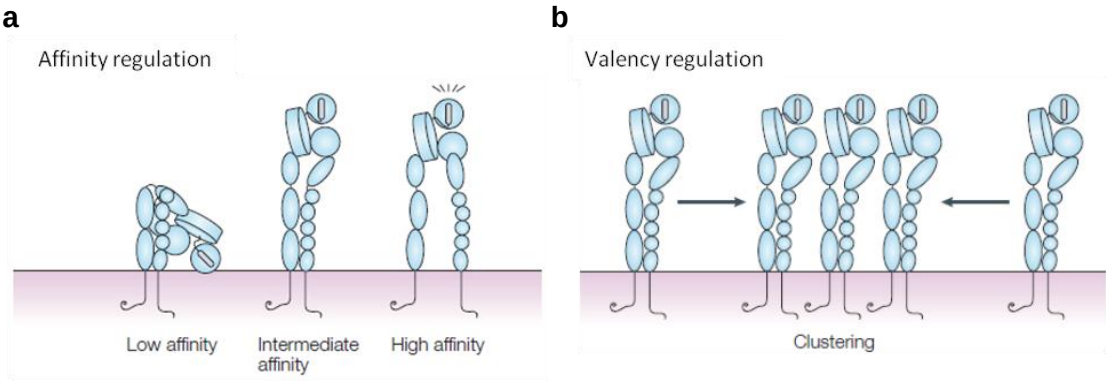

Figure 1.7: Regulation of integrin avidity. Integrin avidity is regulated by their affinity state and valency. **(a)** Integrins (αβ heterodimers) can exhibit three conformational states that are associated with different ligand affinities. In the bent head-piece conformation (left), integrins exhibit low ligand affinity. Conformational changes triggered through inside-out signalling leads to an extension of the head-piece and an increase in ligand affinity (intermediate affinity, middle; high affinity state, right). **(b)** Valency regulation of integrin avidity is described by the clustering of integrins on the cells' surface, which allows multivalent interactions with ligands. (Figure modified from *(Kinashi, 2005)*).

Upon arrest, the cytoskeleton of leukocytes reorganises itself resulting in marked morphological changes from a round, rolling phenotype to a flattened and polarised morphology exhibiting a leading (lamellopodia) and a trailing edge (uropod) (Nourshargh et al., 2010). This process is termed cell spreading and is initiated by outside-in signalling. The induction of F-actin polymerisation at the front and actin-myosin contraction and retraction at the back of the leukocyte allows the cell to crawl intraluminally along a haptotactic gradient of chemoattractants to favoured sites of transmigration (Phillipson et al., 2006; Schenkel et al., 2004). Binding of leukocytic Mac-1 ($\alpha_M\beta_2$ integrin) to endothelial ICAM-1 mediates the extension of leukocyte protrusions into ECs and EC-junctions, which is further associated with EC contraction and opening of interendothelial contacts. Thereby directional crawling might be important for neutrophils and monocytes to enable them to move towards nearby junctions and facilitate subsequent leukocyte transmigration through the endothelium layer (Phillipson et al., 2006; Schenkel et al., 2004).

Leukocyte transendothelial migration (TEM)

Leukocyte migration through the endothelium layer can occur via both paracellular (through endothelial junctions) and to a lesser extent transcellular routes (through the body of the cell) (Ley et al., 2007). To maintain the barrier function of the vessel wall to macromolecules, penetration of leukocytes must occur with minimal disruption of the endothelium. *In vitro* studies have suggested that ECs support leukocyte transmigration via endothelial adhesive platforms (EAP) - acting as pro-adhesive sites - and the formation of docking structures - endothelial projections - around the penetrating leukocyte (Barreiro et al., 2004; Barreiro et al., 2008; Ley and Zhang, 2008; Petri et al., 2011; Carman and Springer, 2004). The formation of these docking structures, which are enriched in ICAM-1 and VCAM-1 might form an air lock type seal around adherent leukocytes and thereby maintain the endothelial barrier function (Phillipson et al., 2008). Furthermore, this encapsulation of the leukocytes might prepare the leukocyte for diapedesis and thus, initiate leukocyte passage through the endothelium. Numerous adhesion molecules, including PECAM-1, ICAM-1, JAM-A, JAM-B, JAM-C, ICAM-2, CD99, CD99L2 and endothelial cell-selective adhesion molecule (ESAM) have been implicated in the response of transendothelial migration (Wegmann et al., 2006; Muller, 2003; Bixel et al., 2007; Thompson et al., 2001; Woodfin et al., 2007; Huang et al., 2006). However, the adhesion molecules involved in diapedesis vary depending on the type of penetrating leukocyte, phase of transmigration and the inflammatory stimulus (Woodfin et al., 2007; Huang et al., 2006; Woodfin et al., 2009; Nourshargh et al., 2006).

Paracellular transmigration - migration of leukocytes through EC junctions appears to be the dominant route. ECs exhibit highly organised molecular complexes that connect adjacent cells. These intercellular junctions are composed of tight junctions (e.g. JAMs and claudins) and adherens junctions (such as VE-Cadherin) (Figure 1.8). Junctional molecules are mostly transmembrane proteins linked to cytoskeletal and intravascular signalling structures. They provide stability of the vessel wall, transfer intracellular signals, and act as paracellular seals controlling vascular permeability to plasma proteins and support controlled passage of circulating cells into the tissue (reviewed in (Dejana et al., 2001)).

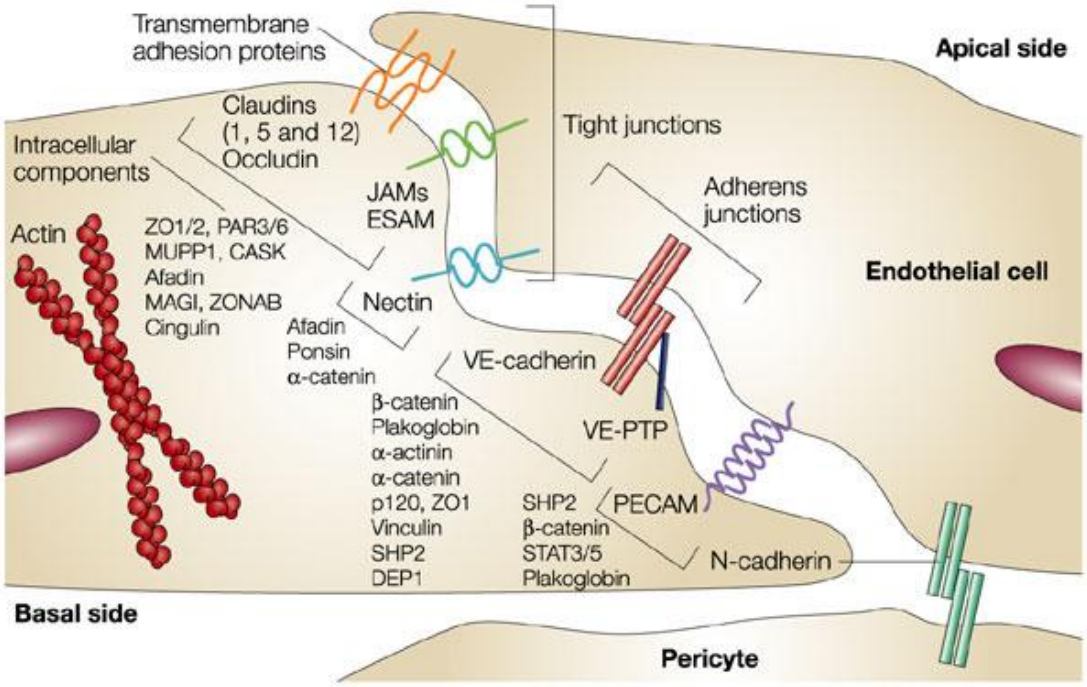

Figure 1.8: Summary of adhesion molecules connecting adjacent ECs. EC-EC junctional molecules include tight junctions and adherens junctions which involve transmembrane proteins (such as JAMs, ESAM, Claudins and VE-Cadherin, respectively) which are linked to cytoskeletal structures and signalling pathways. (Figure from Dejana et *(Dejana, 2004)*).

Paracellular transmigration as a dominant route has been directly demonstrated in genetically modified mice with highly stabilized endothelial junctions (Schulte et al., 2011). Under physiological conditions, junctional molecules that are not directly involved in the migration process themselves (e.g. VE-Cadherin), transiently translocate away from the junctions (Allport et al., 2000; Shaw et al., 2001). The stabilisation of VE-Cadherin in mutant mice led to a resistance to permeability-inducing factors (e.g. VEGF and histamine) due to inhibition of junction dissociation (Schulte et al., 2011). Furthermore, leukocyte transmigration in response to LPS, IL-1β and in a model of immunogen-challenged skin was markedly reduced in this model, indicating the trans-junctional pathway as the main route of leukocyte extravasation. Data from our group suggest that 90% of transmigrating neutrophils use the route through EC junctions as shown in 3 different models of inflammation *in vivo* (inflammation induced by the pro-inflammatory cytokine IL-β, the chemotactic formyl-methionyl-leucyl-phenylalanine (fMLP) and in pathological I/R injury) (Woodfin et al., 2011). Paracellular transmigration is controlled by a well-

coordinated interplay between EC and leukocytic adhesion molecules (Figure 1.9a). Adhesion molecules located within different junctional regions may act at different stages in the process of leukocytes breaching endothelial cell junction (Muller, 2003). In this context, our group recently demonstrated that EC adhesion molecules facilitate leukocyte diapedesis in a sequential manner (Woodfin et al., 2009). Using mice deficient in either ICAM-2, JAM-A or PECAM-1 and IL-1β as a stimulus, ICAM-2 could be identified as an early mediator of leukocyte migration guiding leukocytes to EC junctions, followed by JAM-A, which mediates leukocyte migration through endothelial junctions, with PECAM-1 mediating leukocyte migration through the venular BM. However, this sequential process occurred in a stimulus-specific manner, and in contrast to IL-1β, neutrophil transmigration in response to other inflammatory mediators such as TNF, fMLP or LTB_4 occurred independently of ICAM-2, JAM-A and PECAM-1 (Huang et al., 2006; Nourshargh et al., 2006; Woodfin et al., 2007).

The same adhesion molecules involved in leukocyte migration via the paracellular route are suggested to be involved also in transcellular migration (Feng et al., 1998; Millan et al., 2006; Carman et al., 2007; Marmon et al., 2009a; Marmon et al., 2009b). However, the distinctive mechanisms involved in transcellular migration are not fully understood yet. Transcellular migration is described as the process where leukocytes get engulfed and transported through channels within an endothelial cell (Figure 1.9b). This route of endothelial penetration might be initiated by the formation of leukocyte protrusions that may extend into endothelial invaginations to search for permissive sites (Ley et al., 2007). Interaction of leukocyte protrusions with EC ICAM-1 may lead to the translocation of apical ICAM-1 into vesiculo-vacuolar organelles (VVOs), which might in turn act as a gateway for leukocytes through ECs (Millan et al., 2006). However the physiological relevance of this pathway remains unclear. In mice deficient for CD11b (Mac-1), leukocyte crawling is specifically blocked (Phillipson et al., 2006). In addition, these mice reportedly show a marked increase in incidents of transcellular transmigration through ECs as compared to paracellular transmigration. These findings suggest that blocking migration of leukocytes to preferred junctions may force leukocytes to breach the body of ECs via the transcellular route. Indeed, transcellular leukocyte transmigration appears to predominate in the CNS, where high barrier function is crucial in maintaining the BBB (Engelhardt and Wolburg, 2004).

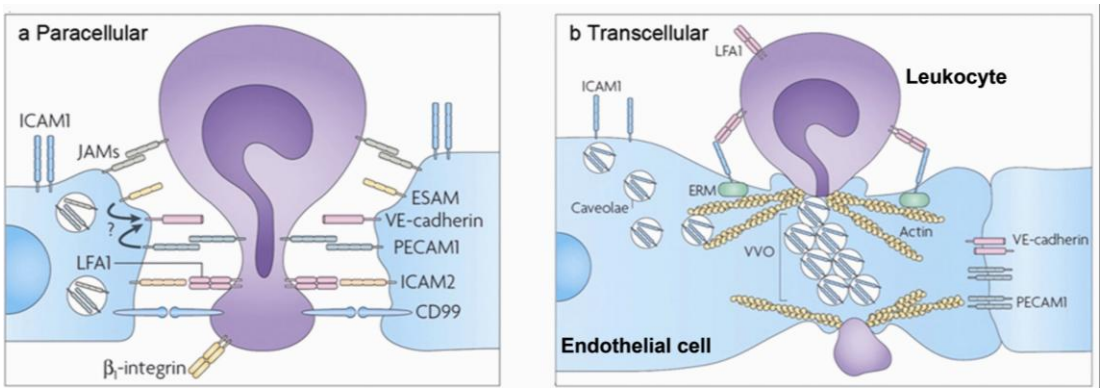

Figure 1.9: Transmigration though the endothelial cell layer. Leukocytes are able to penetrate the endothelial layer through a paracellular or a transcellular route. **(a)** Paracellular migration involves the loosening of interendothelial interactions and migration of leukocytes through these junctions. This process is facilitated by several adhesion molecules, including JAM-A, PECAM-1, ESAM, ICAM-2 and CD99. **(b)** Transcellular migration was shown at thinner and actin-rich areas of endothelial cells through vesiculo-vacuolar organelles (VVOs). These VVOs are formed by ICAM-1-containing calveolae and function as an intracellular "channel" through which leukocytes can migrate. (Figure from (Ley et al., 2007)).

1.3.3 Penetration of the venular BM

After leukocytes breach the endothelium, they then need to cross the vascular BM and the pericytes embedded within it. Whereas penetration of the endothelium can be rapid (within a few minutes), migration through the perivascular BM and pericyte sheath to the interstitial tissue takes much longer (~30 minutes) (Woodfin et al., 2011; Ley et al., 2007). The venular BM is a dense layer (50-300 nm thick) with a pore size of ~50 nm. It consists of a complex network of macromolecules such as proteins, glycoproteins and proteoglycans (Rowe and Weiss, 2008). Predominant components of venular BM involve filamentary proteins such as laminins and collagens interconnected to themselves and other extracellular matrix proteins (Figure 1.10). Both proteins are heterotrimeric glycoproteins composed of several chains, creating distinct isoforms. Laminin α, β and γ chains can form 16 different isoforms. The two main isoforms found in vascular BM are laminin 8 (composed of laminin α4, β1 and γ1 chains; also known as LN-411) and laminin 10 (composed of laminin α5, β1 and γ1 chains; also known as LN-511). Collagen IV is the main collagen type and consists of six different α chains and exists in three different isoforms (Rowe and Weiss, 2008). Different components of the BM are proposed to have biophysically and biochemically different properties to transmigrating leukocytes. As such the degree of covalently cross-linked collagen IV oligomers and

laminin networks might regulate penetration of the BM.(Rowe and Weiss, 2008) In addition, laminin 511 has been suggested to be anti-migratory, whereas laminin 411 is proposed to promote migration as shown in studies analysing neutrophil (Wondimu et al., 2004a) and T-cell migration (Wu et al., 2009). Besides adhesive support for transmigrating leukocytes, the venular BM acts as a depot for matrix-bound regulatory proteins (e.g. growth factors, enzymes, chemokines and thrombotic factors) that might further regulate migration of leukocytes through this structure (Rowe and Weiss, 2008).

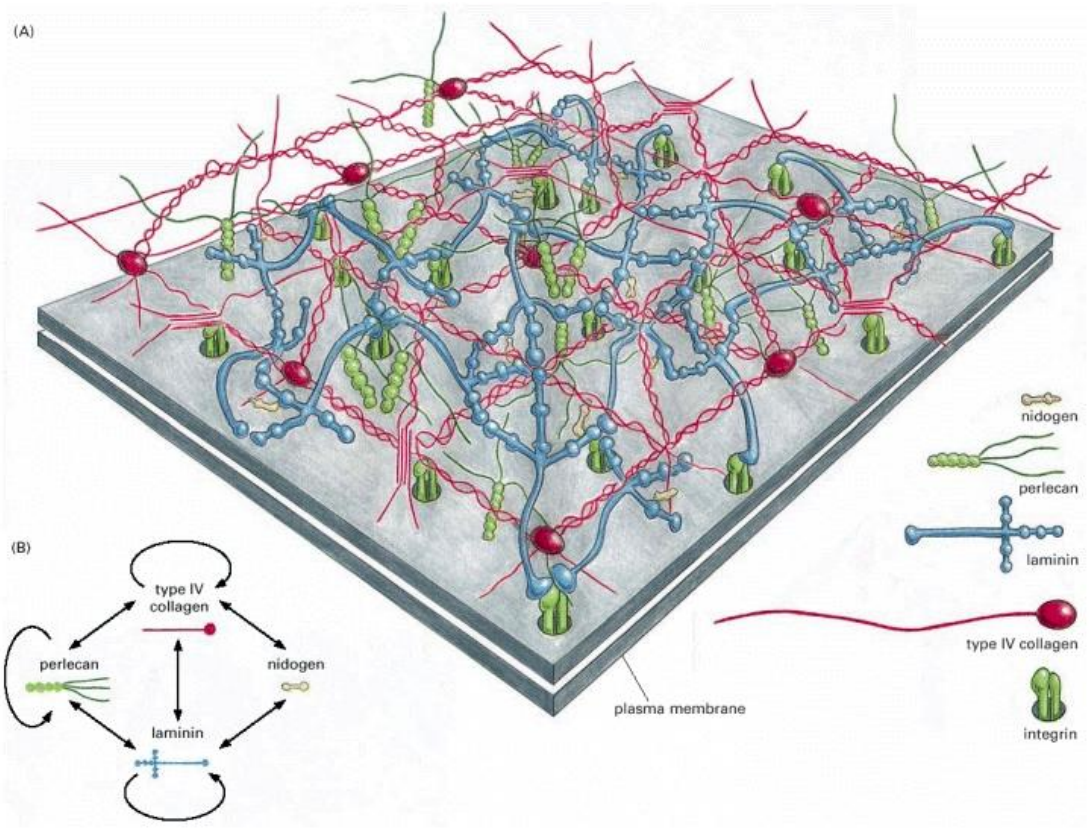

Figure 1.10: Molecular structure and components of basement membranes. Basement membranes are composed of complex network of laminins, collagen and other glycoproteins such as perlecans and nidogens, connected through specific interactions (A). Collagen IV, laminins and perlecans can bind to themselves and can also assembly with other extracellular matrix proteins, whereas nidogens only bind to collagen IV and laminin as indicated by arrows (B). (Figure from *(Alberts B et al., 2002)*).

There is evidence that leukocyte-EC interaction during TEM triggers signals involved in subsequent migration through the BM. This includes phenotypic changes in leukocytes such as upregulation of molecules that are needed for the latter step of breaching the BM (Dangerfield et al., 2002) (Figure 1.11). PECAM-1 has been shown to mediate the expression of members of the β_1-, β_2-, and β_3 integrin families (Newman and Newman, 2003), which might support the passage of leukocytes through the BM by acting as interaction partners for components of the BM. Indeed, PECAM-1-mediated mobilisation of $\alpha_6\beta_1$-integrin (VLA-6; receptor for laminin) from intracellular stores to the cell surface of transmigrating neutrophils allows neutrophils to interact with extracellular matrix in IL-1β-induced inflammation in murine models (Dangerfield et al., 2005; Dangerfield et al., 2002). These molecular interactions, however, are stimulus-dependent (they were not involved in TNF-induced inflammation), indicating the existence of other additional pathways of leukocyte extravasation.

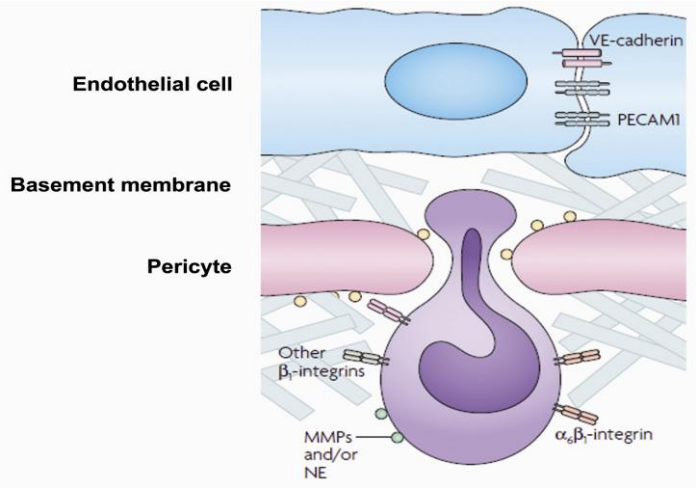

Figure 1.11: Transmigration through BM and the pericyte sheath. Leukocyte migration through the pericyte sheath and vascular BM might be mediated by a chemokine gradient and under certain inflammatory conditions can occur in a β_1-integrin- and protease-dependent manner.(Figure from *(Ley et al., 2007)*).

Leukocyte transmigration through the vascular BM is associated with a transient increase in vascular permeability to macromolecules and reduced barrier function of the BM *in vitro* and *in vivo* (Hurley J.V., 1964; Huber and Weiss, 1989b). Our group recently identified the presence of matrix protein low expression regions (LER) within the BM, sites that are co-localised with gaps between adjacent pericytes (Wang et al., 2006). LERs are defined as areas within the venular BM with lower expression of certain matrix proteins (e.g. collagen type IV, laminin-8, laminin-10, nidogen, but not perlecan) than the average venular level. Although both neutrophils and monocytes have been shown to use these regions to breach the BM, the mechanisms involved seem to differ between the two leukocyte subsets (Voisin et al., 2009). Whereas monocytes squeeze through LERs, neutrophil transmigration through this layer is associated with BM remodelling. During neutrophil transmigration LERs undergo a transient enlargement and decrease in protein content in numerous inflammatory conditions, such as cytokine-, and chemoattractant-induced inflammation and pathological conditions such as I/R injury (Reichel et al., 2008; Reichel et al., 2009; Reichel et al., 2011; Voisin et al., 2009; Voisin et al., 2010; Wang et al., 2006). These regions provide higher permissiveness due to lower protein densities within the extracellular matrix. It is hypothesised that reduced barrier function for leukocytes and at the same time increased permeability to chemoattractants might facilitate leukocyte migration into the interstitial tissue via permissive sites. The underlying mechanism in this transient loss of BM integrity remains unclear. Several *in vitro* and *in vivo* studies suggest a role for proteases (such as matrix metallo proteinases (MMPs) or neutrophil elastase (NE)) in remodelling of BM proteins (Delclaux et al., 1996; Okada et al., 1997) (Voisin et al., 2009). Indeed, transendothelial migration of neutrophils triggers the release of proteases that are stored in intracellular granules and expressed on the surface of leukocytes (Cepinskas et al., 1999; Wang et al., 2005). The hypothesis of subtle disassembly of the BM during leukocyte penetration is further supported by a study from our group, showing fragments of BM (laminin) on the surface of tissue-extravasated neutrophils (Voisin et al., 2009). It is also possible that proteases act as supportive instruments by exposing potential interaction sites for leukocytes or activate chemotactic stimuli within the extracellular matrix (Adair-Kirk et al., 2003; Mydel et al., 2008). However, the involvement of proteases in the process of neutrophil breaching of the BM is controversial (Huber and Weiss, 1989c) and does not seem to be necessary for all leukocyte sub-types (Voisin et al., 2009). Collectively, the precise mechanism of how leukocytes penetrate this tightly packed structure is still under investigation.

1.3.4 Breaching the pericyte layer and potential roles of pericytes during inflammation

In recent years, more insight has been gained into how leukocytes interact with and transmigrate though the EC layer (Ley et al., 2007; Muller, 2009), however, the latter step of leukocyte transmigration - penetrating the pericyte sheath - has been largely neglected and little is known about the role of pericytes during inflammation. This is largely due to difficulties in isolating primary pericytes and their heterogeneous morphology and phenotype *in vivo*.

Following transendothelial migration, leukocytes migrate below the endothelial layer before finally breaching the pericyte sheath. Since LERs are closely associated with gaps between adjacent pericytes we hypothesised that these gaps could be preferred sites of leukocyte emigration through this cellular barrier and that pericytes actively facilitate leukocyte transmigration. This possibility is supported by data from our group (Voisin et al., 2009; Voisin et al., 2010; Wang et al., 2006). Although transcellular pericyte breaching of neutrophils through guinea-pig skin venules in response to fMLP was reported previously as quantified by electron microscopy (Feng et al., 1998), our group has recently shown that neutrophils primarily breach the pericyte layer in mouse cremasteric venules in response to TNF and IL-1β via the paracellular route (Proebstl et al., 2012; Wang et al., 2006; Wang et al., 2012). This suggests tissue- and/or stimulus-specific mechanisms for leukocyte breaching of the pericyte sheath.

Although relatively little is known about the biological activities of pericytes during inflammation, intriguing evidence exist that pericytes are immunoactive and thus, able to modulate inflammatory events. In this context, the ability of pericytes to produce a number of immunoregulatory cytokines, including IL-1β, IL-6, granulocyte-macrophage colony-stimulatory factor (GM-CSF) and TNF has been shown in numerous *in vitro* studies using primary pericytes from several tissues and species (e.g. human, rat and mouse brains, bovine retinas and rat lungs) (Alcendor et al., 2012; Kovac et al., 2011; Kowluru et al., 2010; Fabry et al., 1993; Edelman et al., 2007). Primary pericytes isolated from rat brain or human placenta were further demonstrated to express adhesion molecules such as ICAM-1 and VCAM-1, and major histocompatibility complex (MHC) class I and II molecules on their surface that can be regulated by inflammatory mediators and through which they might interact with immune cells (Balabanov et al., 1999; Maier and Pober, 2011). MHC molecule expression suggests potential antigen-presenting functions for

lymphocytes. Reports have indeed implicated a role for pericytes in T cell exit from the thymus (Zachariah and Cyster, 2010) and in neuroinflammatory processes *in vitro* (Balabanov et al., 1999; Verbeek et al., 1995). In another study, T-cell responses were negatively regulated by human placental pericytes *in vitro* (Maier and Pober, 2011), results that might demonstrate the heterogeneous nature of pericytes in different organs.

More recently, direct interaction of pericytes with cells of the innate immune system (neutrophils and monocytes) and the potential role of pericytes in facilitating transmigration of these cells has been demonstrated *in vivo* (Proebstl et al., 2012; Stark et al., 2013). Using a genetically modified mouse with fluorescent αSMA-positive cells (pericytes and vSMCs) and myeloid leukocytes (e.g. neutrophils), together with intravital confocal microscopy our group was able to analyse pericyte-leukocyte interactions during inflammation in real time *in vivo* (Proebstl et al., 2012). In this study, neutrophils crawled along pericyte processes for approximately 20 min and a distance of ~60 µm before exiting the vessel wall through specific gaps between adjacent pericytes.

ICAM-1 (on pericytes) has been suggested to play a role in this abluminal crawling binding to Mac-1 and LFA-1 on neutrophils in TNF- and IL-1β-induced inflammation. Furthermore, it was shown that pericyte gaps transiently enlarge in response to these pro-inflammatory cytokines (Proebstl et al., 2012; Voisin et al., 2010; Wang et al., 2006) and that neutrophils preferentially employ enlarged pericyte gaps for transmigration. In another study by Wang et al using the mouse cremaster muscle model and primary mouse retina pericytes *in vitro*, TNF- and IL-1β-induced pericyte gap opening was associated with direct pericyte-neutrophil contact (Wang et al., 2012). In this context, neutrophil engagement with primary pericytes *in vitro* induced pericyte relaxation by inhibition of the RhoA/ Rho Kinase ROCK signalling pathway and suppression of actomyosin-based contractility. Inducing cell relaxation *in vivo* by topical application of Tolazoline increased the number of extravasated neutrophils in the murine cremaster muscle, suggesting a supportive role for pericyte gap enlargement in leukocyte transmigration. However, these results are discordant with data obtained from our group where pericyte gaps enlarged even in the absence of neutrophils (using neutrophil-depleted mice) in response to both TNF and IL-1β (Proebstl et al., 2012). Furthermore, Tolazoline applied topically to the tissue affects every tissue cell type and thus, the combined response of all cells might influence leukocyte transmigration, rather than pericyte relaxation on its own.

Hence, the underlying mechanisms of pericyte gap opening and its relevance during different inflammatory reactions is unclear, issues that have been addressed as part of this project.

In addition to facilitating neutrophil transmigration through the pericyte sheath, a distinct population of capillary and arteriolar pericytes (NG-2^{+}) facilitate leukocyte migration within the interstitial tissue to the site of inflammation (Stark et al., 2013). Stark et al. found that human placental pericytes are able to sense DAMPs through PRRs expressed on their surface (including TLR2, TLR4, NLR family, pyrin-containing domain 3 (NLRP3) and N-formyl peptide receptor 2 (FPR2)). When treated with TNF or PRP ligands, ICAM-1 and chemoattractants (CXCL1, CXCL8, macrophage inhibitory factor (MIF), CCL2 and IL-6) became upregulated on these cells, suggesting a role for pericytes in leukocyte attraction. Indeed, in a model of sterile skin injury in the mouse ear *in vivo*, after extravasation from the blood, neutrophils and macrophages showed fast directional migration along capillary and arteriolar pericytes toward the site of inflammation. This event was mediated by pericyte-expressed ICAM-1 and MIF as showed by blocking antibodies against ICAM-1 and a locally introduced MIF inhibitor. Collectively, this study provides evidence for the ability of capillary and arteriolar pericytes to facilitate efficient target finding by leukocytes within the interstitial space and hence, suggests distinct roles for different pericyte subsets.

Collectively, these studies strongly suggest an active role for pericytes in mediating immune modulation and leukocyte transmigration during inflammation. Specifically pericytes might facilitate leukocyte transmigration by secretion and presentation of pro-inflammatory mediators and direct interaction with migrating cells, a topic that is further explored as part of this thesis.

1.4 Aims of this study

To reach the site of infections or injury, leukocytes migrating through venular walls have to penetrate both the endothelial cell layer and the pericyte layer embedded within the BM. A key hypothesis of this study was that pericytes are able to actively participate in the regulation of the inflammation process via direct interaction with leukocytes and its environment, altered morphology and/or regulating the generation of extracellular BM. The present project has addressed several aspects of pericyte biology, collectively aimed at enhancing our understanding of the role of pericytes in inflammation. Specific aims of the project were:

1. **Analysis of expression and regulation of expression of pericyte cell surface molecules capable of supporting an inflammatory response.** To address this objective, the expression of key adhesion molecules on pericyte-like cells (C3H/10T1/2 cells) was characterised *in vitro* under basal and inflammatory conditions using flow cytometry and confocal microscopy. Furthermore the expression of receptors for potent pro-inflammatory cytokines was investigated on primary murine lung pericytes to analyse whether pericytes are able to directly respond to these stimuli.

2. **Investigation of pericyte shape change in response to different inflammatory stimuli**. Leukocytes have previously been shown to preferentially migrate through gaps between adjacent pericytes, gaps that were shown to enlarge in response to TNF and IL-1β. To extend these findings to a wider range of inflammatory mediators, in the present project the impact of multiple chemoattractants (e.g. LTB_4, KC, C5a and fMLP) on pericyte shape change was investigated *in vivo* using confocal microscopy of immunofluorescently labelled murine cremaster muscles.

3. **Analysis of the mechanism of chemoattractant-induced pericyte shape change**. The involvement of neutrophils mediating pericyte gap enlargement in response to neutrophil chemoattractants was analysed in neutrophil-depleted mice. Using antagonists, knockout mice or scavengers of molecules that are vasoactive on perivascular cells, potential secondary mediators involved in chemoattractant-induced pericyte shape change were elucidated *in vivo*.

4. **Analysis of the functional consequence of pericyte shape change during inflammation.** By using confocal microscopy the role of pericyte shape change was investigated in relation to neutrophil transmigration. In addition, an association of BM remodelling to pericyte shape change in inflammation was analysed by elucidating the remodelling and restoration of BM proteins at different stages of inflammatory reactions in parallel with changes in pericyte morphology. As pericytes have been associated with regulating the barrier function of vessel wall to vascular leakage, the role of pericyte shape change in vascular permeability as occurs during inflammation was further analysed. To address this objective, the Miles assay was used and leakage to intravenously injected Evans Blue dye was analysed in response to locally injected chemoattractants.

CHAPTER 2: METHODS AND MATERIALS

2.1 List of reagents

2.1.1 General reagents

Cell culture reagents

Reagent	Details and Source
Dimethyl sulfoxide (DMSO):	Sigma-Aldrich (Poole, Dorset, UK)
Dulbecco's Modified Eagle's Medium (DMEM):	High glucose, GIBCO (Paisley, UK)
Endothelial growth factor (EGF):	Prepotech (London, UK)
Ethylene diamine tetraacetic acid (EDTA):	Sigma-Aldrich (Poole, Dorset, UK)
Fetal bovine serum (FBS):	Gibco (Paisley, UK)
Fibroblast growth factor (FGF):	bFGF, eBioscience (Hatfield, UK)
Hank's Balanced Salt Solution (HBSS):	Gibco (Paisley, UK)
MCDB-131 medium:	Invitrogen (Paisley, UK)
L-Glutamine:	c= 200 mM (100 x), Gibco (Paisley, UK)
Penicillin/Streptomycin:	10 000 units of penicillin and 10 mg/ml streptomycin, Gibco (Paisley, UK)
Phosphate buffered saline (PBS):	1x PBS, pH 7.2, Gibco (Paisley, UK)
Platelet-derived growth factor BB (PDGF-BB):	Peprotech (London, UK)
Trypan blue:	Gibco (Paisley, UK)
Trypsin/EDTA:	1x solution (0.025% Trypsin and 0.01% EDTA, Cascade Biologics, Invitrogen (Paisley, UK)

Anaesthetics

Reagent	Details and Source
Ketamin:	Ketaset® Injection, c= 100 mg/ml, Fort Dodge Animal Health Ltd (Southampton, UK)
Xylazine:	Rompun® 2%, c= 20 mg/ml, Bayer plc. (Newbury, UK)

Enzymes

Reagent	Details and Source
Catalase:	Sigma-Aldrich (Poole, Dorset, UK)
Collagenase II:	Invitrogen (Paisley, UK)
DNAse I:	Sigma-Aldrich (Poole, Dorset, UK)
Myeloperoxidase (MPO):	Sigma-Aldrich (Poole, Dorset, UK)
Proteinase K:	Roche (Burgess Hill, UK)
Superoxide dismutase (SOD):	Sigma-Aldrich (Poole, Dorset, UK)
Trypsin:	Sigma-Aldrich (Poole, Dorset, UK)
TAQ polymerase:	Biotaq DNA polymerase, c= 5u/ µl, Bioline Reagents Ltd. (London, UK)

Other reagents

Reagent	Details and Source
7-Aminoactinomycin D (7-AAD):	Approximately 97%, Sigma (Poole, Dorset, UK)
Actinomycin-D (actD):	From streptomyces species, approximately 97%, Sigma (Poole, Dorset, UK)
Amonium Cloride (NH_4Cl):	Sigma-Aldrich (Poole, Dorset, UK)
Agarose:	Invitrogen (Paisley, UK)
BD Cytofix/Cytoperm™ Kit:	Fixation and permeabilisation kit, BD Biosciences (Oxford, UK)
BD Fc Block™:	Clone 2.4.G2, Pharmingen (Oxford, UK)
Bovine serum albumin (BSA):	New England Biolabs (Hitchin, UK)
Bromophenol Blue:	Sigma-Aldrich (Poole, Dorset, UK)
Deoxynucleotide triphosphates (dNTPs):	Bioline Reagents Ltd. (London, UK)
DNA Ladder:	SmartLadder SF, Eurogentec (Southampton, UK)
Draq5:	Draq5™ nuclear dye, c= 5 mM, Biostatus limited (Shepshed, UK)
Enhanced K-Blue® TMB Substrate:	Oxford Biosystems (Oxford, UK)

Ethanol:	VWR (Soulbury, UK)
Evans Blue dye:	VWR (Soulbury, UK)
Formamide:	VWR (Soulbury, UK)
GelRed:	Biotum, via Cambridge BioScience (Cambridge UK)
Goat serum (GS):	Normal GS, AbD Serotec (Kidlingdon, UK)
Isopropanol:	VWR, (Soulbury, UK)
Magnesium chloride (MgCl2):	Bioline Reagents Ltd. (London, UK)
Molecular biology grade water:	Sigma-Aldrich (Poole, Dorset, UK)
Methanol:	VWR (Soulbury, UK)
Paraformaldehyde (PFA):	VWR (Soulbury, UK)
Rabbit serum (RS):	Normal rabbit serum AbD Serotec (Kidlingdon, UK)
Saline:	Sodium chloride, 0.9% w/v, Baxter Healthcare (Northampton, UK)
Saponin	Sigma-Aldrich (Poole, Dorset, UK)
Sodium Chloride (NaCl):	Fluka BioChemica, Sigma-Aldrich (Poole, Dorset, UK)
Sodium dodecyl sulphate (SDS):	10% SDS solution, Severn Biotech Ltd. (Kidderminister, UK)
Sucrose:	BDH AnalaR®, VWR (Soulbury, UK)
Tris-Acetate-EDTA (TAE) buffer:	UltraPure™ 10x TAE buffer Invitrogen (Paisley, UK)
Tris-HCl:	1 M Tris-HCl solution, pH 8.5, Severn Biotech Ltd. (Kidderminister, UK)
Triton X-100:	Sigma-Aldrich (Poole, Dorset, UK)

2.1.2 List of antibodies

Primary antibodies

Antigen	Details and source
αSMA:	Monoclonal mouse anti-mouse αSMA-Cy3, clone 1A4, Sigma (St. Louis, USA), working conc.: 6.5 µg/ml (confocal microscopy of tissue) Purified monoclonal mouse anti-mouse α-SMA, clone 1A4, Sigma (St. Louis, USA), (directly conjugated to Alexa-488 using the Molecular Probes™ Alexa Fluor® 488 Antibody labelling kit from Invitrogen), working concentration: 10 µg/ml (confocal microscopy of tissue)
CD45:	Monoclonal rat anti-mouse CD45-APC, clone 30-F11, Biolegend. working concentration: 5 µg/ml (confocal microscopy of tissue and flow cytometry)
Collagen type IV:	Purified polyclonal rabbit anti-mouse collagen IV, Abcam (Cambridge UK), working concentration: 5 µg/ml (confocal microscopy)
E-Selectin:	Purified rat anti-mouse E-Selectin, kind gift from Prof. Dorian Haskard (Cardiovascular Sciences, National Heart and Lung Institute, Faculty of Medicine, Hammersmith Campus, Imperial College Academic Health Sciences Centre, Imperial College London, London, UK), working concentration: 2 µg/ml (flow cytometry)
GR-1:	Purified monoclonal rat anti-mouse Ly-6G and Ly-6C (GR1), clone RB6-8C5, BD Pharmingen (Oxford, UK), working concentration: 100 µg/ml or 25 µg/ml (neutrophil depletion), 5 µg/ml (flow cytometry)
ICAM-1:	Purified monoclonal hamster anti-mouse CD54, clone 3E2, BD Pharmingen (Oxford, UK), working concentration: 2 µg/ml (flow cytometry), 5 µg/ml (confocal microscopy of tissue)
ICAM-2:	Purified monoclonal rat anti-mouse CD102, clone 3C4 (mIC2/4), no azide/low endotoxin (NA/LE), BD Pharmingen (Oxford, UK), working concentration: 2 µg/ml (flow cytometry)
IL-1R I:	Purified goat anti-mouse IL-1RI, R&D Systems (Abingdon, UK), working conc.: 10 µg/ml (flow cytometry)
Integrin α_1 (CD49a):	Purified monoclonal Armenian hamster anti-mouse CD49a, clone HMα1, BioLegend (San Diego, USA), working concentration: 1 µg/ml (flow cytometry), 10 µg/ml (confocal microscopy of cultured cells)
Integrin α_2 (CD49b):	Monoclonal Armenian hamster anti-mouse CD49b-PE, clone HMα2, BD Pharmingen (Oxford, UK), working concentration: 1 µg/ml (flow cytometry) Purified monoclonal Armenian hamster anti-mouse CD49b, clone HMα2, BioLegend (San Diego, USA), working concentration: 10 µg/ml (confocal microscopy of cultured cells)

Integrin α_4 (CD49d):	Monoclonal fisher rat anti-mouse CD49d-PE, clone R1-2, BD Pharmingen (Oxford, UK), working concentration: 2 µg/ml (flow cytometry)
Integrin α_5 (CD49e):	Monoclonal Armenian hamster anti-mouse CD49e-PE, clone HMa5-1, eBiosciences (Hatfield, UK), working concentration: 1 µg/ml (flow cytometry) Purified monoclonal Lewis rat anti-mouse CD49e, clone 5H10-27, BD Pharmingen (Oxford, UK), working concentration: 10 µg/ml (confocal microscopy of cultured cells)
Integrin α_6 (CD49f):	Monoclonal rat anti-mouse CD49f-PE, clone GoH3, eBioscience (Hatfield, UK), working concentration: 2 µg/ml (flow cytometry) Monoclonal rat anti-mouse CD49f-A488, clone GoH3, BioLegend (San Diego, USA), working concentration: 10 µg/ml (confocal microscopy of cultured cells)
Integrin β_1 (CD29):	Monoclonal Armenian hamster anti-mouse CD29-PE, clone HMb1-1, BioLegend (San Diego, USA), working concentration: 1 µg/ml (flow cytometry) Purified monoclonal rat anti-mouse CD29, clone MB1.2, Millipore (Watford, UK), working concentration: 10 µg/ml (confocal microscopy of cultured cells)
Integrin β_3 (CD61):	Purified NA/LE monoclonal Armenian hamster anti-mouse CD61, clone 2C9.G2, BD Pharmingen (Oxford, UK), working concentration: 10 µg/ml (flow, cytometry, confocal microscopy of cultured cells)
Integrin β_4 (CD104):	Purified monoclonal fisher rat anti-mouse CD104, clone 346-11A, BD Pharmingen (Oxford, UK), working concentration: 10 µg/ml (flow cytometry)
JAM-A:	Purified monoclonal rat anti-mouse JAM-A, clone BV-II, kind gift from Prof Elisabetta Dejana (Department of Biomolecular Sciences and Biotechnologies, School of Sciences, University of Milan, Italy) generated as previously described (Martin-Padura et al., 1998; Vecchi et al., 1994), working concentration: 2 µg/ml (flow cytometry)
JAM-B:	Purified rat anti-mouse JAM-B, kind gift from Prof Beat Imhof (Department of Pathology and Immunology, Centre Médical Universitaire, Geneva , Switzerland), working concentration: 2 µg/ml (flow cytometry)
JAM-C:	Purified monoclonal rat anti-mouse JAM-C, clone H33, Millipore (Hoddeston Hets, UK), working concentration: 2 µg/ml (flow cytometry)
Laminin:	Purified polyclonal rabbit anti-mouse pan-laminin, Sigma-Aldrich (Poole, Dorset, UK), working concentration: 2.5 µg/ml (confocal microscopy of tissue)
MRP-14:	Purified monoclonal rat anti-mouse MRP-14, clone 2B10, kind gift from Dr. Nancy Hogg (Leukocyte Adhesion Laboratory, Cancer Research UK, London Research Institute, Lincoln's Inn Fields Laboratories, London, UK), working concentration: 7 µg/ml (confocal microscopy of tissue)

NG-2:	Purified polyclonal rabbit anti-mouse NG-2, Chemicon (Billerica, MA 01821, USA), working concentration: 3.3 µg/ml (flow cytometry), 5 µg/ml (confocal microscopy of tissue)
PDGFR-β:	Purified polyclonal goat anti-mouse PDGFR-β, R&D Systems, working concentration: 2 µg/ml (flow cytometry), 5 µg/ml (confocal microscopy of tissue)
PECAM-1 (CD31):	Purified monoclonal rat anti-mouse CD31, clone 390, eBiosciences (Hatfield, UK), (directly conjugated to Alexa-647 using the Molecular Probes™ Alexa Fluor® 647 antibody labelling kit from Invitrogen (Paisley, UK)), working concentration: 2 µg/400 µl saline i.s. (confocal microscopy of tissue)
TNFR I:	Purified goat anti-mouse TNFRI, R&D Systems (Abingdon, UK), working concentration: 10 µg/ml (flow cytometry)
TNFR II:	Purified goat anti-mouse TNFRII, R&D Systems (Abingdon, UK), working concentration: 10 µg/ml (flow cytometry)
Smooth muscle protein α (SM22α):	Purified polyclonal goat anti-mouse SM22α, abcam, working concentration: 5 µg/ml (confocal microscopy of tissue)
Syndecan-2:	Purified polyclonal rabbit anti-mouse Syndecan-2 (M-140), Santa Cruz Biotechnology, Inc. (Santa Cruz, USA), working concentration: 10 µg/ml (flow cytometry)
VCAM-1:	Monoclonal rat anti-mouse CD106-Alexa 647, clone 492 (MVCAM.A), BioLegend (San Diego, USA), working concentration: 5 µg/ml (flow cytometry), 10 µg/ml (confocal microscopy of cultured cells)
VE-Cadherin:	Purified monoclonal rat anti-mouse CD144, clone eBioBV13 (BV13), eBiosciences (Hatfield, UK), working concentration: 2 µg/ml (flow cytometry)

Isotype controls

Isotype	**Details and source**
Armenian hamster IgG_1:	Purified, clone G235-2356, BD Pharmingen (Oxford, UK)
Armenian hamster IgG:	PE-conjugated, clone HTK888, BioLegend (San Diego, USA)
Goat IgGs:	Normal goat IgGs, R&D Systems (Abingdon, UK)
Rabbit IgGs:	Normal rabbit IgGs, Abcam (Cambridge, UK)

Rat IgG_{2a}:	PE-conjugated, clone R35-95, BD Pharmingen (Oxford UK) Purified, clone YTH71.3, AbD Serotec (Kidlingdon, UK) Alexa 647-conjugated, clone RTK2758, BioLegend (San Diego, USA)
Rat IgG_{2b}:	Purified, clone LO-DNP-11, AbD Serotec (Kidlingdon, UK)

Secondary antibodies and streptavidin conjugates

Antigen	**Details and source**
Armenian hamster IgG:	Goat anti-Armenian hamster IgG-biotin, Biolegend (San Diego, USA) Goat anti-Armenian hamster IgG-DyLight 649, BioLegend (San Diego, USA)
Goat IgG:	Rabbit anti-goat IgG-Alexa 488, Invitrogen (Paisley, UK) Rabbit anti-goat IgG-Alexa 633, Invitrogen (Paisley, UK) rabbit anti-goat IgG-Alexa 488, Invitrogen (Paisley, UK)
Rabbit IgG:	Goat anti-rabbit IgG-Alexa 488, Invitrogen (Paisley, UK) Goat anti-rabbit IgG-Alexa 555, Invitrogen (Paisley, UK) Goat anti-rabbit IgG-Alexa 647, Invitrogen (Paisley, UK) Sheep anti-rabbit IgG-PE, AbD Serotec (Kidlingdon, UK)
Rat IgG:	Chicken anti-rat IgG-Alexa 647, Invitrogen (Paisley, UK) Goat anti-rat IgG-Alexa 488, Invitrogen (Paisley, UK)

Biotin-binding protein	**Details and source**
Streptavidin	Streptavidin-Alexa 488, Invitrogen (Paisley, UK)

2.1.3 List of inflammatory stimuli

Stimuli	Details and source
C5a:	Recombinant mouse C5a, Cat. No.: 2150-C5-025/CF, R&D Systems (Abingdon, UK)
CXCL1/keratinocyte-derived chemokine (KC):	Recombinant murine CXCL1, Cat. No.: PMP66, AbD serotec (Kidlington, UK)
Formyl-Methionyl-Leucyl-Phenylalanine (fMLP):	fMLP, Cat. No.: F3506, Sigma (St. Louis, MO, USA)
Interleukin-1β (IL-1β):	Mouse IL-1β, Cat. No.: 401-ML-005/CF, R&D Systems (Abingdon, UK)
Leukotriene B4 (LTB_4):	LTB_4, Cat. No.: 434625, Merck (Hoddeston Hets, UK)
Platelet-activating factor (PAF):	PAF-16, Cat. No.: 511075, Calbiochem, Merck Millipore (Hoddeston Hets, UK)
Tumour necrosis factor-α (TNF-α):	Mouse TNF-α, Cat. No.: 401-ML-010/CF, R&D Systems (Abingdon, UK)

2.2 Cell Culture

2.2.1 Cell lines

The adherent murine fibroblast-like cell line C3H/10T1/2 (clone 8) was obtained from American Type Culture Collection (ATCC; Manassas, USA). These cells were originally isolated from mouse embryos of the C3H strain in 1973 as described by Reznikoff et al. (Reznikoff et al., 1973). In the present study C3H/10T1/2 cells were used due to their pericyte-like properties (Darland and D'Amore, 2001; Hirschi et al., 1998; Proebstl et al., 2012; Walshe et al., 2009).

Culture of C3H/10T1/2 cells

C3H/10T1/2 cells were cultured according to the supplier's protocol. Cells were maintained in DMSO supplemented with 10% heat-inactivated fetal bovine serum (FBS), 2mM L-glutamine, 1% Penicillin (10,000 u/ml)/ Streptomycin (10 mg/ml). Cultured cells were kept in a humidified 5% CO_2 atmosphere at 37°C. C3H/10T1/2 cells were split twice a week when they reached a confluency of about 70 to 80%

and were used for experiments between passage 14 and 20. For harvesting or passaging, the culture medium was aspirated from the cell monolayer. Cells were washed with PBS and detached enzymatically using Trypsin/EDTA (0.025% Trypsin and 0.01% EDTA). 1/6 volume of the cell suspension was then sub-cultured ($5x10^3$ cells per cm^2).

For storage, aliquots of $1x10^6$ cells were suspended in 1 ml DMEM enriched with 20% FBS and 10% DMSO and were frozen at -80°C over night. The following day the vials were transferred into a liquid nitrogen tank.

For usage, cells were thawed at 37°C, suspended in 9 volumes medium and centrifuged at 200 g for 30 min at room temperature. Supernatant was removed and pelleted cells were resuspended in 5 ml medium for further cultivation in 25 cm^2 cell culture flasks. The following day, cells were transferred into 75 cm^2 cell culture flasks.

2.2.2 Isolation and culture of primary murine lung perivascular cells

Isolation of microvascular cells

Cells were isolated from mice expressing green fluorescent protein (GFP) under an αSMA promoter. For this purpose, a slightly modified protocol as described previously for the isolation of perivascular cells from mouse embryos and meninges (Brachvogel et al., 2005) was used. The entire procedure was performed using sterilised instruments (autoclaved and/or sterilisation using 70% ethanol). In adult mice (5-6 weeks old) the lung was removed immediately after euthanizing the animal by cervical dislocation and rinsed with calcium- and magnesium-free PBS. Tissues were mechanically minced into small pieces with a scalpel and digested by incubation in 2 ml collagenase II (200u/ml) in HBSS at 37°C in a shaking bath for 1 h. After initial dissociation, tissues were gently homogenised using successive 5, 1, and 0.2 ml pipettes to loosen microvessel fragments, followed by adding 2% Trypsin/ 100 units DNAse I to the suspension and further incubation at 37°C in a shaking bath for 30 min. To remove undigested tissue and large vessel segments the resulting suspension was subsequently passed through a 100 µm nylon mesh filter and washed with MCDB-131 medium containing 5% FCS. After centrifugation at 300 g for 5 min, the pellet containing microvessel segments and single cells was plated on gelatine-coated (0.05% gelatine) petri dishes in 10 ml proliferation

medium (MCDB131, 5% FCS, 2mM L-glutamine, 1% Penicillin (10 000u/ml)/ Streptomycin (10mg/ml), bFGF (2 ng/ml), PDGF-BB (5 ng/ml), EGF (10 ng/ml); cells obtained from one lung were split onto two 10 cm dishes.

Culture of isolated cells

On the day after cultivation, medium with floating cells (mainly red blood cells) and tissue debris was carefully aspirated and replaced with fresh proliferation medium. Cells were then left undisturbed for 3 days in a humidified 5% CO_2 atmosphere at 37°C to allow cell attachment and pericyte outgrowth. Medium was changed thereafter every second day. Cultures were examined morphologically and by fluorescence for viability and contaminating cell types using an Olympus IX81 motorised inverted microscope (Olympus Medical, Southend-on-Sea, UK). Cells derived from lungs of wild-type mice were used as negative control. Between culture days 5-7, GFP-positive cells started to proliferate and extensive outgrowth of colonies could be observed by microscopy by day 14-20. At this point, ~ $1x10^6$ cells could be obtained from one lung, of which 50 to 70% were positive for αSMA-GFP. From this point, proliferation medium was replaced with MCDB131 medium without growth factors. Cells were split when they reached confluency of about 70-80% and were used for experiments between passages 1 to 5.

Outgrowth cells were characterised for pericyte (αSMA, NG-2 and PDGFR-β), EC (CD31), SMC (SM22α) and leukocyte markers (CD45) as described previously(Maier et al., 2010) using flow cytometry or immunofluorescence staining as described below.

2.2.3 Determination of cell number and viability

Total cell number and viability was assessed by trypan blue exclusion assay. Cells were suspended 1:1 with a 0.4% trypan blue solution. After incubation for 1-3 min at room temperature total cell number and cell viability counts were determined using a Neubauer haematocytometer (VWR International, Leicestershire, UK) as recommended by the manufacturer. Cells that absorbed trypan blue were shown as distinctive blue colour under the microscope and were identified as dead. Whereas

live cells with an intact cell membrane did not take up the stain and were therefore uncoloured.

2.2.4 Cell stimulation with inflammatory mediators

To investigate the cells' responsiveness to proinflammatory cytokines, C3H/10T1/2 cells were seeded in 6-well culture plates at a density of 1 x 10^5 cells/ well maintained in complete medium. The day after cultivation, medium was removed and fresh medium containing the distinct stimulus was added. Cells were treated with either 10 or 100 ng/ml TNFα, 1 or 10 ng/ml IL-1β and stimulated for 4 h at 37°C. Inflammatory stimuli were then removed by washing the cells twice with cold PBS and expression of receptors and adhesion molecules were then analysed via flow cytometry upon staining with specific antibodies (see section 2.2.5).

2.2.5 Analysis of cell surface molecules by flow cytometry

For characterisation of surface expression of immune receptors, adhesion molecules and specific cell markers (for pericytes, ECs, leukocyte) on 10T1/2 cells and/or isolated primary cells a cytometric assay was used as described before (Proebstl et al., 2012). Untreated cells or cells stimulated with different inflammatory mediators were analysed. Cells were harvested with 1 mM EDTA on ice. Subsequently cells were washed twice with ice-cold PBS containing 1% FCS followed by centrifugation for 5 min at 300 g and 4°C. In some experiments murine whole-blood leukocytes isolated by cardiac puncture or via the tail vein were stained. 5×10^5 detached cells or 50 µl whole blood in 10 µl 0.5M EDTA were transferred into 96-well plates. Cells were then incubated in 50 µl 5 µg/ml mouse BD Fc Block™ in PBS/ 1% FCS or the respective serum (25% in PBS/ 1% FCS) for 10 min on ice to block unspecific binding. After the blocking step, 50 µl of primary antibody in PBS/FCS was added. Cells were immunostained for cell-surface receptors (IL-1R I, TNFR I or TNFR II), adhesion molecules (integrin subunits α_1, α_2, α_4, α_5, α_6, β_1, β_3, β_4, JAM-A, JAM-B, JAM-C, ICAM-1, ICAM-2, VCAM-1, E-Selectin, VE-Cadherin or Syndecan-2), pericyte markers (NG-2 or PDGFR-β), for the EC marker CD31 (PECAM-1), leukocyte markers (CD45, Lys6G and Lys6M) or appropriate control antibody (detailed information about antibodies used in this study including concentrations are listed in section 2.1.2). Incubation was performed

for 30 min on ice in the dark. Subsequently stained cells were washed twice with PBS/FCS by centrifugation for 5 min at 300 g. In case of directly conjugated primary antibodies with a fluorochrome, labelled cells were diluted in 300 µl PBS/FCS. If an unconjugated primary antibody was used, cells were further incubated with a fluorescently labelled secondary antibody for 30 min on ice in the dark. Labelled cells were washed twice with PBS/FCS. Red blood cell lysis of whole blood samples was performed following antibody staining. Cells were resuspended in 300 µl ACK lysis buffer (8.024 mg/l NH_4Cl, 1.001 mg/l $KHCO_3$, 3.722 mg/l EDTA, pH 7.3) and incubated at room temperature for 5 min or until solution was clear red. Subsequently cells were pelleted by centrifugation for 5 min at 300 g and 4°C and washed 2 times with PBS/FCS. For flow cytometric analysis, cells were diluted in 300 µl PBS/FCS. To exclude dead cells in the later analysis, 5 µl of 25 µg/ml 7-AAD in PBS was added to all samples.

Samples were acquired on a FACSCalibur flow cytometer (BD Biosciences, Mountain View, CA, USA) using CellQuest acquisition software (BD Biosciences) and analysed using FlowJo software (Tree Star Inc., Ashland, OR, USA). Flow cytometry data are presented as the relative fluorescence intensity (RFI) calculated as the ratio of expression compared to a negative control. Unstained cells and cells incubated with an isotype control antibody were used as negative controls.

2.2.6 Confocal microscopy of immunofluorescently labelled cells

Confocal microscopy of cells was performed in order to analyse the localisation and expression profile of certain molecules expressed by C3H/10T1/2 cells. For this purpose, cells were cultured on 4-well chamber slides at a density of 1.6×10^4 cells/ well in 900 µl complete medium. 24h after culture, cells were washed twice with cold PBS containing 1% FCS. Cells were then fixed and permeabilised with 200 µl/well of fixation/permeabilisation solution (BD Cytofix/Cytoperm^{TM} Kit) for 20 min on ice. Fixed cells were washed twice with BD permeabilisation/washing (perm/wash) buffer and incubated with 200 µl primary antibody in perm/wash buffer for 30 min on ice in the dark. Cells were immunostained for adhesion molecules (integrin subunits α_1, α_5, α_6, β_1 and β_3, and VCAM-1) or appropriate control antibody and the pericyte marker αSMA. After 3 washing steps, if necessary a specific fluorescently labelled secondary antibody (diluted in perm/wash buffer) was applied, as determined by the combination of primary antibody used in the respective experiment. Cells were

incubated for 30 min on ice in the dark followed by 3 washing steps. Cell nuclei were counterstained with Draq5™ (1:1000 in 200 µl perm/wash) for one min and washed again 3 times with perm/wash buffer. Subsequently 200 µl 4% PFA was applied per well to fix the cells for 10 min on ice. Fixed cells were washed 3 times with PBS and mounted with Prolong®Gold antifade reagent at room temperature over night.

Protein expression of immunofluorescently labelled cells seeded on chamber slides was analysed using a Zeiss LSM 5 PASCAL confocal laser-scanning microscope (Carl Zeiss Ltd, Welwyn Garden City, UK) and a 20 x water-dipping Achroplan objective (numerical aperture 0.5 W, PH2), 40 x water-dipping Achroplan objective (numerical aperture 0.8 and resolution 0.37 µm), or a 63 x oil-dipping Plan-APOCHROMAT objective (numerical aperture 1.4, oil). As negative controls, cells were stained using the respective isotype-matched control antibody. The results were corrected for the background readings of the negative control.

2.3 *In vivo* analyses

2.3.1 Mice

C57BL/6 WT mice from either sex were purchased from Harlan–Olac (Bicester, UK).

αSMA-GFP mice were a gift from Prof. Clare Isacke (Breakthrough Breast Cancer Research Centre, The Institute of Cancer Research, London, UK) with authorisation of Prof. Sanai Sato (Department of Medicine, University of Oklahoma, Health Science Center, Oklahoma City, USA). These mice express GFP under the control of the αSMA promoter and have been described elsewhere (Yokota et al., 2006). This mouse strain was backcrossed at least 8 times onto the C57BL/6 background.

Tumour necrosis factor receptor (TNFR) double knockout mice ($TNFR^{-/-}$) lacking both genes *TNFrsf1a* (p55) and *TNFrsf1b* (p75) were purchased from The Jackson Laboratory (stock number: 003243). This strain was generated by intercrossing singly homozygotes for the $TNFrsf1a^{tm1Imx}$ targeted mutation with homozygotes for the $TNFrsf1b^{tm1Imx}$ mutation. Double homozygous mice are viable and fertile. $TNFR^{-/-}$ mice displayed the C57BL/6 background.

Neutrophil-elastase deficient mice ($NE^{-/-}$) were a gift from Prof. Steven Saphiro, MD (Department of Medicine, University of Pittsburgh, Pittsburgh, USA) and were generated by targeted disruption of the NE gene (Belaaouaj et al., 1998). Homozygous mice are viable, fertile and phenotypically normal under physiological (non-inflammatory) conditions. $NE^{-/-}$ mice used were on a C57BL/6 background.

$CX_3CR_1^{GFP/+}$ mice were obtained from the European Mutant Mouse Archive (EMMA, Orleans, France) and generated by targeted gene disruption as previously described (Jung et al., 2000).

All mice were used at an age between 6-12 weeks at an average weight of 25g. As appropriate, age-matched control mice were litter mates or commercially purchased C57BL/6 mice. All experiments were approved by the United Kingdom Home Office according to the Animals Scientific Procedures Act 1986 (ASPA).

2.3.2 Phenotyping and genotyping

Phenotyping of αSMA-GFP mice

To assess the phenotype of αSMA-GFP mice, ear notches were taken using a puncher at weaning age and analysed by fluorescence microscopy. For this purpose, the skin from ear notch samples was carefully separated from cartilage using fine forceps. The subcutaneous tissue was then mounted onto a glass slide and examined using a fluorescence microscope. Animals were considered positive for the GFP transgene, if GFP-positive perivascular cells (PVC) were observed (Figure 2.1).

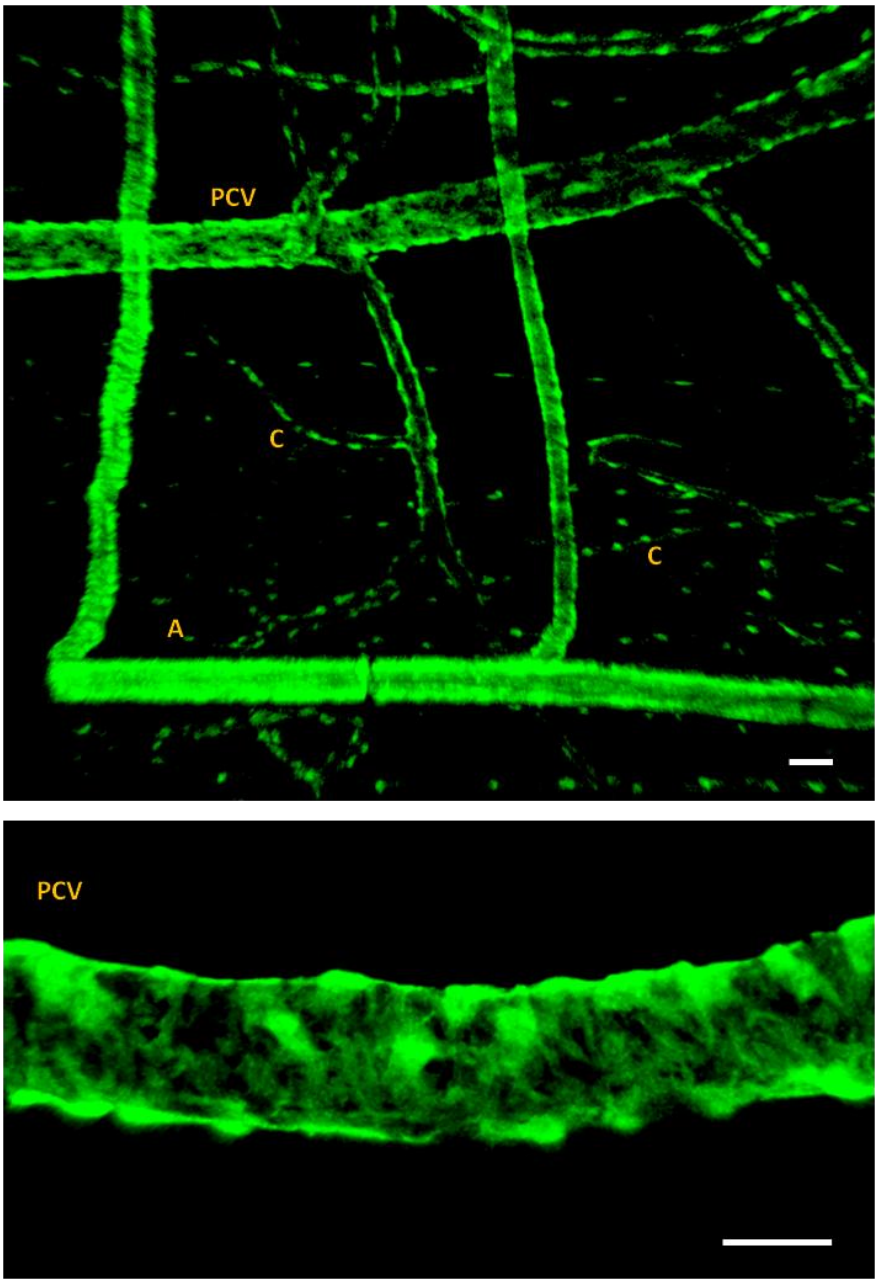

Figure 2.1: Phenotyping of αSMA-GFP mice. Representative 3D-reconstructed confocal images of ear skin from mice expressing GFP under the promoter of αSMA. A, arteriole; C, capillary; PVC, postcapillary venule. Bars, 20 μm.

Genotyping of TNFR double knockout and NE knockout mice

Polymerase chain reaction (PCR) was used to confirm the genotype of $TNFR^{-/-}$ and $NE^{-/-}$ mice used in this study. Ear notch samples or tail biopsies were digested by 4 h incubation in 200 µl lysis buffer (100 mM Tris-HCl, pH8.5; 5 mM EDTA; 0.2% SDS, 200 mM NaCl) containing 10 µg/ml proteinase K at 55°C. To purify the DNA, samples were gently shaken and cooled down for 5 min at room temperature. After 5 min centrifugation at 20,000 g, supernatants were transferred into fresh tubes containing 200 µl isopropanol and mixed well. Subsequently the suspension was centrifuged at 20,000 g for 5 min at room temperature and the resulting supernatant was discarded. 300 µl 70% (v/v) Ethanol was added, followed by centrifugation at 20,000 g for 5 min at room temperature. After removal of supernatants, pellets were air dried for approximately 10 min and resuspended in 50 µl molecular biology grade water. For short-term storage (up to a week) samples were stored at 4°C, or at -20°C if stored for a longer time.

For the PCR, 23 µl mastermix per sample containing distinct primers for each reaction (see Table 2.1) was prepared (Table 2.2, 2.4, 2.3 respectively) and mixed with 2 µl purified DNA. TNFR I (TNFrsf1a) and TNFR II (TNFrsf1b) in TNFR double knockout mice were detected in separate PCRs.

DNA fragments were amplified in a thermal cycler (DNAEngine® Peltier Thermal cycler, Bio-Rad, Hemel Hempstead, UK) using varying reaction times depending on the primers used (Tables 2.3, 2.5, 2.7, respectively).

PCR Primer	Primer sequence
oIMRo834 (TNFR I WT)	5'-GGA TTG TCA CGG TGC CGT TGA AG-3'
oIMRo835 (TNFR I WT)	5'-TGA CAA GGA CAC GGT GTG TGG C-3'
oIMRo836 (mutant)	5'-TGC TGA TGG GGA TAC ATC CAT C-3'
oIMRo837 (mutant)	5'-CCG GTG GAT GTG GAA TGT GTG-3'
oIMRo838 (common)	5'-AGA GCT CCA GGC ACA AGG GC-3'
oIMRo839 (TNFR II WT)	5'-AAC GGG CCA GAC CTC GGG T-3'
WT NE forward primer	5'-GAG AAC ACA GCC CAC CAT G-3'
WT NE reverse primer	5'-GGG CCT GAG AAC ACA CAA AG-3'
Neo forward primer	5'-GAC AAT CGG CTG CTC TGA TG-3'
Neo reverse primer	5'-ATA CTT TCT CGG CAG GAG CAA-3'

Table 2.1: Primers used for genotyping TNFR$^{-/-}$ and NE$^{-/-}$ mice.

Reagent	Volume per sample	Final concentration
Primer 1: oIMRo834 (100 pmol/µl)	0.12 µl	0.5 µM
Primer 2: oIMRo835 (100 pmol/µl)	0.12 µl	0.5 µM
OR		
Primer 3: oIMRo836 (100 pmol/µl)	0.12 µl	0.5 µM
Primer 4: oIMRo837 (100 pmol/µl)	0.12 µl	0.5 µM
dNTPs (10 mM)	0.5 µl	0.2 mM
$MgCl_2$ (50 mM)	1 µl	2 mM
NH_4^+ buffer (10x)	2.5 µl	1 x
TAQ polymerase (5 U/µl)	0.15 µl	0.03 U/ml
dH_2O (molecular biology grade)	18.61 µl	
Total	*23 µl*	

Table 2.2: PCR master mix to amplify either the TNFR I WT or mutant allele.

Initial denaturation	94°C for 3 min	x 1
Denaturation	94°C for 30 sec	35 cycles
Annealing	68°C for 1 min	
Elongation	72°C for 1 min	
Final elongation	72°C for 2 min	x 1

Table 2.3: PCR program for amplifying the TNFR I WT or mutant allele

Reagent	Volume per sample	Final concentration
Primer 1: oIMRo837 (100 pmol/µl)	0.13 µl	0.5 µM
Primer 2: oIMRo838 (100 pmol/µl)	0.26 µl	1 µM
Primer 3: oIMRo839 (100 pmol/µl)	0.13 µl	0.5 µM
dNTPs (10 mM)	0.5 µl	0.2 mM
$MgCl_2$ (50 mM)	1 µl	2 mM
NH_4^+ buffer (10x)	2.5 µl	1 x
TAQ polymerase (5 U/µl)	0.15 µl	0.03 U/ml
dH_2O (molecular biology grade)	18.33 µl	
Total	*23 µl*	

Table 2.4: PCR master mix to amplify both the TNFR II WT and mutant allele.

Initial denaturation	94°C for 3 min	x 1
Denaturation	94°C for 30 sec	35 cycles
Annealing	69°C for 1 min	
Elongation	72°C for 1 min	
Final elongation	72°C for 2 min	x 1

Table 2.5: PCR program for amplifying the TNFR II WT and mutant allele

Reagent	Volume per sample	Final concentration
Primer 1: WT NE forward primer	0.25 µl	1 µM
Primer 2: WT NE reverse primer	0.25 µl	1 µM
OR		
Primer 1: Neo forward primer	0.25 µl	1 µM
Primer 2: Neo reverse primer	0.25 µl	1 µM
dNTPs (10 mM)	0.5 µl	0.2 mM
$MgCl_2$ (50 mM)	0.75 µl	1.5 mM
NH_4^+ buffer (10x)	2.5 µl	1 x
TAQ polymerase (5 U/µl)	0.1 µl	0.005 U/ml
dH_2O (molecular biology grade)	18.65 µl	
Total	*23 µl*	

Table 2.6: PCR master mix to amplify either the NE WT or the mutant allele.

Initial denaturation	94°C for 5 min	x 1
Denaturation	94°C for 30 sec	35 cycles
Annealing	60°C for 30 sec	
Elongation	72°C for 30 sec	
Final elongation	72°C for 10 min	x 1

Table 2.7: PCR program for amplifying the NE WT and mutant allele

Amplified DNA samples (15 µl of each reaction product) were mixed with 2 µl blue agarose gel electrophoresis loading buffer (25 mg bromophenol Blue, 4 g sucrose, 10 ml molecular biology grade water) and separated on a 1% (w/v) agarose gel (in TAE buffer) supplemented with 2 µl GelRed. Samples were run together with a 100-1,000 bp DNA ladder as a marker in an electrophoresis chamber (Mupid® -One electrophoresis system, Eurogentec) at 90 V. Reaction products were visualised and photographed under ultraviolet light on a UV White Darkroom BioImaging system (UVP, Cambridge, UK). The WT TNFR I gene was denoted by a 120 bp fragment, mutant TNFR I gene by a 155 bp, WT TNFR II gene by a 257 bp, TNFR II mutant by a 160 bp, WT NE gene by a 400 bp and mutant NE gene by a 500 bp fragment.

Phenotyping of $CX_3CR_1^{GFP/+}$ mice

Litters of this colony were phenotyped by my colleague Dr. Martina Beyrau using flow cytometry analysis of blood monocytes. Mice heterozygous for CX_3CR_1-GFP were distinguished from homozygous mice by the lower fluorescence intensity of specific monocyte subsets.

2.3.3 Neutrophil depletion

Pure WT C57BL/6 mice were depleted of their circulating neutrophils by intraperitoneal (i.p.) injection of 100 µg anti-GR1 antibody in 500 µl saline as previously described (Wang et al., 2006). Injection was performed 24 h prior to inducing inflammatory responses. Control mice received the same concentration of rat IgG2bκ isotype-matched control antibody. Blood samples taken from the tail vein before and after antibody injection were used to determine the level of neutrophils by Kimura staining (11 ml 0.05% Toluidine Blue, 0.8 ml 0.03% Light green, 0.5 ml saturated saponin in 50% ethanol, 5 ml 1/15M phosphate buffer pH 6.4). This protocol depleted circulating neutrophils by 90% but likely also reduced monocyte levels.

Neutrophil-only depletion was induced in WT C57BL/6 and $CX_3CR_1^{EGFP/+}$ mice by serial i.p. injections of a lower dose of anti-GR1 antibody as previously described (Voisin et al., 2009). 25 µg antibody in 500 µl saline per day was given for 3 days in a row. IgG2bκ isotype control antibody was injected in control animals. The level of neutrophils and monocytes was determined in blood samples taken from the tail vein before and after 3 days of antibody treatment using Kimura staining and/or flow cytometry ($GR1^+$, $GR1^+/CX_3CR_1$-GFP^+ cells, respectively). Mice treated with 3 doses of the anti-GR1 antibody typically showed a depletion of their circulating neutrophils of more than 85%. Of importance, this protocol had no effect on the proportion of blood CX_3CR_1-GFP^+ $GR1^+$ monocytes.

2.3.4 Inhibition of ROS Signalling

In some experiments the role of reactive oxygen species (ROS) molecules on pericyte shape change was analysed using superoxide dismutase (SOD) and catalase as described previously (Woodfin et al., 2011) to scavenge O_2- free radicals, hydrogen peroxide, respectively. Male mice were anaesthetised by i.m. injection of 1 ml/kg ketamin (40 mg) and xylazine (2 mg) in saline. SOD (2,000 U/kg) together with catalase (50,000 U/kg) were injected intravenously (i.v.) into the tail vein of male pure WT C57BL/6 mice immediately prior to induction of inflammation.

2.3.5 Inhibition of PAF-induced responses

Male mice were anaesthetised by i.m. injection of 1 ml/kg ketamin (40 mg) and xylazine (2 mg) in saline. To block PAF-induced responses, male WT C57BL/6 mice were pre-treated with the PAF-antagonist UK 74,505. 150 µl UK 74,505 (0.5 mg/kg bodyweight in saline) was administered i.v. into the tail vein 10 min prior to induction of inflammation as described previously (Young et al., 2002). Control mice received 0.6 mM HCl in saline (vehicle).

2.3.6 Induction of inflammatory reactions in murine tissues

Induction of inflammation in the cremaster muscle

To induce inflammatory responses in the cremaster muscle, inflammatory mediators were injected via the intrascrotal route following sedation. Male mice were anaesthetised by i.m. injection of 1 ml/kg ketamin (40 mg) and xylazine (2 mg) in saline. TNF (300 ng), IL-1β (50 ng), LTB_4 (30 ng), KC (500 ng), C5a (300 ng) or fMLP (5 µg) in 300 µl PBS were administered intrascrotally (i.s.). As a vehicle control 300 µl PBS was injected i.s. alone. Mice were treated for 2, 3, 4, 6, 8, 24, 48 or 72 h as indicated for each experiment. At the end of each *in vivo* test period, mice were sacrificed by cervical dislocation and the cremaster muscle was surgically dissected away, flattened on dental wax and fixed for subsequent *ex vivo* immunofluorescent staining and confocal analysis (see section 2.3.7).

Induction of inflammation in the dorsal skin and ear skin

Mice were anaesthetised by injecting 1 ml/kg ketamine (40 mg) and xylazine (2mg) in saline i.m. Inflammation in the ear skin or dorsal skin was induced via intradermal (i.d.) injection of 30 ng LTB4, 300 ng TNF, 500 ng KC, 300 ng C5a, 5 µg fMLP or 50 ng PAF in 30 µl, 50 µl PBS, respectively. As a vehicle control mice received PBS alone. For injections of the compounds into dorsal skin, the dorsal fur was removed using an electric razor beforehand. Agents under test were injected according to a randomised site injection plan and not more than 8 dorsal sites were injected per mouse (Figure 2.2). At the end of experiments, mice were sacrificed by cervical dislocation. Dorsal skin was removed and injected sites were cut out as circular

patches using a metal puncher (~8 mm in diameter) and ears were cut off using surgical scissors for further analysis.

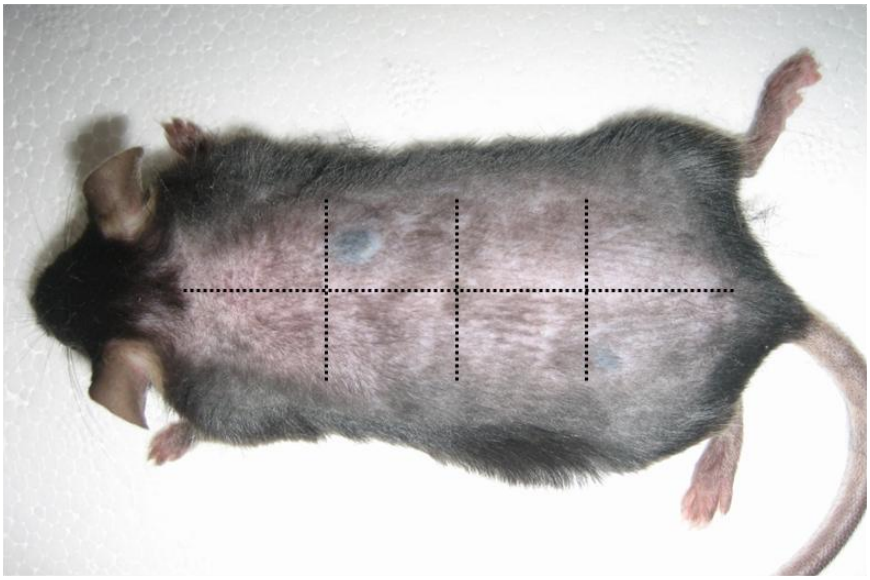

Figure 2.2: Site injection plan of inflammatory mediators in the mouse dorsal skin inflammation model. Mice were anaesthetised and dorsal fur was removed using an electric razor. Inflammatory mediators were injected i.d. in 50 µl PBS at balanced sites as separated by the dotted lines shown in this figure. Not more than eight sites were injected per mouse.

2.3.7 Preparation of lung sections for immunofluorescence labelling

To investigate expression of pericyte markers in the murine lung, lungs were harvested from C57BL/6 WT and αSMA-GFP mice as previously described (Uyechi et al., 2001). For this purpose, initially lungs were inflated as follows to avoid collapsing of the organ. Mice were killed by cervical dislocation and the thoracic cavity was opened exposing the lungs and heart. Warm PBS was perfused into the right heart ventricle to wash out the blood from the vessels for 30 seconds, followed by 4% PFA for 30 seconds. Warmed PBS (42°C) was used as lavage in the open chest cavity to keep subsequent injected agarose solution flowing through the whole lung. After exposing and intubation of the trachea, 800 µl pre-warmed (to 42°C) 3% low-melting point agarose was injected. Subsequently the trachea was quickly closed by making a tight knot with a fine thread. To solidify the agarose, ice-cold PBS was administered around the lungs. Lungs together with the trachea were then removed, fixed over night in 4% PFA at 4°C and stored in PBS at 4°C until tissue sectioning. Lung lobes were dissected and sectioned at 200 µm using a VT12005 vibratome (Leica) at an amplitude set at 1.8 mm and speed of 0.1 mm/s-0.5 mm/s.

Sections were then blocked and permeabilised in PBS supplemented with 25% of the respective serum (10% normal goat serum, 10% FCS and 5% normal mouse serum or 1% normal rabbit serum, 10% FCS and 5% normal mouse serum, depending on the antibody) and 3.75% Triton-X 100 for 7 h at room temperature under agitation. Tissues were stained with fluorescently labelled antibodies followed by image acquisition by confocal microscopy (as described in section 2.3.8).

2.3.8 Immunofluorescent labelling and confocal microscopy

Immunofluorescent labelling of untreated tissues or after stimulation (as described in section 2.3.6) was performed as previously described (Proebstl et al., 2012; Voisin et al., 2009; Voisin et al., 2010; Wang et al., 2006). Following dissection, tissues were fixed immediately in cold 100% methanol or 4% PFA for 30 min at 4°C. After washing in PBS, fixed whole-mounted tissues were blocked and permeabilised in PBS supplemented with 25% of the respective serum (10% normal goat serum, 10% FCS and 5% normal mouse serum or 1% normal rabbit serum, 10% FCS and 5% normal mouse serum, depending on the antibodies used) and 1% Triton-X 100 for 3 h at room temperature while shaking. Tissues were then immunostained for

neutrophils (anti-MRP14), pericytes (anti-αSMA, anti-NG2, anti-PDGFRβ, anti-SM22α), and/or ECs (anti-CD31) and BM components type IV collagen and pan-laminin, or appropriate control antibodies. After incubation with primary antibodies in PBS containing 10% serum (FCS, GS or RS) at 4°C over night or longer, tissues were washed 3 times for 15-30 min in PBS. If necessary, tissues were further incubated with specific fluorescently-conjugated secondary antibodies, as determined by the combination of primary antibody used in the respective experiment. Incubation was performed at 4°C for 3 h in PBS containing 10% serum (FCS, GS or RS). Following 3 washing steps in PBS for 15-30 min, tissues were stored at 4°C in PBS in the dark until analysed using a confocal microscope.

Immunofluorescently labelled tissues were analysed using a Zeiss LSM 5 PASCAL confocal laser-scanning microscope incorporating a x 40 water-dipping objective lens (numerical aperture 0.8 and resolution 0.37 µm), and a 10 x Plan NEOFLUOR objective (numerical aperture 0.3), or with a Leica SP5 confocal microscope (Leica Microsystems, Milton Keynes, UK) incorporating a x 20 water-dipping objective (numerical aperture 1.0 and resolution 0.28 µm). Z-stack images of half post-capillary venules (20-45 µm in diameter) were captured using the multiple track scanning mode at a resolution of 800 x 800 pixels in the x x y plane. Results were corrected for the background readings of the negative control (tissues stained with the respective isotype matched antibody). Images were analysed for leukocyte transmigration, pericyte gaps and BM LERs as described below

Quantification of leukocyte transmigration

Confocal images were analysed for the level of inflammation (number of extravasated leukocytes in the tissue) using the image processing software IMARIS (Bitplane, Zurich, Switzerland) as previously described (Proebstl et al., 2012). Three-dimensional reconstruction of Z-stack images of post-capillary venules (20-45 µm in diameter) were used for analysis. MRP-14 positive neutrophils and/or CX_3CR_1-GFP positive monocytes were counted across 200 µm vessel segments and within 50 µm away from the vessel (above and below of vessel) (Figure 2.3a). The number of transmigrated neutrophils was determined for each vessel segment. At least 3 vessel segments per cremaster muscle (6 per mouse) were quantified and data plotted as mean number of transmigrated cells per mouse.

Quantification of gaps between adjacent pericytes

The image analysing software ImageJ (National Institute of Healths, Bethesda, Maryland, USA) was used to quantify the size (area) and density (average number of gaps per defined vessel area) of gaps between pericytes surrounding post-capillary venules (20-45 µm in diameter). 3D-reconstructed confocal images of half vessels (vessels were split along the longitudinal axis) were artificially displayed on a 2D surface (z-projection, maximum intensity) and converted into 8-bit greyscale projections. Gaps between adjacent pericytes, defined as αSMA-negative regions, were either manually encircled across 200 µm vessel segments (Figure 2.3b) and their area was measured in μm^2 as previously described (Proebstl et al., 2012; Voisin et al., 2010; Wang et al., 2006), or automatically quantified by ImageJ. For automatic analysis, regions of interest (gaps between adjacent pericytes) were defined in binary images (positive/negative in contrast to intensity plots) by creating greyscale cut-off points: To display only pericyte gaps (background) rather than aSMA-positive regions the lower threshold level was set to 0 and the upper threshold level was adjusted so that only areas with low intensities (in terms of pixel) were included (i.e. pericyte gaps). Areas of regions of interest (set between 1-500 μm^2) were measured automatically by ImageJ using the “Analyze Particles” command. The above automatic analysis was developed as part of the present project.

For both, manual and automatic analysis, the values of all ROI areas per vessel segment were totalled. Mean gap size and gap density was determined for each vessel segment. At least 4 vessel segments per mouse were quantified and plotted as mean gap size per mouse, or number of gaps per defined vessel area (1 mm^2) per mouse, respectively.

Quantification of basement membrane low expression regions

As previously described (Voisin et al., 2009; Voisin et al., 2010; Wang et al., 2006; Wang et al., 2012), size and density of venular matrix LERs were determined in 3D images of semi-vessels captured and quantified on a 2D surface using ImageJ. Images were converted into gray scale intensity projection to indicate intensities of pixels from high to low. Regions with less than 60% of average fluorescence intensity as compared with average intensity of the entire vessel segment (200 µm) were defined as LERs (described in (Wang et al., 2006)). These regions were encircled manually and their size, density and fluorescence intensity was measured in at least 4 vessel segments per mouse (Figure 2.3c). Data were plotted as mean LER size per mouse, or number of LERs per defined vessel area (1 mm^2) per mouse, respectively.

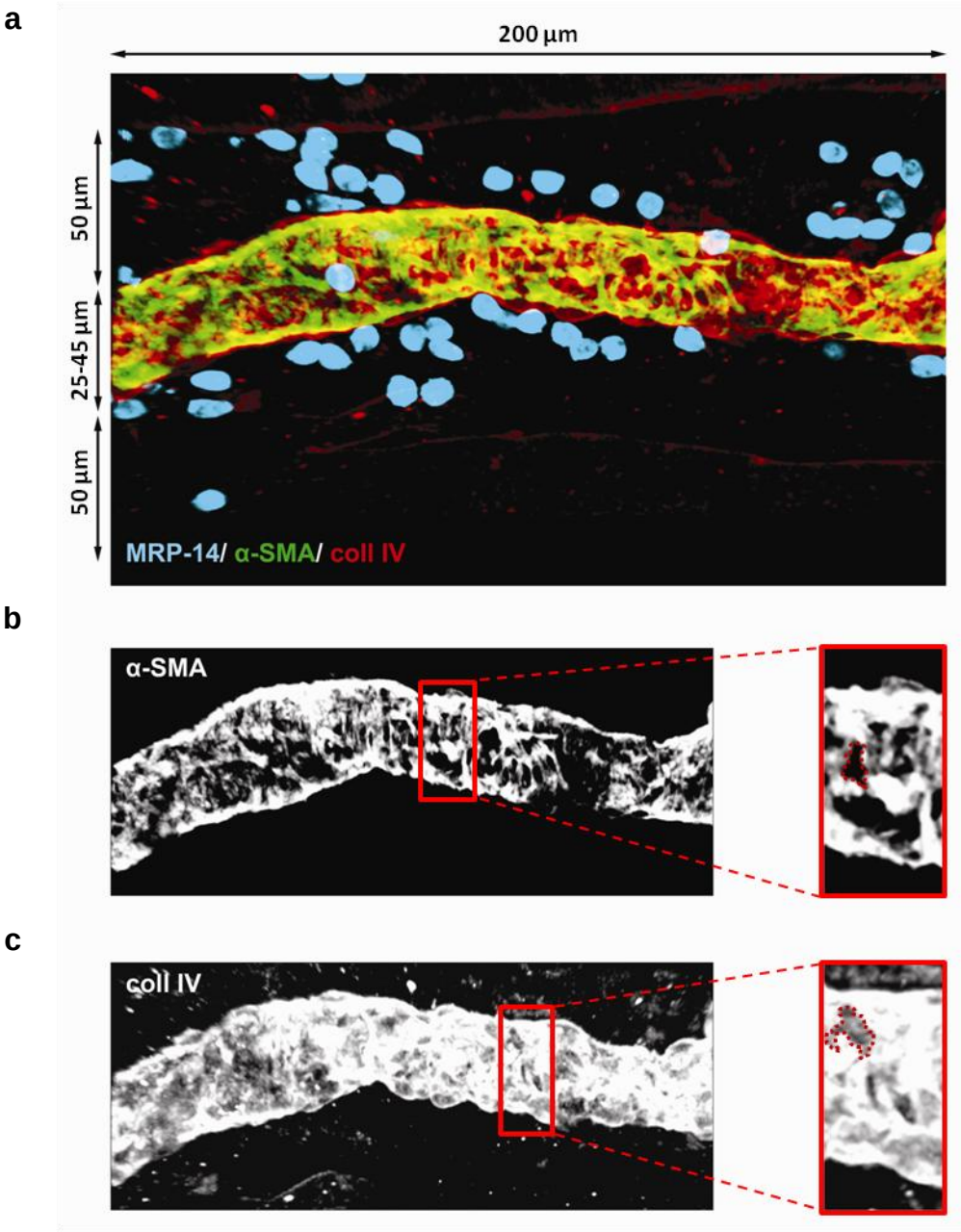

Figure 2.3: Schematic diagram of vasculature and tissue analysis. 200 µm vessel segments of post-capillary venules with a diameter between 25-45 µm were quantified for neutrophil transmigration, gaps between adjacent pericytes and LERs. MRP-14-positive cells were counted across these vessel segments within 50 µm away from the vessel **(a)**. Gaps between adjacent pericytes **(b)** and matrix protein LERs **(c)** were analysed on grey scale intensity projections of the images to quantify their size and density.

2.3.9 *In vivo* vascular permeability assay

Vascular leakage was assessed by measuring the accumulation of plasma-protein-bound Evans Blue dye in the dorsal skin, ear skin and cremaster muscles of animals stimulated with locally injected inflammatory mediators or PBS alone. As previously described (Colom et al., 2012), anaesthetised animals received Evans Blue dye (0.5% in PBS, 5 µl per g bodyweight) i.v. through the tail vein before or after administering the stimulating agents under test as indicated in section 2.3.6. At the end of the experiment animals were sacrificed by cervical dislocation. Sites of injections were removed and incubated in 250 µl formamide at 56°C for 24 h to extract Evans Blue dye from the tissues. The amount of accumulated Evans Blue dye was quantified by spectroscopy at 620 nm using a Spectra MR spectrometer (Dynex technologies Ltd., West Sussex, UK). Results are presented as the optical density at 620 nm (OD_{620}) per mg tissue and per mouse.

In some experiments, mice were pre-treated with one dose of anti-GR1 antibody (100 µg/ 500 µl saline) injected i.p. 24 h before (to deplete circulating neutrophils).

2.3.10 MPO Assay

A myeloperoxidase (MPO) assay was used to quantify neutrophil infiltration in mouse skin samples as previously described (Colom et al., 2012). Freshly dissected dorsal skin samples, or samples rapidly frozen in liquid nitrogen and stored at -80°C, were transferred to in-beaded tubes containing 500 µl homogenizer buffer (600 mM NaCl, 0.5% HTAB, 600 mM KH_2PO_4, 66 mM Na_2HPO_4 in H_2O). Samples were then homogenized using a Precellys homogenizer (Bertin technologies, Montigny-le-Betonneux, France) for 3 cycles at 6500 rpm for 20 second durations and 30 second pauses. After freezing the homogenate with liquid nitrogen and adding further 500 µl homogenizer buffer, the samples were homogenized once more under the same conditions as before. Subsequently the final homogenate was transferred into 1.5 ml tubes and centrifuged at 13,000 g for 10 min at 4°C. Supernatants were either stored at -80°C or used immediately to determine the MPO activity by enzymatic assay.

To assess the MPO activity, tissue extracts were diluted 1:2 in homogenizer buffer. Furthermore a standard curve was set up for each assay using partially purified MPO diluted in PBS (3, 2.5, 2, 1.5, 1, 0.5 and 0 u/ml). 25 µl assay buffer (6.6 mM

Na_2HPO_4, 60 mM KH_2PO_4, 0.5% HTAB; pH 6) was added to 96-well plate and mixed with 25 µl of sample or standard. Wells with 100 µl assay buffer served as negative control (blanks). 100 µl MPO substrate was then added to each well. Enzymatic activity was immediately measured by continually monitoring the change in absorbance at 650 nm for 20 min using a Spectra MR spectrometer (Dynex technologies Ltd., West Sussex, UK). Results are presented as MPO activity (units) per ml tissue lysate.

2.4 Statistical Analysis

Data management and analysis was performed using GraphPad Prism® 4. Data are presented as means ± standard deviation (SD) or standard error of the mean (SEM). Differences between two groups (e.g. untreated versus treated) were analysed for statistical significance using a Student's *t* test. To analyse differences between multiple groups (e.g. different time points) one-way or two-way analysis of variance (ANOVA) followed by Newman-Keuls or Bonferroni multiple comparison test was used. P-values < 0.05 were considered to be statistically significant.

CHAPTER 3: EXPRESSION OF KEY ADHESION MOLECULES AND PRO-INFLAMMATORY RECEPTORS ON PERICYTES *IN VITRO*

3.1 INTRODUCTION

Recruitment of leukocytes from the blood stream through the vessel wall to sites of infection is a crucial event in host defence during injury and infection. ECs and pericytes represent the two cellular components of postcapillary venular walls and together with the BM act as barriers for transmigrating leukocytes (Nourshargh et al., 2010). During inflammation the vessel wall becomes permeable to macromolecules and emigrating leukocytes. It is now well accepted that leukocyte transmigration is driven by interactions between adhesion molecules on immune cells and the endothelium or with the BM extracellular matrix (Hynes and Lander, 1992; van der and Sonnenberg, 2001; Vestweber, 2002). However, mechanisms through which leukocytes interact with pericytes are unknown. This key issue was addressed as part of the present work.

With respect to leukocyte-EC interaction, the importance of numerous adhesion molecules and their regulation during leukocyte transendothelial migration have been demonstrated recently (Ley et al., 2007). Pro-inflammatory mediators such as TNF and IL-1β are able to induce the expression, upregulation and/or re-localisation of endothelial adhesion molecules, a response which is known to stimulate leukocyte adhesion to venular ECs and regulate breaching of the EC barrier (Ley et al., 2007). Although the expression of adhesion molecules (such as ICAM-1 or VCAM-1) on primary pericytes *in vitro* has been demonstrated (Balabanov et al., 1999; Maier and Pober, 2011; Verbeek et al., 1995), their regulation and role during inflammatory processes and leukocyte transmigration *in vivo* is less well studied. Work conduced in our laboratory has previously demonstrated that neutrophils preferentially transmigrate through gaps between adjacent pericytes, sites that are associated with regions of lower deposition of certain BM constituents (LERs) (Voisin et al., 2009; Voisin et al., 2010; Wang et al., 2006). Furthermore there is now evidence for the ability of neutrophils to crawl on capillary and arterial pericytes (Stark et al., 2013), but full details of the associated mechanism are unclear. One hypothesis addressed as part of the present work is that pericytes support leukocyte transmigration via the regulation of adhesion molecule expression on their surface, a response that supports leukocyte-pericyte interaction. In this chapter this

possibility was investigated *in vitro*, an approach that enabled the analysis of a wide range of molecules.

Primary pericytes have been routinely obtained from bovine retinas, an organ where pericyte abundance is particularly high. However, emerging data indicate that pericytes are heterogeneous across different species and thus, might show species-specific properties. Furthermore technical difficulties and the lack of specific markers for pericytes have hampered the isolation and culture of primary pericytes in the past. Therefore pericyte-like cell lines (e.g. C3H/10T1/2 cells) have been commonly used by some groups to analyse pericytes *in vitro*. Reznikoff et al. established the clonal cell line C3H/10T1/2, clone 8 from 14-to 17-day-old C3H mouse embryos in 1973 (Reznikoff et al., 1973). C3H/10T1/2 cells have been derived from whole embryos, so their tissue of origin is unknown. Due to functional similarities (they are able to differentiate into cells of myofibroblast or osteogenic cell lineages such as muscle, adipose, bone, or cartilage cells) (Pinney and Emerson, Jr., 1989), C3H/10T1/2 cells may represent mesenchymal stem cells. In most systems C3H/10T1/2 cells have been used as fibroblasts based on their functional and biochemical properties and morphology (Clemens et al., 2005; Thorsen et al., 2003; Yauk et al., 2008). Cells from this cell line display a stellate fibroblast-like cell shape with several processes protruding from the body of the cell which remains stable for long periods in culture. However, C3H/10T1/2 cells also express markers for perivascular cells (e.g. αSMA and NG-2) and were shown to exhibit similar properties to those obtained from primary perivascular cells (Brachvogel et al., 2007). Previous work from our group further demonstrated the ability of C3H/10T1/2 cells to contract in response to inflammatory stimuli (TNF and IL-1β) similar to pericytes *in vivo* (Proebstl Doris, 2011). Therefore there is reason to propose that this cell line represents pericyte-/smooth muscle cell-like cells and as such have been used in this context in EC co-culture and vascular maturation studies (Darland and D'Amore, 2001; Hirschi et al., 1998; Walshe et al., 2009).

Although C3H/10T1/2 cells may not represent “real” pericytes, this cell line provides a useful opportunity for the analysis of perivascular cell responses *in vitro* and circumvents significant limitations associated with most primary cells (e.g. difficulties in isolation, limited cell survival and differentiation in culture). Hence, C3H/10T1/2 cells were used as pericyte-like cells in this chapter to investigate the expression and regulation of inflammatory relevant surface molecules on these cells. As part of this thesis, a new protocol was also established to isolate and select primary

pericytes from murine tissues and cells isolated with this method were analysed in preliminary works.

3.2 RESULTS

3.2.1 Expression profile of receptors for pro-inflammatory mediators on C3H/10T1/2 cells

Recent findings obtained within our laboratory have shown that TNF and IL-1β can activate blood vessels not only by stimulating ECs but also by acting on pericytes (Proebstl Doris, 2011). Specifically it was shown that post-capillary pericytes *in vivo* and C3H/10T1/2 *cells in vitro* exhibit shape-change in response to TNF and IL-1β. Evidence was obtained within our laboratory for the expression of TNF and IL-1 receptors on pericytes *in vivo* (Proebstl et al., 2012). To extend this work, in preliminary experiments, the expression of TNFR I, TNFR II and IL-1R I was analysed on C3H/10T1/2 cells by flow cytometry. These experiments confirmed previous results obtained from our group (Proebstl Doris, 2011).

C3H/10T1/2 cells were harvested from cell culture using EDTA. Cells in suspension were then fluorescently immunostained for TNFR I, TNFR II and IL-1R I and analysed by flow cytometry. Non-specific background staining was determined by staining cells with an isotype-matched goat IgG antibody. The results from both the specific mAbs and control antibodies were used to present immunoreactive antigen expression by relative fluorescent intensity (RFI). Flow cytometric analysis of at least 6 independent experiments revealed the expression of TNFR I, II and IL-1R I on the cell surface of C3H/10T1/2 cells (Figure 3.1). Mean RFI levels for IL-1R I were relatively low (1.8 ± 0.18), but significantly different when compared to isotype controls (goat IgG) (Figure 3.1b). Specificity of the anti IL-1RI antibody was further verified by Dr. Doris Proebstl using IL-1 receptor antagonist (IL-1ra) in the staining solution, which abolished IL-1RI receptor staining completely (Proebstl Doris, 2011). TNFR I and II, showed comparable RFI levels (5.6 ± 0.6, 5.6 ± 0.6, respectively).

a

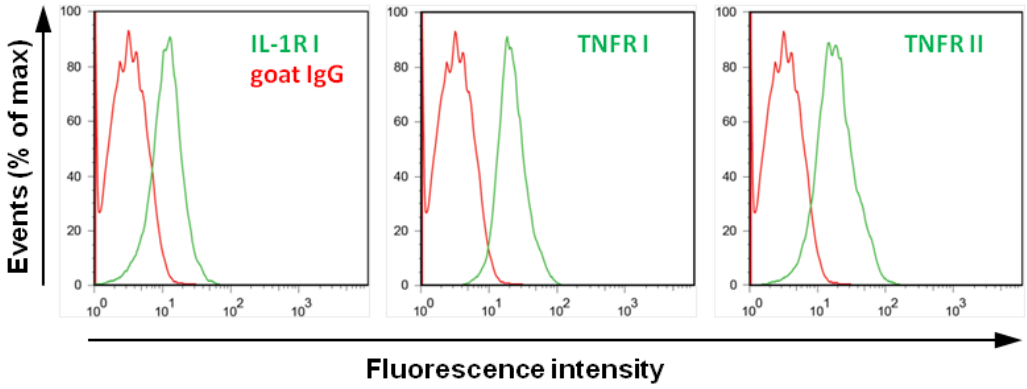

b

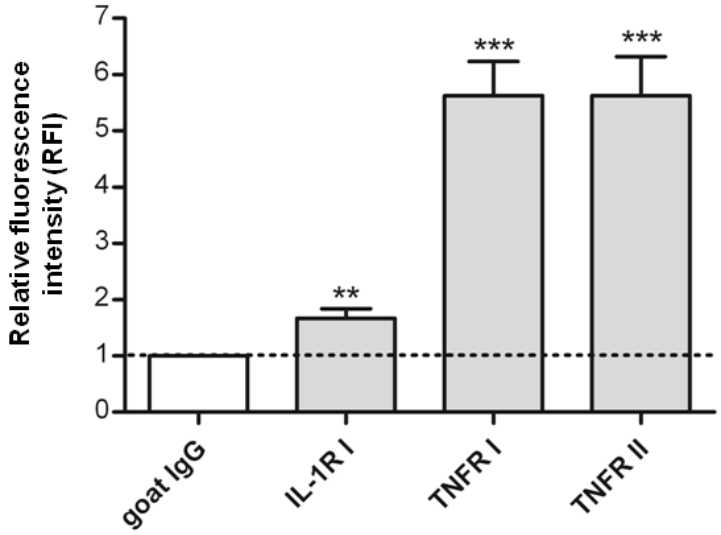

Figure 3.1: C3H/10T1/2 cells express receptors for TNF and IL-1β. Cell-surface expression of IL-1R I, TNFR I and TNFR II on C3H/10T1/2 cells were analysed by flow cytometry. **(a)** Representative histogram plots show overlays of cells stained with anti-TNFR I, -TNFR II, or –IL1R I, respectively (green), and cells stained with an isotype-matched control antibody (red). These plots illustrate the number of events as percentage of the maximum number over a spectrum of increasing fluorescence intensity. **(b)** Data are presented as the relative fluorescence intensity (RFI) normalized to the isotype control. Therefore the dotted line illustrates the isotype control with an RFI of 1 by definition. Bars for IL-1R I, TNFR I and TNFR II, respectively, represent the mean ±SD of at least 6 independent experiments per group. Significant expression levels as compared to the isotype control were determined using Student's *t*-test. (**: $p < 0.01$; ***: $p < 0.001$)

3.2.2 Effects of TNF and IL-1β on expression of key adhesion molecules on C3H/10T1/2 cells

TNF and IL-1β are well known to promote leukocyte transmigration by activating leukocytes and/or inducing the upregulation of adhesion molecules on ECs (e.g. ICAM-1, VCAM-1, E-Selectin). Having demonstrated in this chapter (section 3.2.1) and by Dr. Doris Proebstl (Proebstl Doris, 2011) that C3H/10T1/2 cells express receptors for these cytokines, the potential effect of TNF and IL-1β on adhesion molecule expression on this pericyte-like cells was next investigated.

Initial studies were performed to assess the basal expression levels of certain adhesion molecules, including integrins, junctional adhesion molecule (JAMs) and cellular adhesion molecules (CAMs), on the surface of C3H/10T1/2 cells. In order to do this, C3H/10T1/2 cells were harvested from cell culture flasks using EDTA, fluorescently immunostained and analysed by flow cytometry. As negative control, cells were stained using the respective isotype control antibodies. Immunoreactive antigen expression was assessed in at least 3 independent experiments and presented as RFI. Flow cytometry analysis of resting C3H/10T1/2 cells showed significant expression of integrin subunits α1, α5, α6, β1 and β3, as well as JAM-A, -B, -C, ICAM-1 and VCAM-1 under basal conditions. In contrast, no detectable levels of integrin subunits α2, α4 and β4, or ICAM-2, E-Selectin and VE-Cadherin could be quantified on these cells (Figure 3.2).

To analyse the regulation of these adhesion molecules by pro-inflammatory cytokines, cells seeded in 6-well plates were treated with different concentrations of TNF (10 ng/ml and 100 ng/ml in PBS), IL-1β (1 ng/ml and 10 ng/ml in PBS) or PBS alone for 4 h. Cells were then washed with cold PBS and analysed by flow cytometry as described in the previous paragraph. Whereas the expression levels of the analysed integrins and JAMs remained unchanged following TNF or IL-1β stimulation of cells for 4 h (Figure 3.3a), ICAM-1 and VCAM-1 expressions were significantly up-regulated in response to the cytokines in a dose-dependent manner (Figure 3.3b).

For a selection of molecules, the expression and distribution of adhesion molecules on C3H/10T1/2 cells was also analysed by immunofluorescent staining and confocal microscopy. For this purpose, C3H/10T1/2 cells were grown on 4-well chamber slides, fixed and co-stained with antibodies against adhesion molecules under investigation and the pericyte marker αSMA. To analyse also intracellular

expression of the proteins cells were permeabilised before staining. As a negative control, cells were stained using the respective isotype control antibody. The nucleus was visualized using the nuclear dye Draq5. Confocal microscopy of immunofluorescently labelled cells further confirmed the expression of integrin subunits α5, α6, β1 and β3, and VCAM-1 on unstimulated cells (Figure 3.4). In addition, focal adhesions could be observed for at least α5- and β1-integrin subunits (Figure 3.5), suggesting a functional implication of these molecules in binding to extracellular matrix proteins.

In summary, these data demonstrate that C3H/10T1/2 cells are able to respond to the pro-inflammatory cytokines TNF and IL-1β. Furthermore, as the findings are in line with the limited level of *in vivo* data available (Proebstl et al., 2012), these studies also suggest that C3H/10T1/2 cells act as a useful tool to investigate a wider range of molecular pathways involved in pericyte responses *in vitro*.

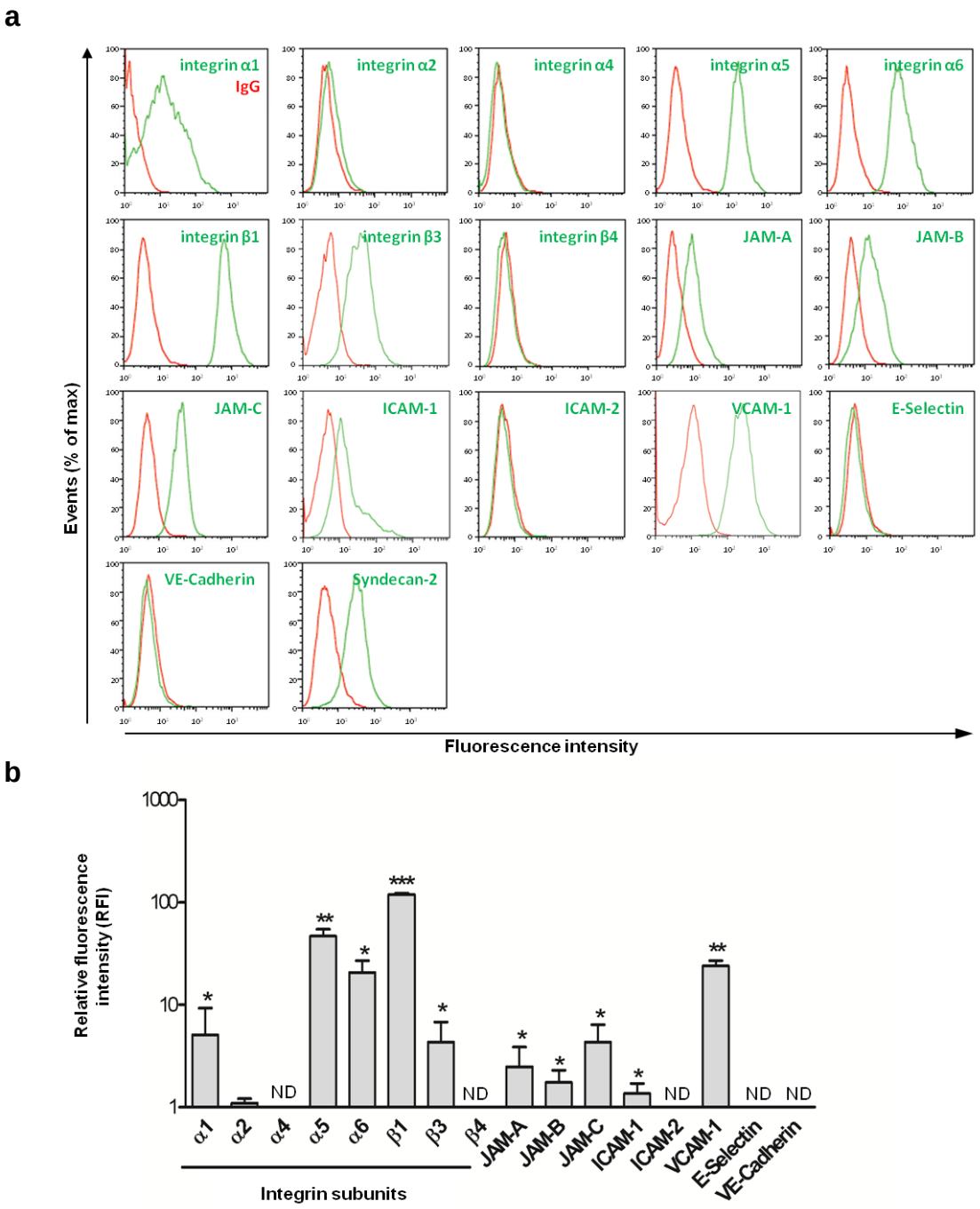

Figure 3.2: Expression of key adhesion molecules on C3H/10T1/2 cells. Cell-surface expression of a diverse range of adhesion molecules on C3H/10T1/2 cells were analysed by flow cytometry. **(a)** Representative histogram overlays show the expression of integrin subunits α1, α5, α6, β1, β3, as well as JAM-A, JAM-B, JAM-C, ICAM-1 and VCAM-1, but not integrin subunits α2, α4, β4, and ICAM-2, E-Selectin and VE-Cadherin on pericyte-like cells *in vitro*. Specific staining is shown by the green line; isotype-matched control staining is shown by the red line. **(b)** Data are presented as the decimal logarithm of the RFI normalized to the isotype control. They represent the mean ±SD of at least 3 independent experiments per group. Significant expression levels as compared to the isotype control were determined using Student's *t*-test. (*: $p < 0.05$; **: $p < 0.01$; ***: $p < 0.001$). ND, not detected.

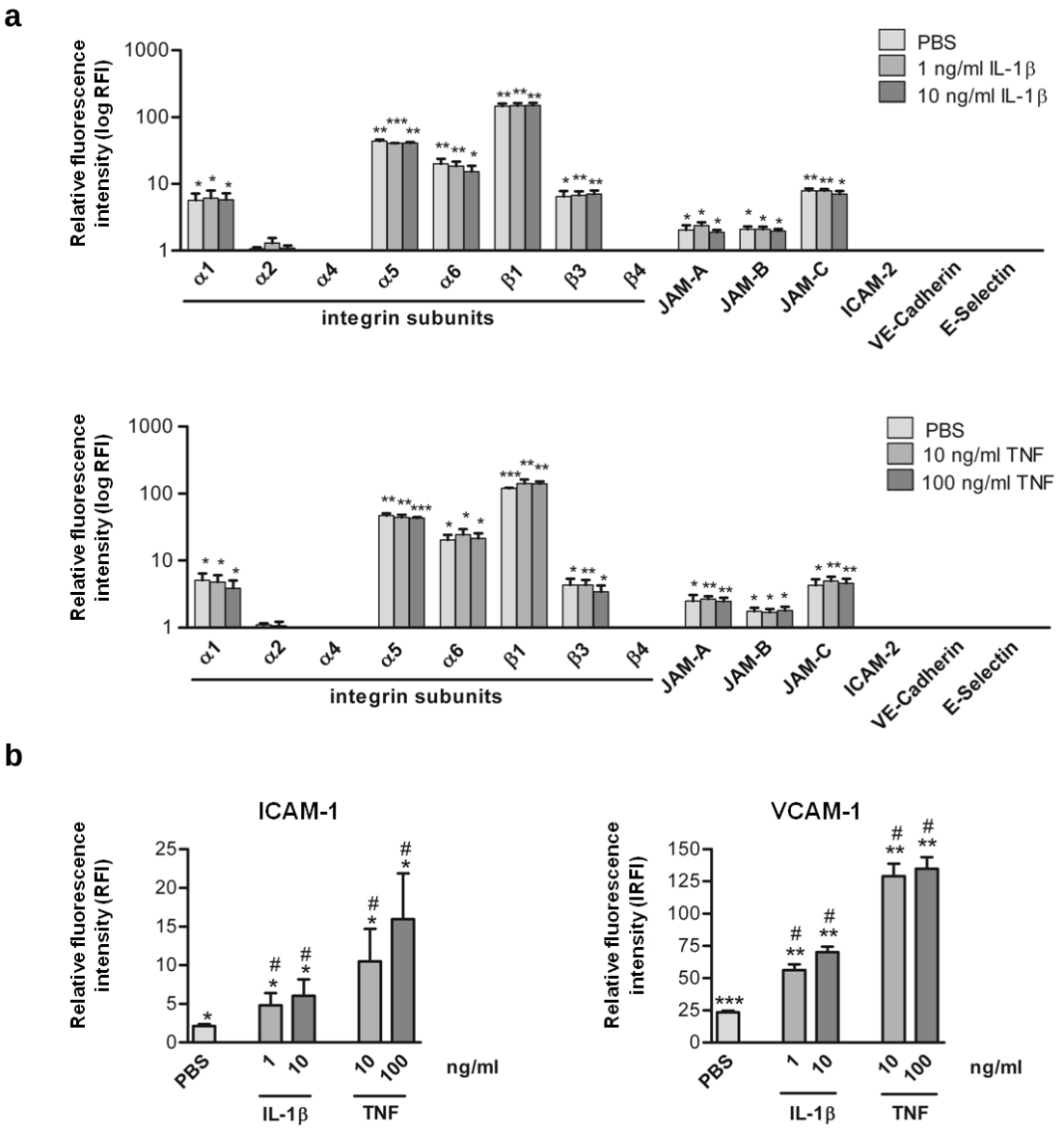

Figure 3.3: Regulation of expression of adhesion molecules on C3H/10T1/2 cells. Cells were cultured in the absence of inflammatory stimuli or treated with 1 or 10 ng/ml IL-1β or 10 or 100 ng/ml TNF for 4 h. Expression levels of adhesion molecules were assessed by flow cytometry analysis. **(a)** C3H/10T1/2 cells showed similar expression levels of integrin subunits α1, α2, α4, α5, α6, β1, β3, β4, and JAM-A, JAM-B, JAM-C, ICAM-2, VE-Cadherin and E-Selectin in PBS, IL-1β- or TNF-treated cells. **(b)** ICAM-1 and VCAM-1 expression were upregulated on C3H/10T1/2 cells following IL-1β and TNF stimulation as compared to PBS controls. Data are presented as the RFI normalized to the isotype control and are displayed on a log (a) or linear (b) scale. They represent the mean ±SD of at least 3 independent experiments. Significant expression levels as compared to the isotype control (marked with asterisks) and differences between PBS control vs. TNF, IL-1β stimulation, respectively (marked with hashes) were determined using Student's *t*-test. (* and #: $p < 0.05$; **: $p < 0.01$; ***: $p < 0.001$).

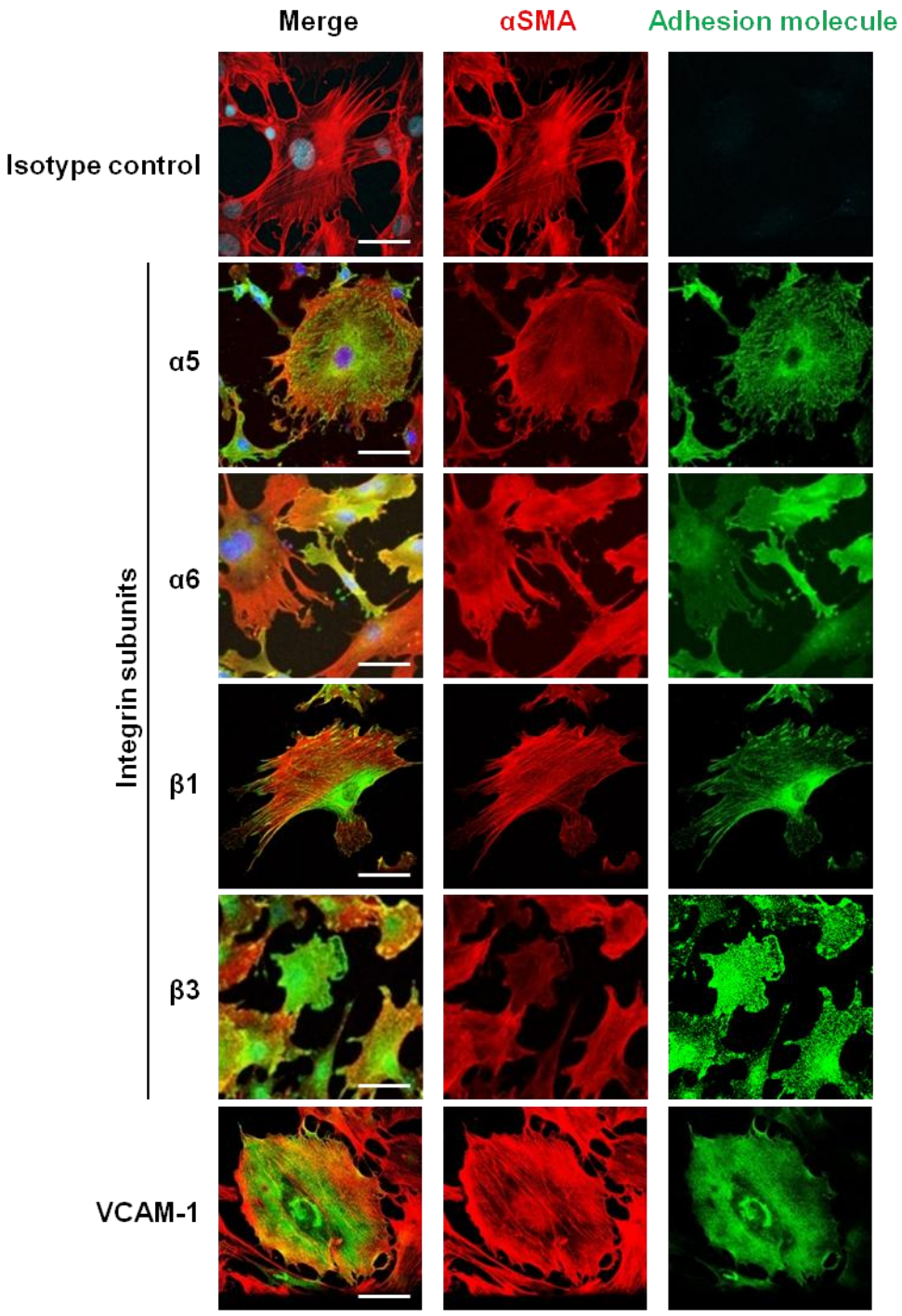

Figure 3.4: Expression pattern of adhesion molecules by C3H/10T1/2 cells. Cells were seeded on 4-well chamber slides, fixed, permeabilised and stained with antibodies against the pericyte marker αSMA (red), the nuclear dye Draq5 (blue) and specific antibodies against indicated adhesion molecules or matched isotype controls (green). Representative confocal images from 3 independent experiments are shown. Bars, 50 µm

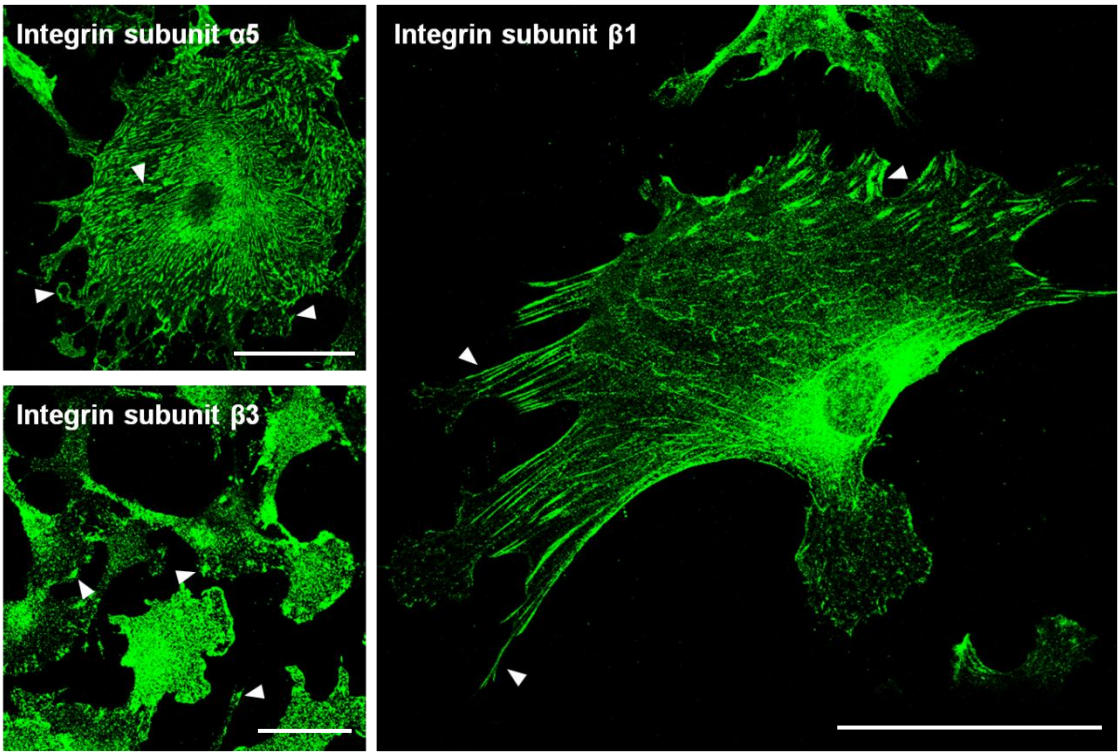

Figure 3.5: Assembly of integrin adhesion structures in cultured C3H/10T1/2 cells. Cells were seeded on 4-well chamber slides, fixed, permeabilised and stained with antibodies against indicated adhesion molecules (green). Integrin clustering leads to assembly of adhesion structures (marked with arrowheads). Representative confocal images out of 3 independent experiments are shown and are the same as shown in Figure 3.4. Bars, 50 µm

3.2.3 Isolation of primary pericytes

To extend the results obtained with the pericyte-like cell line C3H/10T1/2 to a more physiological scenario, studies aimed at using primary pericytes were also initiated. For this purpose a new protocol was established to isolate pericytes from murine lung tissues.

Characterisation of pericyte marker expression in different murine tissues

Prior to isolation, the expression profile of different protein markers reported for pericytes was analysed in immunofluorescently labelled murine tissues (*i.e.* lung sections in comparison to whole-mount cremaster muscles) using confocal microscopy. The characterisation of marker expression on different pericyte subsets is important to be able to identify and sort isolated primary cells in a later step. For these experiments the lung was selected for investigation based on its high vascularisation and hence high abundance of pericytes.

Lungs from WT animals were inflated by injecting low-melting point agarose via the trachea into the lung immediately after cervical dislocation. This was important to preserve the structure of the vasculature. Organs were fixed after removal from the thoracic cavity and sectioned at 200 µm using a vibratome. Subsequently, sections were co-stained using an anti-αSMA antibody together with antibodies against other pericyte markers. Whole mounted cremaster muscles removed from WT animals were used in parallel for comparative analysis. Confocal images were taken from different vessel types (e.g. arteries, venules, capillaries) that were identified using a number of criteria including vessel diameter and morphology of ECs and perivascular cells along the vasculature.

αSMA is a commonly used marker to identify perivascular cells such as pericytes and SMCs (Armulik et al., 2011). This protein is a major constituent of the cytoskeleton and is involved in regulating cell motility, structure and integrity. Immunofluorescence staining of whole mounted murine cremaster muscles (Figure 3.6) and lung sections (Figure 3.7) revealed a high intensity staining on SMCs surrounding arteries, arterioles, pre-capillary arterioles and large veins as characterised by a tightly wrapped perivascular morphology. High expression of αSMA was further detected on postcapillary and collecting venules, defined as vessels with a diameter between 25-50 µm and >50 µm, respectively and exhibiting notable gaps between adjacent pericytes. In contrast, pericytes on capillaries

showed hardly any αSMA staining. These results obtained with murine lung and cremaster muscle are in line with published reports by others, demonstrating the same expression pattern in multiple human organs and murine pancreatic tissues (Morikawa et al., 2002b; Nehls and Drenckhahn, 1991).

Postcapillary pericytes were positively stained for PDGFR-β, as well as pericytes surrounding collecting venules and capillaries, and to a lesser extend SMCs of arterioles. The expression profile of PDGFR-β was similar in both cremaster muscle (Figure 3.6b) and lung tissues (Figure 3.7b). PDGFR-β has been shown to be expressed broadly by developing SMCs and pericytes in almost all organs (except the liver) (Hellstrom et al., 1999), and plays a crucial role in pericyte recruitment to the vessel wall, especially during embryonic development and angiogenesis (Armulik et al., 2011).

NG-2 is a membrane-spanning chondroitin sulphate proteoglycan and is considered as one of the most reliable markers for pericytes (Hughes and Chan-Ling, 2004). NG-2-positive perivascular cells were associated with cells in vessel walls of capillaries, arteries and arterioles, but not postcapillary venules in the cremaster muscle (Figure 3.6b) and in lung sections (Figure 3.7b). Furthermore NG-2 staining was observed on nerves along vessels in the interstitial space. The present findings are consistent with results from a previous study by Murfee et. al., showing an absence of NG-2 expression in pericytes along postcapillary venules in rat lungs (Murfee et al., 2005).

The intracellular protein smooth muscle 22-α (SM22α) is a marker of early differentiated SMCs and is highly expressed by isolated human umbilical artery SMCs (Maier et al., 2010). It was considered to be absent on pericytes (Maier and Pober, 2011). However, in in the present work SM22α labelling covered all mural cells of arterioles, venules and capillaries in the cremaster muscle (Figure 3.6b) and lung tissue (Figure 3.7b). Tissues stained with isotype-matched control antibodies showed no staining, indicating a true positive staining for PDGFR-β, NG-2 and SM22α (Figure 3.6b and 3.7b).

Based on these findings, postcapillary pericytes were characterised as αSMA-, PDGFR-β- and SM22α-positive, but NG-2-negative cells. These markers therefore provide a useful tool to identify pericytes derived from postcapillary venules after isolation and were employed as such as detailed below.

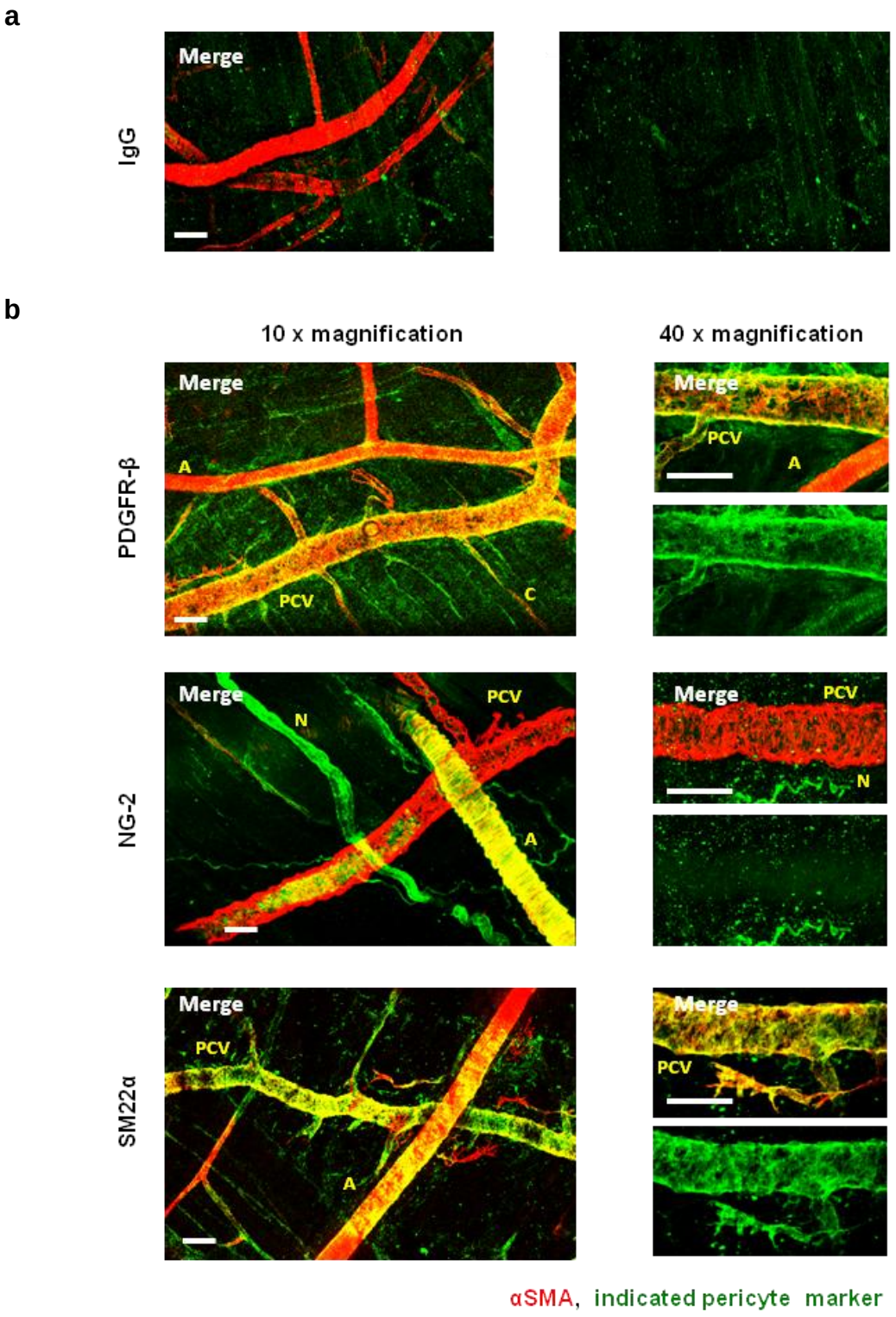

Figure 3.6: Expression profile of pericyte markers in the cremaster muscle. Representative 3D-reconstructed confocal images from independent experiments show different blood vessel types in the murine cremaster muscle. Whole-mount cremaster muscles from unstimulated WT C57BL/6 mice were double-stained for αSMA (red) and the isotype control **(a),** PDGFR-β, NG-2 or SM22α (green) **(b)**. A, arteriole; C, capillary; N, nerve; PCV, postcapillary venule. Bars, 50 µm.

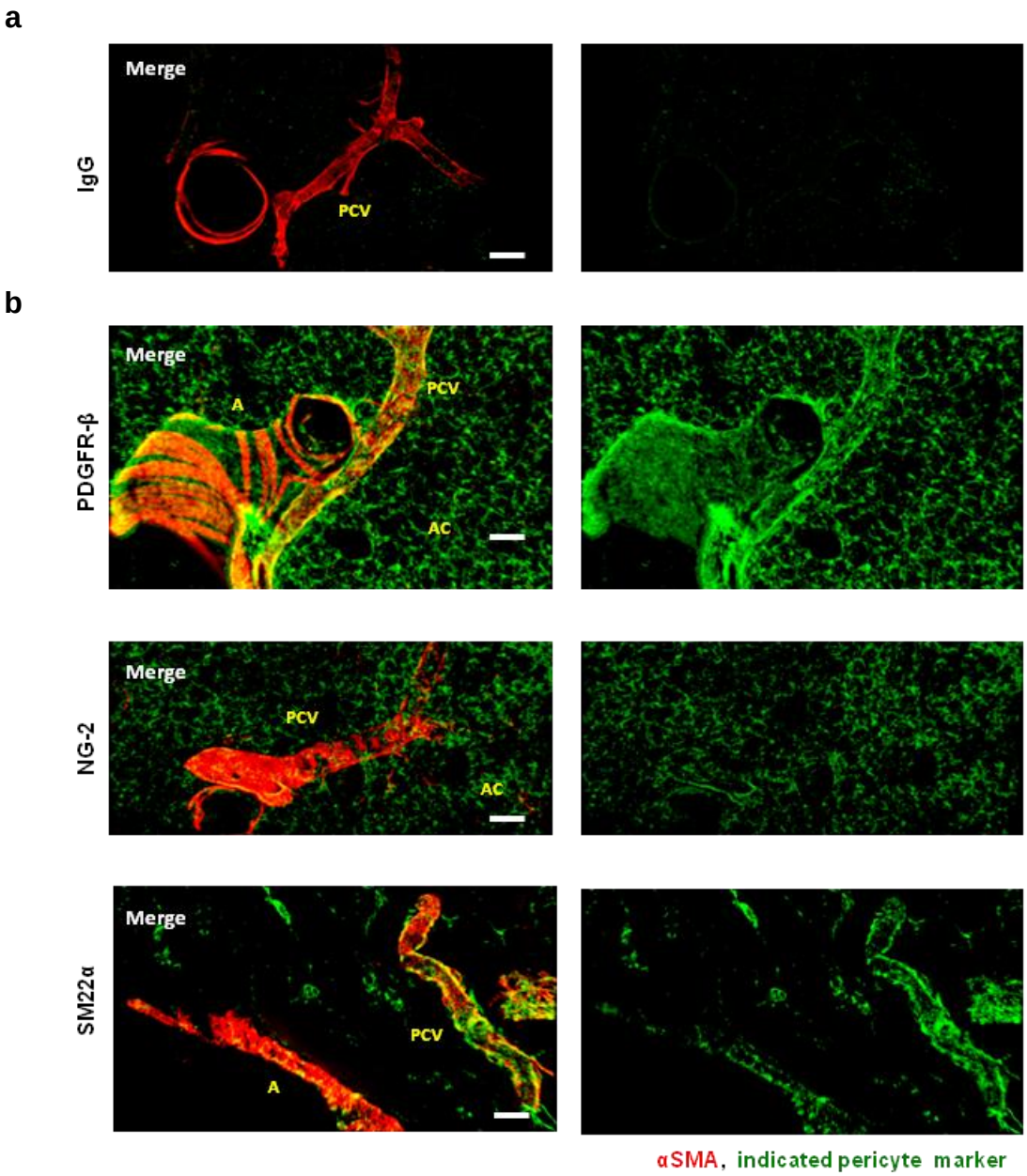

Figure 3.7: Expression profile of pericyte markers in the lung. Representative 3D-reconstructed confocal images from 3 independent experiments show different blood vessel types in the murine lung. Lung vibratome sections from unstimulated WT C57BL/6 mice were double-stained for αSMA (red) and the isotype control **(a)**, PDGFR-β, NG-2 or SM22α (green) **(b)**. A, arteriole; AC, alveolar capillary; PCV, postcapillary venule. Bars, 50 µm.

Characterisation of isolated lung perivascular cells

Primary cells were obtained from mice expressing GFP under the promoter of αSMA using collagenase and trypsin digestion of lungs. Following enzymatic digestion larger tissue fragments and undigested tissue were removed by sieving the resulting solution through a nylon mesh. The flow-through including single cells and microvessel fragments was cultured in medium containing growth factors to support pericyte proliferation. Cells were characterised for their pericyte nature based on their morphology and marker expressions (described above) as assessed by a combination of bright field and fluorescence microscopy, and flow cytometry.

GFP-positive vessel fragments and single cells could be detected directly after digestion from αSMA-GFP as compared to WT cell suspensions (Figure 3.8a). Cultured cells started to attach and spread on gelatine-coated plates by day 2, where cells showing a pericyte-like morphology with highly irregular peripheries and several protrusions could be observed (Figure 3.8b). In some cultures small EC colonies, characterised by a tightly packed, cobble-stone morphology were also present, which were seen only in the first few days in culture and disappeared later (Figure 3.8b, right). Cells started to proliferate within 5 to 7 days and a confluency of about 80-90% was typically visible within 14-20 days (Figure 3.8c).

Using flow cytometry, cells isolated from αSMA-GFP mice and expanded in culture were analysed for pericyte, endothelial cell and leukocyte markers. Dead cells were excluded by 7-Aminoactinomycin D (7-AAD) staining (Figure 3.9a, left panel). A population of usually more than 50% was revealed exhibiting a strong fluorescent signal for GFP (Figure 3.9a, right panel). These αSMA-GFP$^+$ cells further expressed PDGFR-β and lacked markers for leukocytes (CD45) and endothelial cells (CD31). 36% of the αSMA-GFP$^+$ population were also positive for NG-2, likely representing SMC and pericytes surrounding vessel types other than postcapillary venules (Figure 3.9b). Based on analyses of pericyte marker expression in lung sections as described before, α-SMA-EGFP$^+$, PDGFR- β$^+$, NG-2$^-$ cells were considered as postcapillary pericytes.

Morphology and marker expression was shown to be sustained for at least 5 passages, indicating that serially passaged primary cells continued to express a pericytic phenotype within this time frame.

Altogether, these findings outline a valuable method for isolating and culturing murine perivascular cells from lung vasculature of fluorescent αSMA-GFP mouse strain. Primary pericytes (α-SMA-EGFP^{+}, PDGFR- β^{+}, NG-2^{-}) acquired using this protocol were analysed for cell surface expression of cytokine receptors as detailed below.

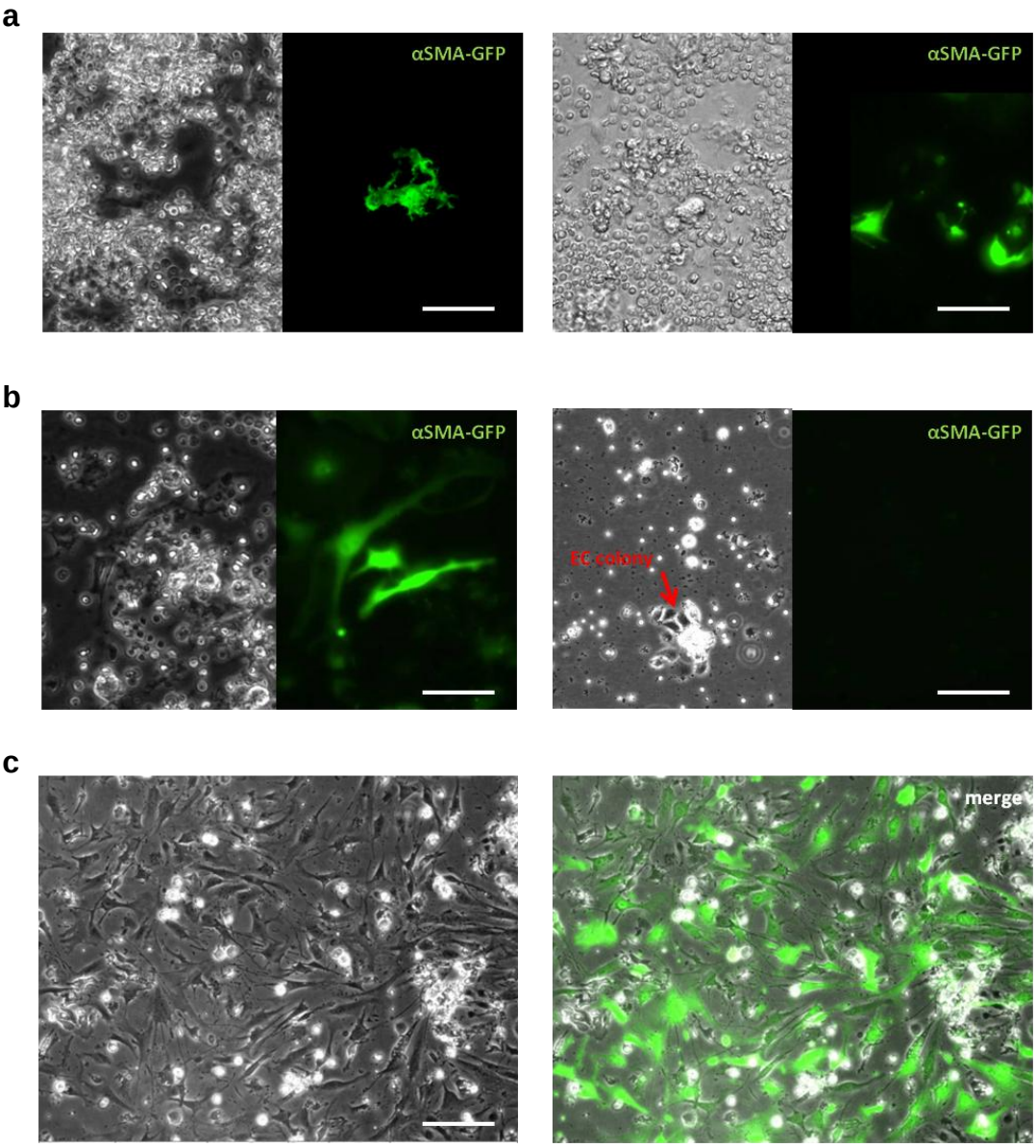

Figure 3.8: Isolated primary lung pericytes in culture. Representative phase contrast and corresponding fluorescent images of cultured primary cells isolated from lungs of αSMA-GFP C57BL/6 mice are shown. **(a)** GFP-positive vessel fragments (left panel) and single cells (right panel) were visible immediately after enzymatic digestion and culture. Mainly erythrocytes could be observed in the phase contrast displays. **(b)** Several processes were extending from the cell bodies of GFP-positive cells in 2-day old cultures (left panels), indicating adhesion and spreading of cells. Also small cobble-stone shaped endothelial cell colonies could be detected in 2-day old cultures, which were negative for GFP (right panels). **(c)** Confluency was typically reached between culture days 14-20, as shown here by phase contrast (left) and fluorescent overlay images (right) of an 18-day old culture. Bars, 50 µm.

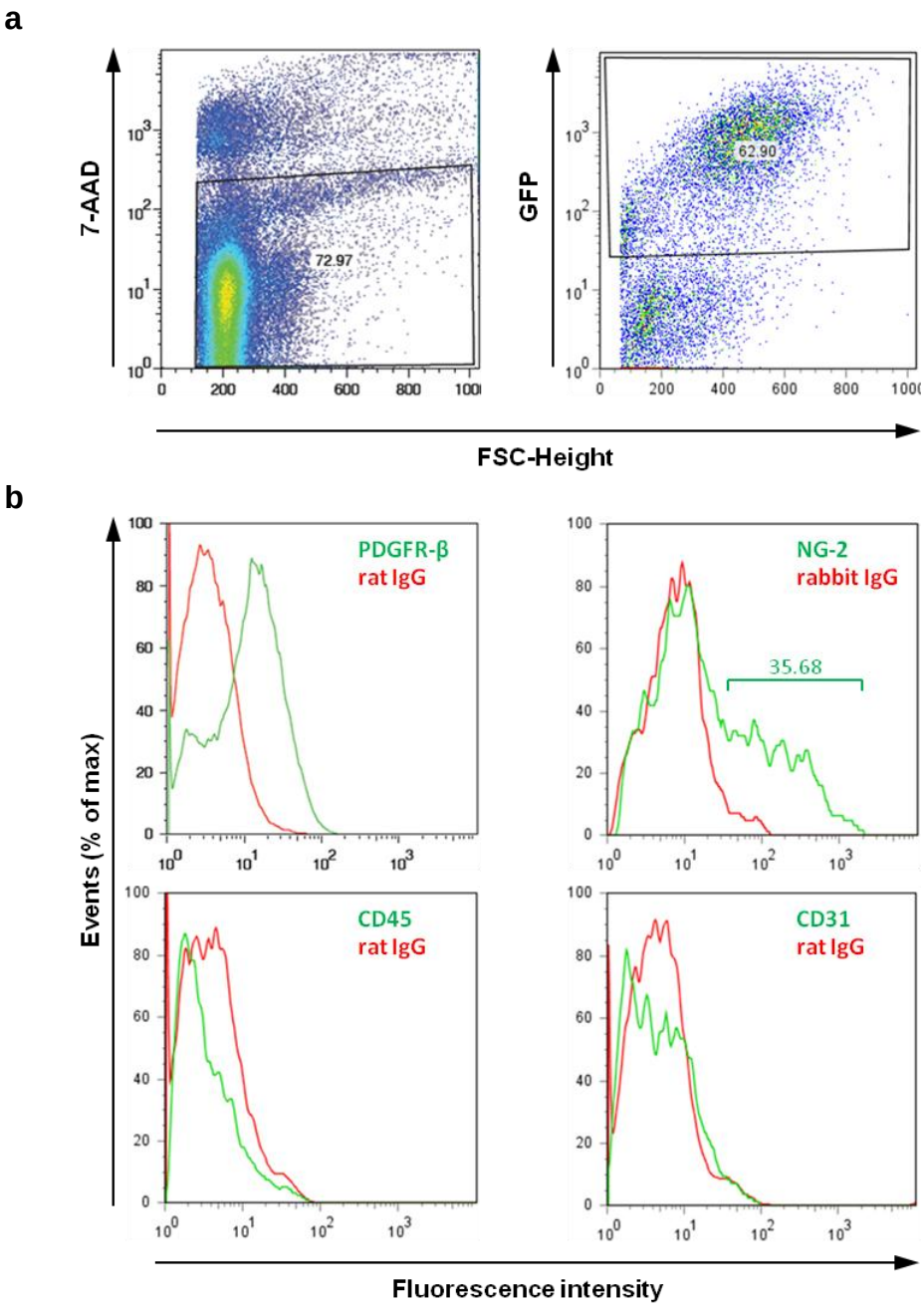

Figure 3.9: Characterisation of cultured primary cells isolated from murine lungs. Primary cells were obtained from αSMA-GFP mice using enzymatic digestion of lungs and cultured for at least seven days. The expression of cell-specific markers on their surface was analysed over five passages using flow cytometry. Representative flow cytometry data from cells at subculture 1 are shown. **(a)** Living cells were gated in dot plots upon incubation with 7-AAD (left). GFP/ FSC-H dot plot shows 62.9% GFP-positive cells (right). **(b)** Histogram overlays of cells gated in (a) (living and GFP-positive cells) show the expression of the pericyte marker PDGFR-β on cultured primary cells. Within the αSMA-GFP$^+$ population an NG-2-positive population of 35.68% of total cells could be detected. αSMA-GFP$^+$ cells lacked markers for leukocytes (CD45) and ECs (CD31). Specific staining is shown by the green line; isotype-matched control staining is shown by the red line. Similar results were obtained in six independent experiments.

3.2.4 Expression of receptors for TNF and IL-1β on isolated primary murine lung pericytes

To further characterise pericytes isolated from lung microvessels, the expression of cytokine receptors and thus, their ability to directly respond to pro-inflammatory mediators was examined. For this purpose, the expression of TNF and IL-1β receptors, namely TNFR I, TNFR II and IL-1R I, respectively, were analysed on mixed primary cells isolated from αSMA-GFP mice between passage 0 and 5. Co-staining for NG-2 allowed us to identify pericytes derived from postcapillary venules, the site where leukocyte transmigration normally occurs during inflammation. Indeed, αSMA-GFP^{+}, NG-2^{-} pericytes expressed significant levels of TNFR I, TNFR II and IL-1R I as shown by flow cytometry analysis (Figure 3.10).

Together with the results obtained from the pericyte-like C3H/10T1/2 cell line, these data further support the concept that pericytes are direct cellular targets for TNF and IL-1β, suggesting a functional role for pericytes in inflammation.

a

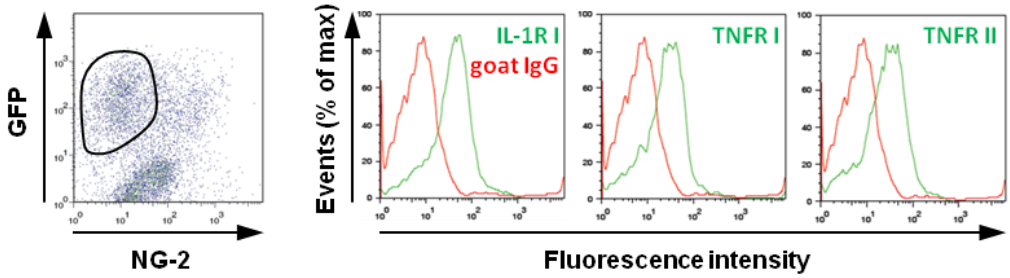

b

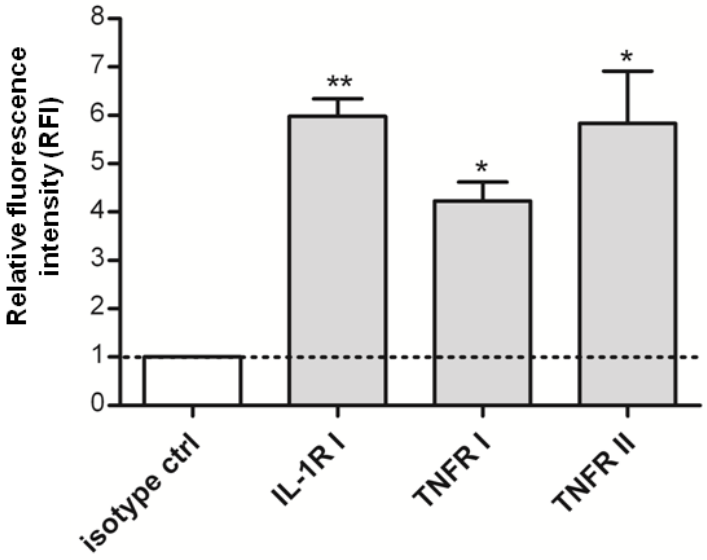

Figure 3.10: Primary murine lung postcapillary pericytes express receptors for TNF and IL-1β. Primary cells were obtained from αSMA-GFP mice using enzymatic digestion of lungs. Cell-surface expression of IL-1R I, TNFR I and TNFR II was analysed over five passages using flow cytometry. Representative flow cytometry data from cells at subculture 3 are shown. **(a)** An αSMA-GFP^{+} NG-2^{-} population was considered to represent pericytes derived from postcapillary venules and were gated in αSMA-EGFP/ NG-2-A647 dot blots (left). Representative histogram plots show overlays of αSMA-GFP^{+} NG-2^{-} cells stained with anti-TNFR I, -TNFR II, or –IL1R I, respectively (green), and cells stained with an isotype matched antibody (red) (right panels). These plots illustrate the number of events as percentage of the maximum number over a spectrum of increasing fluorescence intensity. **(b)** Data are presented as the relative fluorescence intensity (RFI) normalized to the isotype control. Therefore the dotted line illustrates the isotype control with an RFI of 1 by definition. Bars for IL-1R I, TNFR I and TNFR II, respectively, represent the mean ±SD of 3 independent experiments. Significant expression levels as compared to the isotype control were determined using Student's *t*-test. (*: $p < 0.05$; **: $p < 0.01$)

3.3 DISCUSSION

Migration of circulating leukocytes through venular walls to sites of inflammation is a crucial component of host immune response against pathogens and tissue injury. Although there is at present much interest in deciphering the mechanisms of leukocyte transendothelial migration, little attention has been paid to the analysis of the role of pericytes during leukocyte transmigration. In this chapter, a possible role for pericytes in supporting and facilitating leukocyte transmigration during inflammation was investigated *in vitro*. To address this question, the expression of key pro-inflammatory surface molecules on pericytes (including cytokine receptors and adhesion molecules) and the regulation of these molecules upon cytokine stimulation were investigated. To enable investigation of a wider range of molecular pathways, *in vitro* models were used involving the pericyte-like cell line C3H/10T1/2 and primary murine pericytes. C3H/10T1/2 cells are widely used for analysis of pericyte responses *in vitro* as they show similar morphologies and properties to those shown by primary pericytes. To study these cells, flow cytometry and confocal microscopy were employed to investigate the expression of molecules of interest.

In preliminary experiments the expression of receptors for the pro-inflammatory cytokines TNF and IL-1β, namely TNFR I and II, and IL-1R I, respectively, on C3H/10T1/2 cells were analysed in parallel with Dr. Doris Proebstl (Proebstl Doris, 2011). As has been shown for postcapillary pericytes in the murine cremaster muscle *in vivo* (Proebstl et al., 2012), all 3 receptors could be detected on C3H/10T1/2 cells *in vitro*. A recent study performed by Stark et al. further showed the upregulation of TNFR I mRNA expression in human placenta pericytes stimulated with TNF and LPS (Stark et al., 2013). Biological functions of cytokines, chemokines and chemoattractants are mediated by receptors on the cell's surface. ECs are known to express both TNFRs and IL1-R1 and to respond to TNF and IL-1β. However, very little is known about the potential effects of these cytokines on pericytes. Recent data acquired from our group has shown that C3H/10T1/2 cells as well as mouse cremaster muscle pericytes of postcapillary venules *in vivo* exhibit shape change in response to TNF and IL-1β (Proebstl Doris, 2011). In these experiments, pericyte-shape change *in vivo* occurred even in the absence of neutrophils and evidence was presented for expressions of TNF and IL-1 receptors on pericytes. In line with these studies, data acquired in the present project confirmed the expression of cytokine receptors on C3H/10T1/2 cells, indicating that these cells have the potential to directly respond to TNF and IL-1β.

As a next step the expression and regulation of expression of key potential ligands for leukocytes on C3H/10T1/2 cells was investigated. To identify proteins with a role in inflammatory responses, changes in cell-surface expression of various adhesion molecules on the pericyte-like C3H/10T1/2 cells were investigated after TNF or IL-1β stimulation. Cells were treated with different concentrations of either TNF (10 or 100 ng/ml) or IL-1β (1 or 10 ng/ml) for the indicated length of time or were left untreated. Adhesion molecules that were analysed included integrins, junctional adhesion molecules (JAMs) and cellular adhesion molecules (CAMs). Immunoreactive antigen expression was assessed through quantifications of RFI or the percentage of positively stained cells. In this context, C3H/10T1/2 were found to express several integrins (α_1, α_5, α_6, β_1 and β_3), JAMs (JAM-A, -B, -C) and cell adhesion molecules (ICAM-1 and VCAM-1) under basal conditions. In contrast, expression of integrin subunits α_2, α_4 and β_4, as well as ICAM-2, E-Selectin and VE-Cadherin could not be detected on C3H/10T1/2 cells.

At present, few reports are published that demonstrate the expression of adhesion molecules on the surface of pericytes. In line with the present study, ICAM-1 expression has been shown on murine post-capillary pericytes of the cremaster muscle (Proebstl et al., 2012) and capillary pericytes in the ear (Stark et al., 2013) *in vivo*, pericytes of brain tissue from multiple sclerosis patients *ex vivo* (Verbeek et al., 1995) and primary pericytes isolated from rat brains (Balabanov et al., 1999), bovine retinas (Kowluru et al., 2010) and human placentas (Stark et al., 2013). VCAM-1 expression on pericytes has been found on synovial tissue of patients with rheumatoid arthritis (Kriegsmann et al., 1995), brain tissues of multiple sclerosis patients (Verbeek et al., 1995), dermal tissue of patients with bullous pemphigoid (Dahlman-Ghozlan et al., 2004), primary rat (Balabanov et al., 1999) and human brain pericytes (Dahlman-Ghozlan et al., 2004). In contrast, cultured pericytes from human placentas did not express VCAM-1 under basal conditions or following stimulation with Interferon (IFN)-γ or TNF (Maier and Pober, 2011). In agreement with the present results using C3H/10T1/2 cells, E-Selectin expression could also not be detected in this study (Maier and Pober, 2011).

Using an EC-pericyte coculture model α_1, α_3 and α_6 integrin mRNA has been demonstrated to be expressed on bovine retinal pericytes *in vitro,* whereas expression of α_2 and α_4 could not be detected (Stratman et al., 2009). These findings support the data obtained in the present study. Adhesion molecules on pericytes represent possible interaction partners for ECs, adjacent pericytes, BM

components and transmigrating leukocytes. In this context, $\alpha_1\beta_1$ integrin and $\alpha_6\beta_1$ integrin are known as collagen-, laminin-binding integrins, respectively (Humphries et al., 2006). $\alpha_5\beta_1$ and $\alpha_V\beta_3$ integrins bind RGD (arginine-glycine-aspartic acid)-containing soluble and ECM molecules (e.g. fibronectin, vitronectin, fibrinogen, thrombospondin, osteopontin and laminins) (Ruoslahti, 1996). Members of the JAM family have a role in leukocyte transmigration and are involved in EC junction assembly (Bazzoni, 2003). Hence, JAMs on pericytes might possess similar function by binding to ligands in a homophilic (JAMs expressed by adjacent pericytes and/or ECs), and heterophilic way (LFA-1, $\alpha_L\beta_2$ integrin; VLA-4, $\alpha_4\beta_1$ integrin; Mac-1; $\alpha_M\beta_2$ integrin expressed on leukocytes), as has been shown for JAMs on ECs (Bazzoni, 2003; Bradfield et al., 2007). Pericytes might also interact with leukocytes through their expressions of ICAM-1 and VCAM-1, and adhesion molecules on leukocytes that bind ICAM-1 or VCAM-1 are LFA-1 and Mac-1, or VLA-4 (Ley et al., 2007).

The overall role of adhesion molecules on pericytes, however, is not well understood. A key hypothesis of this study was that pro-inflammatory cytokines such as TNF and IL-1β stimulate the expression of proteins necessary for leukocyte interaction on pericytes and that this may mediate leukocyte adhesion and transmigration through gaps between adjacent pericytes. Interestingly, whilst the expression levels of integrins and JAMs did not change following TNF or IL-1β stimulation, ICAM-1 and VCAM-1 were highly up-regulated in response to the cytokines. These results are in agreement with results by others showing the upregulation of both molecules by pericytes following stimulation with inflammatory mediators such as TNF or IFN-γ (Balabanov et al., 1999; Maier and Pober, 2011; Verbeek et al., 1995; Stark et al., 2013). ICAM-1 appears to facilitate neutrophil intravascular crawling through interaction with leukocyte Mac-1 (Phillipson et al., 2006). Thus, pericytic ICAM-1 might have a potential role during transmigration of leukocytes through the pericyte sheath. Indeed, confocal IVM experiments conducted within our group indicate that after transendothelial migration neutrophils crawl along pericyte processes in an ICAM-1 dependent-manner (Proebstl et al., 2012). Blocking antibodies against ICAM-1 diminish abluminal crawling of leukocytes to preferred sites of transmigration through pericyte gaps. However, the inhibitory effect of ICAM-1 blocking antibodies was not absolute, indicating a role for other pericyte-associated adhesion molecules in facilitating neutrophil sub-endothelial transmigration. Although VCAM-1 on pericytes has been suggested to have a role in facilitating T-cell adhesion and migration during multiple sclerosis as

demonstrated in a study using human brain perictytes *in vitro* (Verbeek et al., 1995), at present nothing is known about the role of pericyte VCAM-1 *in vivo* or a role for pericyte VCAM-1 in innate immune responses. In addition to guiding leukocytes to exit sites in venular walls, ICAM-1 on capillary and arteriolar pericytes in the mouse ear has recently been shown to navigate interstitial leukocyte migration to sites of sterile inflammation (Stark et al., 2013). Hence, in line with the well accepted roles of ICAM-1 and VCAM-1 in supporting leukocyte adhesion, these findings suggest an active participation of pericytes in leukocyte migration in inflammation *in vivo*.

At this point, however, it needs to be emphasised that C3H/10T1/2 cells, being isolated from mouse embryos (Reznikoff et al., 1973), may not represent "real" pericytes, but rather mesenchymal stem cells. Hence, these cells might behave differently than pericytes and data obtained with C3H/10T1/2 cells need to be interpreted with caution. As such, to complement the results obtained with these cells with a more physiological approach, as part of this work a protocol was established for the isolation and culture of primary mouse pericytes.

Pericytes have to date been isolated from different species (bovine, mouse, rat, human) and tissues (brain, retina, lung, placenta) (Brachvogel et al., 2005; Doherty and Canfield, 1999; Khoury and Langleben, 1996; Maier et al., 2010; Schor et al., 1995). However, technical difficulties in isolation and characterisation of pericytes due to a lack of a universal specific pericyte marker has made isolation of primary pericytes difficult. Several pericyte markers have been reported in the literature, including αSMA, NG-2, PDGFR-β and desmin. However, the expression of these molecular markers is not necessarily cell-type specific and are not specific to all pericytes. For example NG-2, has been shown to be expressed by capillary pericytes but not by postcapillary pericytes (Murfee et al., 2005). Furthermore NG-2 is also expressed on vSMCs and neuronal cells (Grako and Stallcup, 1995; Levine and Nishiyama, 1996; Murfee et al., 2005) suggesting that NG-2 alone is not a reliable pericyte marker as previously suggested (Hughes and Chan-Ling, 2004). Furthermore, pericytic expression of these markers varies depending on the type of vessels, tissue and changes under different pathological conditions (Chan-Ling et al., 2004; Gerhardt et al., 2000; Hughes and Chan-Ling, 2004). In previous studies, the employed methods of pericyte purification have mostly relied on selective adherence properties and morphological characteristics of the cell populations isolated from pericyte-rich tissues. Thus, the nature of the specific cell type isolated was unclear and likely represented a mixture of perivascular cells including SMCs

and other mesenchymal cells. Therefore the understanding of the expression profile of pericyte markers within the microvascular network in relation to location and morphology of the cells is critical to identify pericytes and isolate them.

In the present study a detailed marker analysis of perivascular cells in the lung and cremaster muscle was carried out prior to isolation. Murine lungs were chosen as a source of pericytes based on their relatively high pericyte density. Although tissues of the blood-brain-barrier (*i.e.* brain, retina) are generally regarded as the sites of highest pericyte abundance (Mathiisen et al., 2010; Sims, 1986), cells from these organs are likely to exhibit organo-specific properties due to the specialised function of the central nervous system.

The expression profile of pericyte markers was analysed on immunofluorescently labelled lung sections and whole-mounted cremaster muscles using confocal microscopy. Pericytes surrounding postcapillary venules and collecting venules as well as SMCs surrounding arterioles, arteries and veins were highly positive for αSMA, whereas capillary pericytes showed hardly any αSMA staining. These results were in line with previous studies using bovine retina, rat mesentery and mouse pancreas (Nehls and Drenckhahn, 1991). Other perivascular cell markers include PDGFR-β and SM22α, which were both expressed in cremasteric postcapillary venular pericytes, whilst NG-2 was only present on capillary pericytes and SMCs, and not on postcapillary pericytes, as previously described in rat tissues (Murfee et al., 2005). The expression profile of the analysed pericyte markers was similar in lung and cremaster tissues. Hence, primary postcapillary pericytes in a mixed population of isolated lung cells were identified as αSMA^+, PDGFR-β^+, $SM22\alpha^+$, NG-2^- cells. Primary cells were isolated by enzymatic digestion of murine lungs and expanded in culture for up to five passages. Indeed, phenotypic characterisation of these cells *in vitro* by flow cytometry revealed a postcapillary pericyte-like population that lacked markers for ECs (CD31) and leukocytes (CD45). Furthermore, isolated primary pericytes expressed receptors for the pro-inflammatory cytokines TNF and IL-1β as shown by immunofluorescence staining for TNFR I, II and IL1R I and flow cytometry analysis.

The similarities of protein marker expression of the isolated cells cultured *in vitro* and pericytes *in vivo* strongly indicate that these cells retain a pericyte-like phenotype in culture for at least five passages and therefore represent a unique and relatively simple tool for studies of these cells *in vitro*. However, it needs to be considered that pericytes might differentiate with increasing passage number and

significantly change their phenotype, a phenomenon that has been shown for many other primary cells, such as SMCs (Orlidge and D'Amore, 1986). Another concern of this method is the presence of contaminating cell populations, especially SMCs and fibroblasts. It is therefore necessary to positively and negatively sort these cells from primary tissue digests or serially propagated cultures (with magnetic beads or flow cytometry cell sorting) prior to their use in assays. Furthermore, it is important to understand that pericytes derived from different tissues –similar to many other cell types- might exhibit organo-typic properties and thus behave differently in culture and different research models. Nevertheless, the method described here provides a novel and relatively simple way to identify postcapillary pericytes from a mixed culture of isolated cells. The use of NG-2 to distinguish between SMCs and postcapillary venular pericytes represents a novel and useful approach to gain a clean pericyte population and study these cells *in vitro*.

In summary, the results presented in this chapter suggest that IL-1β and TNF can act directly on pericytes as shown by the expression of IL-1R I, TNFR I and TNFR II by pericyte-like cells and primary pericytes *in vitro*. Indeed, receptor expression for these cytokines has also been found on pericytes *in vivo* (Proebstl et al., 2012; Stark et al., 2013). Furthermore, the present findings show that pericytes express adhesion molecules *in vitro* that can be upregulated by pro-inflammatory cytokines, suggesting an active participation of pericytes in the regulation of an inflammatory response. *In vivo* evidence has been obtained for the ability of TNF to induce expression of ICAM-1 and chemokines on pericytes, responses that facilitate neutrophil transmigration (Proebstl et al., 2012; Stark et al., 2013). Furthermore, cytokines such as TNF and IL-1β have been reported to induce pericyte shape change *in vitro* (Proebstl et al., 2012) and *in vivo* (Proebstl et al., 2012; Wang et al., 2012). Hence, pericytes are able to actively respond to TNF and IL-1β in a number of models. This represents a novel mechanism through which these cytokines could exert their pro-inflammatory effects. To extend these findings to other types of inflammatory stimuli, the next chapter focused on the impact of neutrophil chemoattractants on pericyte morphology and function.

CHAPTER 4: CHEMOATTRACTANT-INDUCED PERICYTE SHAPE CHANGE *IN VIVO*

4.1 INTRODUCTION

Despite our improved understanding of transendothelial migration of leukocytes, the mechanism whereby immune cells breach the pericyte sheath *in vivo* remains elusive. Studies showing the expression of adhesion molecules such as ICAM-1 and VCAM-1 on pericytes (Balabanov et al., 1999; Dahlman-Ghozlan et al., 2004; Kowluru et al., 2010; Kriegsmann et al., 1995; Maier and Pober, 2011; Proebstl et al., 2012; Stark et al., 2013; Verbeek et al., 1995) (discussed in chapter 3) strongly suggest the participation of these mural cells in the recruitment of leukocytes. In addition, *in vivo* 3D data obtained within our laboratory has been shown that neutrophils preferentially breach the pericyte sheath through gaps between adjacent cells (Wang et al., 2006). More recently, these sites have been shown to transiently enlarge in response to TNF and IL-1β (Proebstl et al., 2012; Wang et al., 2012). Hence, we hypothesise that pericyte shape change might facilitate leukocyte transmigration through a yet unknown mechanism.

TNF- and IL-1β-induced pericyte gap enlargement in postcapillary venules of the cremaster muscle, as induced by local injection of the cytokines, is independent of the presence of neutrophils (Proebstl Doris, 2011; Proebstl et al., 2012). The aim of this chapter was to extent these findings to different types of inflammatory mediators. In the present study, pericyte shape change was analysed in conditions when inflammation was induced by potent neutrophil chemoattractants, namely LTB_4, KC, C5a and fMLP. In contrast to cytokines, which are well known to act directly on vessel wall components such as ECs (Dinarello, 2000), the primary target of chemoattractants is leukocytes (Adams and Lloyd, 1997). In fact, chemoattractants provide directional cues for these cells and hence, allow leukocytes to rapidly migrate towards the site of inflammation. Chemoattractant signals are released endogenously by cells of the immune system and tissue cells upon activation or derived directly from bacterial sources. They are associated with the ability to stimulate specific leukocyte subtypes via primarily G-protein coupled receptors (GPCRs) (Adams and Lloyd, 1997). The main neutrophil chemoattractants include “intermediate” chemoattractants including endogenous lipids such as leukotriene B4 (LTB_4), and CXC chemokines such as

CXCL1/keratinocyte-derived chemokine (KC) and CXCL2/monocyte-inhibitory protein-2 (MIP-2) and “end-target” chemoattractants such as bacterial peptides (e.g. formyl-methionyl-leucyl-phenylalanine (fMLP)) and components of the complement cascade (such as C5a) (Phillipson and Kubes, 2011). These different types of chemoattractants provide a multistep hierarchy of directional cues, with endothelial- and immune-derived intermediate chemoattractants as the first molecular guidance signals regulating directional neutrophil crawling, followed by a prioritised gradient of short-range cues secreted by pathogens (*i.e*. end-target chemoattractants). Chemoattractants act through their respective receptor on target cells, which are all related to the large family of seven-transmembrane-domain rhodopsin-like G protein-coupled receptors (Murphy, 1994). Besides broadly overlapping roles in inducing chemotaxis and adhesion of leukocytes, chemoattractants may have specialised functions in regulating inflammatory responses by stimulating leukocyte degranulation.

In the present chapter, the effect of the neutrophil chemoattractants LTB_4, KC, C5a and fMLP on pericyte morphology was analysed *in vivo*. For this purpose, the murine cremaster muscle was used. Tissue infiltration of neutrophils and pericyte shape change were analysed *ex vivo* by wholemount immunostaining using specific markers for neutrophils and pericytes (MRP-14 and αSMA, respectively), and viewed by confocal microscopy.

4.2 RESULTS

4.2.1 Effect of neutrophil chemoattractants on pericyte morphology in cremasteric postcapillary venules

To analyse the effect of LTB_4, KC, C5a and fMLP on pericyte morphology, cremaster muscles were stimulated locally by i.s. injection. Initial experiments were performed to establish optimal experimental conditions including doses of the respective chemoattractant and/or duration of cremaster muscle stimulation.

The initial doses used for LTB_4, KC, and fMLP in this study were selected based on previous experiments from our group at which significant leukocyte transmigration is elicited in the murine cremaster muscle. In preliminary experiments, the *in vivo* test period for these chemoattractants was established in which a significant change in pericyte morphology could be observed. To induce local inflammation in the cremaster muscle, 30 ng LTB_4, 500 ng KC, or 5 µg fMLP in 300 µl PBS were injected into WT C57BL/6 mice by i.s. injection. 300 µl PBS alone was used as control. After an *in vivo* test period of 2 or 4 h, cremaster muscles were dissected away from the mice, fixed in 4% PFA and immunostained for pericytes and leukocytes using specific markers (αSMA, MRP-14, respectively). Whole-mounted immunofluorescently labelled tissues were then analysed for neutrophil infiltration and pericyte-shape change using confocal microscopy and ImageJ, IMARIS, respectively (as described in section 2.3.8). Some tissues treated with KC for 4 h were prepared by Dr. Mathieu Benoit-Voisin and Amar Ladwa. Independent experiments were performed at least 4 times.

Local injection of LTB_4, KC, and fMLP induced neutrophil transmigration responses that were very low and/or absent in PBS-treated controls (Figure 4.1). Significant LTB_4-induced neutrophil extravasation could be detected 4 h post injection (Figure 4.1b, left). Both, KC and fMLP elicitated neutrophil transmigration within 2 h of stimulation, which was sustained up to 4 h post injection (Figure 4.1b, middle and right). 3D-reconstruced confocal images of postcapillary venules further showed that this response was associated with a change in pericyte morphology as seen through enlargement of gaps between adjacent pericytes (Figure 4.2a, 4.3a and 4.4a). LTB_4 and fMLP stimulation induced significant increase in mean gap size by 4 h post injection as compared to control samples (Figure 4.2b, 4.4b, respectively). Mean gap size under control conditions (PBS) was 7.2 ± 0.26 μm^2. Local injection of LTB_4 and fMLP (both for 4 h) resulted in a mean gap size between adjacent

postcapillary pericytes of 13 ± 0.32 μm^2, 12.54 ± 0.96 μm^2, respectively. In contrast, gap enlargement between adjacent pericytes induced by KC occurred at an earlier time point as a significant increase could be detected 2 h after injection (mean gap size: 12.47 ± 0.6 μm^2; Figure 4.3b). Furthermore the effect of these chemoattractants on the gap density of adjacent pericytes was assessed as defined by the average number of gaps per vessel area (per 1 mm^2). The average gap density of PBS-treated cremaster muscles was 6.649 ± 1.979 gaps/mm^2 and did not significantly change upon stimulation with LTB_4, KC, and fMLP at all time points investigated (Figure 4.2b, 4.3b and 4.4b).

As no reference point for C5a was available in this model, a dose-response curve for C5a to elicit leukocyte transmigration was established. WT C57BL/6 mice received either 100, 300 or 1000 ng C5a in 300 µl PBS or 300 µl PBS alone i.s. 4 h after injection, cremaster muscles were dissected away from the mice, fixed and whole mount tissues were used for immunofluorescence labelling and confocal microscopy as described above. Significant increases in neutrophil transmigration were detected with 300 and 1000 ng C5a, but not 100 ng (Figure 4.5), thus the dose of 300 ng/ 300 µl PBS was used for quantifications of pericyte gaps. As seen in 3D-reconstruced confocal images of postcapillary venules this dose also provoked a significant enlargement of gaps between adjacent pericytes with a mean gap size of 13.64 ± 0.52 μm^2 at 4 h post injection (Figure 4.6). As seen with LTB_4, KC and fMLP, local injection of C5a had no effect on pericyte gap density in this model (Figure 4.6b, right).

In summary, all tested chemoattractants induced pericyte shape change resulting in significant increases in gap size between adjacent cells with an average of 80% as compared to control animals. In contrast, but in agreement with our previous results(Proebstl et al., 2012; Voisin et al., 2010), the average gap density did not significantly change in stimulated tissues (~6600 gaps per mm^2 of vessel surface).

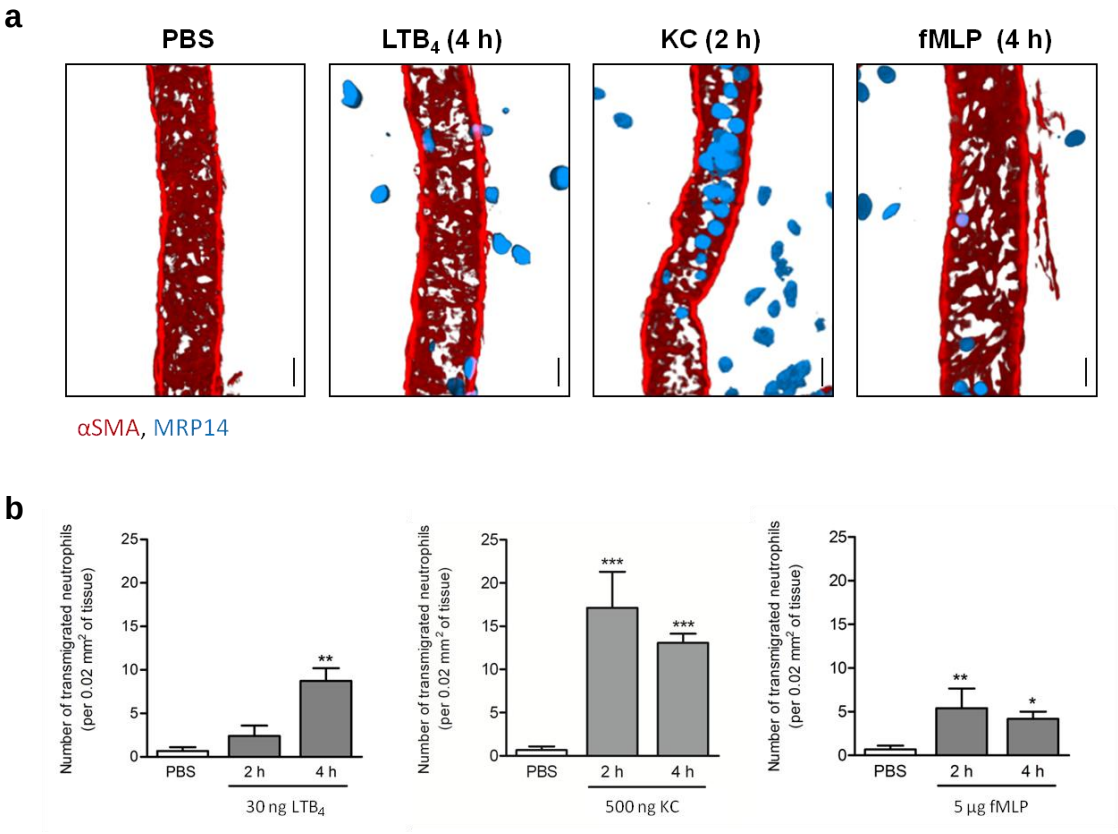

Figure 4.1: LTB_4-, KC- and fMLP-induced neutrophil transmigration. Cremaster muscles of WT C57BL/6 mice were treated with LTB_4 (30ng), KC (500 ng), fMLP (5 µg) or PBS and were dissected away 2 or 4 h after i.s. injections. Tissues were fixed, immunostained for pericytes (αSMA, red) and neutrophils (MRP-14, blue) and analysed for transmigrated neutrophils by confocal microscopy and IMARIS. **(a)** Representative 3D-reconstructed confocal images of post-capillary venules in PBS-, LTB_4-, KC- and fMLP-stimulated cremaster muscles illustrating neutrophil responses are shown. Bars, 20 µm. **(b)** The number of extravasated neutrophils adjacent to 200 µm vessel segments and within 50 µm away from the vessel (0.02 mm^2 area) was quantified in images of 2 or 4 h treated tissues. White Bars represent control samples (PBS, 2 and 4 h pooled together) and grey bars correspond to stimulated tissues (LTB_4, KC or fMLP, for 2 or 4 h). At least 6 vessel segments per mouse (3 per cremaster) were analysed and plotted as mean per mouse. Data are represented as the mean ±SEM of at least 4 mice per condition. Significant differences between groups were determined using one-way ANOVA and Neuman-Keuls multiple comparison test. Differences compared to PBS control are indicated by * ($p < 0.05$), ** ($p < 0.01$) and *** ($p < 0.001$).

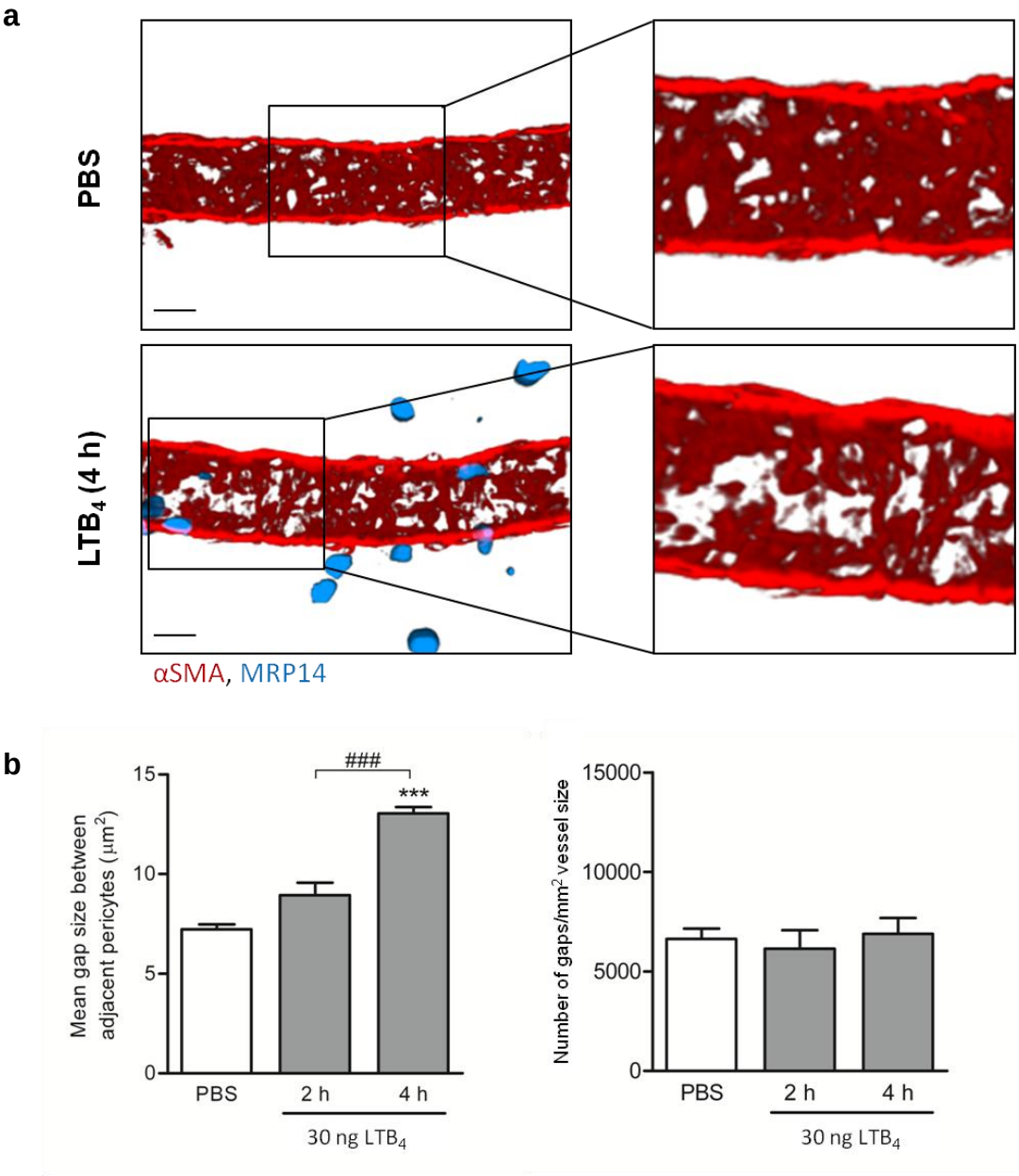

Figure 4.2: LTB_4-induced changes in pericyte gaps. Changes in pericyte gap size and density were quantified in 3D-reconstruced confocal images of cremaster muscles stimulated with LTB_4 or PBS for 2 or 4 h using ImageJ. Images used for analysis were the same as analysed for Figure 4.1. **(a)** Representative 3D-reconstructed confocal images of post-capillary venules in PBS- or LTB_4 (30 ng)-stimulated cremaster muscles illustrate neutrophils (blue) and pericytes (red) with gaps between adjacent cells. The right panels show magnifications of the αSMA channel of the region outlined in the left panels. Bars, 20 µm. **(b)** Pericyte gaps were quantified for their size (left graph) and density (right graph) in 200 µm vessel segments of 2 and 4 h treated tissues. White Bars represent control samples (PBS, 2 and 4 h pooled together) and grey bars correspond to LTB_4- stimulated tissues. At least 6 vessel segments per mouse (3 per cremaster) were analysed and plotted as mean per mouse. Data are represented as the mean ±SEM of at least 4 mice per condition. Significant differences between groups were determined using one-way ANOVA and Neuman-Keuls multiple comparison test. Differences compared to PBS control are marked with asterisks. Differences between time points were marked with hashes. (*** and ###: $p < 0.001$)

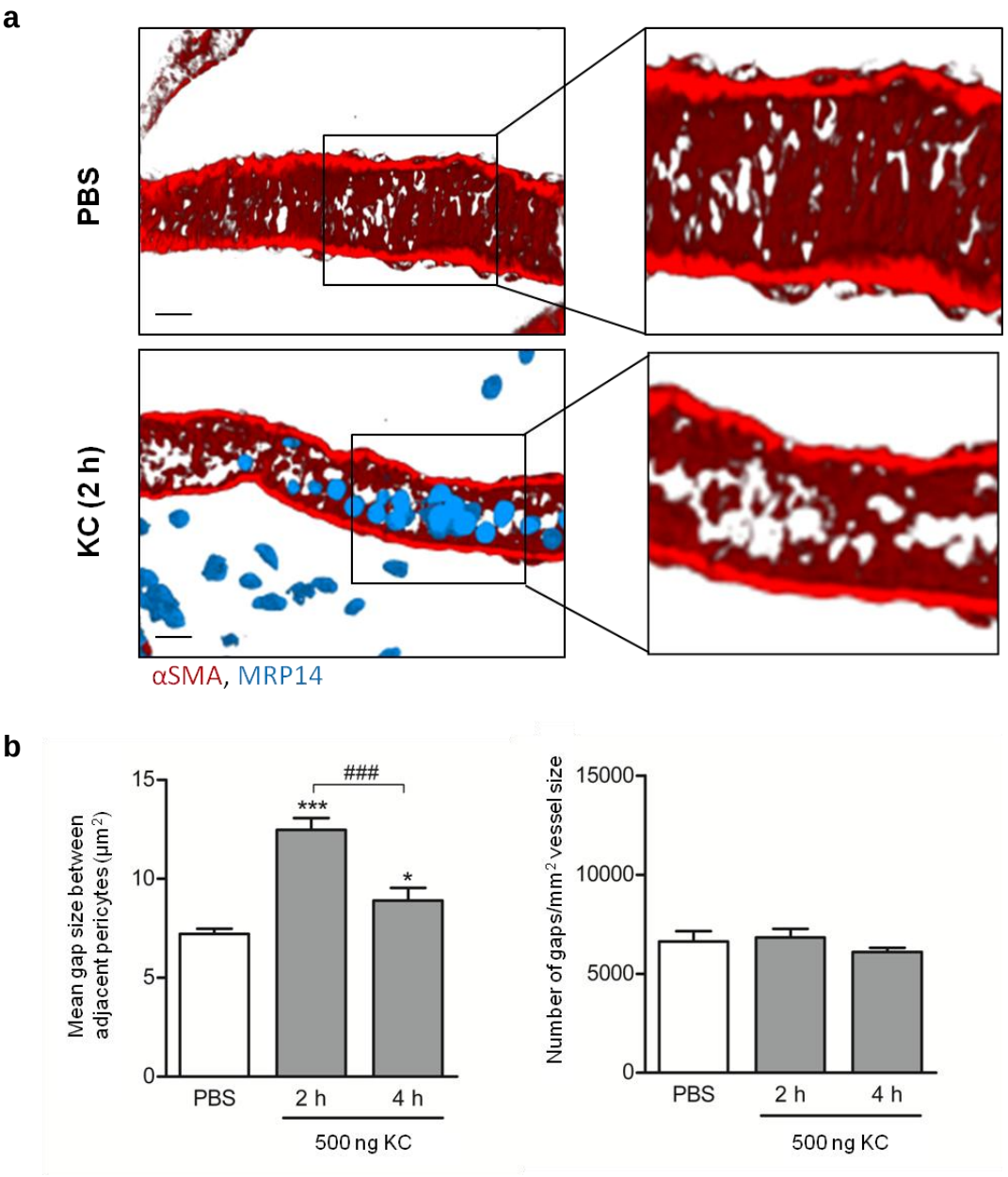

Figure 4.3: KC-induced changes in pericyte gaps. Changes in pericyte gap size and density were quantified in 3D-reconstruced confocal images of cremaster muscles stimulated with KC (500 ng) or PBS for 2 or 4 h using ImageJ. Images used for analysis were the same as analysed for Figure 4.1. **(a)** Representative 3D-reconstructed confocal images of post-capillary venules in PBS- or KC-stimulated cremaster muscles illustrate neutrophils (blue) and pericytes (red) with gaps between adjacent cells. The right panels show magnifications of the αSMA channel of the region outlined in the left panels. Bars, 20 µm. **(b)** Pericyte gaps were quantified for their size (left graph) and density (right graph) in 200 µm vessel segments of 2 and 4 h treated tissues. White Bars represent control samples (PBS, 2 and 4 h pooled together) and grey bars correspond to KC- stimulated tissues. At least 6 vessel segments per mouse (3 per cremaster) were analysed and plotted as mean per mouse. Data are represented as the mean ±SEM of at least 4 mice per condition. Significant differences between groups were determined using one-way ANOVA and Neuman-Keuls multiple comparison test. Differences compared to PBS control are marked with asterisks. Differences between time points were marked with hashes. (*: $p < 0.05$; *** and ###: $p < 0.001$)

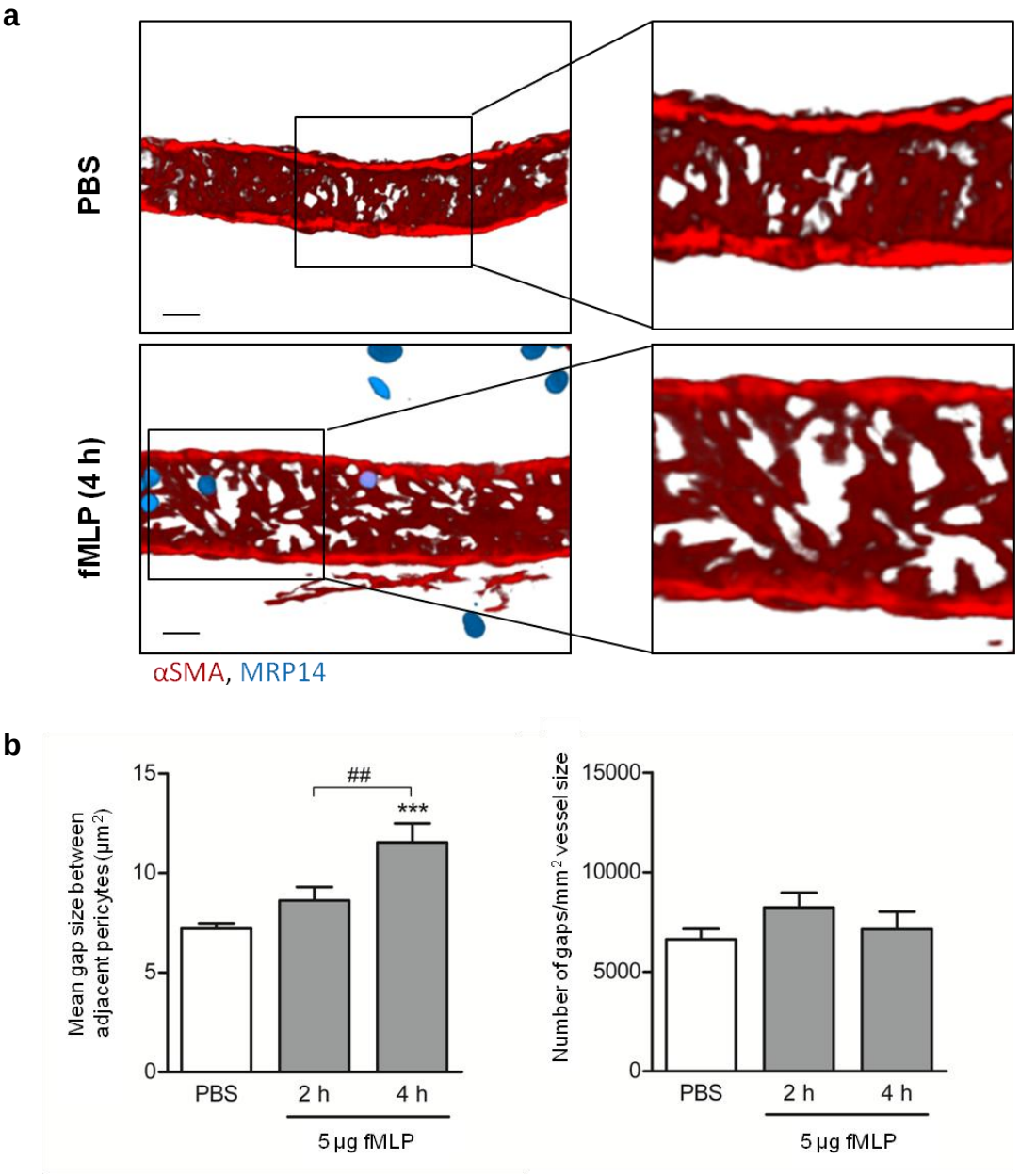

Figure 4.4: fMLP-induced changes in pericyte gaps. Changes in pericyte gap size and density were quantified in 3D-reconstruced confocal images of cremaster muscles stimulated with fMLP (5 µg) or PBS for 2 or 4 h using ImageJ. Images used for analysis were the same as analysed for Figure 4.1. **(a)** Representative 3D-reconstructed confocal images of post-capillary venules in PBS- or fMLP-stimulated cremaster muscles illustrate neutrophils (blue) and pericytes (red) with gaps between adjacent cells. The right panels show magnifications of the αSMA channel of the region outlined in the left panels. Bars, 20 µm. **(b)** Pericyte gaps were quantified for their size (left graph) and density (right graph) in 200 µm vessel segments of 2 and 4 h treated tissues. White Bars represent control samples (PBS, 2 and 4 h pooled together) and grey bars correspond to fMLP- stimulated tissues. At least 6 vessel segments per mouse (3 per cremaster) were analysed and plotted as mean per mouse. Data are represented as the mean ±SEM of at least 4 mice per condition. Significant differences between groups were determined using one-way ANOVA and Neuman-Keuls multiple comparison test. Differences compared to PBS control are marked with asterisks. Differences between time points were marked with hashes. (##: $p < 0.01$; ***: $p < 0.001$)

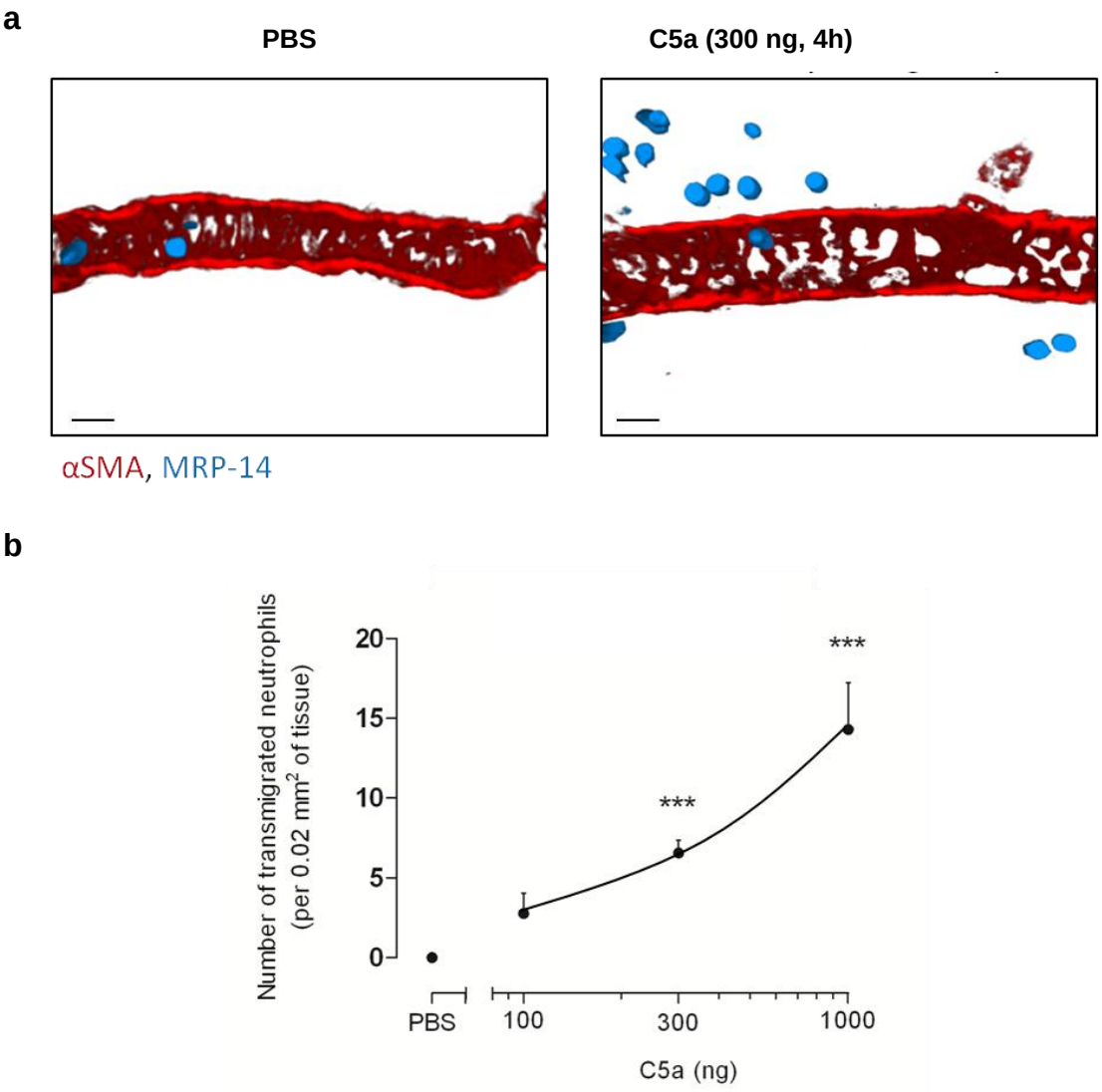

Figure 4.5: C5a-induced neutrophil transmigration. Cremaster muscles of WT C57BL/6 mice were treated with 100, 300, or 1000 ng C5a in 300 µl PBS or PBS alone and dissected 4 h after i.s. injections. Tissues were fixed, immunostained for pericytes (αSMA, red) and neutrophils (MRP-14, blue) and analysed for neutrophil transmigration by confocal microscopy and IMARIS. **(a)** Representative 3D-reconstructed confocal images of post-capillary venules in PBS- and 300 ng C5a- treated cremaster muscles illustrating neutrophil responses are shown. Bars, 20 µm. **(b)** The number of extravasated neutrophils adjacent to 200 µm vessel segments and within 50 µm away from the vessel (0.02 mm^2 area) was quantified using images of tissues treated with PBS or 100, 300, or 1000 ng C5a for 4 h. A dose-response curve is shown. At least 6 vessel segments per mouse (3 per cremaster) were analysed and plotted as mean per mouse. Data are represented as the mean ±SEM of 3 mice per condition. Significant differences between groups were determined using one-way ANOVA and Neuman-Keuls multiple comparison test. Differences compared to PBS control are indicated by *** ($p < 0.001$).

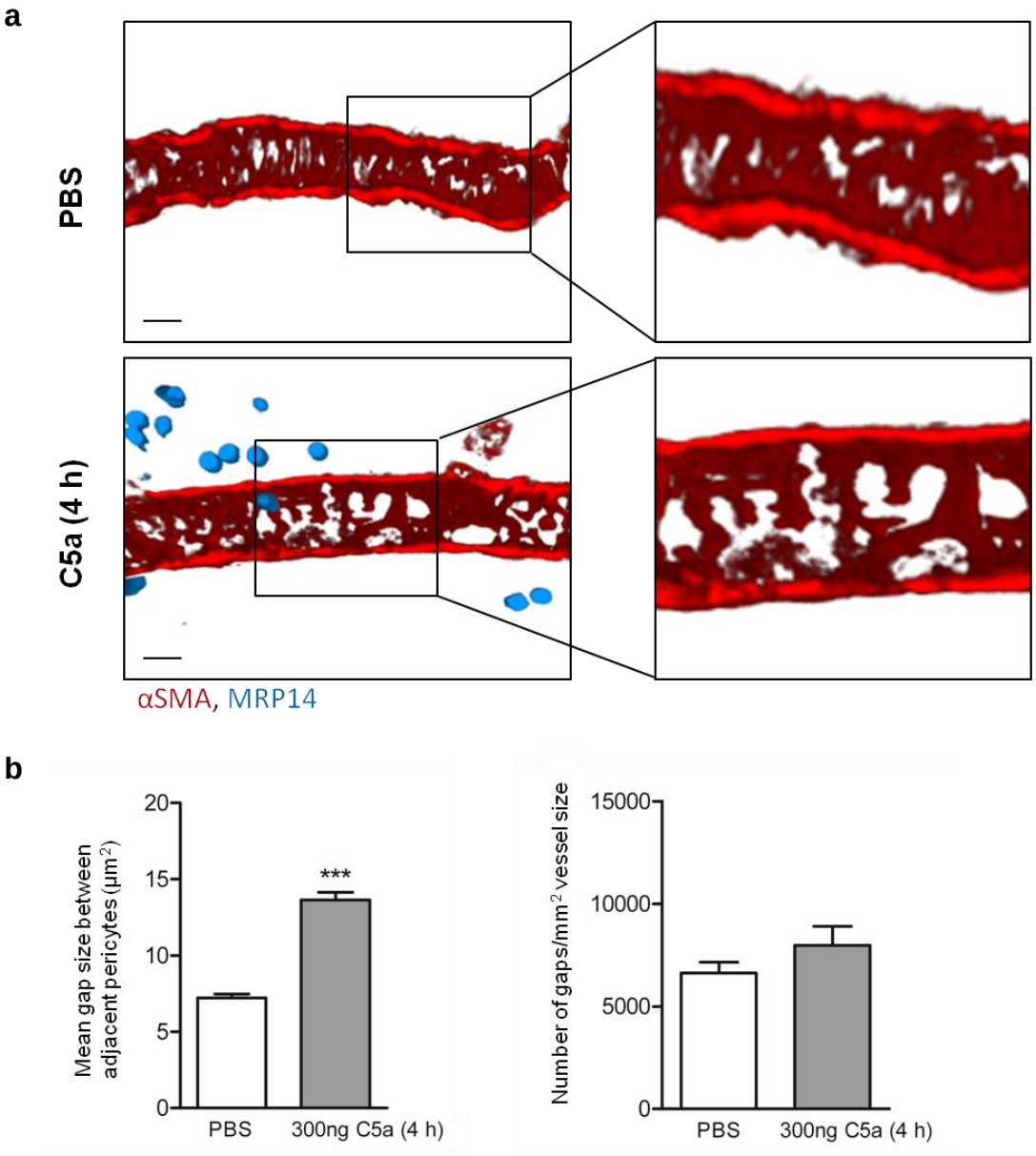

Figure 4.6: C5a-induced changes in pericyte gaps. Changes in pericyte gap size and density were quantified in 3D-reconstruced confocal images of cremaster muscles stimulated with 300 ng C5a or PBS for 4 h using ImageJ. Images used for analysis were the same as analysed for Figure 4.5. **(a)** Representative 3D-reconstructed confocal images of post-capillary venules in PBS- or C5a-stimulated cremaster illustrate neutrophils (blue) and pericytes (red) with gaps between adjacent cells. The right panels show magnifications of the αSMA channel of the region outlined in the left panels. Bars, 20 µm. **(b)** Pericyte gaps were quantified for their size (left graph) and density (right graph) in 200 µm vessel segments of 4 h treated tissues. White Bars represent control samples (PBS) and grey bars correspond to C5a- stimulated tissues. At least 6 vessel segments per mouse (3 per cremaster) were analysed and plotted as mean per mouse. Data are represented as the mean ±SEM of 3 mice per condition. Significant differences between groups were determined using one-way ANOVA and Neuman-Keuls multiple comparison test. Differences compared to PBS control are indicated by *** ($p < 0.001$)

4.2.2 Time course of LTB_4-induced changes in pericyte morphology

To characterise the effect of chemoattractants on pericytes in more detail, time course experiments of LTB_4-induced pericyte shape change was analysed. Inflammation was induced locally by intrascrotal injection of 30ng LTB_4 in 300 µl PBS for 2, 3, 4, 6, 8, 24, 48 and 72 h. Control mice received 300 µl PBS alone. Pericyte shape change was analysed *ex vivo* by wholemount immunostaining and confocal microscopy as described before. At least 3 independent experiments were performed for each treatment.

LTB_4 stimulation led to a gradual and time-dependent increase in mean gap size between 2-8 h after injection of the stimulus as compared to control samples (Figure 4.7, left). Although not significant, a change in pericyte gap size was already noted at 2 h post LTB_4 injection ($p > 0.05$), resulting in a mean gap size of 8.95 ± 0.62 μm^2 and a 24% increase as compared to PBS-injected control tissues. Maximum gap size was achieved within 4 h of LTB_4 treatment (13 ± 0.32 μm^2 and 80% increase as compared to controls). This response was transient and time points beyond 4 h indicated a time-dependent decrease of the size of αSMA-negative areas. Pericyte gap size returned to basal levels by 48 h of LTB_4 stimulation (6.03 ± 0.82 μm^2). The average gap density of PBS-treated cremaster muscles was 7,649 ± 1,979 gaps/mm^2 and did not significantly change upon LTB_4 stimulation at all time points investigated (Figure 4.7, right).

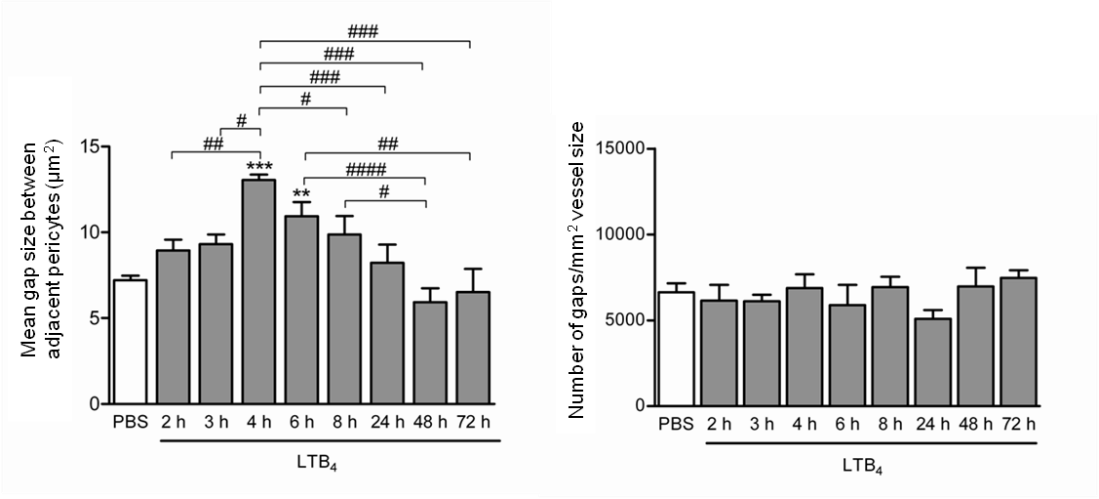

Figure 4.7: LTB_4 induces a time-dependent change in pericyte gap size. Changes in pericyte morphology were quantified in 3D-reconstruced confocal images of cremaster muscles stimulated with LTB_4 (30 ng) or PBS for the indicated *in vivo* test period using ImageJ. Pericyte gaps were quantified for their size (left graph) and density (right graph) in 200 µm vessel segments. White Bars represent control samples (PBS, 2-72h pooled together) and grey bars correspond to LTB_4-stimulated tissues. At least 4 vessel segments per mouse were analysed and plotted as mean per mouse. Data are represented as the mean ±SEM of at least 3 mice per time point. Significant differences between groups were determined using one-way ANOVA and Neuman-Keuls multiple comparison test. Differences compared to PBS control are marked with asterisks. Differences between time points were marked with hashes. (**: $p < 0.01$, ***: $p < 0.001$, #: $p < 0.05$, ##: $p < 0.01$, ###: $p < 0.001$)

4.2.3 Profile of neutrophil transmigration in relation to pericyte gap enlargement

Notably, increased pericyte gap size was associated with an increase in neutrophil transmigration. To compare the time course of neutrophil transmigration in relation to pericyte gap size in more detail, the same confocal images of post-capillary venules as analysed in the previous section (section 4.2.2) were also analysed for extravasated neutrophils (MRP-14 positive cells).

At base line conditions (PBS treatment), only few MRP-14-positive cells were found within the tissue (Figure 4.8, left). Similar to pericyte gap enlargement, i.s. injection of 30 ng LTB_4 elicited neutrophil infiltration in a time-dependent manner starting within 2 h and a peak at 4 h post injection. Time points beyond 4 h indicated a gradual decrease in the neutrophil transmigration response. Although not statistically significant (likely because of a high variability and relatively low n-number), it appears that neutrophils are present within the tissue up to 24 h. Data presented here demonstrate that both, pericyte gap opening and neutrophil transmigration peaked at similar time points (4 h post injection of LTB_4) before returning back to basal levels by 48 h (Figure 4.8). The comparable time frames of these responses suggest a correlation between neutrophil recruitment and pericyte shape change. Thus, the contribution of neutrophils to chemoattractant-induced morphological changes of cremaster muscle venular pericytes was analysed as detailed in the following chapter (chapter 5).

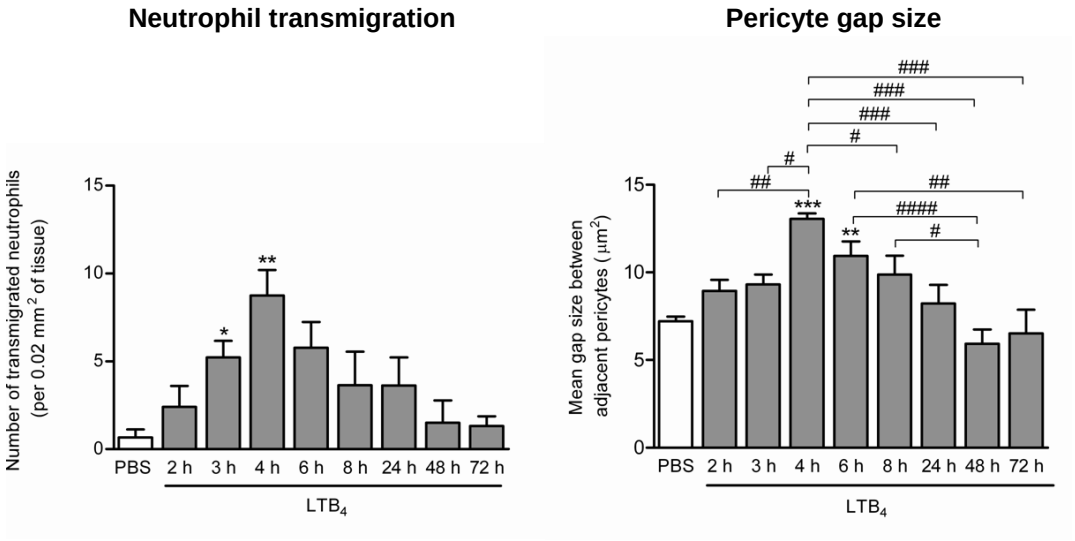

Figure 4.8: Time course of LTB_4-induced neutrophil transmigration and pericyte shape change. Neutrophil and pericyte responses were quantified in 3D-reconstruced confocal images of cremaster muscles stimulated with LTB_4 (30 ng) or PBS for the indicated *in vivo* test period using ImageJ. Images used for analysis were the same as those analysed for Figure 4.7. The number of extravasated neutrophils was quantified adjacent to 200 µm vessel segments and within 50 µm away from the vessel (0.02 mm^2 area) (left). White Bars represent control samples (PBS, 2-72 h pooled together) and grey bars correspond to LTB_4-stimulated tissues. At least 4 vessel segments per mouse were analysed and plotted as mean per mouse. Data are represented as the mean ±SEM of at least 3 mice per time point. Significant differences between groups were determined using one-way ANOVA and Neuman-Keuls multiple comparison test. Differences compared to PBS control are marked with asterisks. Differences between time points were marked with hashes. (**: $p < 0.01$, ***: $p < 0.001$, #: $p < 0.05$, ##: $p < 0.01$, ###: $p < 0.001$)

4.3 DISCUSSION

Data acquired in chapter 3 demonstrated that pericyte-like cells are able to respond to pro-inflammatory cytokines (TNF and IL-1β) by inducing the upregulation of adhesion molecules on their surface. This result suggests that pericytes might be able to directly interact with transmigrating leukocytes and thereby facilitate their penetration of the pericyte sheath. Supporting this idea, leukocytes have been shown to migrate on the abluminal side of ECs along pericyte processes for a significant amount of time in an ICAM-1-dependent manner, before breaching the pericyte layer through gaps between adjacent pericytes (Proebstl et al., 2012). Of interest, these gaps increase in size in response to TNF and IL-1β and transmigrating neutrophils appear to preferentially use enlarged pericyte gaps (Proebstl et al., 2012; Wang et al., 2012). Hence, in addition to direct interaction with leukocytes, pericytes may guide transmigrating leukocytes through the pericyte layer via altered pericyte morphology. When using TNF and IL-1β as inflammatory stimuli, pericyte shape change occurred in a neutrophil-independent manner, and together with the expression of TNFRs and IL-1R on pericytes, this indicates a direct effect of these cytokines on pericytes. To extend these findings to other types of inflammatory mediators, here the impact of a wide range of neutrophil chemoattractants (LTB_4, KC, C5a and fMLP) on pericyte morphology was investigated.

The model employed was that of the mouse cremaster muscle which through its thin and transparent nature enables high resolution analysis of changes in vascular morphology as observed and quantified by immunofluorescent staining and confocal microscopy (Proebstl et al., 2012; Voisin et al., 2009; Voisin et al., 2010; Wang et al., 2006). The findings presented in this chapter show for the first time that chemoattractants (*i.e*. LTB_4, KC, C5a and fMLP) can induce pericyte gap enlargement. However, the average gap density did not significantly change upon stimulation (~6600 gaps per mm^2 of vessel surface) as previously noted for other stimuli (Voisin et al., 2010). This finding indicates that the increase in area likely represents a true enlargement of pre-existing gaps rather than aggregation of several gaps or the generation of new permissive regions.

Cell contraction was the first function suggested for pericytes and described some 100 years earlier by the French scientist and discoverer of pericytes Charles-Marie Benjamin Rouget. With evolving imaging techniques, pericyte contractility could be analysed in more detail and has to date been demonstrated in response to several

vasoactive factors and neurotransmitters (Attwell et al., 2010; Hamilton et al., 2010). Molecular analyses led to the discovery of the activation of kinases with a role in the regulation of vasoconstriction within pericytes (Joyce et al., 1984; Joyce et al., 1985). These kinases include actin, myosin, tropomyosin and cyclic GMP-dependent protein kinase. Of interest, shape change (contractility/relaxation) of pericytes in inflammatory scenarios (*i.e*. stimulation with TNF, IL-1β and LPS) has already been demonstrated for rat lung pericytes *in vitro* (Kerkar et al., 2006; Khoury and Langleben, 1998; Speyer et al., 2000). There is also evidence to suggest that pericyte contractility might be regulated by members of the Rho family of small GTPases (Bryan and D'Amore, 2007; Kutcher and Herman, 2009). More specifically, a study using bovine retinal pericytes identified RhoA as a mediator of pericyte shape change through the disassembly of αSMA stress fibres and formation of non-muscle actin stress fibres. In contrast, other Rho GTPases (Ras-related small GTPases Rac 1 and cdc42) do not seem to be involved in this process (Kolyada et al., 2003; Kutcher et al., 2007). Notably, cytokine-induced pericyte gap opening was recently associated with disassembly of stress fibres and focal adhesion sites and as such it has been suggested that pericyte shape change may occur as a result of cell relaxation rather than contraction (Wang et al., 2012). In this study inhibition of RhoA/Rho kinase (ROCK) signalling and suppression of actomyosin-based contractility upon leukocyte-pericyte interaction *in vitro* led to shape change of mouse primary pericytes. However, at present it is unclear whether the pericyte shape change noted in the mouse cremaster tissue is as a result of cell relaxation or contraction.

In addition, although several studies have shown that pericytes generally exhibit the ability to undergo shape change during inflammatory conditions, the functional role of this phenomenon is yet unknown. Pericyte contraction has most notably been associated with capillary constriction, however, no convincing evidence has to date been found for a definitive role of pericyte shape change in regulating blood flow at the microvascular level (reviewed in (Armulik et al., 2011)). Pericyte shape change during inflammatory conditions might facilitate leukocyte transmigration through enhanced permissiveness to infiltrating cells, the establishment of a chemotactic gradient, regulation of blood flow or other unknown mechanisms.

Although cytokines have previously been shown to induce pericyte shape change both *in vitro* (Kerkar et al., 2006) and *in vivo* (Proebstl et al., 2012; Wang et al., 2012), this is the first report that demonstrates the ability of pericytes to respond to

chemoattractants. All analysed chemoattractants are potent neutrophil stimulators and several studies demonstrate the requirement of neutrophils to induce changes in the vessel wall (e.g. opening of EC junctions and BM remodelling) in response to chemoattractants such as LTB_4 *in vivo* (Bjork et al., 1982; Wedmore and Williams, 1981; Williams and Jose, 1981). Based on these studies, the role of neutrophils in pericyte shape change as mediated by these stimuli was investigated next. In time course experiments, the timeframe of LTB_4-induced pericyte gap enlargement was compared with neutrophil transmigration in the same tissues. Post-capillary venules of the cremaster muscle showed a time-dependent increase in pericyte gap size following LTB_4 stimulation, with a peak at 4 h post injection. Pericyte gap enlargement then gradually returned to basal levels between 4-24 h after LTB_4 treatment. These findings indicate that at sites of inflammation pericytes undergo a time-dependent and transient shape change which may account for their proposed role in regulating microvascular permeability under inflammatory conditions (Hellstrom et al., 2001; Leveen et al., 1994; Sims et al., 1990; Sims et al., 1994).

As expected, local injection of LTB_4 elicited neutrophil transmigration in a time-dependent manner. Interestingly, time course analysis of LTB_4-induced inflammation showed a direct correlation between tissue infiltration of neutrophils and pericyte gap opening, with both responses peaking at 4 h. This is in contrast to TNF-induced inflammation, where pericyte gap enlargement precedes neutrophil transmigration, as has been shown by our group (Proebstl et al., 2012). In addition, the onset and termination of pericyte gap opening has been shown to occur earlier in response to TNF as compared to LTB_4 in the present work. As pericytes express receptors for TNF, the effect of this cytokine on changes in pericyte morphology are considered to be direct and hence possibly more rapid. Hence, these results suggest a role for neutrophils in chemoattractant-, but not cytokine-induced pericyte shape change.

In summary, this chapter describes for the first time the ability of pericytes to respond to neutrophil chemoattractants as indicated by pericyte shape change in chemoattractant-stimulated tissues. The functional consequence of this response is at present unclear, but the observed changes in pericyte shape might contribute to the overall pro-inflammatory effects of certain stimuli. Time course experiments further provided indications for a role for neutrophils in this response, a possibility that was examined as part of the following chapter (chapter 5). However, the underlying mechanism remains to be elucidated, which is part of the next chapter.

CHAPTER 5: MECHANISM OF CHEMOATTRACTANT-INDUCED PERICYTE SHAPE CHANGE *IN VIVO*

5.1 INTRODUCTION

The findings described in chapter 4 showed the ability of neutrophil chemoattractants to act on pericytes by inducing pericyte shape change *in vivo.* In these experiments, pericyte shape change resulted in a marked increase in mean gap size between adjacent cells. The aim of the present chapter was to extend these results by dissecting the mechanism through which these factors induce the observed pericyte shape change. As neutrophils are the main target for the analysed chemoattractants (*i.e.* LTB_4, KC, C5a and fMLP), here the role of neutrophils and neutrophil-derived factors in pericyte gap enlargement was investigated.

Although there exists a wide range of structurally different neutrophil chemoattractants, biochemical and molecular analysis have demonstrated several similarities of functions and mechanisms of actions of chemoattractants on neutrophils (Murphy, 1994; Murphy, 1996). For instance, all of them bind to GPCRs of the 7 transmembrane spanning protein family (Murphy, 1994; Pierce et al., 2002). Members of these receptors include the formyl peptide receptor 1 (FPR1), chemokine receptors of the CCR and CXCR families, leukotriene receptors BLTs and C5aR that are all expressed on the surface of neutrophils. During acute inflammation, chemoattractants mediate rapid neutrophil accumulation in the vascular lumen and guide leukocyte migration through the vessel wall into the tissue (Fernandez et al., 1978; Ford-Hutchinson et al., 1980; Schiffmann et al., 1975). In addition, chemoattractants activate neutrophils by inducing degranulation and release of degrading enzymes, antimicrobial molecules, pro-inflammatory stimuli and production of oxygen-derived free radicals (Dahinden et al., 1983; Goetzl and Pickett, 1980; Showell et al., 1982; Sumimoto et al., 1984). Besides directly acting on neutrophils, chemoattractants can indirectly induce changes in vascular wall properties such as vasodilatation and reduced barrier function of vessels (Hurley J.V., 1964; Bjork et al., 1982; Wedmore and Williams, 1981). Specifically, chemoattractants have been shown to indirectly act on ECs by inducing the opening of EC junctions and impairing its barrier function to plasma fluid and macromolecules, an effect that occurred in a neutrophil-dependent manner (Bjork et al., 1982; Wedmore and Williams, 1981). In addition, a number of studies have

demonstrated the ability of chemoattractants to mediate vascular BM remodelling via neutrophil activation (Hurley J.V., 1964; Reichel et al., 2009; Voisin et al., 2010; Voisin et al., 2009). In this context, recent data from our group and others have shown that neutrophil transmigration as induced by a variety of stimuli is associated with enlargement of regions within the venular BM that exhibit lower protein expression (LERs) (Reichel et al., 2009; Voisin et al., 2010; Voisin et al., 2009). The findings of the present study for the first time reports on the impact of neutrophil chemoattractants on pericytes as demonstrated by pericyte shape change *in vivo*. Although neutrophils have been shown to play an important role in mediating changes in the vessel wall, *i.e*. in inducing vascular permeability and BM remodelling, the precise mechanisms through which these responses are mediated is less well understood. Work presented in the previous chapter gave indications for a temporal association between chemoattractant-induced neutrophil migration and pericyte gap opening. Hence, as part of this chapter the role of neutrophils in chemoattractant-induced pericyte gap opening and the potential role of neutrophil-derived secondary mediators in this response was investigated.

5.2 RESULTS

5.2.1 Role of neutrophils in chemoattractant-induced pericyte shape change

To analyse the mechanism by which chemoattractants induce pericyte shape change, the role of neutrophils in this response was analysed in mice depleted of their circulating neutrophils. For this purpose, WT mice received a single dose of 100 µg anti-GR1 antibody RB6-8C5 i.p. 24 h before inflammation was induced. Control mice received either rat IgG i.p. and PBS i.s., anti-GR1 i.p. and PBS i.s., or rat IgG i.p. and LTB_4 i.s. Three independent experiments were performed.

Pericyte gaps were quantified for their size and density 4 h post LTB_4 injection by immunofluorescent staining and confocal microscopy as previously described (chapter 2, section 2.3.8). Furthermore, the amount of neutrophils within a blood sample taken before and after antibody treatment and the level of extravasated neutrophils in the tissue were assessed. As confirmed by Kimura staining and confocal microscopy, treatment with the anti-GR1 antibody depleted almost all neutrophils (> 80%) (Figure 5.1, left). In contrast, a high number of extravasated neutrophils were present when mice were treated with the IgG control in response to LTB_4. Whilst mice treated with the control antibody showed an increase in pericyte gap size 4 h post LTB_4 injection, this increase was absent in neutrophil-depleted mice (Figure 5.1, right). These results indicate that neutrophils can mediate the enlargement of pericyte gaps following LTB_4 stimulation.

As the concentration of the GR1-antibody used for the experiments described above appeared to also deplete monocytes, based on these experiments the potential involvement of monocytes/macrophages in mediating pericyte shape change cannot be ruled out. Thus, a more specific protocol for analysis of the role of neutrophils in this response was next employed. To induce specific neutropenia, WT mice or mice exhibiting green monocytes ($CX_3CR_1^{GFP/+}$ mice) were injected with a lower dose of anti-GR1 antibody (25 µg) given i.p. over 3 days prior to induction of inflammatory reactions as previously described(Voisin et al., 2009). Treatment with the anti-GR1 antibody depleted almost all circulating neutrophils (> 82%), but not monocytes as confirmed by flow cytometry in $CX3CR1^{GFP/+}$ animals (Figure 5.2).

Using this protocol, quantitative analysis using confocal microscopy of immunofluorescently stained cremaster muscles showed no neutrophil infiltration in mice depleted of their circulating neutrophils in response to LTB_4 (4 h) as compared

to control IgG antibody-treated animals (Figure 5.3, left and 5.4 top). In contrast, monocyte transmigration in GR1-treated animals was similar to the response obtained in animals injected with an IgG control antibody and relatively low as compared to neutrophils in undepleted animals (Figure 5.3, right).

Similar to the experiments described above (using the high dose of GR-1 antibody) the specific depletion of neutrophils also abolished LTB_4-induced pericyte gap opening (Figure 5.4, bottom). Of interest, the same results were achieved when cremaster muscles were stimulated with KC or C5a (Figure 5.4, bottom). In contrast, when cremaster muscles were stimulated with the pro-inflammatory cytokine IL-1β, pericyte shape change was independent of neutrophils as the pericyte gap size increased at similar levels in both control IgG-treated and neutrophil-depleted animals. These results are in line with previous results showing the expression of IL-1R on pericytes and the ability of IL-1β to directly induce pericyte shape change *in vitro* and *in vivo* in a neutrophil-independent manner (Proebstl et al., 2012). Altogether, these results suggest that pericyte shape change can occur in a neutrophil-dependent manner when inflammation is induced by neutrophil-specific chemoattractants.

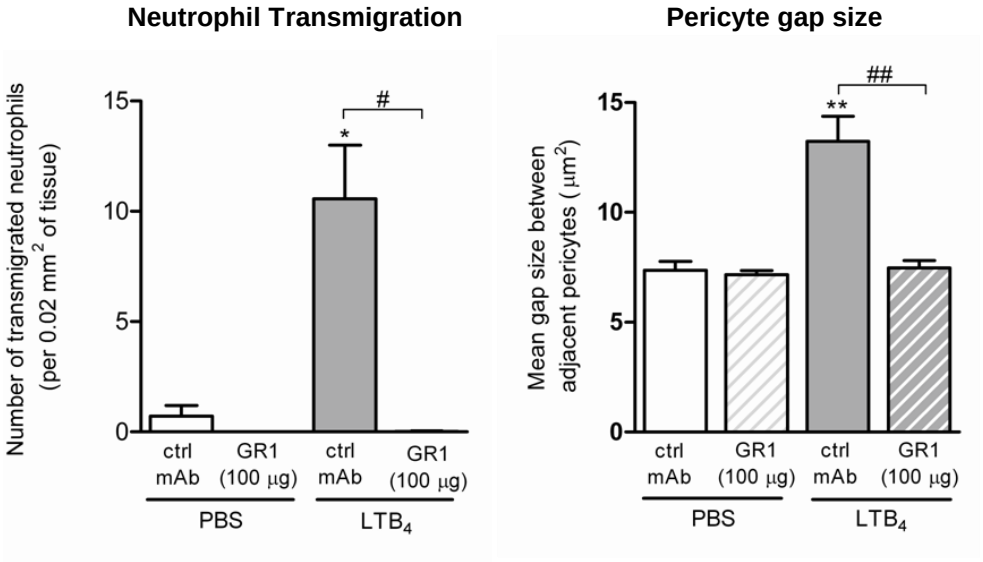

Figure 5.1: LTB_4-induced pericyte shape change in neutrophil-depleted mice. WT mice were depleted of their neutrophils by i.p. injection of 100 µg anti-GR1 antibody 24 h prior to LTB_4 (30 ng) or PBS i.s. injection. Control mice received an isotype-matched control antibody i.p. Cremaster muscles were dissected away 4 h after LTB_4 or PBS injection, fixed and immunostained for neutrophils (MRP-14) and pericytes (αSMA) for confocal analysis. Number of transmigrated neutrophils (left) and the size of gaps between adjacent pericytes (right) were quantified. White bars represent control samples (PBS, 4 h) and grey bars correspond to LTB_4-stimulated tissues which received control antibody. Patterned bars correspond to mice depleted of their circulating neutrophils and treated with PBS (patterned white) or LTB_4 (patterned grey). 3 vessel segments per cremaster muscle (6 per mouse) were analysed and plotted as mean per mouse. Data are presented as the mean ±SD of 3 independent experiments. Significant differences between groups were determined using Student's *t*-test. Differences between depleted and undepleted groups are marked with hashes (#: $p < 0.05$, ##: $p < 0.01$), differences to PBS-treatment are indicated by asterisks. (*: $p < 0.05$, **: $p < 0.01$)

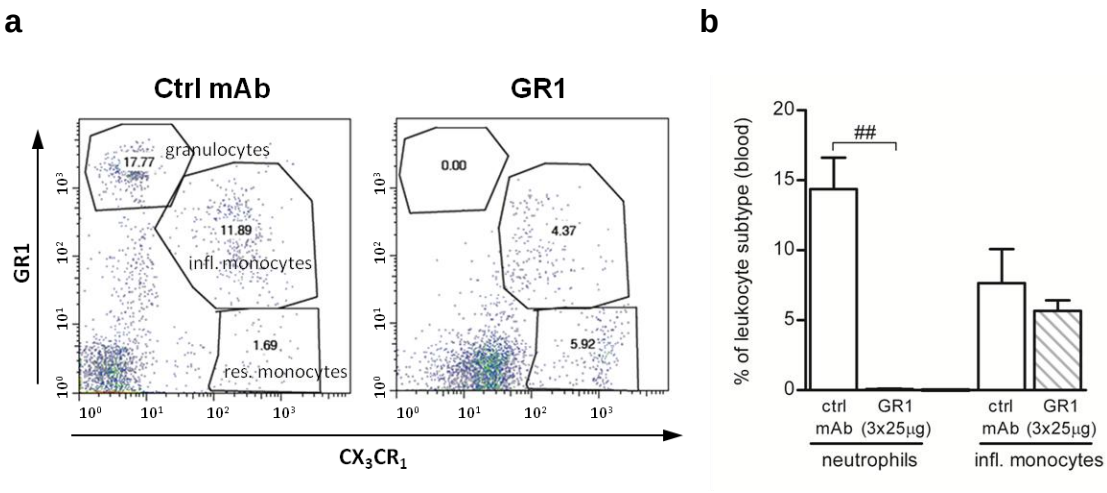

Figure 5.2: Blood neutrophil and monocyte counts in mice treated with low concentrations of GR1 antibody. $CX_3CR_1^{GFP/+}$ mice were depleted of their neutrophils by 3 doses of 25 µg anti-GR1 antibody. Control mice received the same amount of isotype-matched control antibody i.p. Blood samples were taken 24 h after the last injection and stained with an anti-GR1 antibody for flow cytometric analysis. **(a)** Dot plots show $GR1^+$ $CX_3CR_1^-$ granulocytes (neutrophils), $GR1^-$ $CX_3CR_1^+$ resident monocytes and $GR1^+$ $CX_3CR_1^+$ inflammatory monocytes of blood taken from control IgG (left) or GR1 antibody treated mice (right). Numbers within the outlined gates indicate the percentage of the respective leukocyte subset within the blood sample. **(b)** Graph represents the percentage of neutrophils and monocytes from blood samples taken from control IgG (white) or GR1 antibody treated mice (patterned) as analysed by flow cytometry. Data are presented as the mean ±SD of 3 independent experiments. Significant differences between groups were determined using Student's *t*-test. Differences between depleted and undepleted groups are marked with hashes (##: $p < 0.01$).

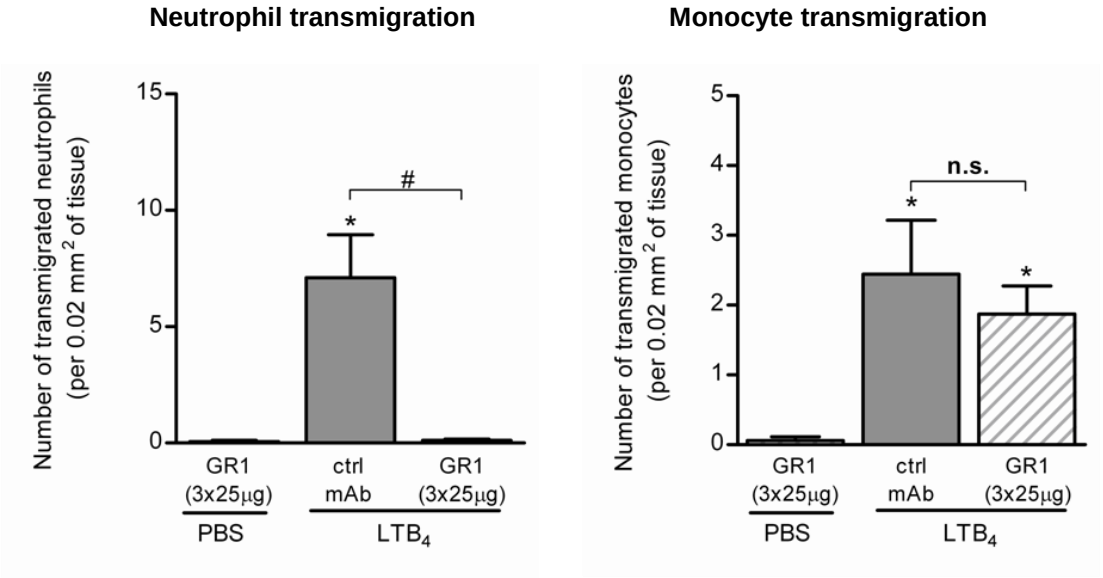

Figure 5.3: Neutrophil and monocyte transmigration in response to LTB_4 in mice treated with low concentrations of GR1 antibody or. $CX_3CR_1^{GFP/+}$ mice were depleted of their neutrophils by 3 doses of 25 µg anti-GR1 antibody i.p. Control mice received the same amount of isotype-matched control antibody. LTB_4 (30 ng) or PBS was given i.s. 24 h after the last dose. Cremaster muscles were dissected away 4 h after stimulus injection, fixed and immunostained for neutrophils (MRP-14) for confocal analysis. Number of transmigrated MRP-14 positive neutrophils (left) and CX_3CR_1-positive monocytes (right) were quantified. Filled bars represent mice which received control antibody; patterned bars correspond to mice depleted of their circulating neutrophils. 3 vessel segments per cremaster muscle (6 per mouse) were analysed and plotted as mean per mouse. Data are presented as the mean ±SD of 3 independent experiments. Significant differences between groups were determined using Student's *t*-test. Differences between depleted and undepleted groups are marked with hashes (#: p), differences to PBS-treatment are indicated by asterisks. (*: $p < 0.05$).

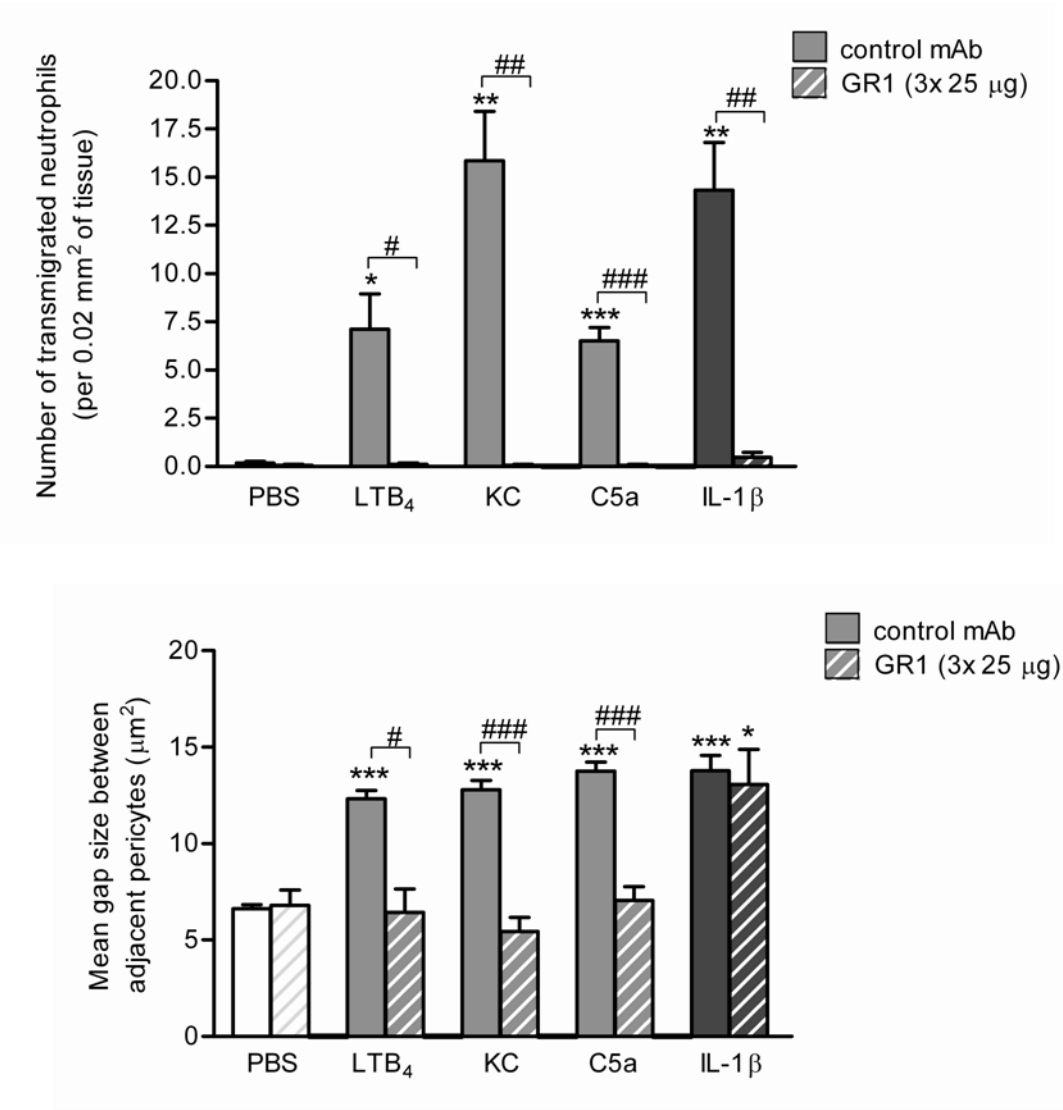

Figure 5.4: Neutrophil chemoattractant-induced pericyte shape change in neutrophil-, but not monocyte-depleted mice. WT or $CX_3CR_1^{GFP/+}$ mice were depleted of their neutrophils by 3 doses of 25 µg anti-GR1 antibody i.p. Control mice received the same amount of isotype-matched control antibody. LTB_4 (30 ng), KC (500 ng), C5a (300 ng), IL-1β (50 ng) or PBS was given i.s. 24 h after the last dose. Cremaster muscles were dissected away 2 h (KC) or 4 h (LTB_4, C5a, IL-1β) after stimuli injection or 2 and 4h post PBS injections (results pooled together). Tissues were fixed and immunostained for neutrophils (MRP-14) and pericytes (αSMA) for confocal analysis. Number of transmigrated neutrophils (top) and size of gaps between adjacent pericytes (bottom) were quantified. White bars represent control samples (PBS) and grey bars correspond to LTB_4-stimulated tissues which received control antibody. Patterned bars correspond to mice depleted of their circulating neutrophils and treated with PBS (patterned white) or inflammatory stimuli (patterned grey). At least 4 vessel segments per mouse were analysed and plotted as mean per mouse. Data are presented as the mean ±SD of 3 independent experiments. Significant differences between groups were determined using Student's *t*-test. Differences between depleted and undepleted groups are marked with hashes (#: $p < 0.05$, ##: $p < 0.01$, ###: $p < 0.001$), differences to PBS-treatment are indicated by asterisks. (*: $p < 0.05$, **: $p < 0.01$, ***: $p < 0.001$).

5.2.2 Role of secondary mediators in regulating pericyte shape change

The data so far suggest that, in contrast to cytokine-induced inflammation, neutrophil chemoattractants induce a neutrophil-dependent change in pericyte morphology leading to an increase in size of gaps between adjacent cells. It was hypothesised that in chemoattractant-induced inflammation, neutrophils rapidly release a secondary mediator that acts on pericytes. Hence, a number of neutrophil-derived factors that have been shown to be vasoactive on SMCs were investigated for their ability to stimulate changes in pericyte morphology in response to LTB_4. Independent experiments were performed at least 3 times for each condition.

LTB_4 stimulation of neutrophils leads to a rapid release of platelet-activating factor (PAF) (Tessner et al., 1989), a phospholipid that has been shown to stimulate SMC contraction (Soloviev and Braquet, 1991; Stimler et al., 1981). To elucidate the potential role of PAF in mediating LTB_4-induced pericyte gap opening, mice were pre-treated with the PAF antagonist UK 74,505 before inducing inflammatory responses by i.s. injection of LTB_4 for 4 h. Stimulated whole mount cremaster muscles were immunostained for MRP-14 (neutrophils) and αSMA (pericytes) and analysed for neutrophil transmigration and changes in pericyte morphology by confocal microscopy. Treatment of mice with UK 74,505 abolished PAF-induced neutrophil transmigration almost completely as confirmed by confocal microscopy of PAF-induced dermal inflammation in mouse ears (Figure 5.5a). In contrast, blocking PAF receptors had no effect on neutrophil transmigration or pericyte gap opening in response to LTB_4 (Figure 5.5b).

Activated neutrophils, e.g. upon stimulation with LTB_4, also release tissue-destructive oxygen-derived free radicals (Sumimoto et al., 1984), which in turn are able to augment contraction of SMCs (uch-Schwelk et al., 1989b). Thus, the role of reactive oxygen intermediates in mediating pericyte responses to LTB_4 was analysed next using confocal microscopy and immunofluorescent staining. Neutrophil extravasation following 4 h LTB_4 was prevented by combined treatment of mice with the ROS scavenger SOD and catalase as shown by the absence of neutrophils within tissues (Figure 5.6a and 5.b, left). Of interest, in assessing the site of arrest of neutrophils, in SOD and catalase treated mice almost no neutrophils could be detected within the vessel wall (Figure 5.6b, middle) but high number of neutrophils were seen within the vessel lumen (Figure 5.6a and 5.6b right). These results indicate that reactive oxygen intermediates contribute to the process of neutrophil transmigration at the level of the endothelium in response to LTB_4.

However, ROS scavenging had no effect on LTB_4-induced pericyte shape change (Figure 5.7). Similarly, NE (also released by LTB_4-stimulated neutrophils (Young et al., 2007)) was not required for LTB_4-induced pericyte gap opening as analysed in mice deficient for NE (Figure 5.8, left). $NE^{-/-}$ mice further showed similar neutrophil transmigration following 4 h LTB_4 as compared to WT animals (Figure 5.8, left).

Results obtained in this laboratory have previously demonstrated that the pro-inflammatory cytokine TNF can directly act on pericytes to induce pericyte shape-change both *in vivo* and *in vitro* (Proebstl et al., 2012). As this molecule can also be generated and released from neutrophils upon stimulation with mediators such as LTB_4 or KC (Chou et al., 2010; Gaudreault and Gosselin, 2009; Saiwai et al., 2010; Vieira et al., 2009), the role of TNF was investigated in the context of neutrophil-dependent pericyte shape-change. Stimulated whole mount cremaster muscles of WT and $TNFR^{-/-}$ mice were immunostained for MRP-14 (neutrophils) and αSMA (pericytes) and analysed for neutrophil transmigration and changes in pericyte morphology as before. In both, WT and $TNFR^{-/-}$ mice neutrophil transmigration responses into the tissue were similar upon stimulation with LTB_4 (4 h; Figure 5.9 and 5.10, top), KC (2 h) or C5a (4 h; Figure 5.10, top). Interestingly, quantification of pericyte gap size showed that in contrast to WT animals, chemoattractant-induced increase in pericyte gap size was absent in TNFR-deficient mice (Figure 5.9, and 5.10, bottom).

As a control, $TNFR^{-/-}$ were also stimulated with TNF. As expected, neutrophil transmigration and pericyte shape change in response to TNF were both abolished in these animals (Figure 5.11, left). When cremaster muscles were stimulated with the pro-inflammatory cytokine IL-1β, pericyte shape change was independent of TNFR signalling as both, WT and TNFR-deficient animals showed significant enlargement of gaps between adjacent pericytes (Figure 5.11, right). These results are in line with previous results showing the ability of IL-1β to directly induce pericyte shape change *in vivo* (Proebstl et al., 2012) and suggest that neutrophil-dependent chemoattractant, but not cytokine-induced, changes in pericyte morphology are triggered through TNFR signalling.

a

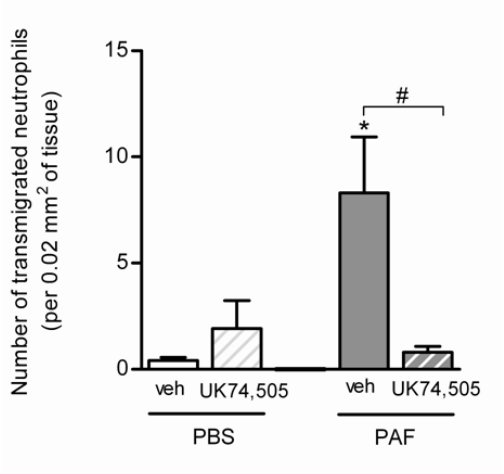

b

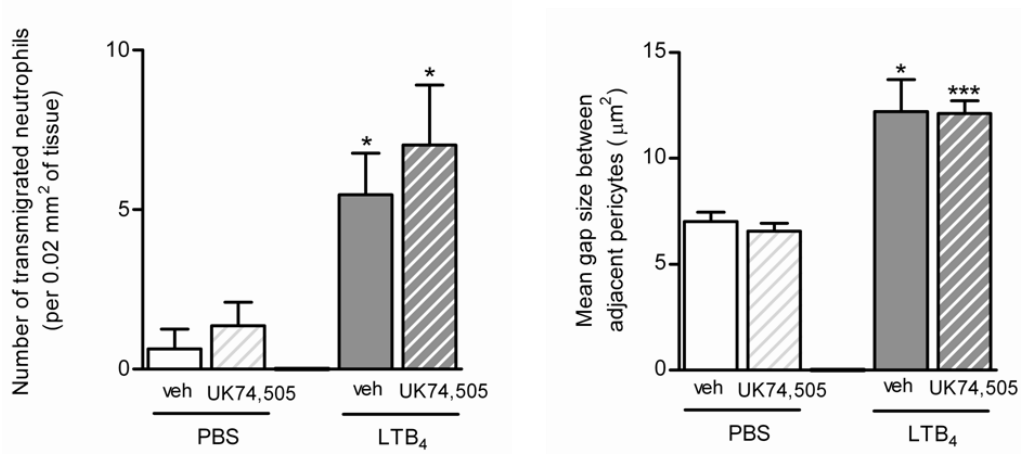

Figure 5.5: Effect of PAF antagonist UK74, 505 on LTB_4-induced pericyte shape change. LTB_4 (30 ng) or PBS was injected i.s. 10 min after i.v. injection of UK74, 505 or vehicle control. To test the efficiency of UK74, 505, PAF was injected i.d. into the ear skin of the same animals. Tissues were extracted 4 h after stimulation, fixed, permeabilised and stained for neutrophils (MRP-14) and pericytes (αSMA) for confocal analysis. Number of transmigrated neutrophils was quantified in ear skin stimulated with PAF **(a)** and cremaster muscles stimulated with LTB_4 **(b, left)**. Furthermore the size of gaps between adjacent pericytes was analysed in post-capillary venules of the cremaster muscle **(b, right)**. White bars represent control samples (PBS) and grey bars correspond to PAF-, LTB_4-stimulated tissues. Patterned bars correspond to mice injected with the PAF antagonist UK74, 505. 3 vessel segments per cremaster muscle (6 per mouse) were analysed and plotted as mean per mouse. Data are presented as the mean ±SD of at least 3 independent experiments. Significant differences between groups were determined using Student's *t*-test. Differences to corresponding PBS controls are indicated by asterisks (*: $p < 0.05$, ***: $p < 0.001$) and differences between vehicle and UK74, 505 treated groups are marked with hashes (#: $p < 0.05$).

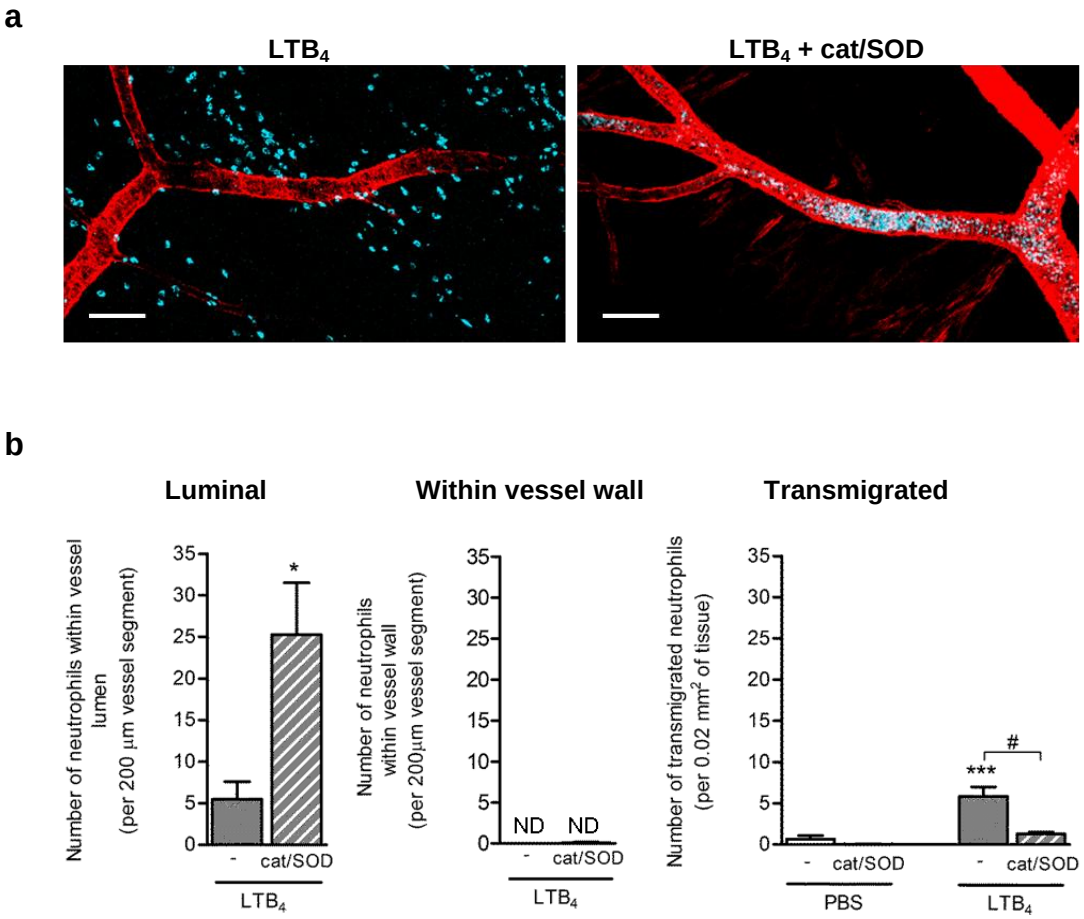

Figure 5.6: Effect of ROS scavengers on LTB_4-induced neutrophil transmigration. LTB_4 or PBS was injected i.s. immediately after i.v. injection of catalase+SOD. Uninjected animals served as control. Tissues were extracted 4 h after stimulation, fixed, permeabilised and stained for neutrophils (MRP-14) and pericytes (αSMA) for confocal analysis. **(a)** Representative 3D-reconstructed confocal images of LTB_4-treated postcapillary venules in the absence (left) or presence of cat/SOD. Bars, 50 µm **(b)** Number of neutrophils within the lumen (left), within the vessel wall (middle) and transmigrated neutrophils (right) were analysed. Patterned bars correspond to mice injected with the catalase/SOD cocktail and filled bars to control mice. 3 vessel segments per cremaster muscle (6 per mouse) were analysed and plotted as mean per mouse. Data are presented as the mean ±SD of at least 3 independent experiments. Significant differences between groups were determined using Student's *t*-test. Differences to corresponding PBS controls are indicated by asterisks (*: $p < 0.05$, ***: $p < 0.001$) and differences between untreated and cat/SOD-treated groups are marked with hashes (#: $p < 0.05$).

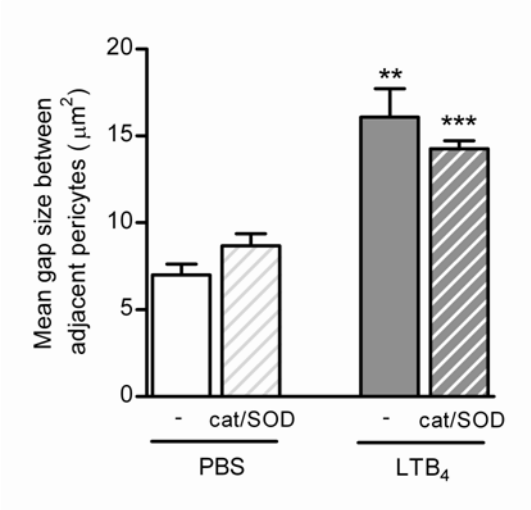

Figure 5.7: Effect of ROS scavengers on LTB_4-induced pericyte shape change. LTB_4 (30 ng) or PBS was injected i.s. immediately after i.v. injection of catalase+SOD. Uninjected animals served as control. Tissues were extracted 4 h after stimulation, fixed, permeabilised and stained for neutrophils (MRP-14) and pericytes (αSMA) for confocal analysis. Size of pericyte gaps was analysed in the same images used for Figure 5.6. Patterned bars correspond to mice injected with the catalase/SOD cocktail and filled bars to control mice. 3 vessel segments per cremaster muscle (6 per mouse) were analysed and plotted as mean per mouse. Data are presented as the mean ±SD of at least 3 independent experiments. Significant differences between groups were determined using Student's *t*-test. Differences to corresponding PBS controls are indicated by asterisks (**: $p < 0.01$, ***: $p < 0.001$).

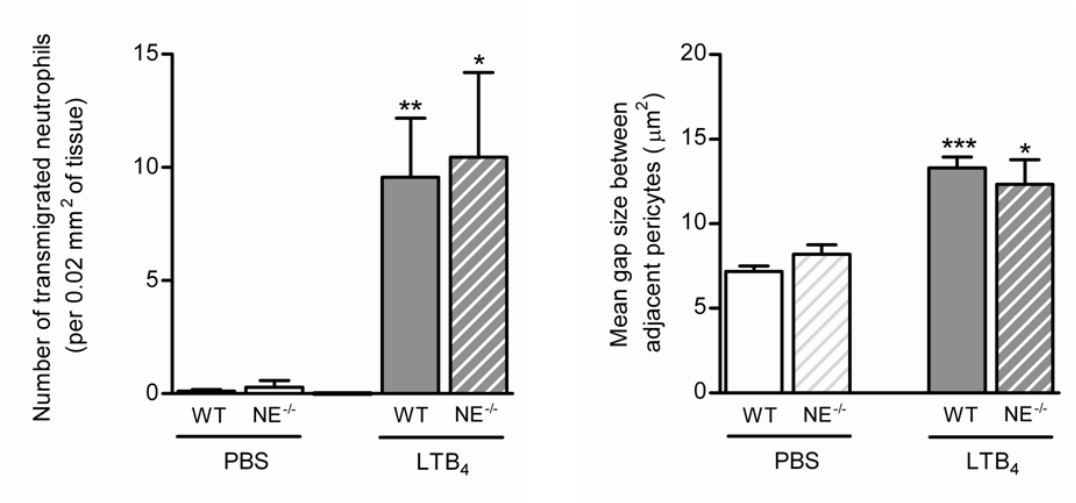

Figure 5.8: Effect of NE-deficiency on LTB_4-induced pericyte shape change. LTB_4 (30 ng) or PBS was injected i.s. into WT or $NE^{-/-}$ mice. Tissues were extracted 4 h after stimulation, fixed, permeabilised and stained for neutrophils (MRP-14) and pericytes (αSMA) for confocal analysis. Number of transmigrated neutrophils (left) and the size of pericyte gaps (right) were analysed in the cremaster muscle. Patterned bars correspond to $NE^{-/-}$ mice and filled bars to WT mice. 3 vessel segments per cremaster muscle (6 per mouse) were analysed and plotted as mean per mouse. Data are presented as the mean ±SD of at least 3 independent experiments. Significant differences between groups were determined using Student's *t*-test. Differences to corresponding PBS controls are indicated by asterisks (*: $p < 0.05$, **: $p < 0.01$, ***: $p < 0.001$).

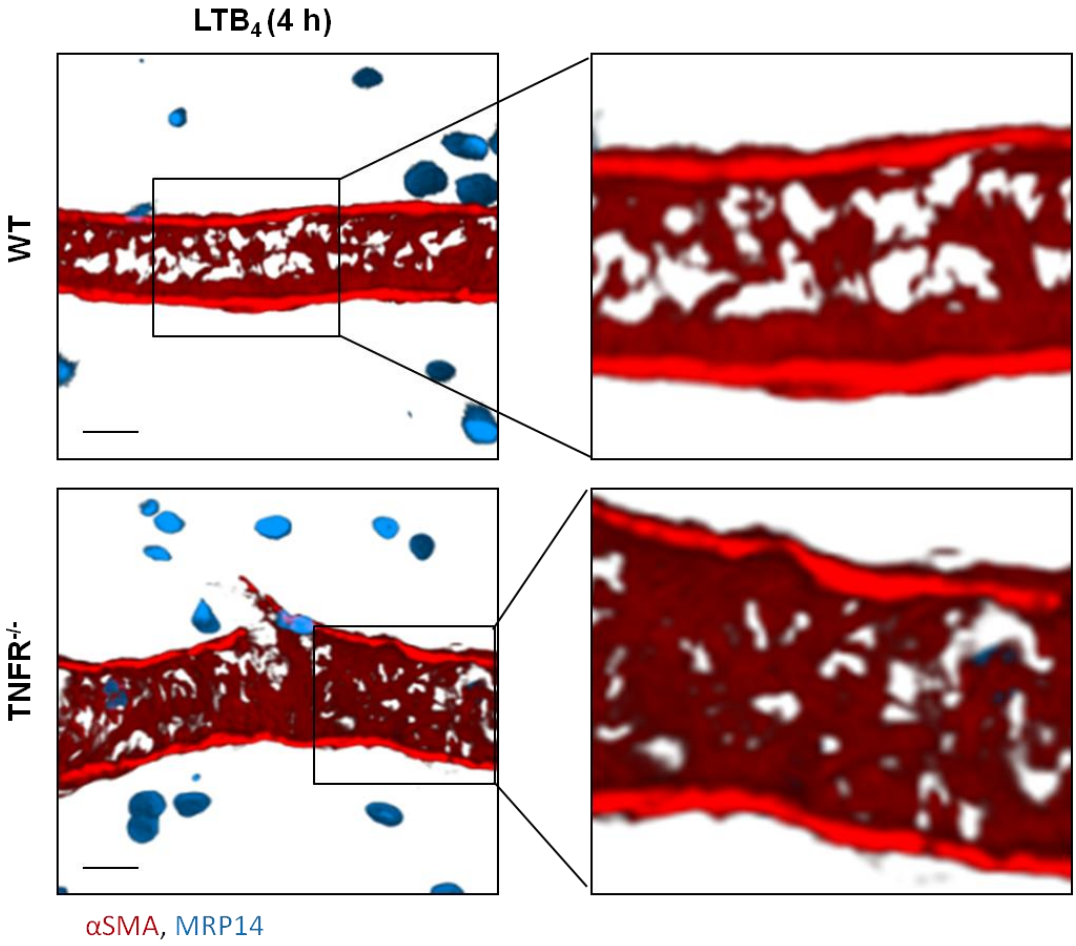

Figure 5.9: Effect of TNFR-deficiency on LTB_4-induced pericyte shape change. LTB_4 (30 ng) was injected i.s. into WT and $TNFR^{-/-}$ mice. Cremaster muscles were dissected away 4 h after stimulation, fixed, permeabilised and stained for neutrophils (MRP-14) and pericytes (αSMA) for confocal analysis. Representative 3D-reconstructed confocal images of LTB_4-treated cremasteric postcapillary venules of WT (top) and $TNFR^{-/-}$ mice (bottom) illustrating neutrophils (blue) and pericytes (red) with gaps between adjacent cells. The right panels show magnifications of the αSMA channel of the region outlined in the left panels. Bars, 20 µm.

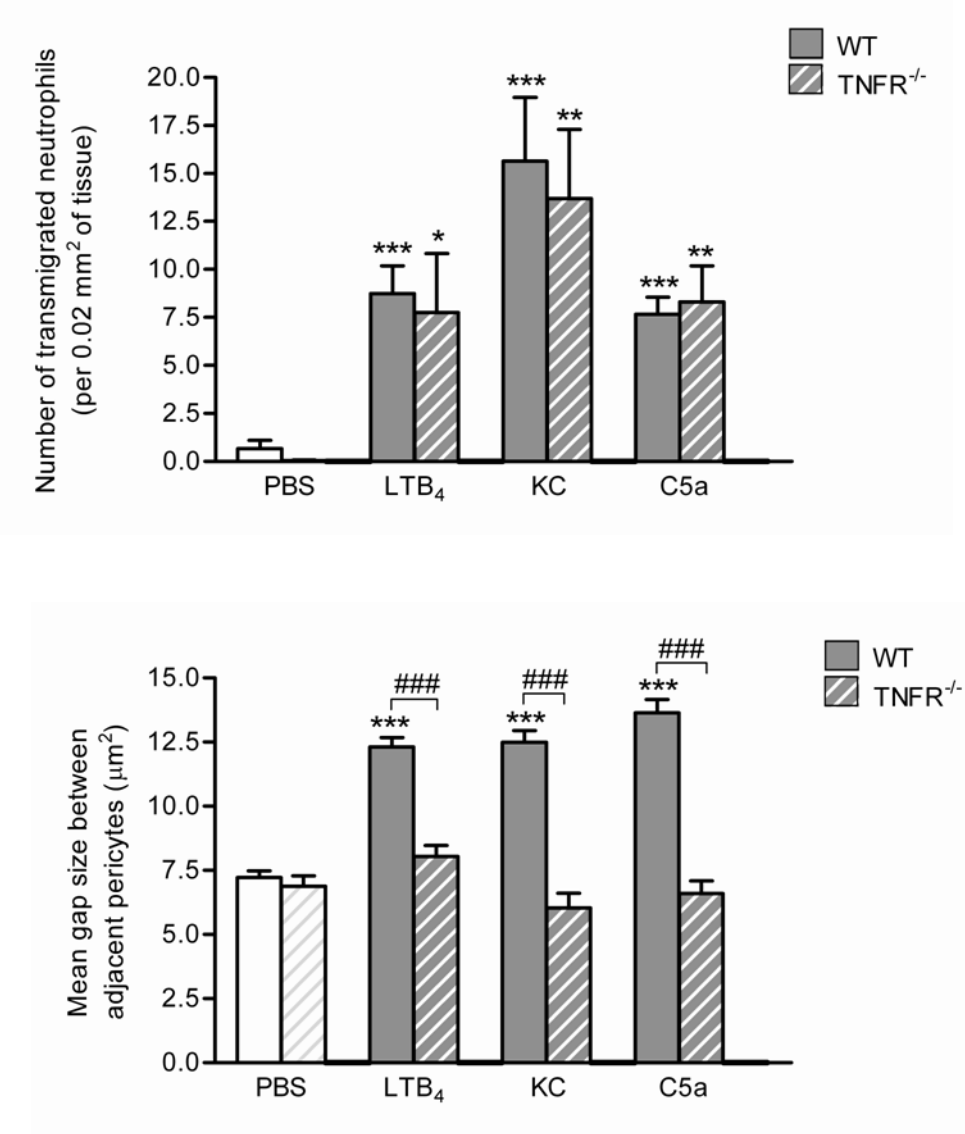

Figure 5.10: Effect of TNFR-deficiency on chemoattractant-induced pericyte shape change. LTB_4 (30 ng), KC (500 ng), C5a (300 ng) or PBS was injected i.s. into WT or $TNFR^{-/-}$ mice. Tissues were extracted 2 h (KC) or 4 h (LTB_4, C5a) after stimulation, fixed, permeabilised and stained for neutrophils (MRP-14) and pericytes (αSMA) for confocal analysis. Number of transmigrated neutrophils (top) and the size of pericyte gaps (bottom) were analysed in the cremaster muscle. Patterned bars correspond to $TNFR^{-/-}$ mice and filled bars to WT mice. 3 vessel segments per cremaster muscle (6 per mouse) were analysed and plotted as mean per mouse. Data are presented as the mean ±SD of at least 3 independent experiments. Significant differences between groups were determined using Student's *t*-test. Differences to corresponding PBS controls are indicated by asterisks (*: $p < 0.05$, **: $p < 0.01$, ***: $p < 0.001$). Differences between mouse strains are marked by hashes (###: $p < 0.001$).

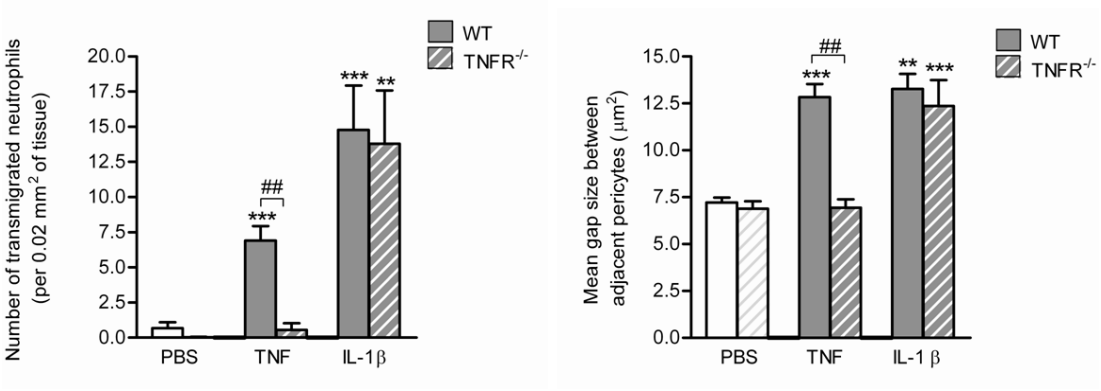

Figure 5.11: Effect of TNFR-deficiency on TNF- and IL-1β-induced pericyte shape change. TNF (300 ng), IL-1β (50 ng) or PBS were injected i.s. into WT or TNFR$^{-/-}$ mice. Tissues were extracted 2 h (TNF) or 4 h (IL-1β) after stimulation, fixed, permeabilised and stained for neutrophils (MRP-14) and pericytes (αSMA) for confocal analysis. Number of transmigrated neutrophils (left) and the size of pericyte gaps (right) were analysed in the cremaster muscle. Patterned bars correspond to TNFR$^{-/-}$ mice and filled bars to WT animals. 3 vessel segments per cremaster muscle (6 per mouse) were analysed and plotted as mean per mouse. Data are presented as the mean ±SD of at least 3 independent experiments. Significant differences between groups were determined using Student's *t*-test. Differences to corresponding PBS controls are indicated by asterisks (**: $p < 0.01$, ***: $p < 0.001$). Differences between mouse strains are marked by hashes (##: $p < 0.01$).

5.3 DISCUSSION

Post-capillary venules are composed of 2 cellular components, the ECs and the pericytes, and networks of tightly packed matrix proteins forming the venular BM. During inflammation, neutrophils have to interact and penetrate all 3 structures (Nourshargh et al., 2010). Gaps between adjacent pericytes are preferential exit points for neutrophils to penetrate the pericyte sheath, sites that have been shown to transiently enlarge in response to cytokines such as TNF and IL-1β (Proebstl et al., 2012). In addition, the present study demonstrates for the first time the ability of different types of neutrophil chemoattractants, namely "intermediate" chemoattractants (LTB_4 and KC) and "end-target" chemoattractants (fMLP and C5a) to act on pericytes *in vivo*. Collectively, the results presented in this chapter shed further light onto the cellular and molecular mechanisms that mediate pericyte shape change in inflammation.

Based on previous studies showing the importance of neutrophils in changes in different vessel wall components as induced by chemoattractants (Hurley J.V., 1964; Voisin et al., 2010; Wedmore and Williams, 1981) and results presented in chapter 4, showing a temporal association between pericyte shape change and neutrophil transmigration, the role of neutrophils in this response was investigated. Indeed, using neutropenic mice (as induced by antibody-based depletion of neutrophils), pericyte gap opening in response to LTB_4, KC, and C5a, was completely abolished. This provides direct evidence for the importance of neutrophils in mediating pericyte shape change. Previous studies have further demonstrated the ability of at least LTB_4 and C5a to direct chemotaxis of monocytes and macrophages (Smith et al., 1980). However the involvement of these leukocyte subsets in pericyte shape change could be ruled out as the concentration of GR1-antibody used in this study was sufficient to deplete circulating neutrophils, but not monocytes or macrophages.

Using IL-1β as a stimulus, enlargement of pericyte gaps occurred independently of neutrophils, a phenomenon that was also previously shown for TNF (Proebstl et al., 2012). The same study also showed the expression of both TNFRs and IL-1R on pericytes, indicating the ability of pericytes to directly respond to these cytokines. LTB_4 acts through the G-protein coupled membrane receptors BLT_1 (a high affinity receptor) and BLT_2 (a low affinity receptor) (Tager and Luster, 2003). BLT_1 is mainly expressed by leukocytes, whereas BLT_2 is also found in the tissue. Both receptors were recently found to be expressed on human endothelial cells *in vitro* (Qiu et al.,

2006), however, their involvement in inflammatory responses remains unclear. There is so far no evidence of either the presence of LTB_4 receptors or a direct biological effect of this chemoattractant on pericytes.

Though elegant studies associated a link between chemoattractant-induced neutrophil migration and changes in vessel wall properties five decades ago (Hurley J.V., 1964), the molecular mechanisms of this phenomenon have remained unknown. Mediators such as LTB_4, KC, or C5a are not only potent chemotactic molecules for neutrophils, but also activate these cells and induce the generation and/or release of numerous proinflammatory molecules such as proteases, cytokines, vasoactive factors and ROS that could affect pericyte morphology (Adams and Lloyd, 1997; Ford-Hutchinson et al., 1980). The present study thus investigated the impact of possible secondary mediators in neutrophil-dependent chemoattractant-induced pericyte shape-change. Blocking PAF- or ROS-induced signalling, representing two vasoactive mediators (Soloviev and Braquet, 1991; Stimler et al., 1981; uch-Schwelk et al., 1989a) that are released by neutrophils in chemoattractant-induced inflammation (Sumimoto et al., 1984; Tessner et al., 1989), did not overcome pericyte shape-change in the present model. Similar results were observed in mice deficient in the serine protease NE. Notably, in mice pre-treated with ROS scavengers, neutrophil transmigration into tissues was inhibited at the level of the endothelium with neutrophils accumulating within the vascular lumen. As pericyte gaps still increased under these circumstances, these data suggest that transmigration itself is not essential for the occurrence of pericyte shape change.

Of interest, altered pericyte morphology was completely abolished in $TNFR^{-/-}$ mice upon LTB_4, KC or C5a stimulation, demonstrating that chemoattractant-induced changes in pericyte gaps are triggered by endogenously released TNF. This is supported by the fact that TNF can directly induce the enlargement of pericyte gaps since the cells express the receptors for this cytokine (Proebstl et al., 2012). Although monocytes are the primary source of TNF, neutrophils have also been shown to release TNF e.g. following LPS (Bazzoni et al., 1991; Dubravec et al., 1990), GM-CSF (Lindemann et al., 1989), Y-IgG (Bazzoni et al., 1991) or upon exposure to *Candida albicans* (Djeu et al., 1990) *in vitro*. However, conflicting data exists in the literature concerning the endogenous generation of neutrophil-derived TNF in response to chemoattractants. TNF has been shown to be secreted by human and mouse neutrophils *ex vivo* in response to LTB_4 (Gaudreault and

Gosselin, 2009). KC injected intraperitoneally into mice has also been demonstrated to induce a dose- and time-dependent increase in TNF protein expression, a response that occurred in parallel with recruitment of neutrophils (Vieira et al., 2009). TNF mRNA was further detected in isolated neutrophils after *in vivo* spinal cord injury, a response that was absent in neutrophils isolated from $BLT1^{-/-}$ mice, indicating a role for LTB_4 in mediating TNF expression (Saiwai et al., 2010). Furthermore, upregulated TNF mRNA levels downstream of LTB_4- signalling have been demonstrated in a murine model of inflammatory arthritis (Chou et al., 2010). In contrast, using the same model, TNF was not detected in synovial tissue in a study performed a few years earlier (Kim et al., 2006). TNF mRNA expression was also not detected upon fMLP, C5a or LTB_4 stimulation of cultured human neutrophils (Cassatella et al., 1997). The discrepancy between these studies might be partly due to different time points analysed, different concentrations of stimulating factors used, or differences between mRNA and protein expression. In addition, in our model we cannot exclude the possibility that the endogenous TNF comes from other sources than neutrophils. Pericytes themselves for example express low constitutive TNF *in vitro* that can be upregulated upon stimulation (Alcendor et al., 2012; Kovac et al., 2011; Kowluru et al., 2010). Although monocytes can also generate TNF in response to chemoattractants (Cavaillon et al., 1990; Schindler et al., 1990), in our hands, the level of monocyte infiltration was minimal and only depletion of neutrophils, but not monocytes, led to inhibition of pericyte shape change. Another potential mechanism for endogenous TNF release could be through the interaction of neutrophils with endothelium via β2 integrins (CD11/CD18), which can be upregulation on the surface of neutrophils upon chemoattractant stimulation (Sanchez-Madrid et al., 1983; Wallis et al., 1986). Further studies, however, are needed to better understand the source of TNF and the underlying mechanism of its synthesis and release.

CHAPTER 6: ROLE OF TNF IN CHEMOATTRACTANT-INDUCED VASCULAR FUNCTION AND BM REMODELLING

6.1 INTRODUCTION

As demonstrated in chapters 4 and 5, chemoattractant-induced inflammation was associated with changes in pericyte morphology in a neutrophil- and TNF-dependent manner. In addition, chemoattractants such as LTB_4 are further linked with neutrophil-dependent changes in the vascular wall properties *in vivo* including reduced barrier function of vessels to plasma proteins (Bjork et al., 1982; Wedmore and Williams, 1981), and BM remodelling (Voisin et al., 2009; Voisin et al., 2010). However, the molecular mechanisms of these phenomena are not well understood. The aim of this chapter was to investigate the potential role of endogenous TNF in mediating chemoattractant-induced vascular permeability and changes in the BM structure, specifically BM deposition post inflammation.

Inflammation is intimately associated with an increase in vascular permeability leading to leakage of plasma fluid, proteins and macromolecules into the extravascular tissue resulting in oedema. This can occur via a transcellular route through interendothelial junctions or paracellular through transcytosis (Komarova and Malik, 2010). The most common described mechanism of vascular leakage is leakage via EC junctions in postcapillary venules (20-60 µm in diameter) (Majno and Palade, 1961; Baluk et al., 1997; McDonald et al., 1999), structures tightly regulated by complexes of EC junctional molecules (e.g. components of adherence and tight junctions) (Dejana et al., 2009; Taddei et al., 2008). Stimuli directly able to induce rapid and transient increased vascular permeability are low molecular weight mediators such as histamine, serotonin, bradykinin and substance P (Baluk et al., 1997; Di et al., 1971). In addition, activated neutrophils in response to chemical stimuli are able to regulate the barrier properties of venular walls to plasma proteins (Wedmore and Williams, 1981). In this context, Williams and Morley suggested a two mediator model for regulation of permeability, where the first mediator stimulates ECs to increase vascular permeability, and the second mediator (e.g. prostaglandins) acts in synergy to potentiate the response by increasing arteriolar vasodilation and thus, increased blood flow (Williams and Morley, 1973). Although it is well known that neutrophils can mediate vascular leakage in response to chemoattractants such as LTB_4 and C5a (Bjork et al., 1982; Wedmore and Williams,

1981; Arfors et al., 1987; Kaslovsky et al., 1990a), the precise mechanism through which neutrophils can provoke reduced barrier function of venular walls is not known.

Pericytes are embedded within vascular BM, representing an additional barrier for transmigrating cells and macromolecules. In a study performed by Hurley in 1964, carbon particles could only fully breach the vessel wall under conditions of EC permeability and leukocyte transmigration (Hurley J.V., 1964). In the absence of emigrating leukocytes the particles accumulated at the luminal side of the BM, suggesting a barrier function of this structure. In addition, early electron microscopy studies revealed a generally higher number of transmigrating neutrophils within the BM layer as compared to cells breaching the EC barrier, indicating a high resistance of the BM to emigrating cells and macromolecules (HURLEY, 1963). Hence, following transendothelial migration, leukocytes remain in the sub-endothelial space for a considerable amount of time before penetrating the pericyte sheath and the vascular BM. Neutrophils have been shown to breach these layers preferentially through regions of low matrix protein expression (LER), sites that are directly aligned with pericyte gaps. Similar to pericyte gaps, these LERs undergo a transient increase in size in response to a number of inflammatory stimuli (Reichel et al., 2008; Reichel et al., 2009; Reichel et al., 2011; Voisin et al., 2009; Voisin et al., 2010).

Vascular BMs are composed of independent networks of laminin and collagen, which form molecular bridges involving other glycoproteins such as perlecan and nidogen (Rowe and Weiss, 2008). The venular BM envelops pericytes and provides structural support for the vessel wall and adhesive support for emigrating cells. Both pericytes and ECs contribute to the generation of venular BM; however, as pericyte gaps are aligned with so-called LERs, the existence of significant gaps between adjacent pericytes seems to account for the generation of these leukocyte-permissive sites.

Matrix protein LERs have been identified in the collagen IV, laminin-511, laminin-411 and nidogen networks (Voisin et al., 2009; Voisin et al., 2010; Wang et al., 2006). We and others demonstrated increased LERs in tissues stimulated with several inflammatory stimuli including TNF, IL-1β, CCL2, LTB_4, MIP1a, CCL3, LPS and I/R (Reichel et al., 2009; Reichel et al., 2011; Voisin et al., 2009; Voisin et al., 2010; Wang et al., 2006). The mechanisms involved in leukocyte breaching of this barrier *in vivo* are poorly understood, but leukocyte proteases have been implicated

in this process (Delclaux et al., 1996; Wang et al., 2006). Furthermore, the expression of integrins on leukocytes that function as receptors for laminins and collagen IV (e.g. $\alpha_2\beta_1$ and $\alpha_6\beta1$) are upregulated during transmigration, indicating that adhesive contacts between leukocytes and BM components may play a role in this phase of leukocyte transmigration (Bohnsack, 1992; Frieser et al., 1996; Werr et al., 1998; Werr et al., 2000). Interestingly, different BM components have been shown to exhibit distinct adhesive properties for leukocytes and hence may play an active role in regulating neutrophil transmigration through this barrier (Sixt et al., 2001).

As data presented in the previous chapter (chapter 5) indicated a role for chemoattractant-induced TNF in regulation of pericyte morphology, the potential functional role of endogenous TNF in chemoattractant-induced vascular permeability and BM remodelling was analysed as part of the present chapter.

6.2 RESULTS

6.2.1 Role of endogenous TNF in chemoattractant-induced vascular permeability

Experiments were carried out to investigate the role of TNF in chemoattractant-induced vascular permeability. For this purpose, chemoattractant-induced vascular leakage was assessed in different inflammatory models (dorsal skin, ear skin and cremaster muscle) using Evans Blue as a tracer.

Role of neutrophils in chemoattractant-induced plasma leakage

In preliminary studies, vascular leakage of i.v. injected Evans Blue in response to LTB_4 was compared in neutrophil-depleted and undepleted mice using the dorsal skin and ear skin models. In line with previous studies (Bjork et al., 1982; Wedmore and Williams, 1981), vascular leakage as induced by local injection of LTB_4 (5 minutes after Evans Blue injection i.v.) and stimulation for 4 h was absent in neutrophil-depleted mice (treated with 100 µg GR1 antibody 24 h prior stimulation) as compared to mice treated with control antibody (Figure 6.1).

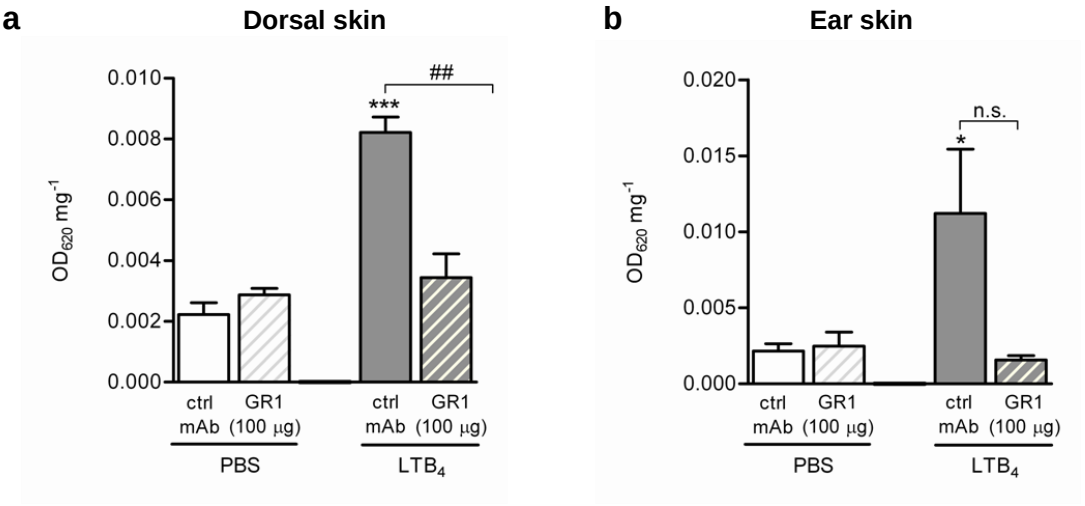

Figure 6.1: LTB_4-induced vascular leakage of intravenous Evans Blue in neutrophil-depleted mice. WT C57BL/6 mice were depleted of their circulating neutrophils by 100 µg GR1 antibody given 24 h before inducing the inflammatory reaction. Control mice received an isotype-matched control antibody. 5 min after i.v. injection of Evans Blue dye, LTB_4 (30 ng) or PBS were injected i.d. into the dorsal skin and ear skin. 4 h post induction of inflammation, dorsal skin and ear were removed and analysed for Evans Blue dye influx into the tissue as measured by the change in OD_{620} using a spectrometer. **(a)** dorsal skin**, (b)** ear skin, respectively. White bars represent control samples (PBS) and grey bars correspond to LTB_4-stimulated tissues of undepleted (filled) or neutrophil-depleted mice (patterned). Data are represented as the mean ±SD of 3 independent experiments. Significant differences between groups were determined using Student's *t*-test. Differences compared to PBS control are marked with asterisks. Differences between depleted and undepleted groups were marked with hashes. (*: $p < 0.05$, ***: $p < 0.001$, ##: $p < 0.01$)

LTB_4-induced vascular permeability in WT and $TNFR^{-/-}$ mice in different vascular beds

To elucidate the mechanism of how neutrophils provoke reduced barrier function of venular walls in response to chemoattractants, the potential role of TNF as a secondary mediator was next analysed. WT and $TNFR^{-/-}$ mice were injected i.v. with Evans Blue as a tracer followed by i.d. injections of LTB_4 or PBS into the dorsal skin. To analyse neutrophil transmigration, separate mice were treated with LTB_4 or PBS only (without injecting Evans Blue) in parallel and MPO activity, as a marker for neutrophils, was measured. Independent experiments were performed 3 times. As expected, LTB_4 induced vascular leakage within 4 h of treatment as seen by the extravasated dye at injection sites and assessed by spectrometry (Figure 6.2a). Interestingly, this response was absent in $TNFR^{-/-}$ mice, mice that exhibited similar neutrophil transmigration as compared to control mice (Figure 6.2b) and reduced pericyte gap opening. These results were confirmed in different vascular beds including the ear skin and cremaster muscles (Figures 6.3, 6.4, respectively).

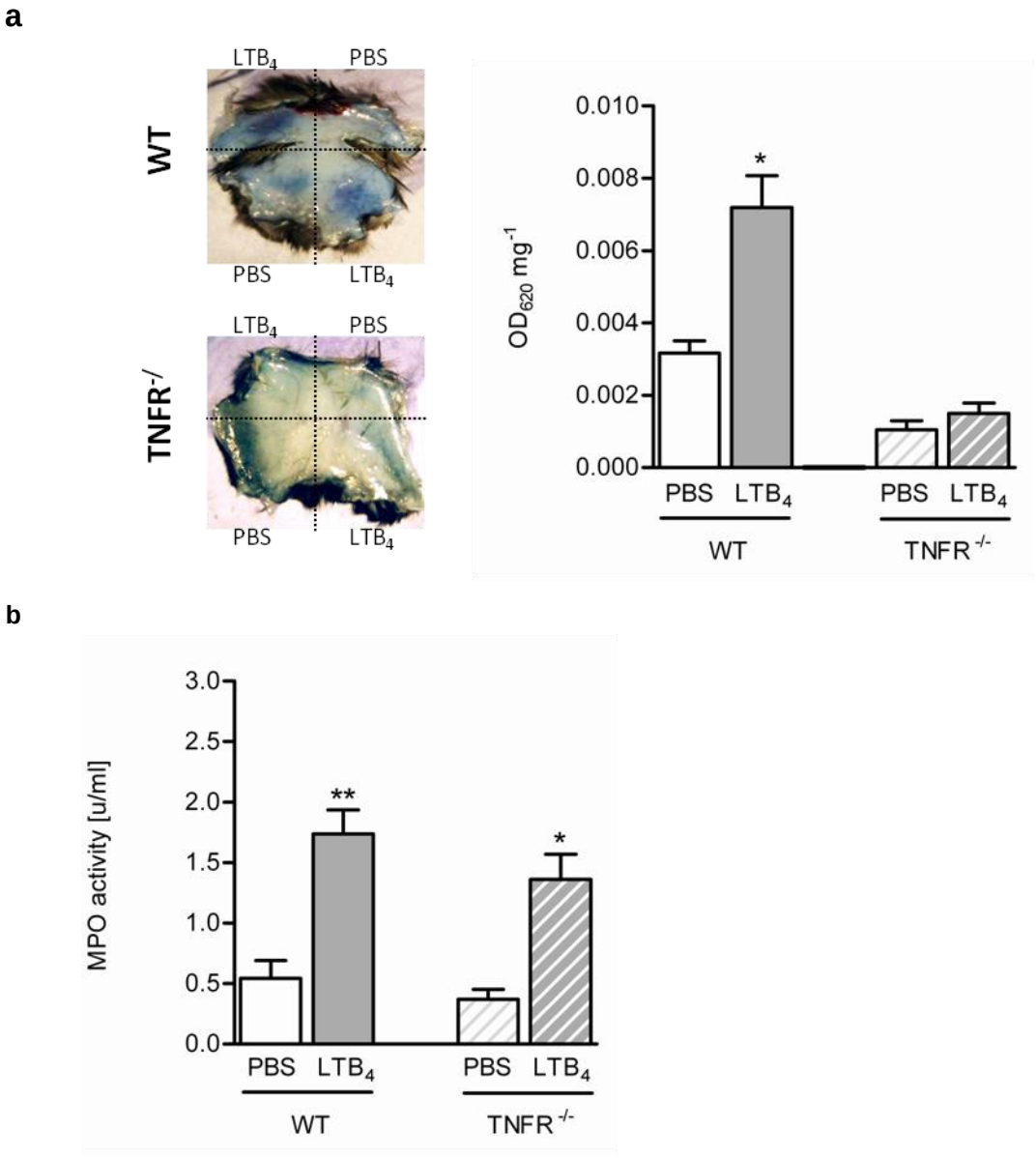

Figure 6.2: LTB_4-induced vascular leakage of intravenous Evans Blue in the dorsal skin of WT and $TNFR^{-/-}$ mice. (a) WT C57BL/6 and $TNFR^{-/-}$ mice received i.v. injections of Evans Blue dye 5 min prior to i.d. injection of LTB_4 (30 ng) or PBS into the dorsal skin. Dorsal skin was removed 4 h post induction of inflammation (left) and analysed for Evans Blue influx into the tissue as measured by the change in OD_{620} using a spectrometer (right). **(b)** Neutrophil transmigration was analysed in terms of MPO activity in separate mice, which did not receive Evans blue, but were treated with LTB_4 or PBS for 4 h in parallel. White bars represent control samples (PBS) and grey bars correspond to LTB_4-stimulated tissues of WT (filled) or $TNFR^{-/-}$ mice (patterned). Data are represented as the mean ±SD of 3 independent experiments. Significant differences between groups were determined using Student's *t*-test. Differences compared to PBS control are marked with asterisks. Differences between WT and $TNFR^{-/-}$ mice were marked with hashes. (*: $p < 0.05$, **: $p < 0.01$; ##: $p < 0.01$)

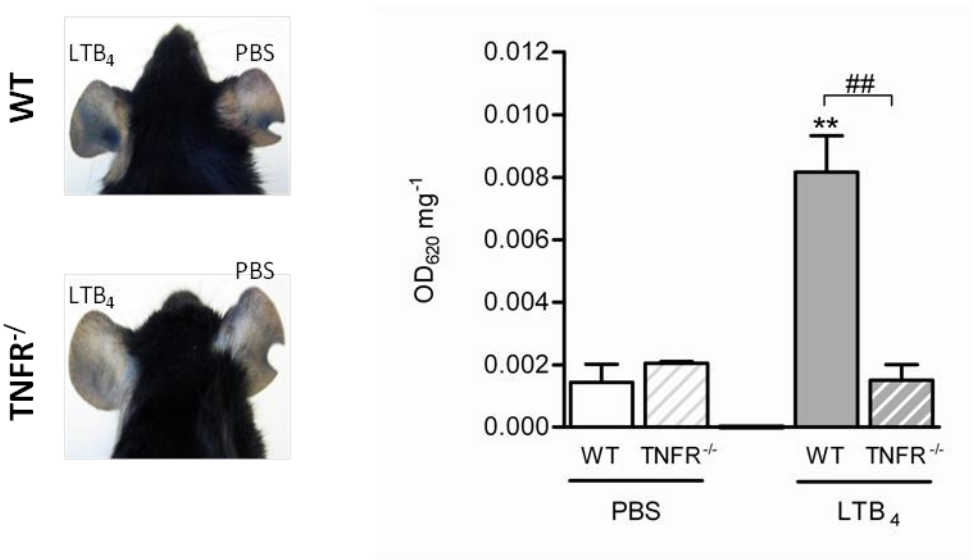

Figure 6.3: LTB_4-induced vascular leakage of intravenous Evans Blue in the ear skin of WT and $TNFR^{-/-}$ mice. WT C57BL/6 and $TNFR^{-/-}$ mice received i.v. injections of Evans Blue dye 5 min prior to i.d. injection of LTB_4 (30 ng) or PBS into the ear skin (left). Ear skin was removed 4 h post induction of inflammation and analysed for Evans Blue influx into the tissue as measured by the change in OD_{620} using a spectrometer (right). White bars represent control samples (PBS) and grey bars correspond to LTB_4-stimulated tissues of WT (filled) or $TNFR^{-/-}$ mice (patterned). Data are represented as the mean ±SD of 3 independent experiments. Significant differences between groups were determined using Student's *t*-test. Differences compared to PBS control are marked with asterisks. Differences between WT and $TNFR^{-/-}$ mice were marked with hashes. (**: $p < 0.01$; ##: $p < 0.01$)

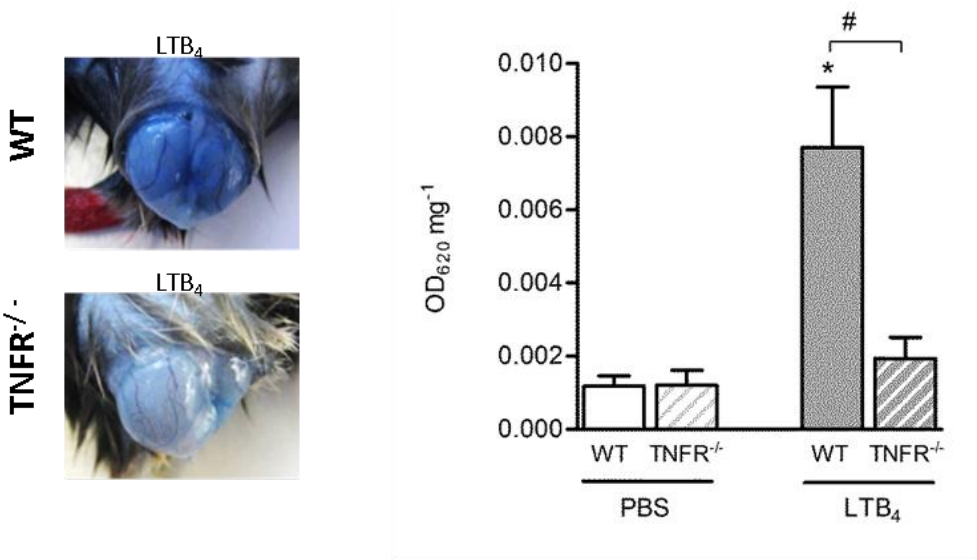

Figure 6.4: LTB_4-induced vascular leakage of intravenous Evans Blue in the cremaster muscle of WT and $TNFR^{-/-}$ mice. WT C57BL/6 and $TNFR^{-/-}$ mice received i.v. injections of Evans Blue dye 5 min prior to i.s. injection of LTB_4 930 ng) or PBS (left). Cremaster muscles were removed 4 h post induction of inflammation and analysed for Evans Blue influx into the tissue as measured by the change in OD_{620} using a spectrometer (right). White bars represent control samples (PBS) and grey bars correspond to LTB_4-stimulated tissues of WT (filled) or $TNFR^{-/-}$ mice (patterned). Data are represented as the mean ±SD of 3 independent experiments. Significant differences between groups were determined using Student's *t*-test. Differences compared to PBS control are marked with asterisks. Differences between WT and $TNFR^{-/-}$ mice were marked with hashes. (*: $p < 0.05$; # < 0.05)

Kinetics of chemoattractant-induced vascular permeability in WT and TNFR$^{-/-}$ mice

To further investigate the role of TNF in chemoattractant-induced vascular permeability and the potential relationship of this response with pericyte gap opening, time course experiments were performed and the kinetics of vascular leakage as induced by LTB_4, KC, and C5a were analysed in WT and TNFR$^{-/-}$ mice using the dorsal skin model. To analyse the rate of vascular leakage over certain time windows (*i.e.* 0-30, 30-60, 90-120 and 210-240 min of the inflammatory response), inflammatory stimuli were injected i.d. at different time points prior to i.v. Evans Blue: 4, 2, 1 and 0.5 h before scarifying the animal. Evans Blue was injected for the last ~28 min.

These experiments showed a rapid induction of vascular leakage within the first 30 min for all the chemoattractants tested, responses that progressively declines at later time points (Figure 6.5). As shown before for LTB_4 (Figure 6.2, 6.3 and 6.4), KC- and C5a-induced increase in vessel wall permeability was also dependent on the presence of TNF signalling, as mice deficient for both TNF receptors showed no (KC) or reduced vascular leakage (C5a) as compared to WT animals (Figure 6.5c and d). Furthermore, locally injected TNF also induced a rapid increase in vascular permeability (between 0-30 min) in the dorsal skin model (Figure 6.6). These data indicate for the first time a role of TNF as a secondary mediator of chemoattractant-induced vascular permeability.

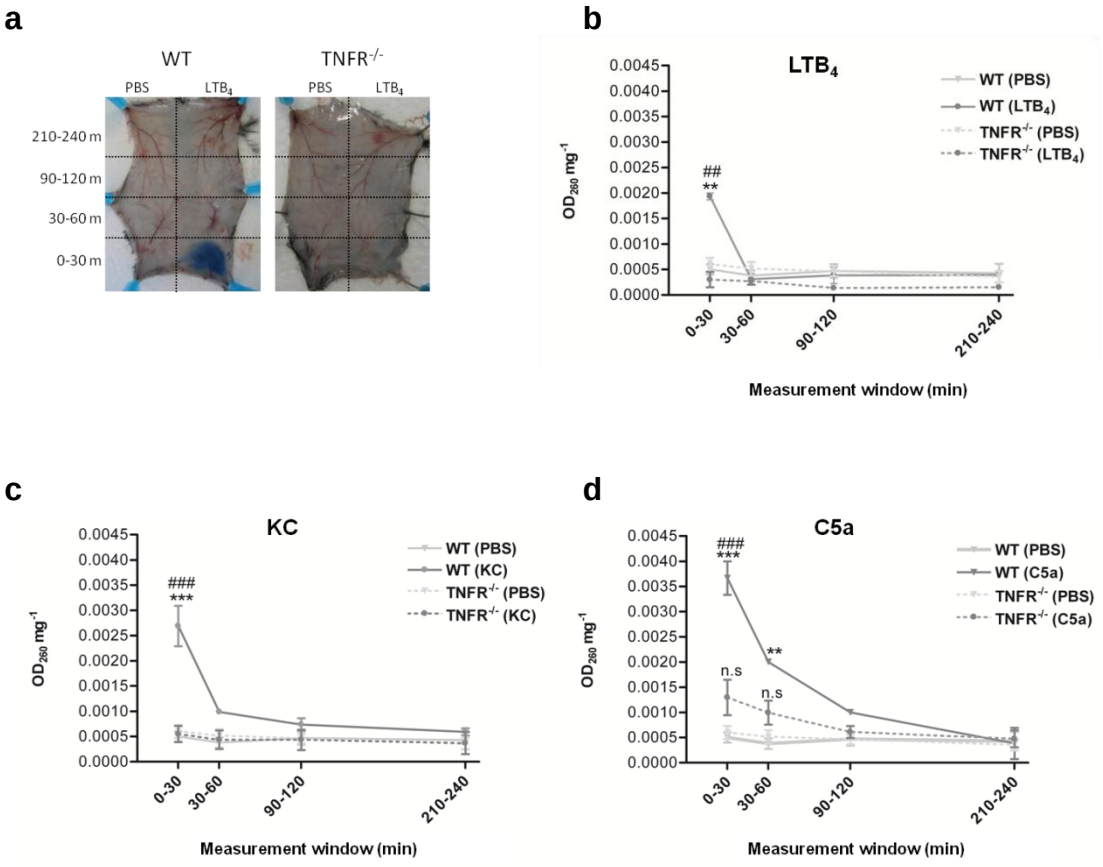

Figure 6.5: Kinetics of chemoattractant-induced vascular permeability in the dorsal skin of WT and TNFR$^{-/-}$ mice. WT C57BL/6 and TNFR$^{-/-}$ were injected with LTB_4 (30 ng), KC (500 ng), C5a (300 ng) or PBS i.d. at 240, 120, 60 and 30 min before the end of the experiments. Evans Blue dye was injected i.v. immediately after the last stimuli injection (30 min time point). At the end of the experiment, dorsal skin was removed and analysed for Evans Blue dye influx into the tissue as measured as the change in OD_{620} using a spectrometer. **(a)** Dorsal skin is shown after stimulation with LTB_4 or PBS and extraction from WT (left) and TNFR$^{-/-}$ mice (right) indicating vascular leakage in terms of blue dye within the tissue. **(b-d)** Kinetics of LTB_4-, KC- and C5a-induced vascular leakage, respectively were analysed in WT and TNFR$^{-/-}$ mice. Light grey lines represent control samples (PBS) and dark grey lines correspond to LTB_4-stimulated tissues of WT (uniform) or TNFR$^{-/-}$ mice (patterned). Data are represented as the mean ±SEM of 3 independent experiments. Significant differences between groups were determined using two-way ANOVA and Bonferroni's test. Differences between stimulus and PBS control are marked with asterisks. Differences between strains (WT and TNFR$^{-/-}$) are marked with hashes. (**: $p < 0.01$, ***: $p < 0.001$; ##: $p < 0.01$, ###: $p < 0.001$)

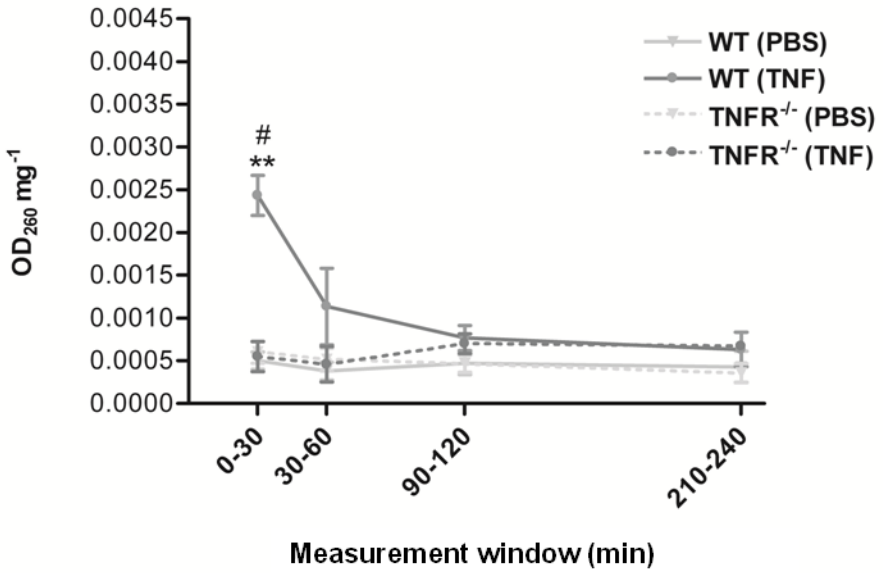

Figure 6.6: Kinetics of TNF-induced vascular permeability in the dorsal skin of WT and TNFR$^{-/-}$ mice. WT C57BL/6 and TNFR$^{-/-}$ were injected with TNF (300 ng) or PBS i.d. at 240, 120, 60 and 30 min before the end of the experiments. Evans Blue dye was injected i.v. immediately after the last stimuli injection (30 min time point). At the end of experiment, dorsal skin was removed and analysed for Evans Blue influx into the tissue as measured as the change in OD_{620} using a spectrometer. Light grey lines represent control samples (PBS) and dark grey lines correspond to LTB_4-stimulated tissues of WT (uniform) or TNFR$^{-/-}$ mice (patterned). Data are represented as the mean ±SEM of 3 independent experiments. Significant differences between groups were determined using two-way ANOVA and Bonferroni's test. Differences between stimuli and PBS control are marked with asterisks. Differences between strains (WT and TNFR$^{-/-}$) are marked with hashes. (**: $p < 0.01$; #: $p < 0.05$)

6.2.2 Role of TNF in regulating post-inflammatory BM remodelling

Pericyte gaps are directly associated with sites of venular BM LERs, regions that are preferred exit points for transmigrating leukocytes and undergo a transient increase in size in response to a number of inflammatory stimuli, similar to pericyte gaps (Reichel et al., 2008; Reichel et al., 2009; Reichel et al., 2011; Voisin et al., 2009; Voisin et al., 2010; Wang et al., 2006). The role of TNF in regulating chemoattractant-induced changes in BM composition was analysed next. For this purpose, the remodelling of LERs within the extracellular matrix of cremasteric post-capillary venules in LTB_4–stimulated tissues of WT and $TNFR^{-/-}$ mice was investigated by immunofluorescence staining and confocal microscopy.

Profile of LTB_4-induced BM protein LER enlargement

In initial experiments the time course of LTB_4-induced LER remodelling was analysed. For this purpose, the size of LERs within the venular BM was quantified in tissues extracted 4, 24, 48 and 72 h after i.s. LTB_4 injection as compared to PBS-treated tissues using ImageJ as described in chapter 2, section 2.3.7. Collagen IV and laminin were chosen for this characterisation because they represent the major matrix components of the venular BM.

As previously demonstrated (Wang et al., 2006; Voisin et al., 2009; Voisin et al., 2010), staining of tissues with anti-collagen IV antibody revealed a heterogeneous expression of this BM protein and the presence of LERs which were aligned with pericyte gaps (Figure 6.7). Furthermore, LTB_4 stimulation led to a gradual increase in mean size of collagen IV LERs in post-capillary venules of WT animals, a response that peaked at 4 h (Figure 6.7 and 6.8a). Similar results were obtained for the BM protein laminin using a pan-laminin antibody (Figure 6.8b). Whilst in unstimulated tissues the mean size of post-capillary venule collagen IV and laminin LERs were 6.45 ± 0.63 μm^2, 5.54 ± 0.84μm^2, respectively, these increased to 10.72 ± 0.44 μm^2, 11.68 ± 1.95 μm^2, respectively, in response to local LTB_4 (4 h test period). Thus, a 4 h LTB_4 reaction induced a 66% and 110% increase in collagen IV and laminin LER size, respectively, as compared to control tissues.

LERs remained enlarged up to 24 h and returned to basal levels by 48 h post LTB_4 stimulation. No significant differences in the densities of collagen IV and laminin LERs could be observed. The number of LE sites per unit area was comparable

between laminin and collagen IV and ranged between 14281 - 9614 sites/mm^2 and 13929 - 10580 sites/mm^2, respectively (Figure 6.8, right panels).

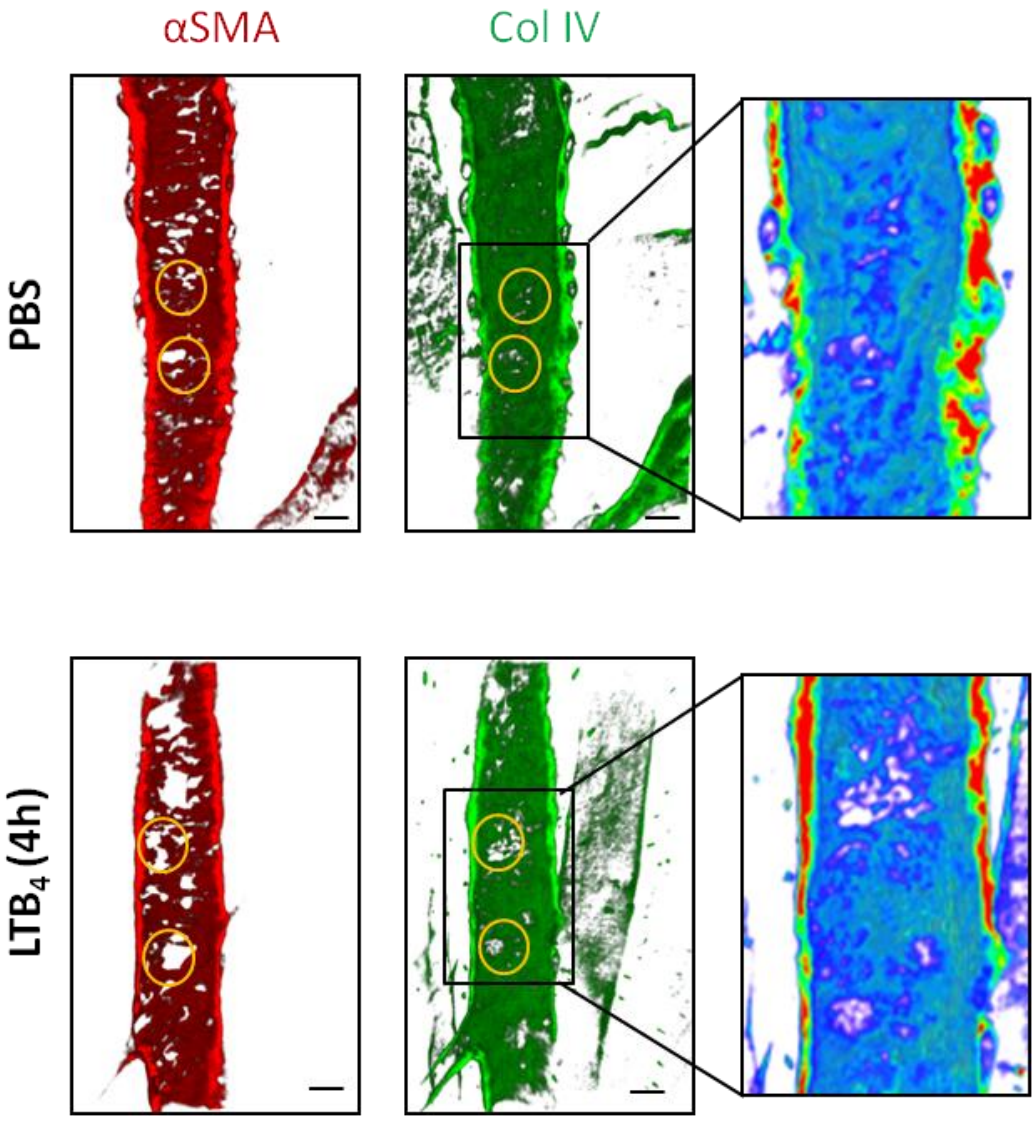

Figure 6.7: Time-dependent change in collagen type IV LERs in response to LTB_4. Cremaster muscles were treated with PBS or LTB_4 (30 ng) for 4 h. Tissues were fixed, permeabilised and stained with antibodies against αSMA (pericytes) and collagen IV. Representative 3D-reconstructed single channel confocal images of PBS- or LTB_4-treated post-capillary venules display the pericyte layer (red) and venular BM collagen type IV (green). Gaps between adjacent pericytes and BM LERs are shown (encircled). The corresponding intensity profiles of collagen IV with a spectrum colour code (blue indicating low-intensity-sites and red indicating high-intensity-sites) are also shown in a higher magnification (right). Scale bar, 20 µm

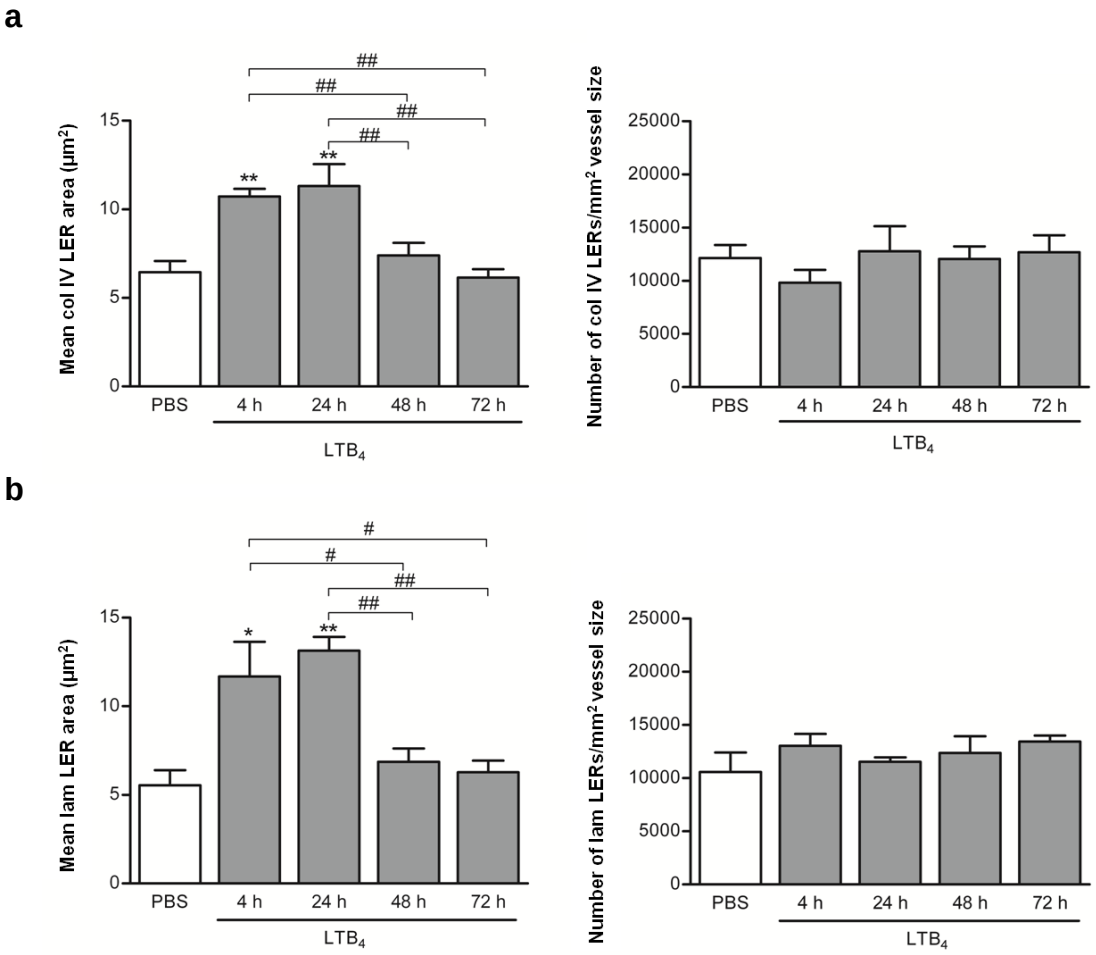

Figure 6.8: Time-dependent change in collagen type IV and laminin LERs in response to LTB_4. Changes in venular BM morphology were quantified in 3D-reconstruced confocal images of cremaster muscles stimulated with LTB_4 (30 ng) or PBS for the indicated length of time using ImageJ. Images used for analysis were the same as analysed for Figure 5.1 and 5.3. Collagen Type IV **(a)** and laminin **(b)** LERs were quantified for their size (left) and density (right) in 200 µm vessel segments. White Bars represent control samples (PBS, 4-72h pooled together) and grey bars correspond to LTB_4-stimulated tissues. At least 4 vessel segments per mouse were analysed and plotted as mean per mouse. Data are represented as the mean ±SEM of at least 3 independent experiments. Significant differences between groups were determined using one-way ANOVA and Neuman-Keuls multiple comparison test. Differences between LTB_4 and PBS control are marked with asterisks. Differences between time points were marked with hashes. (**: $p < 0.01$, ***: $p < 0.001$, #: $p < 0.05$, ##: $p < 0.01$, ###: $p < 0.001$)

Mechanisms of LTB_4-induced alterations in BM composition

Recent data obtained from our laboratory showed that emigrating neutrophils appear to preferentially use enlarged gaps between adjacent pericytes to exit the vessel wall, sites that are colocalised with BM LERs (Proebstl et al., 2012). It is hypothesised that the composition of the BM might regulate leukocyte transmigration as different matrix constituents exhibit different biochemical and biophysical properties (Wu et al., 2009; Wondimu et al., 2004b; Kenne et al., 2010; Hallmann et al., 2005; Rowe and Weiss, 2008). However, despite the fact that pericyte gap opening was absent in $TNFR^{-/-}$ mice, TNFR-deficiency had no impact on the number of transmigrated neutrophils in LTB_4 stimulated tissues as described in chapter 5. To analyse the effect of TNF on BM remodelling/regeneration and to directly compare the profile of neutrophil transmigration in $TNFR^{-/-}$ animals in relation to changes in pericyte and BM morphology, time course experiments were performed. For this purpose, the same tissues were used as described for pericyte shape change. Independent experiments were performed at least 3 times.

LTB_4 was injected i.s. into WT or $TNFR^{-/-}$ mice and cremaster muscles were dissected away after different *in vivo* test periods, fixed and used whole mounted for immunofluorescent staining for confocal analysis. Neutrophils, pericytes and BM were visualised using an anti-MRP-14, anti-αSMA, and anti-collagen IV antibody, respectively. Both, WT and $TNFR^{-/-}$ mice showed a time-dependent increase in LER size post LTB_4 stimulation of cremaster muscles *in vivo,* a response that peaked at 4 h post inflammation (Figure 6.9 and 6.10). These results suggest that in contrast to pericyte shape change, TNFR deficiency has no effect on BM LER remodelling in response to LTB_4. Interestingly however, whilst the size of collagen IV LERs was back to basal level by 48 h in WT mice, in TNFR deficient mice the LERs remained enlarged at 48 h post LTB_4 and was back to basal level by 72 h. These results indicate that LTB_4-induced TNF release might contribute to the regeneration of venular BM *in vivo* and hence post inflammation BM remodelling.

Quantification of MRP-4 positive cells in these tissues showed that TNFR-deficient mice exhibited a similar onset of neutrophil transmigration following LTB_4 as compared to WT animals (Figure 6.10). Although $TNFR^{-/-}$ mice showed collagen IV LER enlargement, a response that was previously reported to be neutrophil-protease-dependent(Wang et al., 2006), pericyte shape change was absent in these mice throughout the whole time course. 24 h post LTB_4 injection both groups still exhibited a significant level of transmigrated neutrophils within the tissue as

compared to PBS-treated cremaster muscles. Of note, although not significant, the number of neutrophils within the tissue at this time point seemed to be higher in TNFR-deficient mice as compared to WT animals.

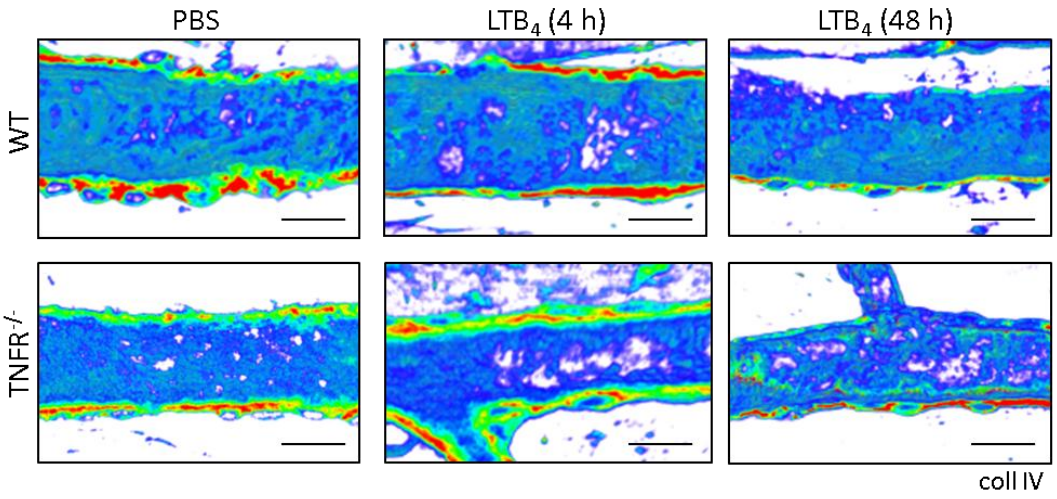

Figure 6.9: Profile of LTB_4-induced BM deposition in WT and $TNFR^{-/-}$ mice. WT C57BL/6 and $TNFR^{-/-}$ mice received LTB_4 (30 ng) or PBS as a control. Cremaster muscles were extracted 4 or 48 h post injection, fixed and immunostained for confocal analysis. Intensity profiles of collagen IV with a spectrum colour coding (blue indicating low-intensity-sites and red indicating high-intensity sites) are shown of WT (top) and $TNFR^{-/-}$ post-capillary venules (bottom) treated with PBS (4 h) or LTB_4 for 4 or 48 h. Scale bar, 20 µm

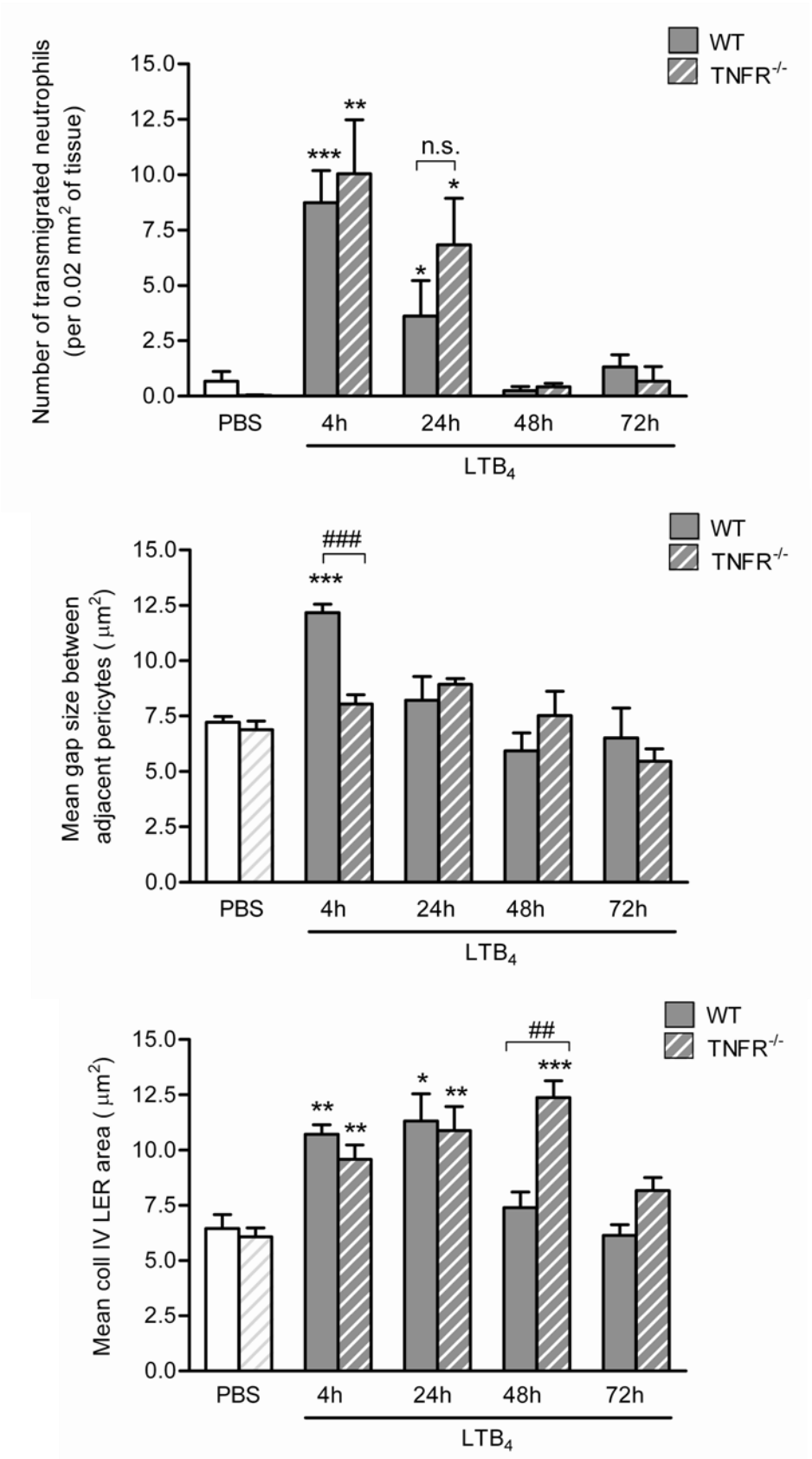
WT
TNFR-/-
Number of transmigrated neutrophils (per 0.02 mm2 of tissue)
15.0
12.5
10.0
7.5
5.0
2.5
0.0
***
**
n.s.
*
*
PBS
4h
24h
48h
72h
LTB4
WT
TNFR-/-
Mean gap size between adjacent pericytes (μm2)
###
***
PBS
4h
24h
48h
72h
LTB4
WT
TNFR-/-
Mean coll IV LER area (μm2)
##
**
**
*
**
***
PBS
4h
24h
48h
72h
LTB4

Figure 6.10: Profile of LTB_4-induced neutrophil transmigration in relation to pericyte shape change and BM deposition in WT and $TNFR^{-/-}$ mice. WT C57BL/6 and $TNFR^{-/-}$ mice received LTB_4 (30 ng) or PBS as a control. Cremaster muscles were extracted at different time points, fixed and immune-stained for confocal analysis. Neutrophil transmigration (top), pericyte gap size (middle) and BM LER remodelling/deposition were quantified in 3D-reconstruced confocal images of 200 µm post-capillary vessel segments using ImageJ. Images of WT animals used for analysis were the same as analysed for Figure 6.8. White bars represent control samples (PBS, 2-72h pooled together) and grey bars correspond to LTB_4-stimulated tissues of WT (filled) or $TNFR^{-/-}$ mice (patterned). At least 4 vessel segments per mouse were analysed and plotted as mean per mouse. Data are represented as the mean ±SEM of at least 3 independent experiments. Significant differences between groups were determined using two-way ANOVA and Bonferroni multiple comparison test. Differences compared to PBS control are marked with asterisks. Differences between time points were marked with hashes. (*: $p < 0.05$, **: $p < 0.01$, ***: $p < 0.001$, ##: $p < 0.01$, ###: $p < 0.001$)

6.3 DISCUSSION

Inflammation induced by injury or infection is characterised by changes in vascular morphology, plasma protein and fluid leakage and leukocyte transmigration. In inflammation evoked by chemoattractants, these responses are dependent on neutrophil activation (Hurley J.V., 1964; Wang et al., 2006; Wedmore and Williams, 1981). As such, the presence and/or intact adhesive function of neutrophils has been shown to be required for the induction of vascular permeability (Arfors et al., 1987; Wedmore and Williams, 1981), BM remodelling (Wang et al., 2006) and pericyte shape change (as shown in this study) in response to chemotactic stimuli. However, the underlying mechanisms by which neutrophils may control these events are less well understood. Chapter 5 demonstrated the pivotal role of endogenous TNF in chemoattractant-evoked pericyte shape change. Here the role of this cytokine as a secondary mediator in inducing vascular leakage and BM remodelling/deposition was investigated using $TNFR^{-/-}$ mice. In addition, the temporal association of changes in vascular morphology, pericyte shape change, LER enlargement, and neutrophil transmigration were studied in both WT and TNFR-deficient mice.

To analyse the role of TNF in vascular leakage as induced by chemoattractants, permeability assays were performed *in vivo* using i.v. Evans Blue as a tracer. In line with experiments by others (Bjork et al., 1982; Wedmore and Williams, 1981), plasma protein leakage into the tissue was strictly neutrophil-dependent in our model as determined in studies with neutrophil-depleted mice. Furthermore, LTB_4-, C5a- and KC-induced permeability was rapid and transient as infiltration of plasma fluid into the tissue could be observed within 30 min post tissue stimulation. Of interest, vascular leakage in response to LTB_4, C5a and KC was absent in $TNFR^{-/-}$ mice. This was confirmed in different vascular beds including the dorsal skin, ear skin and cremaster muscle models. Hence, our data demonstrate for the first time a pivotal role for TNF in vascular permeability in response to chemoattractants.

Neutrophil chemoattractants (C5a des Arg, fMLP and LTB_4), in contrast to IL-1β, have been shown to induce rapid plasma protein leakage, which is unaffected by local inhibition of protein synthesis (Rampart and Williams, 1988). This suggests a rapid release of preformed mediators and is in line with our findings that vascular leakage is dependent on endogenous TNF. A study performed by Wong et al showed that exogenously administered TNF and IFN-γ induces a redistribution of VE-cadherin from EC junctions and increased vascular permeability in the rat

(Wong et al., 1999). However, the exact mechanism through which TNF mediates chemoattractant-induced vascular permeability in our model (chemoattractant-stimulated murine tissues) remains to be explored. LTB_4-stimulated human neutrophils have been shown to induce rapid EC permeability *in vitro* via the release of heparin-binding protein (HBP) (Di et al., 2009). It is however unclear whether HBP is also involved in the mouse models used in the present study and if so whether it acts downstream or upstream of TNF. This and possible differences between species needs to be further investigated.

The potential role of chemoattractant-induced TNF in regulation of vascular BM remodelling was also investigated. The vascular BM envelops pericytes and - similar to pericytes - undergoes morphological changes during inflammation as evoked by numerous inflammatory stimuli (Reichel et al., 2008; Reichel et al., 2009; Reichel et al., 2011; Voisin et al., 2009; Voisin et al., 2010; Wang et al., 2006). The BM layer is heterogeneous and sites of lower matrix protein expression (LERs) are preferably used by transmigrating leukocytes (Voisin et al., 2010; Wang et al., 2006). In the present study, a time-dependent and transient enlargement of collagen IV and laminin LERs in response to LTB_4 was demonstrated. In contrast to pericyte gap size, TNFR deficiency had no effect on LTB_4-induced LER enlargement. This is in accordance with the concept that BM remodelling is strictly neutrophil-dependent and requires protease activity (Wang et al., 2006). However, in comparison to WT animals (LER size was back to basal levels by 48 h), LER enlargement was prolonged in $TNFR^{-/-}$ mice and returned to basal levels by 72 h, suggesting a role for TNF downstream of LTB_4 in post-inflammatory BM deposition.

As leukocyte transmigration through the vascular BM is associated with a transient increase in vascular permeability and reduced barrier function (Huber and Weiss, 1989a; Hurley J.V., 1964), BM deposition post inflammation might regulate leukocyte transmigration by reconstituting the barrier function of the vessel wall. Indeed, $TNFR^{-/-}$ mice showed a trend towards higher levels of neutrophils within the tissue at later time points (24 h). This sustained neutrophil response might suggest a role for BM deposition in the termination of the neutrophil transmigration response. However, further studies are required to analyse a possible connection between these events.

Due to the close association of collagen and laminin LERs with pericyte gaps, pericytes are hypothesised to regulate the heterogeneous morphology of the BM. By regulating the composition of the BM, pericytes might control their biochemical

and biophysical property. Pericytes have previously been shown to be a source of extracellular matrix proteins both *in vitro* and *in vivo* (Cohen et al., 1980; Fujiwara et al., 2010; Hallmann et al., 2005; Mandarino et al., 1993; Stratman et al., 2009; Canfield et al., 1990). Thus, these mural cells might be involved in regulating the re-generation of extracellular BM post inflammation and hence, regulate the re-sealing of LERs towards basal levels during the resolution phase of inflammation. Post-inflammatory BM generation by pericytes might involve similar mechanisms to that involved in wound healing, where growth factors such as TGF-β regulate the remodelling of wound tissues through collagen secretion by myofibroblasts (Dulmovits and Herman, 2012). Furthermore pericytes have been shown to produce extracellular matrix proteins during vasculogenesis, a response that was dependent on the pericyte-derived matrix metalloproteinase inhibitor TIMP-3 (Stratman et al., 2009). However, generation of extracellular matrix proteins in the context of inflammation has not been shown yet. Thus, further studies are needed to analyse whether pericytes indeed stimulate *de novo* synthesis of matrix components in chemoattractant-driven inflammatory reactions and in response to TNF. In addition, the functional consequence of this phenomenon in relation to neutrophil transmigration response requires further investigations.

CHAPTER 7: GENERAL DISCUSSION

7.1 Project overview

The venular wall acts as a semi-permeable barrier at the interface between circulating blood and the interstitial tissue, controlling the passage of cells (such as leukocytes) and macromolecules in and out of the bloodstream. Leukocyte exit from the blood during inflammatory conditions occurs via highly regulated processes involving specific interactions with all 3 components of the vessel wall: *i.e*. the endothelium, the pericyte sheath and the venular BM (Nourshargh et al., 2010). Lack of regulation of leukocyte recruitment can, however, lead to severe pathological inflammatory diseases such as myocardial infarction, stroke, rheumatoid arthritis, acute respiratory distress syndrome and inflammatory bowel disease (Luster et al., 2005; Mackay, 2008).

To understand the complex regulation of leukocyte transmigration in health and disease, the analysis of all components involved in this process including inflammatory cells, inflammatory mediators, ECs, BM and pericytes is required. This PhD thesis aimed to investigate the responses of pericytes in inflammatory conditions in relation to the key inflammatory responses of leukocyte transmigration and vascular permeability.

The presented data demonstrate the ability of pericytes to directly and indirectly respond to different types of inflammatory mediators, including cytokines and chemoattractants. Furthermore, the findings discovered the cellular mechanisms that mediate pericyte shape change in chemoattractant-induced inflammation and identified endogenous TNF as a crucial mediator in chemoattractant-induced inflammation. Thus, the findings of the present study contribute to our understanding of pericyte biology in inflammation and have opened novel avenues for future research. The following discussion gives an overview of possible functions of pericytes in inflammation and discusses the potential role of TNF in chemoattractant-induced responses, including pericyte shape change, BM protein deposition and vascular permeability.

7.1.1 Pericytes are able to respond to inflammatory mediators

Expression of inflammation modulating surface molecules on pericytes

The recruitment and activation of neutrophils into inflamed tissue involves a tightly regulated and complex process of interactions of leukocytes with different components of the venular wall (Nourshargh et al., 2010). Although the role of adhesion molecules has been well documented in leukocyte-EC interactions, little is known about adhesion molecules on pericytes, not to mention their regulation during inflammatory scenarios. In this study, the pericyte-like cell line C3H/10T1/2 was found to express several adhesion molecules (integrins, JAMs, CAMs), as investigated by confocal microscopy and flow cytometry. In addition, the expression of receptors for cytokines (TNFR I, TNFR II and IL-1R I) could be confirmed. This is in line with previous *in vitro* studies suggesting that pericytes generally express adhesion molecules at basal levels (Maier and Pober, 2011; Verbeek et al., 1995; Stratman et al., 2009; Balabanov et al., 1999). Low levels of constitutive ICAM-1 (Balabanov et al., 1999; Maier and Pober, 2011; Verbeek et al., 1995), LFA-3 (Maier and Pober, 2011) and β1-integrins (Stratman et al., 2009) have previously been detected on unstimulated primary pericytes isolated from several species and organs (rat brain, human brain, human placenta and bovine retina). The overall role of these surface molecules on pericytes, however, is not well understood.

Adhesion molecules expressed by pericytes might represent possible interaction partners for ECs, BM compounds and transmigrating leukocytes as has been shown for ECs (Figure 7.1) (Muller, 2003; van der and Sonnenberg, 2001; Vestweber, 2002). Since C3H/10T1/2 cells expressed receptors for main BM components including the integrins $\alpha_1\beta_1$ (collagen receptor), $\alpha_6\beta_1$ (laminin receptor) and $\alpha_5\beta_1$ (fibronectin receptor), these adhesion molecules might be involved in pericyte-BM interactions and thus, might have a role in supporting the structure of the vessel wall and/or BM remodelling. The expression of JAMs on pericytes might regulate cell-cell interactions with adjacent cells via homophilic interactions. In addition, expression of JAMs on pericytes might enable these mural cells to associate with leukocytes as they bind β_2 integrins LFA-1 and Mac-1 as well as with the β_1 integrin $\alpha_4\beta_1$ (Bazzoni, 2003; Bradfield et al., 2007). Pericytes might also regulate leukocyte interactions through ICAM-1 and VCAM-1, molecules that have been shown to be expressed on both C3H10/T1/2 cells and pericytes *in vitro* and *in vivo*.

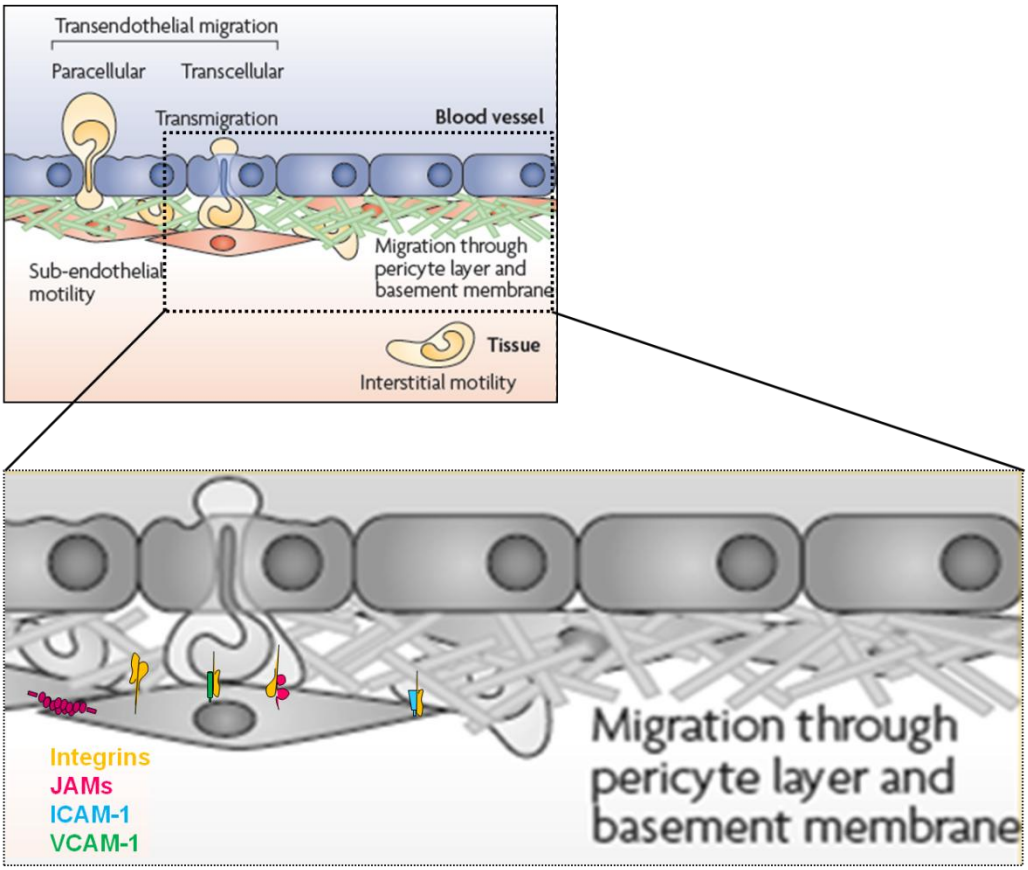

Figure 7.1: Adhesion molecules on pericytes. Adhesion molecules expressed by pericytes such as integrins, members of the JAM family, ICAM-1 and VCAM-1 might represent possible interaction partners for transmigrating leukocytes, adjacent pericytes, ECs and BM components. (Figure modified from *(Nourshargh et al., 2010)*).

Whereas all integrins and JAMs analysed in the present study showed no change in expression levels upon TNF and IL-1β stimulation of C3H/10T1/2 cells, ICAM-1 and VCAM-1 were both upregulated in response to these cytokines. Thus, these pericyte-like cells are able to directly respond to TNF and IL-1β. In addition, upregulation of ICAM-1 and VCAM-1 on pericytes suggests that these adhesion molecules may be regulated on pericytes at sites of inflammation. Similar results were previously reported for primary pericytes in culture. In this context, ICAM-1 upregulation could be detected on rat and human brain pericytes, bovine retinal pericytes and human placental pericytes in response to TNF, IFN-γ, LPS, high glucose, fMLP and necrotic cell lysates *in vitro* (Kowluru et al., 2010; Maier and Pober, 2011; Verbeek et al., 1999; Stark et al., 2013). In contrast, VCAM-1 was not expressed on unstimulated or TNF-stimulated human placental pericytes in culture

(Maier and Pober, 2011), but upregulation has been detected on primary pericytes isolated from human brain upon TNF treatment (Verbeek et al., 1995).

Both, ICAM-1 and VCAM-1 expression by pericytes were further associated with inflammatory diseases as demonstrated using biopsy samples of patients with rheumatoid arthritis (Kriegsmann et al., 1995), multiple sclerosis (Verbeek et al., 1995) and bullous pemphigoid (Dahlman-Ghozlan et al., 2004). Hence, these studies strongly suggest that direct pericyte-leukocyte interaction can occur and that adhesion molecules on pericytes are regulated during inflammation.

Recent *in vivo* data obtained within our laboratory and by others showed that TNF-stimulated murine tissues also exhibited increased ICAM-1 expression on pericytes as compared to PBS-treated controls (Stark et al., 2013; Proebstl et al., 2012). Functional assays using confocal IVM further suggested a role for adhesion molecules on post-capillary pericytes in innate immune responses (Proebstl et al., 2012). Interestingly, after penetration of the EC layer leukocytes crawl along pericyte processes. Sub-endothelial neutrophil migration was hardly seen in pericyte-deficient regions and seemed to be regulated by pericyte-leukocyte interactions. Similar to neutrophil crawling on ECs (Phillipson et al., 2006), ICAM-1 was shown in this study to drive neutrophil crawling on pericytes through interaction with the integrins Mac-1 and LFA-1 on neutrophils. However, as ICAM-1 blocking antibodies did not completely abolish sub-endothelial neutrophil crawling, other pericyte-associated adhesion molecules might be involved in this process.

In addition to facilitating neutrophil transmigration through the pericyte sheath, adhesion molecules on pericytes might also have other functions. Interactions between capillary and arterial pericytes and extravasated neutrophils and monocytes via ICAM-1 for example have recently been shown to facilitate their directional migration within the interstitial tissue (Stark et al., 2013). Pericytes have also been implicated in adaptive immune responses in neuroinflammatory processes and T-cell development *in vitro* and a role for pericytic ICAM-1 and VCAM-1 has been suggested in this process (Balabanov et al., 1999; Verbeek et al., 1995; Zachariah and Cyster, 2010). Furthermore, adhesion molecules on pericytes including integrins and members of the JAM family might play a role in mediating inflammatory responses by enabling pericyte-EC and pericyte-pericyte crosstalk and/or signalling through direct contact with BM components. However, these hypotheses remain elusive and further experiments are required.

Pericyte shape change in response to neutrophil chemoattractants

In addition to regulating the expression of adhesion molecules on pericytes, TNF and IL-1β were recently shown to induce changes in pericyte morphology, resulting in an increase in size of gaps between adjacent pericytes (Proebstl et al., 2012). As part of this thesis, the effects and mechanisms of several neutrophil chemoattractants including LTB_4, KC, C5a and fMLP on pericyte gap size were investigated *in vivo*. Results demonstrate that these neutrophil chemoattractants not only induce the migration of neutrophils into stimulated tissue, but also cause an increase in the size of pericyte gaps and BM protein LERs as analysed by immunofluorescent staining and confocal microscopy (Figure 7.2).

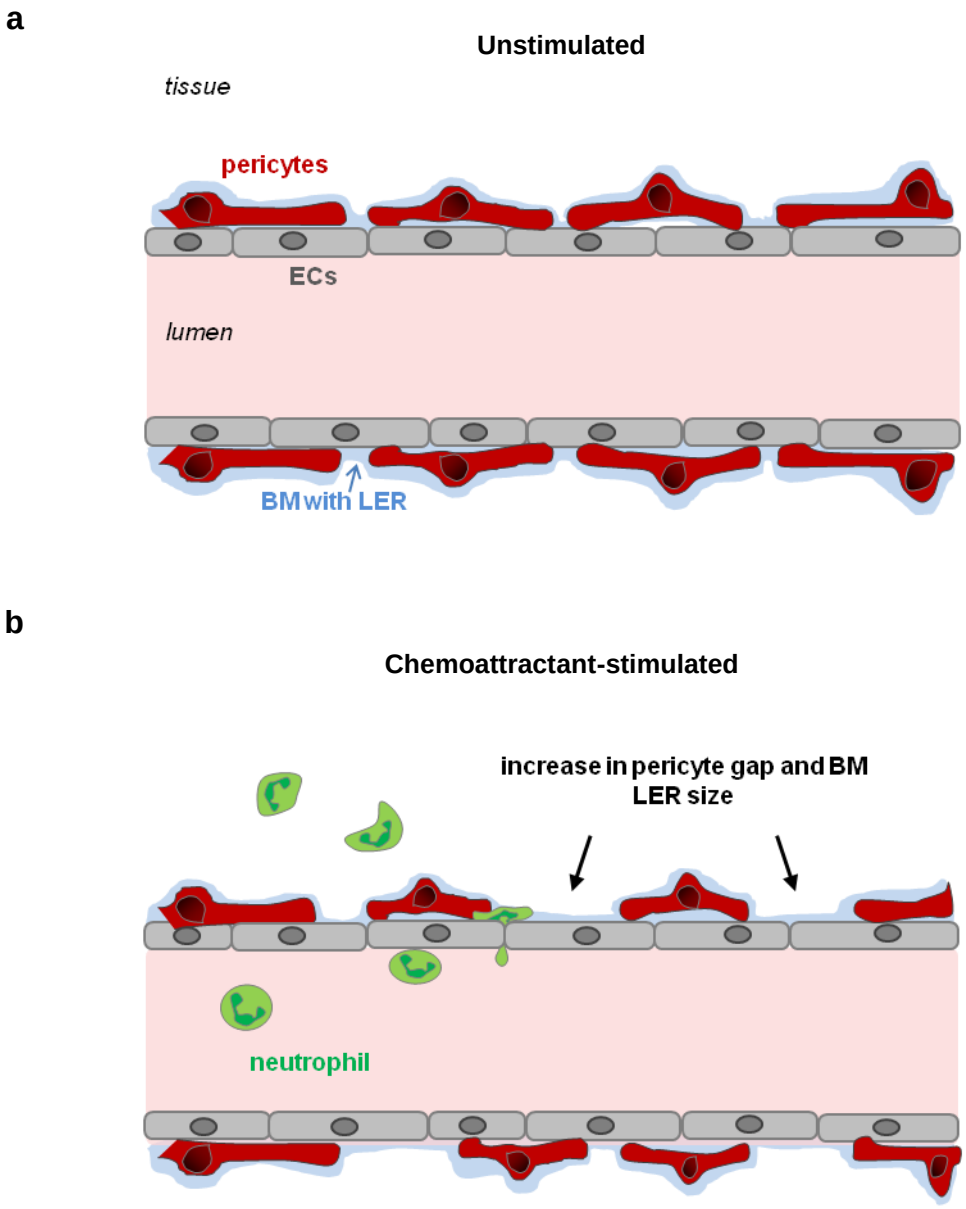

Figure 7.2: Chemoattractants induce changes in vascular morphology. **(a)** Venular walls (sites of neutrophil transmigration) consist of the endothelium (grey), the pericyte layer (red) and their associated BM (blue). Whilst ECs form a monolayer with tight junctions between adjacent cells, pericytes form a discontinuous network around blood vessels, often with notable gaps between adjacent pericytes. These gaps are aligned with LERs, venular wall regions that have been previously shown to act as preferential exit sites by transmigrating leukocytes. **(b)** Inflammation induced by local injection of chemoattractants (e.g. LTB_4, KC, C5a) was associated with leukocyte transmigration and an increase in size of gaps between adjacent pericytes and BM LERs in postcapillary venules.

A comparison of LTB_4-induced pericyte gap-opening and neutrophil transmigration revealed that these events occurred within comparable time frames, both responses peaking at 4 h post tissue stimulation. Using neutropenic mice, as induced by antibody-based depletion of circulating neutrophils, the results demonstrated that the enlargement of pericyte gaps in response to chemoattractants is strictly neutrophil-dependent. This is in contrast to responses induced by the pro-inflammatory cytokines TNF and IL-1β that can induce pericyte shape change in a neutrophil-independent manner via direct activation of pericyte expressed TNF and IL-1 receptors (Proebstl et al., 2012). To date there is no evidence for the presence of chemoattractant receptors on pericytes or the ability of chemoattractants to directly stimulate pericytes. Indeed, chemoattractants such as LTB_4 are thought to primarily stimulate and recruit leukocytes as part of the host immune response (Bjork et al., 1982; Di et al., 2009; Ford-Hutchinson et al., 1980). Hence, pericyte gap enlargement in response to LTB_4 might be an indirect effect of this chemoattractant on neutrophils.

As pericyte gap enlargement occurred within 4 h of stimulation, we hypothesised that pericyte stimulation is mediated by rapidly released secondary factors. Neutrophils possess a high amount of granules and secretory vesicles within their cytoplasm, containing antimicrobial and cytotoxic substances, enzymes, and cytoplasmic membrane receptors (Ford-Hutchinson et al., 1980). During inflammation as induced by chemoattractants, activated neutrophils can release these substances following degranulation. Thus, the roles of several vasoactive factors, including PAF and ROS which are released by neutrophils following chemoattractant-induced inflammation (Auch-Schwelk et al., 1989; Kerkar et al., 2001; Soloviev and Braquet, 1991; Sumimoto et al., 1984; Tessner et al., 1989) were analysed on stimulating pericyte shape change. Furthermore, the role of NE was investigated, as this serine protease is able to cleave BM components which might in turn regulate pericyte shape change. However, neither PAF nor ROS or NE had an effect on pericyte morphology in response to LTB_4, as analysed in mice treated with a PAF-antagonist, ROS scavengers or as analysed in $NE^{-/-}$ mice, respectively. Notably, when ROS scavengers were used, pericyte gap opening occurred even in the absence of neutrophil transmigration (neutrophils accumulated within the vessel). This suggests that direct leukocyte-pericyte interaction is not crucial for the induction of pericyte shape change.

In contrast, a pivotal role for TNF in chemoattractant-induced pericyte gap enlargement was shown as this response was completely abolished in $TNFR^{-/-}$ mice upon LTB_4, KC or C5a stimulation. Although activated macrophages are thought to be the primary source of TNF (Cavaillon et al., 1990; Schindler et al., 1990), neutrophils are also able to release TNF in different models of inflammation as induced by chemoattractants (KC or LTB_4) (Chou et al., 2010; Gaudreault and Gosselin, 2009; Saiwai et al., 2010; Vieira et al., 2009) or other inflammatory mediators such as LPS and Y-IgG or upon exposure to *Candida albicans* (Bazzoni et al., 1991; Djeu et al., 1990; Dubravec et al., 1990; Haziot et al., 1993; Vieira et al., 2009). Though still a matter of debate (Kim et al., 2006), neutrophil-derived TNF expression downstream of the BLT1 (LTB_4 receptor) signalling pathway has been shown recently in a murine model of inflammatory arthritis *in vivo* (Chou et al., 2010). Quantitative RT-PCR of mRNA isolated from transmigrated neutrophils after spinal cord injury further revealed increased levels of TNF, which were abolished in BLT1-knockout mice and mice treated with a LTB_4 receptor antagonist (Saiwai et al., 2010). In another study by Gaudreault and Gosselin LTB_4 induced TNF secretion from isolated human neutrophils by potentiating CpG-mediated intracellular signalling (Gaudreault and Gosselin, 2009). Taken together, these studies indicate that TNF expression can be induced downstream of LTB_4-BLT1 signalling. However, further studies are needed to clarify whether neutrophils indeed secrete TNF in our model or whether this cytokine is secreted from other cells, such as ECs or pericytes in response to activated neutrophils directly or indirectly. Other potential sources of TNF and experimental approaches to investigate such issues in future studies are discussed in section 7.1.3., 7.2.1, respectively.

Another issue that requires resolving is whether the observed changes in pericyte morphology noted in the present study are due to pericyte contraction or relaxation, as both phenomena have been shown in pericytes in response to different inflammatory mediators. Pericyte contraction can occur in response to VEGF (Donoghue et al., 2006), vasoactive substances such as histamine (Kelley et al., 1987), serotonin (Speyer et al., 2000; Kelley et al., 1987) and bradykinin (Speyer et al., 2000), and inflammatory mediators such as PAF (Khoury and Langleben, 1998), TNF (Kerkar et al., 2006), IL-1β (Kerkar et al., 2006) and LPS (Khoury and Langleben, 1998; Speyer et al., 2000). TNF and IL-1β both activate small GTPases such as RhoA, Rac 1 and cdc42, which are known to regulate the actin cytoskeleton (Puls et al., 1999). Cdc41 is involved in regulating signalling pathways that control cell morphology by filopodial extension, Rac1 promotes an actin-dependent

protrusion activity via lamellopodia formation, and RhoA promotes focal adhesion and microfilament bundle assembly (Jaffe and Hall, 2005). Of interest, contractility of primary bovine retinal pericytes as observed by a marked decrease in cell size are mediated by RhoA–dependent disassembly of αSMA stress fibres and formation of non-muscle actin fibres (Kolyada et al., 2003); Rac1 and cdc42 appear to be not involved in pericyte shape change (Kolyada et al., 2003; Kutcher et al., 2007; Kutcher and Herman, 2009). In contrast, in another study IL-1β-induced pericyte shape change in postcapillary venules of the cremaster muscle has been recently associated with suppression of RhoA/ROCK signalling and hence, pericyte relaxation rather than contraction (Wang et al., 2012). However, whether pericyte shape change in our model of chemoattractant-induced responses is due to contraction or relaxation needs to be analysed in future experiments.

7.1.2 Suggested roles of pericyte shape change during inflammation

As shown recently by our group, pericyte gaps are aligned with BM LERs. These sites are preferentially used as exit points by transmigrating neutrophils, indicating a functional implication of these sites in leukocyte trafficking (Voisin et al., 2009; Voisin et al., 2010; Wang et al., 2006; Proebstl et al., 2012). Hence, it was hypothesised that besides direct leukocyte-pericyte interactions through adhesion molecules, pericytes may also regulate leukocyte extravasation through altered morphology and/or regulating the generation of extracellular BM. As a result, the role of active pericyte shape change in several aspects of inflammation, including neutrophil transmigration, BM remodelling and deposition, and vascular permeability was investigated (Figure 7.3). For this purpose, $TNFR^{-/-}$ mice were used, mice in which pericyte gap opening in response to chemoattractants was inhibited.

Role of pericyte shape change in leukocyte transmigration?

In WT mice, the highest level of neutrophil transmigration in response to LTB_4 was observed at the 4 h time point, when also pericyte gap size was at its maximum. However, blocking pericyte gap enlargement in $TNFR^{-/-}$ mice had no effect on the number of transmigrated neutrophils in our model. In an earlier study performed by our group, quantifications of the size of gaps used by transmigrating leukocytes revealed that migration of neutrophils into surrounding tissues primarily occurs

through enlarged gaps (Proebstl et al., 2012). Despite the tempting conclusion that leukocytes are attracted by increased pericyte gaps and hence, pericyte shape change supports leukocyte transmigration, it could also be that leukocyte engagement with the pericytes itself causes the gap enlargement as has been shown previously for LERs (Voisin et al., 2010; Wang et al., 2006). This is supported by a recent study demonstrating that PMN-pericyte contact mediates a change in pericyte morphology by inhibiting RhoA/ROCK signalling *in vitro* and *in vivo* (Wang et al., 2012). However, in contrast to this study, where Tolazoline-induced pericyte shape change (relaxation) facilitated PMN transmigration, in the present work neutrophil transmigration occurred independently of pericyte gap enlargement and was indeed evident under conditions where pericyte shape change was blocked, *i.e*. in $TNFR^{-/-}$ mice. Based on these results, the role of TNF signalling in pericyte shape change needs to be investigated.

Whilst the present results did not show a significant difference in the onset of LTB_4-induced neutrophil transmigration response between WT and $TNFR^{-/-}$ mice, a trend towards prolonged neutrophil infiltration could be observed in TNFR-deficient animals. Hence, the data indicate that pericyte shape change is not required for neutrophil transmigration per se, but might have a role in the termination of neutrophil transmigration. One possibility is that pericytes can negatively regulate leukocyte transmigration via venular contraction; but again, this requires further analysis.

Role of pericyte shape change in regulating BM deposition?

Pericytes synthesise and are embedded within the venular BM. With a pore size of ~50nm, the vascular BM represents a barrier with a high resistance to transmigrating leukocytes and macromolecules (Rowe and Weiss, 2008). During inflammation, leukocyte transmigration through this layer is associated with a transient increase in permeability and reduced barrier function (Huber and Weiss, 1989a; Hurley J.V., 1964). Similar to the pericyte sheath, the BM undergoes morphological changes in response to inflammatory stimuli (Reichel et al., 2008; Reichel et al., 2009; Reichel et al., 2011; Voisin et al., 2009; Voisin et al., 2010; Wang et al., 2006). In the present study, LTB_4 induced a transient enlargement of collagen type IV and laminin LERs within the vascular BM. This response has been shown previously to be strictly neutrophil-dependent (Voisin et al., 2010; Wang et

al., 2006). BM remodelling in response to LTB_4 was independent of TNF signalling and pericyte shape change in that LERs still increased in size when pericyte gap opening was completely blocked in $TNFR^{-/-}$ mice. In contrast, the enlargement of LERs was prolonged in these animals. Since $TNFR^{-/-}$ mice further exhibited a higher neutrophil transmigration response at later time points as compared to WT animals (not significant), LER size might have a role in regulating leukocyte transmigration. This hypothesis is supported by *in vitro* studies in which native EC-derived BM deposits delay neutrophil adhesion and migration depending on the concentration (Burton et al., 2011; Butler et al., 2008). The composition of BM can both facilitate and inhibit leukocyte transmigration due to the biophysical (Rowe and Weiss, 2008) and/or biochemical (Wondimu et al., 2004a), (Wu et al., 2009) properties of different BM components. As pericytes contribute to the generation of the BM and LERs are closely associated with pericyte gaps, pericytes are hypothesised to regulate the heterogeneous morphology of the BM. By regulating the size of LERs, pericytes might play an indirect role in regulating leukocyte transmigration through this layer. However, it has not yet been shown, whether inflammatory mediators indeed stimulate BM production and deposition by pericytes, and whether this impacts the transmigration response *in vivo*.

Pericytes express receptors for key BM components including integrins $\alpha_1\beta_1$, $\alpha_2\beta_1$ (collagen receptors), $\alpha_3\beta_1$, $\alpha_6\beta_1$, $\alpha_7\beta_1$, $\alpha_6\beta_4$ (laminin receptors), $\alpha_4\beta_1$ and $\alpha_5\beta_1$ (fibronectin receptors) (Silva et al., 2008). Hence, *in vivo* pericytes may be able to detect changes in the BM morphology and consequently respond to them through adhesive mechanisms. As suggested previously for αSMA-positive myofibroblasts in fibrosis (Dulmovits and Herman, 2012), pericyte contraction may mediate the generation of *de novo* BM proteins through tightening previously secreted BM proteins and thereby generating space for further BM deposition.

Pericyte shape change and vascular permeability

Pericytes are associated with regulating vascular permeability by increasing the resistance of EC monolayers *in vitro* (Dohgu et al., 2005; McGuire et al., 2011; Dente et al., 2001; Hayashi et al., 2004) and regulating vascular leakage in the blood-brain barrier *in vivo* (Armulik et al., 2010; Daneman et al., 2010). However, whether pericytes also regulate vascular permeability during inflammation is not clear yet. An *in vitro* study using a pericyte-EC coculture model suggested that

inflammatory mediators (TNF and IL-1β) decrease the vascular barrier function by inducing pericyte shape change (Kerkar et al., 2006). However, in the present model vascular leakage to i.v. Evans Blue, as induced by chemoattractants, preceded pericyte gap opening. This argues against the hypothesis that pericyte shape change as observed following LTB_4, KC and C5a treatment regulates vascular permeability during inflammation. However, vascular permeability might regulate pericyte shape change instead. Inflammation-induced tissue oedema is part of the host defence and regulates the supply of inflammatory mediators, antibodies, fibrin and other plasma proteins to the tissue. Hence, it is possible that factors in the plasma exudate might have a role in pericyte shape change. In this context, recent studies conducted by my colleague Dr Mathieu-Benoit Voisin demonstrated that under conditions where leukocyte transmigration is inhibited at the level of ECs (using an ICAM-1 blocking antibody 30 min post LTB_4 injection), whilst pericyte gap enlargement was suppressed, vascular permeability was unaltered. These results indicate that increased leakage of plasma proteins is not sufficient to induce pericyte shape change. Furthermore, these data suggest that TNF regulates both processes, *i.e.* vascular permeability and pericyte shape change, in an independent-manner.

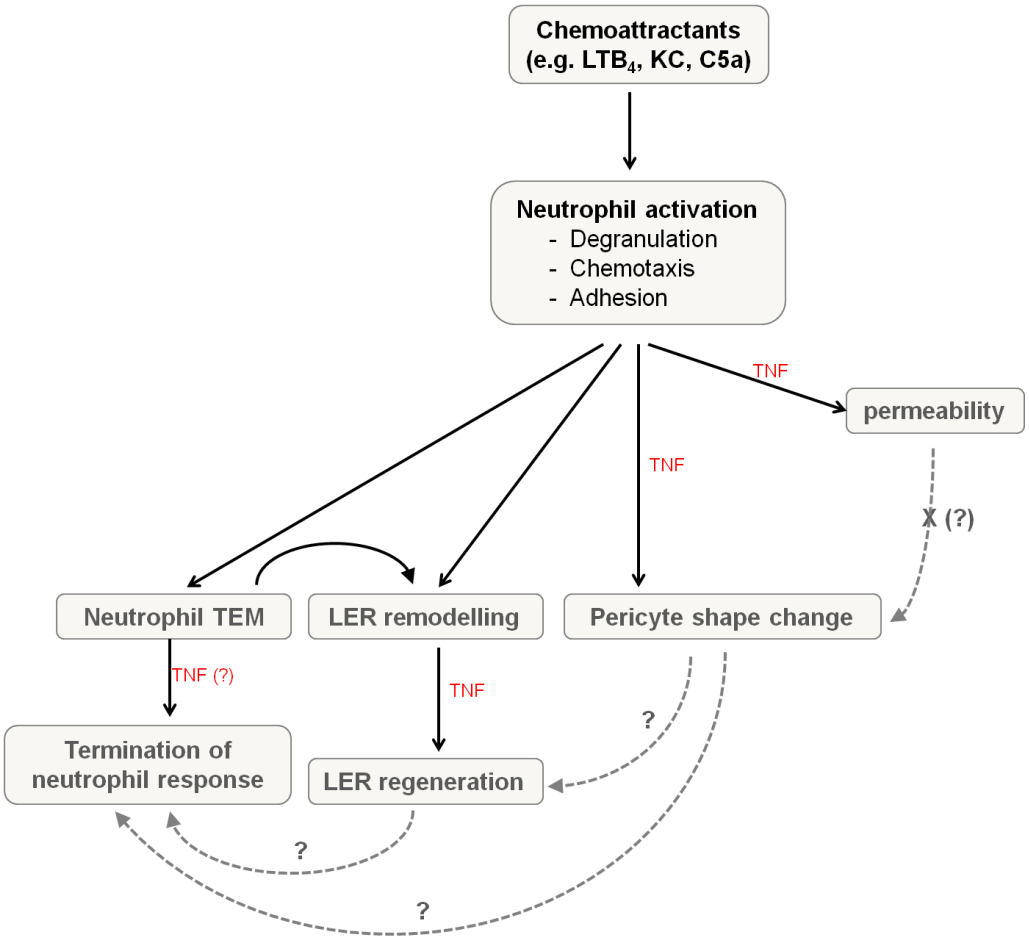

Figure 7.3: Proposed consequences of chemoattractant-induced pericyte shape change. Chemoattractants such as LTB_4, KC or C5a activate neutrophils and induce vascular permeability, neutrophil transmigration, pericyte shape change and BM LER remodelling. Vascular permeability was reduced in $TNFR^{-/-}$ mice, mice where pericyte gap opening in response to these stimuli was completely absent. Due to the time discrepancy (permeability preceded pericyte gap opening) it is unlikely that the increase in pericyte gap size regulates plasma leakage during inflammation. Neutrophil transmigration, which mediates BM LER enlargement, occurred independently of pericyte gap opening. In contrast, post-inflammatory BM deposition was delayed in $TNFR^{-/-}$ mice, a process that might regulate the termination of neutrophil responses as a trend for higher levels of neutrophils within the tissue were visible in $TNFR^{-/-}$ mice at later time points.

7.1.3 TNF as a secondary mediator of chemoattractant-induced changes in vascular morphology and permeability

Chemoattractants mediate the directional movement of leukocytes along a chemotactic gradient to sites of inflammation and hence, represent potent inducers of neutrophil transmigration. In addition, these molecules can indirectly (*i.e.* via activation of leukocytes) modify components of the vessel wall leading to vascular vasodilation and reduced barrier function (Bjork et al., 1982; Wedmore and Williams, 1981). Many aspects of the mechanism of action of these factors, however, remain unclear. Specifically, although it is known that neutrophils are the main target of chemoattractants, how chemoattractants regulate vascular morphology remains elusive. The results of the present study demonstrate for the first time the ability of different types of neutrophil chemoattractants, namely "end-target" chemoattractants (fMLP and C5a) and "intermediate" chemoattractants (LTB_4 and KC) to act on pericytes by inducing shape change of these cells *in vivo*. While specifically the impairment of the vessel wall barrier function was directly correlated with the rapid recruitment and interactions of neutrophils with vascular ECs after inducing inflammation (Wedmore and Williams, 1981), the exact molecular pathway is unknown. The findings of this thesis demonstrate a role for TNF as a secondary mediator in chemoattractant-induced responses (Figure 7.4). LTB_4-, KC- and C5a- induced pericyte shape change and vascular leakage were strictly TNF-dependent as demonstrated through the use of TNFR-deficient mice. In addition, chemoattractant-induced endogenous TNF might also play a role in BM deposition post inflammation since the enlargement of LERs was prolonged in TNFR-deficient mice. Whilst leukocytes are the main targets for chemoattractants, TNF is well known to act on ECs (Orlinick and Chao, 1998; Hehlgans and Pfeffer, 2005) and its ability to directly act on pericytes has also recently been shown (Proebstl et al., 2012).

C5a des Arg, fMLP and LTB_4 induce rapid plasma protein leakage in the rabbit skin *in vivo* which is unaffected by local inhibition of protein synthesis (Rampart and Williams, 1988), suggesting that this process involves rapid release of preformed mediators by neutrophils. Furthermore, the loss of barrier function is associated with the interaction of neutrophils with the endothelium via β_2 integrins expressed on the surface of leukocytes (Arfors et al., 1987; Gautam et al., 2000; Kaslovsky et al., 1990b). In these studies, inhibition of neutrophil-EC interactions via the use of an anti-β2 integrin blocking antibody, was shown to suppress plasma protein leakage *in*

vivo. This suggests the need for direct contact between neutrophils and ECs. The mechanisms involved in TNF release and origin of this cytokine in our model are not known. Although the principal cellular source of TNF is activated macrophages, the depletion of only neutrophils led to the inhibition of pericyte shape-change. Indeed, neutrophils are able to release TNF downstream of chemoattractants such as LTB_4 and KC (Chou et al., 2010; Gaudreault and Gosselin, 2009; Saiwai et al., 2010; Vieira et al., 2009). TNF can also be secreted by a number of other cell types including ECs, SMCs, mast cells and pericytes (Stark et al., 2013; Donnahoo et al., 1999), and thus, interaction of neutrophils with these cells, as suggested above, might play a role in vascular leakage via the induction of intracellular signalling leading to TNF secretion by these cells.

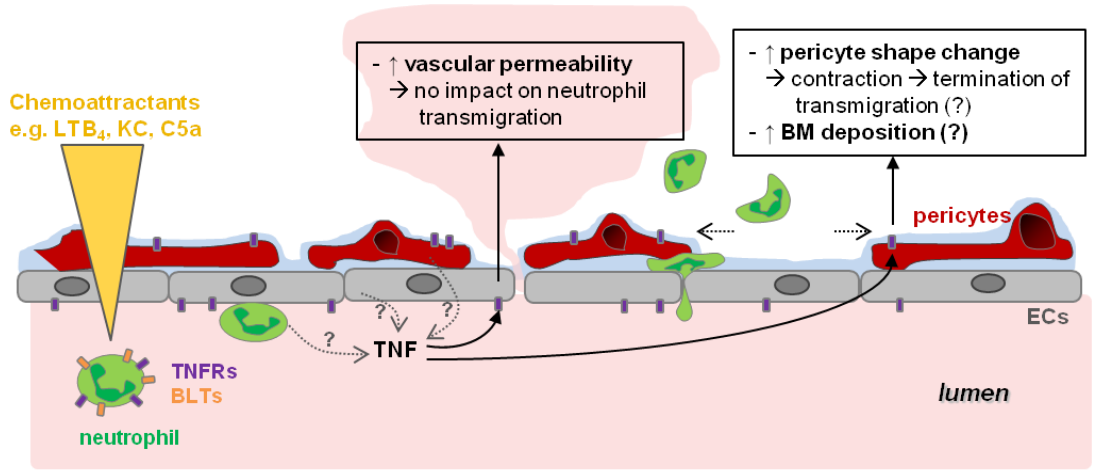

Figure 7.4: Endogenous TNF as a secondary mediator of chemoattractant-induced changes in vascular morphology and permeability. Chemoattractants such as LTB_4, KC and C5a activate neutrophils and promote their adhesion to the endothelium, as well as induce neutrophil-dependent alterations in the vessel wall. Based on the present findings, endogenously secreted TNF acts as a secondary mediator of these neutrophil chemoattractants by mediating vascular leakage, pericyte shape change and potentially post-inflammatory BM deposition. The source of TNF is not clear, but might involve the neutrophils themselves, ECs and/or pericytes.

7.2 Open questions and future perspectives

7.2.1 What is the source of TNF in chemoattractant-induced inflammation?

Chemoattractant-induced TNF may be produced by a number of different cell types, including macrophages, ECs, neutrophils, mast cells, vSMCs and pericytes (Stark et al., 2013; Donnahoo et al., 1999), however, the precise cellular source in our model is unclear. To investigate the involvement of neutrophils in TNF release, ELISA and/or western blot analysis of tissue lysates from neutrophil-depleted as compared to undepleted tissues could be analysed. In addition, supernatants of isolated bone marrow neutrophils (using percoll density gradient centrifugation) stimulated with chemoattractants *in vitro* could be assayed for secreted TNF. Similar experiments could be performed in the presence of cultured pericytes and/or ECs to compare possible contributions of these cell types. As signalling through β_2 integrins as induced by neutrophil-EC interactions was associated with vascular permeability (Arfors et al., 1987; Gautam et al., 2000; Kaslovsky et al., 1990b), the role of neutrophil adhesion in chemoattractant-induced endogenous TNF should be investigated. For this purpose, anti-β2 integrin blocking antibodies can be used, which block the adhesion of neutrophils to the endothelium. To analyse whether direct contact is also required for pericyte shape change the effect of these blockers on pericyte morphology could be analysed *in vivo* by immunofluorescent staining and confocal microscopy or *in vitro* using primary pericytes and time-lapse imaging.

7.2.2 How does TNF induce pericyte shape change? Do ECs act as supporters in this event?

Pericytes and ECs both express receptors for TNF (TNFR I and TNFR II) (Proebstl et al., 2012) and are thus able to directly respond to this cytokine. In addition, both cell types are in close interaction with each other and EC-pericyte cross-talk via direct contact or soluble factors play a crucial role in developmental and angiogenic events (Armulik et al., 2011). Co-culture experiments with primary pericytes and ECs could be established to investigate whether ECs play a supportive role in pericyte shape change and possibly the ability of pericytes to generate BM constituents. Pericyte shape change in pericyte-EC co-culture models could be compared to pericytes alone using time-lapse microscopy. Furthermore, co-cultures of $TNFR^{-/-}$ pericytes (isolated from $TNFR^{-/-}$ mice) with WT ECs and vice versa could

be analysed to selectively investigate the involvement of these cell-types in TNF-induced pericyte responses.

7.2.3 What is the functional consequence of pericyte shape change?

Does it support the migration of leukocyte subtypes other than neutrophils through the pericyte sheath?

Different leukocyte subsets have been shown to use different mechanisms to penetrate the BM (Voisin et al., 2009). Whilst neutrophil transmigration does not require pericyte shape change as was shown in this study, pericyte shape change might play a role in the transmigration of other leukocyte subtypes. In addition, as neutrophils are the first leukocytes to enter sites of infection or injury, it is possible that they prepare the way (e.g. by inducing pericyte shape change) for other leukocyte subsets that follow later. Hence, future experiments should investigate the potential role of pericyte shape change in facilitating the transmigration of leukocyte subtypes other than neutrophils (e.g. monocytes). For this purpose, Lys-EGFP mice which exhibit EGFP-labelled myelomonocytic cells could be stained for monocyte markers to differentiate monocytes from neutrophils. Monocyte-pericyte interactions and monocyte transmigration through the pericyte sheath could be analysed in $TNFR^{-/-}$ mice (where neutrophils are still present, but pericyte gaps do not increase in size) and/or neutrophil-depleted mice as compared to WT and non-depleted animals using confocal IVM.

Is there a role in the regulation of BM deposition? – And does this impact the termination of neutrophil transmigration?

Previous *in vitro* studies suggest that native EC-derived BM consituents delay neutrophil adhesion and migration depending on the concentration deposited (Burton et al., 2011; Butler et al., 2008). Furthermore, different BM components exhibit distinctive adhesion properties for leukocytes (Hallmann et al., 2005; Sixt et al., 2001; Korpos et al., 2010). Hence, the composition of the BM might play a role in the regulation of leukocyte transmigration. Due to the close association of collagen and laminin LERs with pericyte gaps, pericytes are thought to be responsible for the heterogeneous expression profile of the BM. It would be of

interest to assess whether inflammatory stimuli can act on pericytes to induce *de-novo* synthesis of matrix components, a response that could contribute to the "resealing" of the BM towards its basal state post inflammation and may indeed impact the termination rate of neutrophil migration. Thus, future *in vivo* experiments could aim to investigate the relative contribution of pericytes and ECs to this process.

Preliminary *in vitro* or *ex vivo* experiments could be performed to quantify the expression of BM components by qPCR (stimulated vs. control tissue extracts or primary pericytes), by flow cytometry of permeabilised cells or via immunofluorescence staining and confocal microscopy. Later, these studies could be complemented with more physiological studies *in vivo*. This could include the establishment of a new method based on fluorescence in situ hybridisation (FISH) to analyse the localisation of transcription of BM components *in vivo*. The impact of pericyte-derived BM deposition on leukocyte transmigration could be investigated *in vitro* using a transwell assay, where pericytes are stimulated to produce extracellular matrix proteins for different amount of time before neutrophils are added. Furthermore, the role of pericyte shape change in this process could be analysed *in vitro* using inhibitors or activators of cell contraction or relaxation (e.g. Forskolin, Blebbistatin or lysophosphatidic acid, respectively). Since these reagents would affect all cell types if used *in vivo* and hence could potentially have significant non-specific effects, the drugs Norepinephrine (vasoconstrictor) and Tolazoline (vasodilator) could be used in mouse models. Mice expressing Lifeact-GFP (Riedl et al., 2010) might provide a powerful tool for this study *in vivo* showing the formation of actin stress fibres.

7.2.4 Is pericyte gap opening specific to certain inflammatory mediators and/or tissues? Or is it a general phenomenon of inflammation?

So far, pericyte gap opening has been shown in response to cytokines (TNF and IL-1β) (Proebstl et al., 2012), as well as different types of neutrophil chemoattractants (LTB_4, KC, C5a and fMLP) as part of this study, and hence, in acute inflammation. It would be of interest to investigate this phenomenon in the content of a wider range of stimuli to assess its generality and also occurrence in models of chronic inflammation and disease models. For this purpose multiple mediators and experimental models of chronic inflammation (e.g. experimental autoimmune

encephalomyelitis as a model for multiple sclerosis), as well as ischemia/reperfusion injury could be investigated. Also, vasoactive mediators that do not induce neutrophil transmigration, such as histamine, bradykinin or serotonin could be analysed for their effect on pericyte gap enhancement.

In addition, changes in pericyte morphology could be compared in different vascular beds. Experiments performed by my colleague Dr Doris Proebstl previously showed a similar pattern of cytokine-induced pericyte gap enlargement in both the cremaster muscle and ear skin (Proebstl et al., 2012), indicating that this response might not be tissue-specific. This study further demonstrated that post-capillary venules of the mesentery exhibit pericyte gaps much bigger than those noted in postcapillary venules of the cremaster muscle and ear skin under basal conditions. Thus, investigations into pericyte responses in relation to leukocyte trafficking and vascular permeability under inflammatory conditions in the mesentery would be of particular interest.

7.3 Concluding remarks

TNF is a pro-inflammatory cytokine that is implicated to the pathogenesis of numerous inflammatory conditions such as rheumatoid arthritis and cardiovascular disorders (Beutler et al., 1985; Ferrari, 1999). It is not usually expressed under healthy conditions, but increased levels in serum and tissue are detected during inflammation and infectious conditions. The vast success of anti-TNF therapies (e.g. in patients with rheumatoid arthritis and Crohn's disease (Feldman et al., 1998)) has indicated that better understanding of TNF functions and TNF-driven inflammation has a real potential for extending the current use of TNF blockers. Collectively, the findings of this work have shed significant light onto the mechanism by which neutrophil chemoattractants exert their pro-inflammatory effects, findings that could be exploited for additional therapeutic strategies that target TNF.

REFERENCES

Abbas A and Lichtman A. Cellular and Molecular Immunology. 5th edition. 2005.

Abramsson,A., Berlin,O., Papayan,H., Paulin,D., Shani,M., and Betsholtz,C. (2002). Analysis of mural cell recruitment to tumor vessels. Circulation *105*, 112-117.

Adair-Kirk,T.L., Atkinson,J.J., Broekelmann,T.J., Doi,M., Tryggvason,K., Miner,J.H., Mecham,R.P., and Senior,R.M. (2003). A site on laminin alpha 5, AQARSAASKVKVSMKF, induces inflammatory cell production of matrix metalloproteinase-9 and chemotaxis. J. Immunol. *171*, 398-406.

Adams,D.H. and Lloyd,A.R. (1997). Chemokines: leucocyte recruitment and activation cytokines. Lancet *349*, 490-495.

Al,A.A., Taboada,C.B., Gassmann,M., and Ogunshola,O.O. (2011). Astrocytes and pericytes differentially modulate blood-brain barrier characteristics during development and hypoxic insult. J. Cereb. Blood Flow Metab *31*, 693-705.

Alberts B, Johnson A, and Lewis J. Molecular Biology of the Cell. 4th edition. 2002.

Alcendor,D.J., Charest,A.M., Zhu,W.Q., Vigil,H.E., and Knobel,S.M. (2012). Infection and upregulation of proinflammatory cytokines in human brain vascular pericytes by human cytomegalovirus. J. Neuroinflammation. *9*, 95.

Allport,J.R., Muller,W.A., and Luscinskas,F.W. (2000). Monocytes induce reversible focal changes in vascular endothelial cadherin complex during transendothelial migration under flow. J. Cell Biol. *148*, 203-216.

Alon,R., Hammer,D.A., and Springer,T.A. (1995). Lifetime of the P-selectin-carbohydrate bond and its response to tensile force in hydrodynamic flow. Nature *374*, 539-542.

Arfors,K.E., Lundberg,C., Lindbom,L., Lundberg,K., Beatty,P.G., and Harlan,J.M. (1987). A monoclonal antibody to the membrane glycoprotein complex CD18 inhibits polymorphonuclear leukocyte accumulation and plasma leakage in vivo. Blood *69*, 338-340.

Armulik,A., Abramsson,A., and Betsholtz,C. (2005). Endothelial/pericyte interactions. Circ. Res. *97*, 512-523.

Armulik,A., Genove,G., and Betsholtz,C. (2011). Pericytes: developmental, physiological, and pathological perspectives, problems, and promises. Dev. Cell *21*, 193-215.

Armulik,A., Genove,G., Mae,M., Nisancioglu,M.H., Wallgard,E., Niaudet,C., He,L., Norlin,J., Lindblom,P., Strittmatter,K., Johansson,B.R., and Betsholtz,C. (2010). Pericytes regulate the blood-brain barrier. Nature *468*, 557-561.

Attwell,D., Buchan,A.M., Charpak,S., Lauritzen,M., Macvicar,B.A., and Newman,E.A. (2010). Glial and neuronal control of brain blood flow. Nature *468*, 232-243.

Auch-Schwelk,W., Katusic,Z.S., and Vanhoutte,P.M. (1989). Contractions to oxygen-derived free radicals are augmented in aorta of the spontaneously hypertensive rat. Hypertension *13*, 859-864.

Balabanov,R., Beaumont,T., and Dore-Duffy,P. (1999). Role of central nervous system microvascular pericytes in activation of antigen-primed splenic T-lymphocytes. J. Neurosci. Res. *55*, 578-587.

Baluk,P., Hirata,A., Thurston,G., Fujiwara,T., Neal,C.R., Michel,C.C., and McDonald,D.M. (1997). Endothelial gaps: time course of formation and closure in inflamed venules of rats. Am. J. Physiol *272*, L155-L170.

Barber,A.J., Gardner,T.W., and Abcouwer,S.F. (2011). The significance of vascular and neural apoptosis to the pathology of diabetic retinopathy. Invest Ophthalmol. Vis. Sci. *52*, 1156-1163.

Barreiro,O., Vicente-Manzanares,M., Urzainqui,A., Yanez-Mo,M., and Sanchez-Madrid,F. (2004). Interactive protrusive structures during leukocyte adhesion and transendothelial migration. Front Biosci. *9*, 1849-1863.

Barreiro,O., Zamai,M., Yanez-Mo,M., Tejera,E., Lopez-Romero,P., Monk,P.N., Gratton,E., Caiolfa,V.R., and Sanchez-Madrid,F. (2008). Endothelial adhesion receptors are recruited to adherent leukocytes by inclusion in preformed tetraspanin nanoplatforms. J. Cell Biol. *183*, 527-542.

Bazzoni,F., Cassatella,M.A., Laudanna,C., and Rossi,F. (1991). Phagocytosis of opsonized yeast induces tumor necrosis factor-alpha mRNA accumulation and protein release by human polymorphonuclear leukocytes. J. Leukoc. Biol. *50*, 223-228.

Bazzoni,G. (2003). The JAM family of junctional adhesion molecules. Curr. Opin. Cell Biol. *15*, 525-530.

Belaaouaj,A., McCarthy,R., Baumann,M., Gao,Z., Ley,T.J., Abraham,S.N., and Shapiro,S.D. (1998). Mice lacking neutrophil elastase reveal impaired host defense against gram negative bacterial sepsis. Nat. Med. *4*, 615-618.

Bell,R.D., Winkler,E.A., Sagare,A.P., Singh,I., LaRue,B., Deane,R., and Zlokovic,B.V. (2010). Pericytes control key neurovascular functions and neuronal phenotype in the adult brain and during brain aging. Neuron *68*, 409-427.

Bergers,G. and Song,S. (2005). The role of pericytes in blood-vessel formation and maintenance. Neuro. Oncol. *7*, 452-464.

Betsholtz,C. (2004). Insight into the physiological functions of PDGF through genetic studies in mice. Cytokine Growth Factor Rev. *15*, 215-228.

Beutler,B., Milsark,I.W., and Cerami,A.C. (1985). Passive immunization against cachectin/tumor necrosis factor protects mice from lethal effect of endotoxin. Science *229*, 869-871.

Bianchi,M.E. (2007). DAMPs, PAMPs and alarmins: all we need to know about danger. J. Leukoc. Biol. *81*, 1-5.

Bixel,M.G., Petri,B., Khandoga,A.G., Khandoga,A., Wolburg-Buchholz,K., Wolburg,H., Marz,S., Krombach,F., and Vestweber,D. (2007). A CD99-related antigen on endothelial cells mediates neutrophil but not lymphocyte extravasation in vivo. Blood *109*, 5327-5336.

Bjork,J., Hedqvist,P., and Arfors,K.E. (1982). Increase in vascular permeability induced by leukotriene B4 and the role of polymorphonuclear leukocytes. Inflammation *6*, 189-200.

Bohnsack,J.F. (1992). CD11/CD18-independent neutrophil adherence to laminin is mediated by the integrin VLA-6. Blood *79*, 1545-1552.

Brachvogel,B., Moch,H., Pausch,F., Schlotzer-Schrehardt,U., Hofmann,C., Hallmann,R., von der,M.K., Winkler,T., and Poschl,E. (2005). Perivascular cells expressing annexin A5 define a novel mesenchymal stem cell-like population with the capacity to differentiate into multiple mesenchymal lineages. Development *132*, 2657-2668.

Brachvogel,B., Pausch,F., Farlie,P., Gaipl,U., Etich,J., Zhou,Z., Cameron,T., von der,M.K., Bateman,J.F., and Poschl,E. (2007). Isolated Anxa5+/Sca-1+ perivascular cells from mouse meningeal vasculature retain their perivascular phenotype in vitro and in vivo. Exp. Cell Res. *313*, 2730-2743.

Bradfield,P.F., Nourshargh,S., urrand-Lions,M., and Imhof,B.A. (2007). JAM family and related proteins in leukocyte migration (Vestweber series). Arterioscler. Thromb. Vasc. Biol. *27*, 2104-2112.

Brighton,C.T., Lorich,D.G., Kupcha,R., Reilly,T.M., Jones,A.R., and Woodbury,R.A. (1992). The pericyte as a possible osteoblast progenitor cell. Clin. Orthop. Relat Res. 287-299.

Bryan,B.A. and D'Amore,P.A. (2007). What tangled webs they weave: Rho-GTPase control of angiogenesis. Cell Mol. Life Sci. *64*, 2053-2065.

Burton,V.J., Butler,L.M., McGettrick,H.M., Stone,P.C., Jeffery,H.C., Savage,C.O., Rainger,G.E., and Nash,G.B. (2011). Delay of migrating leukocytes by the basement membrane deposited by endothelial cells in long-term culture. Exp. Cell Res. *317*, 276-292.

Butler,L.M., Khan,S., Ed,R.G., and Nash,G.B. (2008). Effects of endothelial basement membrane on neutrophil adhesion and migration. Cell Immunol. *251*, 56-61.

Cai,X., Lin,Y., Friedrich,C.C., Neville,C., Pomerantseva,I., Sundback,C.A., Zhang,Z., Vacanti,J.P., Hauschka,P.V., and Grottkau,B.E. (2009). Bone marrow derived pluripotent cells are pericytes which contribute to vascularization. Stem Cell Rev. *5*, 437-445.

Campbell,J.J., Hedrick,J., Zlotnik,A., Siani,M.A., Thompson,D.A., and Butcher,E.C. (1998). Chemokines and the arrest of lymphocytes rolling under flow conditions. Science *279*, 381-384.

Campbell,J.J., Qin,S., Bacon,K.B., Mackay,C.R., and Butcher,E.C. (1996). Biology of chemokine and classical chemoattractant receptors: differential requirements for adhesion-triggering versus chemotactic responses in lymphoid cells. J. Cell Biol. *134*, 255-266.

Canfield,A.E., Allen,T.D., Grant,M.E., Schor,S.L., and Schor,A.M. (1990). Modulation of extracellular matrix biosynthesis by bovine retinal pericytes in vitro: effects of the substratum and cell density. J. Cell Sci. *96 (Pt 1)*, 159-169.

Canfield,A.E., Sutton,A.B., Hoyland,J.A., and Schor,A.M. (1996). Association of thrombospondin-1 with osteogenic differentiation of retinal pericytes in vitro. J. Cell Sci. *109 (Pt 2)*, 343-353.

Carman,C.V., Sage,P.T., Sciuto,T.E., de la Fuente,M.A., Geha,R.S., Ochs,H.D., Dvorak,H.F., Dvorak,A.M., and Springer,T.A. (2007). Transcellular diapedesis is initiated by invasive podosomes. Immunity. *26*, 784-797.

Carman,C.V. and Springer,T.A. (2004). A transmigratory cup in leukocyte diapedesis both through individual vascular endothelial cells and between them. J. Cell Biol. *167*, 377-388.

Cassatella,M.A., Gasperini,S., and Russo,M.P. (1997). Cytokine expression and release by neutrophils. Ann. N. Y. Acad. Sci. *832*, 233-242.

Cavaillon,J.M., Fitting,C., and Haeffner-Cavaillon,N. (1990). Recombinant C5a enhances interleukin 1 and tumor necrosis factor release by lipopolysaccharide-stimulated monocytes and macrophages. Eur. J. Immunol. *20*, 253-257.

Cepinskas,G., Sandig,M., and Kvietys,P.R. (1999). PAF-induced elastase-dependent neutrophil transendothelial migration is associated with the mobilization of elastase to the neutrophil surface and localization to the migrating front. J. Cell Sci. *112 (Pt 12)*, 1937-1945.

Chan-Ling,T., Page,M.P., Gardiner,T., Baxter,L., Rosinova,E., and Hughes,S. (2004). Desmin ensheathment ratio as an indicator of vessel stability: evidence in normal development and in retinopathy of prematurity. Am. J. Pathol. *165*, 1301-1313.

Chou,R.C., Kim,N.D., Sadik,C.D., Seung,E., Lan,Y., Byrne,M.H., Haribabu,B., Iwakura,Y., and Luster,A.D. (2010). Lipid-cytokine-chemokine cascade drives neutrophil recruitment in a murine model of inflammatory arthritis. Immunity. *33*, 266-278.

Clemens,F., Verma,R., Ramnath,J., and Landolph,J.R. (2005). Amplification of the Ect2 proto-oncogene and over-expression of Ect2 mRNA and protein in nickel compound and methylcholanthrene-transformed 10T1/2 mouse fibroblast cell lines. Toxicol. Appl. Pharmacol. *206*, 138-149.

Cohen,M.P., Frank,R.N., and Khalifa,A.A. (1980). Collagen production by cultured retinal capillary pericytes. Invest Ophthalmol. Vis. Sci. *19*, 90-94.

Collett,G.D. and Canfield,A.E. (2005). Angiogenesis and pericytes in the initiation of ectopic calcification. Circ. Res. *96*, 930-938.

Colom,B., Poitelon,Y., Huang,W., Woodfin,A., Averill,S., Del,C.U., Zambroni,D., Brain,S.D., Perretti,M., Ahluwalia,A., Priestley,J.V., Chavakis,T., Imhof,B.A., Feltri,M.L., and Nourshargh,S. (2012). Schwann cell-specific JAM-C-deficient mice reveal novel expression and functions for JAM-C in peripheral nerves. FASEB J. *26*, 1064-1076.

Constantin,G., Majeed,M., Giagulli,C., Piccio,L., Kim,J.Y., Butcher,E.C., and Laudanna,C. (2000). Chemokines trigger immediate beta2 integrin affinity and mobility changes: differential regulation and roles in lymphocyte arrest under flow. Immunity. *13*, 759-769.

Courtoy,P.J. and Boyles,J. (1983). Fibronectin in the microvasculature: localization in the pericyte-endothelial interstitium. J. Ultrastruct. Res. *83*, 258-273.

Crisan,M., Yap,S., Casteilla,L., Chen,C.W., Corselli,M., Park,T.S., Andriolo,G., Sun,B., Zheng,B., Zhang,L., Norotte,C., Teng,P.N., Traas,J., Schugar,R., Deasy,B.M., Badylak,S., Buhring,H.J., Giacobino,J.P., Lazzari,L., Huard,J., and Peault,B. (2008). A perivascular origin for mesenchymal stem cells in multiple human organs. Cell Stem Cell *3*, 301-313.

Cuevas,P., Gutierrez-Diaz,J.A., Reimers,D., Dujovny,M., Diaz,F.G., and Ausman,J.I. (1984). Pericyte endothelial gap junctions in human cerebral capillaries. Anat. Embryol. (Berl) *170*, 155-159.

Dahinden,C.A., Fehr,J., and Hugli,T.E. (1983). Role of cell surface contact in the kinetics of superoxide production by granulocytes. J. Clin. Invest *72*, 113-121.

Dahlman-Ghozlan,K., Ortonne,J.P., Heilborn,J.D., and Stephansson,E. (2004). Altered tissue expression pattern of cell adhesion molecules, ICAM-1, E-selectin and VCAM-1, in bullous pemphigoid during methotrexate therapy. Exp. Dermatol. *13*, 65-69.

Dalkara,T., Gursoy-Ozdemir,Y., and Yemisci,M. (2011). Brain microvascular pericytes in health and disease. Acta Neuropathol. *122*, 1-9.

Daneman,R., Zhou,L., Kebede,A.A., and Barres,B.A. (2010). Pericytes are required for blood-brain barrier integrity during embryogenesis. Nature *468*, 562-566.

Dangerfield,J., Larbi,K.Y., Huang,M.T., Dewar,A., and Nourshargh,S. (2002). PECAM-1 (CD31) homophilic interaction up-regulates alpha6beta1 on transmigrated neutrophils in vivo and plays a functional role in the ability of alpha6 integrins to mediate leukocyte migration through the perivascular basement membrane. J. Exp. Med. *196*, 1201-1211.

Dangerfield,J.P., Wang,S., and Nourshargh,S. (2005). Blockade of alpha6 integrin inhibits IL-1beta- but not TNF-alpha-induced neutrophil transmigration in vivo. J. Leukoc. Biol. *77*, 159-165.

Darland,D.C. and D'Amore,P.A. (2001). TGF beta is required for the formation of capillary-like structures in three-dimensional cocultures of 10T1/2 and endothelial cells. Angiogenesis. *4*, 11-20.

Dejana,E. (2004). Endothelial cell-cell junctions: happy together. Nat. Rev. Mol. Cell Biol. *5*, 261-270.

Dejana,E., Spagnuolo,R., and Bazzoni,G. (2001). Interendothelial junctions and their role in the control of angiogenesis, vascular permeability and leukocyte transmigration. Thromb. Haemost. *86*, 308-315.

Dejana,E., Tournier-Lasserve,E., and Weinstein,B.M. (2009). The control of vascular integrity by endothelial cell junctions: molecular basis and pathological implications. Dev. Cell *16*, 209-221.

Delclaux,C., Delacourt,C., D'Ortho,M.P., Boyer,V., Lafuma,C., and Harf,A. (1996). Role of gelatinase B and elastase in human polymorphonuclear neutrophil migration across basement membrane. Am. J. Respir. Cell Mol. Biol. *14*, 288-295.

Dente,C.J., Steffes,C.P., Speyer,C., and Tyburski,J.G. (2001). Pericytes augment the capillary barrier in in vitro cocultures. J. Surg. Res. *97*, 85-91.

Di,G.A., Kenne,E., Wan,M., Soehnlein,O., Lindbom,L., and Haeggstrom,J.Z. (2009). Leukotriene B4-induced changes in vascular permeability are mediated by neutrophil release of heparin-binding protein (HBP/CAP37/azurocidin). FASEB J. *23*, 1750-1757.

Di,R.M., Giroud,J.P., and Willoughby,D.A. (1971). Studies on the mediators of the acute inflammatory response induced in rats in different sites by carrageenan and turpentine. J. Pathol. *104*, 15-29.

Diaz-Flores,L., Gutierrez,R., Lopez-Alonso,A., Gonzalez,R., and Varela,H. (1992). Pericytes as a supplementary source of osteoblasts in periosteal osteogenesis. Clin. Orthop. Relat Res. 280-286.

Diaz-Flores,L., Gutierrez,R., Varela,H., Rancel,N., and Valladares,F. (1991). Microvascular pericytes: a review of their morphological and functional characteristics. Histol. Histopathol. *6*, 269-286.

Dinarello,C.A. (2000). Proinflammatory cytokines. Chest *118*, 503-508.

Djeu,J.Y., Serbousek,D., and Blanchard,D.K. (1990). Release of tumor necrosis factor by human polymorphonuclear leukocytes. Blood *76*, 1405-1409.

Doherty,M.J., Ashton,B.A., Walsh,S., Beresford,J.N., Grant,M.E., and Canfield,A.E. (1998). Vascular pericytes express osteogenic potential in vitro and in vivo. J. Bone Miner. Res. *13*, 828-838.

Doherty,M.J. and Canfield,A.E. (1999). Gene expression during vascular pericyte differentiation. Crit Rev. Eukaryot. Gene Expr. *9*, 1-17.

Dohgu,S., Takata,F., Yamauchi,A., Nakagawa,S., Egawa,T., Naito,M., Tsuruo,T., Sawada,Y., Niwa,M., and Kataoka,Y. (2005). Brain pericytes contribute to the induction and up-regulation of blood-brain barrier functions through transforming growth factor-beta production. Brain Res. *1038*, 208-215.

Donnahoo,K.K., Shames,B.D., Harken,A.H., and Meldrum,D.R. (1999). Review article: the role of tumor necrosis factor in renal ischemia-reperfusion injury. J. Urol. *162*, 196-203.

Donoghue,L., Tyburski,J.G., Steffes,C.P., and Wilson,R.F. (2006). Vascular endothelial growth factor modulates contractile response in microvascular lung pericytes. Am. J. Surg. *191*, 349-352.

Dore-Duffy,P., Katychev,A., Wang,X., and Van,B.E. (2006). CNS microvascular pericytes exhibit multipotential stem cell activity. J. Cereb. Blood Flow Metab *26*, 613-624.

Dubravec,D.B., Spriggs,D.R., Mannick,J.A., and Rodrick,M.L. (1990). Circulating human peripheral blood granulocytes synthesize and secrete tumor necrosis factor alpha. Proc. Natl. Acad. Sci. U. S. A *87*, 6758-6761.

Dulmovits,B.M. and Herman,I.M. (2012). Microvascular remodeling and wound healing: A role for pericytes. Int. J. Biochem. Cell Biol. *44*, 1800-1812.

Edelman,D.A., Jiang,Y., Tyburski,J.G., Wilson,R.F., and Steffes,C.P. (2007). Cytokine production in lipopolysaccharide-exposed rat lung pericytes. J. Trauma *62*, 89-93.

Engelhardt,B. and Wolburg,H. (2004). Mini-review: Transendothelial migration of leukocytes: through the front door or around the side of the house? Eur. J. Immunol. *34*, 2955-2963.

Fabris,L. and Strazzabosco,M. (2011). Epithelial-mesenchymal interactions in biliary diseases. Semin. Liver Dis. *31*, 11-32.

Fabry,Z., Fitzsimmons,K.M., Herlein,J.A., Moninger,T.O., Dobbs,M.B., and Hart,M.N. (1993). Production of the cytokines interleukin 1 and 6 by murine brain microvessel endothelium and smooth muscle pericytes. J. Neuroimmunol. *47*, 23-34.

Farrington-Rock,C., Crofts,N.J., Doherty,M.J., Ashton,B.A., Griffin-Jones,C., and Canfield,A.E. (2004). Chondrogenic and adipogenic potential of microvascular pericytes. Circulation *110*, 2226-2232.

Feldman,M., Taylor,P., Paleolog,E., Brennan,F.M., and Maini,R.N. (1998). Anti-TNF alpha therapy is useful in rheumatoid arthritis and Crohn's disease: analysis of the mechanism of action predicts utility in other diseases. Transplant. Proc. *30*, 4126-4127.

Feng,D., Nagy,J.A., Pyne,K., Dvorak,H.F., and Dvorak,A.M. (1998). Neutrophils emigrate from venules by a transendothelial cell pathway in response to FMLP. J. Exp. Med. *187*, 903-915.

Fernandez,H.N., Henson,P.M., Otani,A., and Hugli,T.E. (1978). Chemotactic response to human C3a and C5a anaphylatoxins. I. Evaluation of C3a and C5a leukotaxis in vitro and under stimulated in vivo conditions. J. Immunol. *120*, 109-115.

Fernandez-Klett,F., Offenhauser,N., Dirnagl,U., Priller,J., and Lindauer,U. (2010). Pericytes in capillaries are contractile in vivo, but arterioles mediate functional hyperemia in the mouse brain. Proc. Natl. Acad. Sci. U. S. A *107*, 22290-22295.

Ferrari,R. (1999). The role of TNF in cardiovascular disease. Pharmacol. Res. *40*, 97-105.

Ferrari-Dileo,G., Davis,E.B., and Anderson,D.R. (1996). Glaucoma, capillaries and pericytes. 3. Peptide hormone binding and influence on pericytes. Ophthalmologica *210*, 269-275.

Finger,E.B., Puri,K.D., Alon,R., Lawrence,M.B., von Andrian,U.H., and Springer,T.A. (1996). Adhesion through L-selectin requires a threshold hydrodynamic shear. Nature *379*, 266-269.

Finlay,B.B. and Hancock,R.E. (2004). Can innate immunity be enhanced to treat microbial infections? Nat. Rev. Microbiol. *2*, 497-504.

Ford-Hutchinson,A.W., Bray,M.A., Doig,M.V., Shipley,M.E., and Smith,M.J. (1980). Leukotriene B, a potent chemokinetic and aggregating substance released from polymorphonuclear leukocytes. Nature *286*, 264-265.

Frieser,M., Hallmann,R., Johansson,S., Vestweber,D., Goodman,S.L., and Sorokin,L. (1996). Mouse polymorphonuclear granulocyte binding to extracellular matrix molecules involves beta 1 integrins. Eur. J. Immunol. *26*, 3127-3136.

Fujimoto,T. and Singer,S.J. (1987). Immunocytochemical studies of desmin and vimentin in pericapillary cells of chicken. J. Histochem. Cytochem. *35*, 1105-1115.

Fujiwara,K., Jindatip,D., Kikuchi,M., and Yashiro,T. (2010). In situ hybridization reveals that type I and III collagens are produced by pericytes in the anterior pituitary gland of rats. Cell Tissue Res. *342*, 491-495.

Furuhashi,M., Sjoblom,T., Abramsson,A., Ellingsen,J., Micke,P., Li,H., Bergsten-Folestad,E., Eriksson,U., Heuchel,R., Betsholtz,C., Heldin,C.H., and Ostman,A. (2004). Platelet-derived growth factor production by B16 melanoma cells leads to increased pericyte abundance in tumors and an associated increase in tumor growth rate. Cancer Res. *64*, 2725-2733.

Gaudreault,E. and Gosselin,J. (2009). Leukotriene B4 potentiates CpG signaling for enhanced cytokine secretion by human leukocytes. J. Immunol. *183*, 2650-2658.

Gautam,N., Herwald,H., Hedqvist,P., and Lindbom,L. (2000). Signaling via beta(2) integrins triggers neutrophil-dependent alteration in endothelial barrier function. J. Exp. Med. *191*, 1829-1839.

Gerhardt,H., Wolburg,H., and Redies,C. (2000). N-cadherin mediates pericytic-endothelial interaction during brain angiogenesis in the chicken. Dev. Dyn. *218*, 472-479.

Goetzl,E.J. and Pickett,W.C. (1980). The human PMN leukocyte chemotactic activity of complex hydroxy-eicosatetraenoic acids (HETEs). J. Immunol. *125*, 1789-1791.

Grako,K.A. and Stallcup,W.B. (1995). Participation of the NG2 proteoglycan in rat aortic smooth muscle cell responses to platelet-derived growth factor. Exp. Cell Res. *221*, 231-240.

Hallmann,R., Horn,N., Selg,M., Wendler,O., Pausch,F., and Sorokin,L.M. (2005). Expression and function of laminins in the embryonic and mature vasculature. Physiol Rev. *85*, 979-1000.

Hamilton,N.B., Attwell,D., and Hall,C.N. (2010). Pericyte-mediated regulation of capillary diameter: a component of neurovascular coupling in health and disease. Front Neuroenergetics. *2*.

Hashizume,H., Baluk,P., Morikawa,S., McLean,J.W., Thurston,G., Roberge,S., Jain,R.K., and McDonald,D.M. (2000). Openings between defective endothelial cells explain tumor vessel leakiness. Am. J. Pathol. *156*, 1363-1380.

Hayashi,K., Nakao,S., Nakaoke,R., Nakagawa,S., Kitagawa,N., and Niwa,M. (2004). Effects of hypoxia on endothelial/pericytic co-culture model of the blood-brain barrier. Regul. Pept. *123*, 77-83.

Haziot,A., Tsuberi,B.Z., and Goyert,S.M. (1993). Neutrophil CD14: biochemical properties and role in the secretion of tumor necrosis factor-alpha in response to lipopolysaccharide. J. Immunol. *150*, 5556-5565.

Hehlgans,T. and Pfeffer,K. (2005). The intriguing biology of the tumour necrosis factor/tumour necrosis factor receptor superfamily: players, rules and the games. Immunology *115*, 1-20.

Hellstrom,M., Gerhardt,H., Kalen,M., Li,X., Eriksson,U., Wolburg,H., and Betsholtz,C. (2001). Lack of pericytes leads to endothelial hyperplasia and abnormal vascular morphogenesis. J. Cell Biol. *153*, 543-553.

Hellstrom,M., Kalen,M., Lindahl,P., Abramsson,A., and Betsholtz,C. (1999). Role of PDGF-B and PDGFR-beta in recruitment of vascular smooth muscle cells and pericytes during embryonic blood vessel formation in the mouse. Development *126*, 3047-3055.

Herman,I.M. and D'Amore,P.A. (1985). Microvascular pericytes contain muscle and nonmuscle actins. J. Cell Biol. *101*, 43-52.

Hirschi,K.K. and D'Amore,P.A. (1996). Pericytes in the microvasculature. Cardiovasc. Res. *32*, 687-698.

Hirschi,K.K., Rohovsky,S.A., and D'Amore,P.A. (1998). PDGF, TGF-beta, and heterotypic cell-cell interactions mediate endothelial cell-induced recruitment of 10T1/2 cells and their differentiation to a smooth muscle fate. J. Cell Biol. *141*, 805-814.

Hobbs,S.K., Monsky,W.L., Yuan,F., Roberts,W.G., Griffith,L., Torchilin,V.P., and Jain,R.K. (1998). Regulation of transport pathways in tumor vessels: role of tumor type and microenvironment. Proc. Natl. Acad. Sci. U. S. A *95*, 4607-4612.

Huang,M.T., Larbi,K.Y., Scheiermann,C., Woodfin,A., Gerwin,N., Haskard,D.O., and Nourshargh,S. (2006). ICAM-2 mediates neutrophil transmigration in vivo: evidence for stimulus specificity and a role in PECAM-1-independent transmigration. Blood *107*, 4721-4727.

Huber,A.R. and Weiss,S.J. (1989a). Disruption of the subendothelial basement membrane during neutrophil diapedesis in an in vitro construct of a blood vessel wall. J. Clin. Invest *83*, 1122-1136.

Huber,A.R. and Weiss,S.J. (1989c). Disruption of the subendothelial basement membrane during neutrophil diapedesis in an in vitro construct of a blood vessel wall. J. Clin. Invest *83*, 1122-1136.

Huber,A.R. and Weiss,S.J. (1989b). Disruption of the subendothelial basement membrane during neutrophil diapedesis in an in vitro construct of a blood vessel wall. J. Clin. Invest *83*, 1122-1136.

Hughes,S. and Chan-Ling,T. (2004). Characterization of smooth muscle cell and pericyte differentiation in the rat retina in vivo. Invest Ophthalmol. Vis. Sci. *45*, 2795-2806.

Humphries,J.D., Byron,A., and Humphries,M.J. (2006). Integrin ligands at a glance. J. Cell Sci. *119*, 3901-3903.

Hurley J.V. (1964). Acute inflammation: The effect of concurrent leukocyte emigration and increased permeability on particle retention by the vascular wall. Br. J. Exp. Pathol. *45*, 627-633.

Hurley,J.V. (1963). An electron microscopic study of leucocytic emigration and vascular permeability in rat skin. Aust. J. Exp. Biol. Med. Sci. *41*, 171-186.

Hynes,R.O. and Lander,A.D. (1992). Contact and adhesive specificities in the associations, migrations, and targeting of cells and axons. Cell *68*, 303-322.

Jaffe,A.B. and Hall,A. (2005). Rho GTPases: biochemistry and biology. Annu. Rev. Cell Dev. Biol. *21*, 247-269.

Joyce,N.C., DeCamilli,P., and Boyles,J. (1984). Pericytes, like vascular smooth muscle cells, are immunocytochemically positive for cyclic GMP-dependent protein kinase. Microvasc. Res. *28*, 206-219.

Joyce,N.C., Haire,M.F., and Palade,G.E. (1985). Contractile proteins in pericytes. I. Immunoperoxidase localization of tropomyosin. J. Cell Biol. *100*, 1379-1386.

Jung,S., Aliberti,J., Graemmel,P., Sunshine,M.J., Kreutzberg,G.W., Sher,A., and Littman,D.R. (2000). Analysis of fractalkine receptor CX(3)CR1 function by targeted deletion and green fluorescent protein reporter gene insertion. Mol. Cell Biol. *20*, 4106-4114.

Kansas,G.S. (1996). Selectins and their ligands: current concepts and controversies. Blood *88*, 3259-3287.

Kanwar,S., Bullard,D.C., Hickey,M.J., Smith,C.W., Beaudet,A.L., Wolitzky,B.A., and Kubes,P. (1997). The association between alpha4-integrin, P-selectin, and E-selectin in an allergic model of inflammation. J. Exp. Med. *185*, 1077-1087.

Kaslovsky,R.A., Horgan,M.J., Lum,H., McCandless,B.K., Gilboa,N., Wright,S.D., and Malik,A.B. (1990b). Pulmonary edema induced by phagocytosing neutrophils. Protective effect of monoclonal antibody against phagocyte CD18 integrin. Circ. Res. *67*, 795-802.

Kaslovsky,R.A., Horgan,M.J., Lum,H., McCandless,B.K., Gilboa,N., Wright,S.D., and Malik,A.B. (1990a). Pulmonary edema induced by phagocytosing neutrophils. Protective effect of monoclonal antibody against phagocyte CD18 integrin. Circ. Res. *67*, 795-802.

Kelley,C., D'Amore,P., Hechtman,H.B., and Shepro,D. (1987). Microvascular pericyte contractility in vitro: comparison with other cells of the vascular wall. J. Cell Biol. *104*, 483-490.

Kenne,E., Soehnlein,O., Genove,G., Rotzius,P., Eriksson,E.E., and Lindbom,L. (2010). Immune cell recruitment to inflammatory loci is impaired in mice deficient in basement membrane protein laminin alpha4. J. Leukoc. Biol. *88*, 523-528.

Kerkar,S., Speyer,C., Tyburski,J., and Steffes,C. (2001). Reactive oxygen metabolites induce a biphasic contractile response in microvascular lung pericytes. J. Trauma *51*, 440-445.

Kerkar,S., Williams,M., Blocksom,J.M., Wilson,R.F., Tyburski,J.G., and Steffes,C.P. (2006). TNF-alpha and IL-1beta increase pericyte/endothelial cell co-culture permeability. J. Surg. Res. *132*, 40-45.

Khoury,J. and Langleben,D. (1996). Platelet-activating factor stimulates lung pericyte growth in vitro. Am. J. Physiol *270*, L298-L304.

Khoury,J. and Langleben,D. (1998). Effects of endotoxin on lung pericytes in vitro. Microvasc. Res. *56*, 71-84.

Kim,M., Carman,C.V., and Springer,T.A. (2003). Bidirectional transmembrane signaling by cytoplasmic domain separation in integrins. Science *301*, 1720-1725.

Kim,N.D., Chou,R.C., Seung,E., Tager,A.M., and Luster,A.D. (2006). A unique requirement for the leukotriene B4 receptor BLT1 for neutrophil recruitment in inflammatory arthritis. J. Exp. Med. *203*, 829-835.

Kinashi,T. (2005). Intracellular signalling controlling integrin activation in lymphocytes. Nat. Rev. Immunol. *5*, 546-559.

Kolyada,A.Y., Riley,K.N., and Herman,I.M. (2003). Rho GTPase signaling modulates cell shape and contractile phenotype in an isoactin-specific manner. Am. J. Physiol Cell Physiol *285*, C1116-C1121.

Komarova,Y. and Malik,A.B. (2010). Regulation of endothelial permeability via paracellular and transcellular transport pathways. Annu. Rev. Physiol *72*, 463-493.

Korpos,E., Wu,C., Song,J., Hallmann,R., and Sorokin,L. (2010). Role of the extracellular matrix in lymphocyte migration. Cell Tissue Res. *339*, 47-57.

Kovac,A., Erickson,M.A., and Banks,W.A. (2011). Brain microvascular pericytes are immunoactive in culture: cytokine, chemokine, nitric oxide, and LRP-1 expression in response to lipopolysaccharide. J. Neuroinflammation. *8*, 139.

Kowluru,R.A., Zhong,Q., and Kanwar,M. (2010). Metabolic memory and diabetic retinopathy: role of inflammatory mediators in retinal pericytes. Exp. Eye Res. *90*, 617-623.

Kriegsmann,J., Keyszer,G.M., Geiler,T., Brauer,R., Gay,R.E., and Gay,S. (1995). Expression of vascular cell adhesion molecule-1 mRNA and protein in rheumatoid synovium demonstrated by in situ hybridization and immunohistochemistry. Lab Invest *72*, 209-214.

Kutcher,M.E. and Herman,I.M. (2009). The pericyte: cellular regulator of microvascular blood flow. Microvasc. Res. *77*, 235-246.

Kutcher,M.E., Kolyada,A.Y., Surks,H.K., and Herman,I.M. (2007). Pericyte Rho GTPase mediates both pericyte contractile phenotype and capillary endothelial growth state. Am. J. Pathol. *171*, 693-701.

Larson,D.M., Carson,M.P., and Haudenschild,C.C. (1987). Junctional transfer of small molecules in cultured bovine brain microvascular endothelial cells and pericytes. Microvasc. Res. *34*, 184-199.

Lawrence,M.B., Kansas,G.S., Kunkel,E.J., and Ley,K. (1997). Threshold levels of fluid shear promote leukocyte adhesion through selectins (CD62L,P,E). J. Cell Biol. *136*, 717-727.

Leveen,P., Pekny,M., Gebre-Medhin,S., Swolin,B., Larsson,E., and Betsholtz,C. (1994). Mice deficient for PDGF B show renal, cardiovascular, and hematological abnormalities. Genes Dev. *8*, 1875-1887.

Levine,J.M. and Nishiyama,A. (1996). The NG2 chondroitin sulfate proteoglycan: a multifunctional proteoglycan associated with immature cells. Perspect. Dev. Neurobiol. *3*, 245-259.

Ley,K., Laudanna,C., Cybulsky,M.I., and Nourshargh,S. (2007). Getting to the site of inflammation: the leukocyte adhesion cascade updated. Nat. Rev. Immunol. *7*, 678-689.

Ley,K. and Zhang,H. (2008). Dances with leukocytes: how tetraspanin-enriched microdomains assemble to form endothelial adhesive platforms. J. Cell Biol. *183*, 375-376.

Lindahl,P., Johansson,B.R., Leveen,P., and Betsholtz,C. (1997). Pericyte loss and microaneurysm formation in PDGF-B-deficient mice. Science *277*, 242-245.

Lindemann,A., Riedel,D., Oster,W., Ziegler-Heitbrock,H.W., Mertelsmann,R., and Herrmann,F. (1989). Granulocyte-macrophage colony-stimulating factor induces cytokine secretion by human polymorphonuclear leukocytes. J. Clin. Invest *83*, 1308-1312.

Luster,A.D., Alon,R., and von Andrian,U.H. (2005). Immune cell migration in inflammation: present and future therapeutic targets. Nat. Immunol. *6*, 1182-1190.

Mackay,C.R. (2008). Moving targets: cell migration inhibitors as new anti-inflammatory therapies. Nat. Immunol. *9*, 988-998.

Maier,C.L. and Pober,J.S. (2011). Human placental pericytes poorly stimulate and actively regulate allogeneic CD4 T cell responses. Arterioscler. Thromb. Vasc. Biol. *31*, 183-189.

Maier,C.L., Shepherd,B.R., Yi,T., and Pober,J.S. (2010). Explant outgrowth, propagation and characterization of human pericytes. Microcirculation. *17*, 367-380.

Majno and Joris (2004). Cells, Tissues, and Disease: Principles of General Pathology.

Majno and Palade,G.E. (1961). Studies on inflammation. 1. The effect of histamine and serotonin on vascular permeability: an electron microscopic study. J. Biophys. Biochem. Cytol. *11*, 571-605.

Mandarino,L.J., Sundarraj,N., Finlayson,J., and Hassell,H.R. (1993). Regulation of fibronectin and laminin synthesis by retinal capillary endothelial cells and pericytes in vitro. Exp. Eye Res. *57*, 609-621.

Marmon,S., Cammer,M., Raine,C.S., and Lisanti,M.P. (2009a). Transcellular migration of neutrophils is a quantitatively significant pathway across dermal microvascular endothelial cells. Exp. Dermatol. *18*, 88-90.

Marmon,S., Hinchey,J., Oh,P., Cammer,M., de Almeida,C.J., Gunther,L., Raine,C.S., and Lisanti,M.P. (2009b). Caveolin-1 expression determines the route of neutrophil extravasation through skin microvasculature. Am. J. Pathol. *174*, 684-692.

Martin-Padura,I., Lostaglio,S., Schneemann,M., Williams,L., Romano,M., Fruscella,P., Panzeri,C., Stoppacciaro,A., Ruco,L., Villa,A., Simmons,D., and Dejana,E. (1998). Junctional adhesion molecule, a novel member of the immunoglobulin superfamily that distributes at intercellular junctions and modulates monocyte transmigration. J. Cell Biol. *142*, 117-127.

Mathiisen,T.M., Lehre,K.P., Danbolt,N.C., and Ottersen,O.P. (2010). The perivascular astroglial sheath provides a complete covering of the brain microvessels: an electron microscopic 3D reconstruction. Glia *58*, 1094-1103.

McDonald,B., Pittman,K., Menezes,G.B., Hirota,S.A., Slaba,I., Waterhouse,C.C., Beck,P.L., Muruve,D.A., and Kubes,P. (2010). Intravascular danger signals guide neutrophils to sites of sterile inflammation. Science *330*, 362-366.

McDonald,D.M., Thurston,G., and Baluk,P. (1999). Endothelial gaps as sites for plasma leakage in inflammation. Microcirculation. *6*, 7-22.

McEver,R.P. (2002). Selectins: lectins that initiate cell adhesion under flow. Curr. Opin. Cell Biol. *14*, 581-586.

McGuire,P.G., Rangasamy,S., Maestas,J., and Das,A. (2011). Pericyte-derived sphingosine 1-phosphate induces the expression of adhesion proteins and modulates the retinal endothelial cell barrier. Arterioscler. Thromb. Vasc. Biol. *31*, e107-e115.

Millan,J., Hewlett,L., Glyn,M., Toomre,D., Clark,P., and Ridley,A.J. (2006). Lymphocyte transcellular migration occurs through recruitment of endothelial ICAM-1 to caveola- and F-actin-rich domains. Nat. Cell Biol. *8*, 113-123.

Morikawa,S., Baluk,P., Kaidoh,T., Haskell,A., Jain,R.K., and McDonald,D.M. (2002b). Abnormalities in pericytes on blood vessels and endothelial sprouts in tumors. Am. J. Pathol. *160*, 985-1000.

Morikawa,S., Baluk,P., Kaidoh,T., Haskell,A., Jain,R.K., and McDonald,D.M. (2002a). Abnormalities in pericytes on blood vessels and endothelial sprouts in tumors. Am. J. Pathol. *160*, 985-1000.

Muller,W.A. (2003). Leukocyte-endothelial-cell interactions in leukocyte transmigration and the inflammatory response. Trends Immunol. *24*, 327-334.

Muller,W.A. (2009). Mechanisms of transendothelial migration of leukocytes. Circ. Res. *105*, 223-230.

Murfee,W.L., Skalak,T.C., and Peirce,S.M. (2005). Differential arterial/venous expression of NG2 proteoglycan in perivascular cells along microvessels: identifying a venule-specific phenotype. Microcirculation. *12*, 151-160.

Murphy,D.D. and Wagner,R.C. (1994). Differential contractile response of cultured microvascular pericytes to vasoactive agents. Microcirculation. *1*, 121-128.

Murphy,P.M. (1994). The molecular biology of leukocyte chemoattractant receptors. Annu. Rev. Immunol. *12*, 593-633.

Murphy,P.M. (1996). Chemokine receptors: structure, function and role in microbial pathogenesis. Cytokine Growth Factor Rev. *7*, 47-64.

Mydel,P., Shipley,J.M., ir-Kirk,T.L., Kelley,D.G., Broekelmann,T.J., Mecham,R.P., and Senior,R.M. (2008). Neutrophil elastase cleaves laminin-332 (laminin-5) generating peptides that are chemotactic for neutrophils. J. Biol. Chem. *283*, 9513-9522.

Nakagawa,S., Deli,M.A., Nakao,S., Honda,M., Hayashi,K., Nakaoke,R., Kataoka,Y., and Niwa,M. (2007). Pericytes from brain microvessels strengthen the barrier integrity in primary cultures of rat brain endothelial cells. Cell Mol. Neurobiol. *27*, 687-694.

Nakano,M., Atobe,Y., Goris,R.C., Yazama,F., Ono,M., Sawada,H., Kadota,T., Funakoshi,K., and Kishida,R. (2000). Ultrastructure of the capillary pericytes

and the expression of smooth muscle alpha-actin and desmin in the snake infrared sensory organs. Anat. Rec. *260*, 299-307.

Nehls,V. and Drenckhahn,D. (1991). Heterogeneity of microvascular pericytes for smooth muscle type alpha-actin. J. Cell Biol. *113*, 147-154.

Nehls,V. and Drenckhahn,D. (1993). The versatility of microvascular pericytes: from mesenchyme to smooth muscle? Histochemistry *99*, 1-12.

Newman,P.J. and Newman,D.K. (2003). Signal transduction pathways mediated by PECAM-1: new roles for an old molecule in platelet and vascular cell biology. Arterioscler. Thromb. Vasc. Biol. *23*, 953-964.

Nisancioglu,M.H., Betsholtz,C., and Genove,G. (2010). The absence of pericytes does not increase the sensitivity of tumor vasculature to vascular endothelial growth factor-A blockade. Cancer Res. *70*, 5109-5115.

Nourshargh,S., Hordijk,P.L., and Sixt,M. (2010). Breaching multiple barriers: leukocyte motility through venular walls and the interstitium. Nat. Rev. Mol. Cell Biol. *11*, 366-378.

Nourshargh,S., Krombach,F., and Dejana,E. (2006). The role of JAM-A and PECAM-1 in modulating leukocyte infiltration in inflamed and ischemic tissues. J. Leukoc. Biol. *80*, 714-718.

Okada,S., Kita,H., George,T.J., Gleich,G.J., and Leiferman,K.M. (1997). Migration of eosinophils through basement membrane components in vitro: role of matrix metalloproteinase-9. Am. J. Respir. Cell Mol. Biol. *17*, 519-528.

Orlidge,A. and D'Amore,P.A. (1986). Cell specific effects of glycosaminoglycans on the attachment and proliferation of vascular wall components. Microvasc. Res. *31*, 41-53.

Orlidge,A. and D'Amore,P.A. (1987). Inhibition of capillary endothelial cell growth by pericytes and smooth muscle cells. J. Cell Biol. *105*, 1455-1462.

Orlinick,J.R. and Chao,M.V. (1998). TNF-related ligands and their receptors. Cell Signal. *10*, 543-551.

Patan,S. (1998). TIE1 and TIE2 receptor tyrosine kinases inversely regulate embryonic angiogenesis by the mechanism of intussusceptive microvascular growth. Microvasc. Res. *56*, 1-21.

Peppiatt,C.M., Howarth,C., Mobbs,P., and Attwell,D. (2006). Bidirectional control of CNS capillary diameter by pericytes. Nature *443*, 700-704.

Petri,B., Kaur,J., Long,E.M., Li,H., Parsons,S.A., Butz,S., Phillipson,M., Vestweber,D., Patel,K.D., Robbins,S.M., and Kubes,P. (2011). Endothelial LSP1 is involved in endothelial dome formation, minimizing vascular permeability changes during neutrophil transmigration in vivo. Blood *117*, 942-952.

Phillipson,M., Heit,B., Colarusso,P., Liu,L., Ballantyne,C.M., and Kubes,P. (2006). Intraluminal crawling of neutrophils to emigration sites: a molecularly distinct process from adhesion in the recruitment cascade. J. Exp. Med. *203*, 2569-2575.

Phillipson,M., Kaur,J., Colarusso,P., Ballantyne,C.M., and Kubes,P. (2008). Endothelial domes encapsulate adherent neutrophils and minimize increases in vascular permeability in paracellular and transcellular emigration. PLoS. One. *3*, e1649.

Phillipson,M. and Kubes,P. (2011). The neutrophil in vascular inflammation. Nat. Med. *17*, 1381-1390.

Pierce,K.L., Premont,R.T., and Lefkowitz,R.J. (2002). Seven-transmembrane receptors. Nat. Rev. Mol. Cell Biol. *3*, 639-650.

Pinney,D.F. and Emerson,C.P., Jr. (1989). 10T1/2 cells: an in vitro model for molecular genetic analysis of mesodermal determination and differentiation. Environ. Health Perspect. *80*, 221-227.

Proebstl Doris. An investigation into murine pericyte shape change in response to inflammatory stimuli in vitro and in vivo. 2011.

Proebstl,D., Voisin,M.B., Woodfin,A., Whiteford,J., D'Acquisto,F., Jones,G.E., Rowe,D., and Nourshargh,S. (2012). Pericytes support neutrophil subendothelial cell crawling and breaching of venular walls in vivo. J. Exp. Med. *209*, 1219-1234.

Puls,A., Eliopoulos,A.G., Nobes,C.D., Bridges,T., Young,L.S., and Hall,A. (1999). Activation of the small GTPase Cdc42 by the inflammatory cytokines TNF(alpha) and IL-1, and by the Epstein-Barr virus transforming protein LMP1. J. Cell Sci. *112 (Pt 17)*, 2983-2992.

Puri,K.D., Doggett,T.A., Huang,C.Y., Douangpanya,J., Hayflick,J.S., Turner,M., Penninger,J., and Diacovo,T.G. (2005). The role of endothelial PI3Kgamma activity in neutrophil trafficking. Blood *106*, 150-157.

Qiu,H., Johansson,A.S., Sjostrom,M., Wan,M., Schroder,O., Palmblad,J., and Haeggstrom,J.Z. (2006). Differential induction of BLT receptor expression on human endothelial cells by lipopolysaccharide, cytokines, and leukotriene B4. Proc. Natl. Acad. Sci. U. S. A *103*, 6913-6918.

Rampart,M. and Williams,T.J. (1988). Evidence that neutrophil accumulation induced by interleukin-1 requires both local protein biosynthesis and neutrophil CD18 antigen expression in vivo. Br. J. Pharmacol. *94*, 1143-1148.

Reichel,C.A., Lerchenberger,M., Uhl,B., Rehberg,M., Berberich,N., Zahler,S., Wymann,M.P., and Krombach,F. (2011). Plasmin inhibitors prevent leukocyte accumulation and remodeling events in the postischemic microvasculature. PLoS. One. *6*, e17229.

Reichel,C.A., Rehberg,M., Bihari,P., Moser,C.M., Linder,S., Khandoga,A., and Krombach,F. (2008). Gelatinases mediate neutrophil recruitment in vivo: evidence for stimulus specificity and a critical role in collagen IV remodeling. J. Leukoc. Biol. *83*, 864-874.

Reichel,C.A., Rehberg,M., Lerchenberger,M., Berberich,N., Bihari,P., Khandoga,A.G., Zahler,S., and Krombach,F. (2009). Ccl2 and Ccl3 mediate neutrophil recruitment via induction of protein synthesis and generation of lipid mediators. Arterioscler. Thromb. Vasc. Biol. *29*, 1787-1793.

Reznikoff,C.A., Brankow,D.W., and Heidelberger,C. (1973). Establishment and characterization of a cloned line of C3H mouse embryo cells sensitive to postconfluence inhibition of division. Cancer Res. *33*, 3231-3238.

Riedl,J., Flynn,K.C., Raducanu,A., Gartner,F., Beck,G., Bosl,M., Bradke,F., Massberg,S., Aszodi,A., Sixt,M., and Wedlich-Soldner,R. (2010). Lifeact mice for studying F-actin dynamics. Nat. Methods *7*, 168-169.

Rot,A. (2010). Chemokine patterning by glycosaminoglycans and interceptors. Front Biosci. *15*, 645-660.

Rowe,R.G. and Weiss,S.J. (2008). Breaching the basement membrane: who, when and how? Trends Cell Biol. *18*, 560-574.

Ruoslahti,E. (1996). RGD and other recognition sequences for integrins. Annu. Rev. Cell Dev. Biol. *12*, 697-715.

Sadik,C.D., Kim,N.D., and Luster,A.D. (2011). Neutrophils cascading their way to inflammation. Trends Immunol. *32*, 452-460.

Saiwai,H., Ohkawa,Y., Yamada,H., Kumamaru,H., Harada,A., Okano,H., Yokomizo,T., Iwamoto,Y., and Okada,S. (2010). The LTB4-BLT1 axis mediates neutrophil infiltration and secondary injury in experimental spinal cord injury. Am. J. Pathol. *176*, 2352-2366.

Sanchez-Madrid,F., Nagy,J.A., Robbins,E., Simon,P., and Springer,T.A. (1983). A human leukocyte differentiation antigen family with distinct alpha-subunits and a common beta-subunit: the lymphocyte function-associated antigen (LFA-1), the C3bi complement receptor (OKM1/Mac-1), and the p150,95 molecule. J. Exp. Med. *158*, 1785-1803.

Sato,M., Suzuki,S., and Senoo,H. (2003). Hepatic stellate cells: unique characteristics in cell biology and phenotype. Cell Struct. Funct. *28*, 105-112.

Schenkel,A.R., Mamdouh,Z., and Muller,W.A. (2004). Locomotion of monocytes on endothelium is a critical step during extravasation. Nat. Immunol. *5*, 393-400.

Schiffmann,E., Corcoran,B.A., and Wahl,S.M. (1975). N-formylmethionyl peptides as chemoattractants for leucocytes. Proc. Natl. Acad. Sci. U. S. A *72*, 1059-1062.

Schindler,R., Gelfand,J.A., and Dinarello,C.A. (1990). Recombinant C5a stimulates transcription rather than translation of interleukin-1 (IL-1) and tumor necrosis factor: translational signal provided by lipopolysaccharide or IL-1 itself. Blood *76*, 1631-1638.

Schor,A.M., Allen,T.D., Canfield,A.E., Sloan,P., and Schor,S.L. (1990). Pericytes derived from the retinal microvasculature undergo calcification in vitro. J. Cell Sci. *97 (Pt 3)*, 449-461.

Schor,A.M., Canfield,A.E., Sutton,A.B., Arciniegas,E., and Allen,T.D. (1995). Pericyte differentiation. Clin. Orthop. Relat Res. 81-91.

Schrimpf,C. and Duffield,J.S. (2011). Mechanisms of fibrosis: the role of the pericyte. Curr. Opin. Nephrol. Hypertens. *20*, 297-305.

Schulte,D., Kuppers,V., Dartsch,N., Broermann,A., Li,H., Zarbock,A., Kamenyeva,O., Kiefer,F., Khandoga,A., Massberg,S., and Vestweber,D. (2011). Stabilizing the VE-cadherin-catenin complex blocks leukocyte extravasation and vascular permeability. EMBO J. *30*, 4157-4170.

Serhan,C.N., Chiang,N., and Van Dyke,T.E. (2008). Resolving inflammation: dual anti-inflammatory and pro-resolution lipid mediators. Nat. Rev. Immunol. *8*, 349-361.

Shamri,R., Grabovsky,V., Gauguet,J.M., Feigelson,S., Manevich,E., Kolanus,W., Robinson,M.K., Staunton,D.E., von Andrian,U.H., and Alon,R. (2005). Lymphocyte arrest requires instantaneous induction of an extended LFA-1 conformation mediated by endothelium-bound chemokines. Nat. Immunol. *6*, 497-506.

Shaw,S.K., Bamba,P.S., Perkins,B.N., and Luscinskas,F.W. (2001). Real-time imaging of vascular endothelial-cadherin during leukocyte transmigration across endothelium. J. Immunol. *167*, 2323-2330.

Shepro,D. and Morel,N.M. (1993). Pericyte physiology. FASEB J. *7*, 1031-1038.

Shimada,T., Kitamura,H., and Nakamura,M. (1992). Three-dimensional architecture of pericytes with special reference to their topographical relationship to microvascular beds. Arch. Histol. Cytol. *55 Suppl*, 77-85.

Showell,H.J., Naccache,P.H., Borgeat,P., Picard,S., Vallerand,P., Becker,E.L., and Sha'afi,R.I. (1982). Characterization of the secretory activity of leukotriene B4 toward rabbit neutrophils. J. Immunol. *128*, 811-816.

Silva,R., D'Amico,G., Hodivala-Dilke,K.M., and Reynolds,L.E. (2008). Integrins: the keys to unlocking angiogenesis. Arterioscler. Thromb. Vasc. Biol. *28*, 1703-1713.

Sima,A.A., Chakrabarti,S., Garcia-Salinas,R., and Basu,P.K. (1985). The BB-rat--an authentic model of human diabetic retinopathy. Curr. Eye Res. *4*, 1087-1092.

Simon,S.I., Hu,Y., Vestweber,D., and Smith,C.W. (2000). Neutrophil tethering on E-selectin activates beta 2 integrin binding to ICAM-1 through a mitogen-activated protein kinase signal transduction pathway. J. Immunol. *164*, 4348-4358.

Sims,D.E. (1986). The pericyte--a review. Tissue Cell *18*, 153-174.

Sims,D.E., Miller,F.N., Donald,A., and Perricone,M.A. (1990). Ultrastructure of pericytes in early stages of histamine-induced inflammation. J. Morphol. *206*, 333-342.

Sims,D.E., Miller,F.N., Horne,M.M., and Edwards,M.J. (1994). Interleukin-2 alters the positions of capillary and venule pericytes in rat cremaster muscle. J. Submicrosc. Cytol. Pathol. *26*, 507-513.

Sixt,M., Hallmann,R., Wendler,O., Scharffetter-Kochanek,K., and Sorokin,L.M. (2001). Cell adhesion and migration properties of beta 2-integrin negative polymorphonuclear granulocytes on defined extracellular matrix molecules. Relevance for leukocyte extravasation. J. Biol. Chem. *276*, 18878-18887.

Smith,M.J., Ford-Hutchinson,A.W., and Bray,M.A. (1980). Leukotriene B: a potential mediator of inflammation. J. Pharm. Pharmacol. *32*, 517-518.

Soloviev,A.I. and Braquet,P. (1991). Platelet-activating factor (PAF) induces contraction of saponin-skinned smooth muscle of coronary artery. Lipids *26*, 1274-1276.

Soriano,P. (1994). Abnormal kidney development and hematological disorders in PDGF beta-receptor mutant mice. Genes Dev. *8*, 1888-1896.

Sperandio,M., Smith,M.L., Forlow,S.B., Olson,T.S., Xia,L., McEver,R.P., and Ley,K. (2003). P-selectin glycoprotein ligand-1 mediates L-selectin-dependent leukocyte rolling in venules. J. Exp. Med. *197*, 1355-1363.

Speyer,C.L., Steffes,C.P., Tyburski,J.G., and Ram,J.L. (2000). Lipopolysaccharide induces relaxation in lung pericytes by an iNOS-independent mechanism. Am. J. Physiol Lung Cell Mol. Physiol *278*, L880-L887.

Stark,K., Eckart,A., Haidari,S., Tirniceriu,A., Lorenz,M., von Bruhl,M.L., Gartner,F., Khandoga,A.G., Legate,K.R., Pless,R., Hepper,I., Lauber,K., Walzog,B., and Massberg,S. (2013). Capillary and arteriolar pericytes attract innate leukocytes exiting through venules and 'instruct' them with pattern-recognition and motility programs. Nat. Immunol. *14*, 41-51.

Stimler,N.P., Bloor,C.M., Hugli,T.E., Wykle,R.L., McCall,C.E., and O'Flaherty,J.T. (1981). Anaphylactic actions of platelet-activating factor. Am. J. Pathol. *105*, 64-69.

Stratman,A.N., Malotte,K.M., Mahan,R.D., Davis,M.J., and Davis,G.E. (2009). Pericyte recruitment during vasculogenic tube assembly stimulates endothelial basement membrane matrix formation. Blood *114*, 5091-5101.

Sumimoto,H., Takeshige,K., and Minakami,S. (1984). Superoxide production of human polymorphonuclear leukocytes stimulated by leukotriene B4. Biochim. Biophys. Acta *803*, 271-277.

Sundberg,C., Ivarsson,M., Gerdin,B., and Rubin,K. (1996). Pericytes as collagen-producing cells in excessive dermal scarring. Lab Invest *74*, 452-466.

Sundd,P., Gutierrez,E., Koltsova,E.K., Kuwano,Y., Fukuda,S., Pospieszalska,M.K., Groisman,A., and Ley,K. (2012). 'Slings' enable neutrophil rolling at high shear. Nature *488*, 399-403.

Suri,C., Jones,P.F., Patan,S., Bartunkova,S., Maisonpierre,P.C., Davis,S., Sato,T.N., and Yancopoulos,G.D. (1996). Requisite role of angiopoietin-1, a ligand for the TIE2 receptor, during embryonic angiogenesis. Cell *87*, 1171-1180.

Taddei,A., Giampietro,C., Conti,A., Orsenigo,F., Breviario,F., Pirazzoli,V., Potente,M., Daly,C., Dimmeler,S., and Dejana,E. (2008). Endothelial adherens junctions control tight junctions by VE-cadherin-mediated upregulation of claudin-5. Nat. Cell Biol. *10*, 923-934.

Tager,A.M. and Luster,A.D. (2003). BLT1 and BLT2: the leukotriene B(4) receptors. Prostaglandins Leukot. Essent. Fatty Acids *69*, 123-134.

Takahashi,K., Brooks,R.A., Kanse,S.M., Ghatei,M.A., Kohner,E.M., and Bloom,S.R. (1989). Production of endothelin 1 by cultured bovine retinal endothelial cells and presence of endothelin receptors on associated pericytes. Diabetes *38*, 1200-1202.

Takeuchi,O. and Akira,S. (2010). Pattern recognition receptors and inflammation. Cell *140*, 805-820.

Tessner,T.G., O'Flaherty,J.T., and Wykle,R.L. (1989). Stimulation of platelet-activating factor synthesis by a nonmetabolizable bioactive analog of platelet-activating factor and influence of arachidonic acid metabolites. J. Biol. Chem. *264*, 4794-4799.

Thompson,R.D., Noble,K.E., Larbi,K.Y., Dewar,A., Duncan,G.S., Mak,T.W., and Nourshargh,S. (2001). Platelet-endothelial cell adhesion molecule-1 (PECAM-1)-deficient mice demonstrate a transient and cytokine-specific role for PECAM-1 in leukocyte migration through the perivascular basement membrane. Blood *97*, 1854-1860.

Thorsen,V.A., Vorland,M., Bjorndal,B., Bruland,O., Holmsen,H., and Lillehaug,J.R. (2003). Participation of phospholipase D and alpha/beta-protein kinase C in growth factor-induced signalling in C3H10T1/2 fibroblasts. Biochim. Biophys. Acta *1632*, 62-71.

Uyechi,L.S., Gagne,L., Thurston,G., and Szoka,F.C., Jr. (2001). Mechanism of lipoplex gene delivery in mouse lung: binding and internalization of fluorescent lipid and DNA components. Gene Ther. *8*, 828-836.

van der,F.A. and Sonnenberg,A. (2001). Function and interactions of integrins. Cell Tissue Res. *305*, 285-298.

van Zwieten,E.J., Ravid,R., Swaab,D.F., and Van de,W.T. (1988). Immunocytochemically stained vasopressin binding sites on blood vessels in the rat brain. Brain Res. *474*, 369-373.

Vecchi,A., Garlanda,C., Lampugnani,M.G., Resnati,M., Matteucci,C., Stoppacciaro,A., Schnurch,H., Risau,W., Ruco,L., Mantovani,A., and . (1994). Monoclonal antibodies specific for endothelial cells of mouse blood vessels. Their application in the identification of adult and embryonic endothelium. Eur. J. Cell Biol. *63*, 247-254.

Verbeek,M.M., Otte-Holler,I., Ruiter,D.J., and de Waal,R.M. (1999). Human brain pericytes as a model system to study the pathogenesis of cerebrovascular amyloidosis in Alzheimer's disease. Cell Mol. Biol. *45*, 37-46.

Verbeek,M.M., Westphal,J.R., Ruiter,D.J., and de Waal,R.M. (1995). T lymphocyte adhesion to human brain pericytes is mediated via very late antigen-4/vascular cell adhesion molecule-1 interactions. J. Immunol. *154*, 5876-5884.

Vestweber,D. (2002). Regulation of endothelial cell contacts during leukocyte extravasation. Curr. Opin. Cell Biol. *14*, 587-593.

Vestweber,D. and Blanks,J.E. (1999). Mechanisms that regulate the function of the selectins and their ligands. Physiol Rev. *79*, 181-213.

Vieira,S.M., Lemos,H.P., Grespan,R., Napimoga,M.H., Dal-Secco,D., Freitas,A., Cunha,T.M., Verri,W.A., Jr., Souza-Junior,D.A., Jamur,M.C., Fernandes,K.S., Oliver,C., Silva,J.S., Teixeira,M.M., and Cunha,F.Q. (2009). A crucial role for TNF-alpha in mediating neutrophil influx induced by endogenously generated or exogenous chemokines, KC/CXCL1 and LIX/CXCL5. Br. J. Pharmacol. *158*, 779-789.

Voisin,M.B., Probstl,D., and Nourshargh,S. (2010). Venular basement membranes ubiquitously express matrix protein low-expression regions: characterization in multiple tissues and remodeling during inflammation. Am. J. Pathol. *176*, 482-495.

Voisin,M.B., Woodfin,A., and Nourshargh,S. (2009). Monocytes and neutrophils exhibit both distinct and common mechanisms in penetrating the vascular basement membrane in vivo. Arterioscler. Thromb. Vasc. Biol. *29*, 1193-1199.

Wallis,W.J., Hickstein,D.D., Schwartz,B.R., June,C.H., Ochs,H.D., Beatty,P.G., Klebanoff,S.J., and Harlan,J.M. (1986). Monoclonal antibody-defined functional epitopes on the adhesion-promoting glycoprotein complex (CDw18) of human neutrophils. Blood *67*, 1007-1013.

Wallow,I.H., Bindley,C.D., Reboussin,D.M., Gange,S.J., and Fisher,M.R. (1993). Systemic hypertension produces pericyte changes in retinal capillaries. Invest Ophthalmol. Vis. Sci. *34*, 420-430.

Walshe,T.E., Saint-Geniez,M., Maharaj,A.S., Sekiyama,E., Maldonado,A.E., and D'Amore,P.A. (2009). TGF-beta is required for vascular barrier function, endothelial survival and homeostasis of the adult microvasculature. PLoS. One. *4*, e5149.

Wang,S., Cao,C., Chen,Z., Bankaitis,V., Tzima,E., Sheibani,N., and Burridge,K. (2012). Pericytes regulate vascular basement membrane remodeling and govern neutrophil extravasation during inflammation. PLoS. One. *7*, e45499.

Wang,S., Dangerfield,J.P., Young,R.E., and Nourshargh,S. (2005). PECAM-1, alpha6 integrins and neutrophil elastase cooperate in mediating neutrophil transmigration. J. Cell Sci. *118*, 2067-2076.

Wang,S., Voisin,M.B., Larbi,K.Y., Dangerfield,J., Scheiermann,C., Tran,M., Maxwell,P.H., Sorokin,L., and Nourshargh,S. (2006). Venular basement membranes contain specific matrix protein low expression regions that act as exit points for emigrating neutrophils. J. Exp. Med. *203*, 1519-1532.

Wedmore,C.V. and Williams,T.J. (1981). Control of vascular permeability by polymorphonuclear leukocytes in inflammation. Nature *289*, 646-650.

Wegmann,F., Petri,B., Khandoga,A.G., Moser,C., Khandoga,A., Volkery,S., Li,H., Nasdala,I., Brandau,O., Fassler,R., Butz,S., Krombach,F., and Vestweber,D. (2006). ESAM supports neutrophil extravasation, activation of Rho, and VEGF-induced vascular permeability. J. Exp. Med. *203*, 1671-1677.

Wei,J., Bhattacharyya,S., Tourtellotte,W.G., and Varga,J. (2011). Fibrosis in systemic sclerosis: emerging concepts and implications for targeted therapy. Autoimmun. Rev. *10*, 267-275.

Werr,J., Johansson,J., Eriksson,E.E., Hedqvist,P., Ruoslahti,E., and Lindbom,L. (2000). Integrin alpha(2)beta(1) (VLA-2) is a principal receptor used by neutrophils for locomotion in extravascular tissue. Blood *95*, 1804-1809.

Werr,J., Xie,X., Hedqvist,P., Ruoslahti,E., and Lindbom,L. (1998). beta1 integrins are critically involved in neutrophil locomotion in extravascular tissue In vivo. J. Exp. Med. *187*, 2091-2096.

Williams,T.J. and Jose,P.J. (1981). Mediation of increased vascular permeability after complement activation. Histamine-independent action of rabbit C5a. J. Exp. Med. *153*, 136-153.

Williams,T.J. and Morley,J. (1973). Prostaglandins as potentiators of increased vascular permeability in inflammation. Nature *246*, 215-217.

Wondimu,Z., Geberhiwot,T., Ingerpuu,S., Juronen,E., Xie,X., Lindbom,L., Doi,M., Kortesmaa,J., Thyboll,J., Tryggvason,K., Fadeel,B., and Patarroyo,M. (2004b). An endothelial laminin isoform, laminin 8 (alpha4beta1gamma1), is secreted by blood neutrophils, promotes neutrophil migration and extravasation, and protects neutrophils from apoptosis. Blood *104*, 1859-1866.

Wondimu,Z., Geberhiwot,T., Ingerpuu,S., Juronen,E., Xie,X., Lindbom,L., Doi,M., Kortesmaa,J., Thyboll,J., Tryggvason,K., Fadeel,B., and Patarroyo,M. (2004a). An endothelial laminin isoform, laminin 8 (alpha4beta1gamma1), is secreted by blood neutrophils, promotes neutrophil migration and extravasation, and protects neutrophils from apoptosis. Blood *104*, 1859-1866.

Wong,R.K., Baldwin,A.L., and Heimark,R.L. (1999). Cadherin-5 redistribution at sites of TNF-alpha and IFN-gamma-induced permeability in mesenteric venules. Am. J. Physiol *276*, H736-H748.

Woodfin,A., Reichel,C.A., Khandoga,A., Corada,M., Voisin,M.B., Scheiermann,C., Haskard,D.O., Dejana,E., Krombach,F., and Nourshargh,S. (2007). JAM-A mediates neutrophil transmigration in a stimulus-specific manner in vivo: evidence for sequential roles for JAM-A and PECAM-1 in neutrophil transmigration. Blood *110*, 1848-1856.

Woodfin,A., Voisin,M.B., Beyrau,M., Colom,B., Caille,D., Diapouli,F.M., Nash,G.B., Chavakis,T., Albelda,S.M., Rainger,G.E., Meda,P., Imhof,B.A., and Nourshargh,S. (2011). The junctional adhesion molecule JAM-C regulates polarized transendothelial migration of neutrophils in vivo. Nat. Immunol. *12*, 761-769.

Woodfin,A., Voisin,M.B., Imhof,B.A., Dejana,E., Engelhardt,B., and Nourshargh,S. (2009). Endothelial cell activation leads to neutrophil transmigration as supported by the sequential roles of ICAM-2, JAM-A, and PECAM-1. Blood *113*, 6246-6257.

Wu,C., Ivars,F., Anderson,P., Hallmann,R., Vestweber,D., Nilsson,P., Robenek,H., Tryggvason,K., Song,J., Korpos,E., Loser,K., Beissert,S., Georges-Labouesse,E., and Sorokin,L.M. (2009). Endothelial basement membrane laminin alpha5 selectively inhibits T lymphocyte extravasation into the brain. Nat. Med. *15*, 519-527.

Yamagishi,S., Fujimori,H., Yonekura,H., Tanaka,N., and Yamamoto,H. (1999). Advanced glycation endproducts accelerate calcification in microvascular pericytes. Biochem. Biophys. Res. Commun. *258*, 353-357.

Yauk,C.L., Polyzos,A., Rowan-Carroll,A., Kortubash,I., Williams,A., and Kovalchuk,O. (2008). Tandem repeat mutation, global DNA methylation, and regulation of DNA methyltransferases in cultured mouse embryonic fibroblast cells chronically exposed to chemicals with different modes of action. Environ. Mol. Mutagen. *49*, 26-35.

Yemisci,M., Gursoy-Ozdemir,Y., Vural,A., Can,A., Topalkara,K., and Dalkara,T. (2009). Pericyte contraction induced by oxidative-nitrative stress impairs capillary reflow despite successful opening of an occluded cerebral artery. Nat. Med. *15*, 1031-1037.

Yokota,T., Kawakami,Y., Nagai,Y., Ma,J.X., Tsai,J.Y., Kincade,P.W., and Sato,S. (2006). Bone marrow lacks a transplantable progenitor for smooth muscle type alpha-actin-expressing cells. Stem Cells *24*, 13-22.

Young,R.E., Thompson,R.D., and Nourshargh,S. (2002). Divergent mechanisms of action of the inflammatory cytokines interleukin 1-beta and tumour necrosis factor-alpha in mouse cremasteric venules. Br. J. Pharmacol. *137*, 1237-1246.

Young,R.E., Voisin,M.B., Wang,S., Dangerfield,J., and Nourshargh,S. (2007). Role of neutrophil elastase in LTB4-induced neutrophil transmigration in vivo assessed with a specific inhibitor and neutrophil elastase deficient mice. Br. J. Pharmacol. *151*, 628-637.

Zachariah,M.A. and Cyster,J.G. (2010). Neural crest-derived pericytes promote egress of mature thymocytes at the corticomedullary junction. Science *328*, 1129-1135.

Zarbock,A., Lowell,C.A., and Ley,K. (2007). Spleen tyrosine kinase Syk is necessary for E-selectin-induced alpha(L)beta(2) integrin-mediated rolling on intercellular adhesion molecule-1. Immunity. *26*, 773-783.